UNIVERSITÀ
DEGLI STUDI
DI PADOVA

Sede Amministrativa: Università degli Studi di Padova
Dipartimento di Innovazione Meccanica e Gestionale

SCUOLA DI DOTTORATO DI RICERCA IN INGEGNERIA INDUSTRIALE
INDIRIZZO: INGEGNERIA DELLA PRODUZIONE INDUSTRIALE
CICLO XXIV

ACCURACY OF GEOMETRICAL MEASUREMENTS USING COMPUTED TOMOGRAPHY

Direttore della Scuola: Ch.mo Prof. Paolo Francesco Bariani
Coordinatore d'indirizzo: Ch.mo Prof. Enrico Savio
Supervisore: Ch.mo Prof. Enrico Savio
Correlatore: Ing. Simone Carmignato

Dottorando: Anna Pierobon

Preface

This thesis has been prepared as one of the requirements of the Ph.D. degree. The work has been carried out from January 2009 to December 2011 at DIMEG - Dipartimento di Innovazione Meccanica e Gestionale, University of Padova, Italy, under the supervision of Prof. Enrico Savio and Dr. Simone Carmignato.

From August 2010 to November 2010, four months were spent at the Physikalisch-Technische Bundesanstalt), the National Metrology Institute of Germany in Braunschweig (PTB).

First of all I would like to thank my supervisors Prof. Enrico Savio and Dr. Simone Carmignato together with Prof. Leonardo De Chiffre for their inspiration and for their precise and accurate contributions to my work. Furthermore, I would like to express my gratitude to Dr Härtig, Dr. Bartscher, Dr. Neuschaefer-Rube and their colleagues at PTB. Moreover I would like to thank the staff of Elettra Synchrotron Syrmep Beam Line for the precious collaboration during the Ph.D. period. Finally I am really grateful to my Ph.D. colleagues and in particular to Ing. Balcon.

I would like to dedicate my Ph.D. thesis to my precious Parents Daniela&Fulvio, to my Sister Marta, to my Brothers Samuele, Davide and Giovanni, and last but not least to Alex.

"Es soll nicht genügen, dass man Schritte tue, die einst zum Ziele führen, sondern jeder Schritt soll Ziel sein und als Schritt gelten"[1]

Goethe

[1]It is not enough to take steps which may someday lead to a goal; each step must be itself a goal and a step likewise

Abstract

At the state of the art recently there has been increased interest in applying X-ray Computed Tomography (CT) to the task of dimensional measurements since it offers several opportunities which are not possible with conventional tactile or optical measurement devices as for example: complete and non-destructive components' inspections, determination of inner and outer geometries, simultaneous material and geometrical control, high-density point-clouds in relatively short time.
Due to these advantages, CT reveals to be a very promising non-contact measuring technique and several manufacturers and research centres are now investing in the further development of metrological CT systems for both research and industrial applications.
However, dimensional measurements from CT data are still lacking in traceability, due to difficulties in evaluating their uncertainty and in determining metrological performances of CT systems. In order to investigate these limitations, the main objective of the present work has been to contribute to the development of methods and calibrated objects for performance verification of CT systems.

The first part of the Ph.D. thesis is dedicated to the study of the state of the art of Computed Tomography systems, from the first CT applications (medical ones) to the new promising ones for dimensional metrology purposes.

Further on in a second part the state of the art related to the performance verification of CT systems is described, with particular focus on the field of dimensional metrology. In details some important national and international standards have been described together with alternative solutions coming from several research centers

and universities. The analysis of the state of the art leads to the developments of new procedures and related calibrated objects at *Laboratory of Industrial and Geometrical Metrology* of University of Padova. In particular two items are presented Pan Flute Gauge and CT Tetrahedron.

In a third part, the investigation on another calibrated object called PTB Tetrahedron is presented during a four months experience at PTB (*Physikalisch-Technische Bundesanstalt*) in Braunschweig, Germany.

Moreover, as described in the first parts of the Ph.D. thesis, CT systems are still not completely recognized as reference measuring instruments with well known metrological performances. An interlaboratory comparison has been considered to be an indispensable means to establish the effectiveness and comparability of measurement methods and to validate uncertainty claims. For this reason, the University of Padova organized the first international intercomparison of CT systems for dimensional metrology (*CT Audit* project) and an exhaustive extract from the official project report is presented.

Finally preliminary investigations on metrological structure resolution are described. It is an important metrological characteristic of CT systems that is still not clearly described in terms of definitions and testing procedures. The working draft ISO Standard 10360-11 defined the metrological structure resolution is defined as “the size of the smallest structure that can be measured dimensionally”. According to the previous definition, a dedicated item, called *Hourglass* has been created in order to test the metrological resolution and first results have been achieved and presented.

Sommario

Allo stato dell'arte, negli ultimi anni la tomografia computerizzata a raggi x (TC) si sta rivelando una tecnologia molto promettente nell'ambito della metrologia dimensionale, soprattutto perché, rispetto ai sistemi di misura tradizionali (tattili e ottici), essa presenta diversi vantaggi tra i quali la possibilità di controllare geometricamente parti interne di componenti senza doverli scomporre o distruggere, di verificare contemporaneamente la qualità dimensionale e dei materiali, di ricostruire tridimensionalmente gli oggetti con nuvole di punti ad alta densità in un tempo relativamente breve. Grazie a questi vantaggi, quindi, la tomografia computerizzata si è rivelata una tecnica di misura non a contatto molto interessante e molti produttori di sistemi TC e centri di ricerca stanno investendo nello sviluppo e nello studio di sistemi di tomografia a raggi x metrologici sia per uso industriale che nell'ambito di ricerca. Tuttavia, sono presenti alcuni limiti legati a problemi di riferibilità della misura e di stima dell'incertezza del processo di misurazione. L'obiettivo principale di questo lavoro di dottorato vuole quindi essere un contributo allo sviluppo di metodi e relativi campioni tarati per la verifica delle prestazioni di sistemi TC.

La prima parte della tesi di dottorato è dedicata allo studio dello stato dell'arte dei sistemi di tomografia computerizzata, partendo dalle prime applicazioni a livello medicale per approdare agli ultimi promettenti utilizzi nel campo della metrologia dimensionale.

In seguito è presentata una seconda parte dello studio dello stato dell'arte e alla verifica delle prestazioni dei sistemi TC, con particolare attenzione alle applicazioni metrologico dimensionali. In particolare sono presentate le proposte di verifica di

prestazione di alcune norme nazionali e internazionali e delle proposte sperimentali di centri di ricerca e università. L'analisi dello stato dell'arte ha portato allo sviluppo di nuove procedure e di nuovi campioni tarati presso il Laboratorio di metrologia industriale e geometrica dell'Università di Padova. In particolare sono descritti i campioni "Pan Flute Gauge" e "CT Tetrahedron".

In una terza parte, viene riportato il lavoro relativo a un ulteriore campione "PTB Tetrahedron" sviluppatosi nell'ambito di un'esperienza di quattro mesi presso il centro metrologico tedesco PTB a Braunschweig (*Physikalisch-Technische Bundesanstalt*).

Inoltre, come descritto nella prima parte del lavoro, i sistemi TC non sono ancora universalmente accettati come strumenti di misura di riferimento metrologico. Per questo motivo, un confronto interlaboratorio è stato ritenuto indispensabile per stabilire lo stato dei sistemi metrologici TC internazionale. L'Università di Padova ha quindi organizzato il primo interconfronto internazionale tra laboratori che utilizzano sistemi di tomografia computerizzata per misure metrologico dimensionale (Progetto *CT Audit*). Un esauriente estratto del rapporto ufficiale del progetto è presentato nel lavoro di dottorato.

Infine, sono descritti gli studi preliminari riguardanti la risoluzione metrologica strutturale. Essa è una caratteristica metrologica importante dei sistemi TC, anche se non è ancora chiaramente descritta in termini di definizione e di verifica con appositi test. La bozza di lavoro ISO 10360-11 definisce la risoluzione metrologica strutturale come "la misura della più piccola struttura che può essere valutata dimensionalmente". Partendo da questa definizione, è stato creato un campione, denominato "Hourglass", per la valutazione della risoluzione strutturale e sono presentati i primi risultati raggiunti.

Table of Contents

Chapter 1

Introduction to Computed Tomography

Chapter 1 illustrates the state of the art related to Computed Tomography used for several applications, with main focus on Dimensional Metrology field.

1. History of Computed Tomography

It was on 8th November 1895. Wilhelm Conrad Röntgen, a German physicist, while experimenting with an electric discharge in a vacuum tube, noticed a glow on a phosphored screen which was located at some distance from the tube. He analyzed how to stop the radiation with the insertion of objects in the way of the new kind of rays. Finally he could see a showed image of his bones' hand, through putting his hand in front of the screen. He discovered both x-rays and radiography [1]. An x-ray is a form of electromagnetic radiation. Its wavelength ranges from few picometers to a few nanometers.

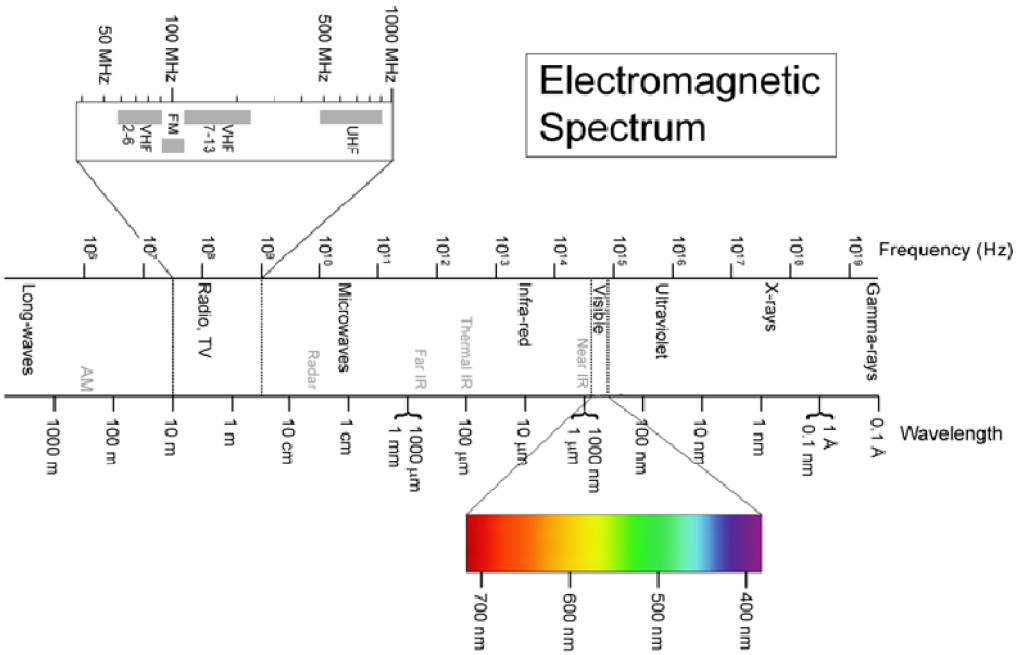

Fig 1.1: Electromagnetic Spectrum [2]

The energy of each x-ray photon E is proportional to its frequency v, and is described by the following expression:

$$E = h\nu = \frac{hc}{\lambda} \qquad (1)$$

, where *h* is Planck' constant (6.63 x 10^{-34} Js), c is the speed of the light (3 x 10^{8} m/s) and λ is the wavelength of the x-ray. [3]

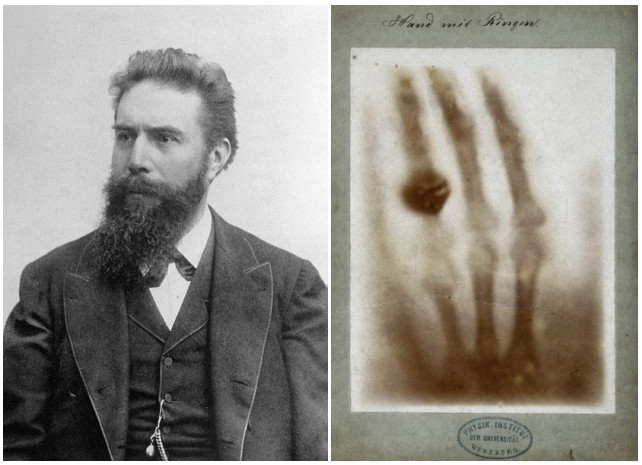

Fig. 1.2: a) Wilhelm Conrad Röntgen b) First x-ray picture (radiograph) taken by Röntgen [4]

Some years later (1901) Röntgen received the Nobel Prize in Physics.

Immediately this discover was considered very important especially in medical applications and first 2D radiography had been done. However, in order to diagnose in a better way anyhow of problems, a 2D radiography of a 3D object was not considered enough and the idea of projections data from several different angles came out. In details, the cross sectional imaging of a sample from data obtained from many different directions is called tomography [1]. Tomography derived from two Greek words: "tomos" (τόμος) which means section or cutting and "graphien" (γράφω), to write. In 1969 Godfrey N. Hounsfield developed the first x-ray computed tomography scanner together with A.M. Cormack.

The history of Computed Tomography started very recently. In early 1900s the Italian radiologist Alessandro Vallebona proposed a method to represent a single slice of the body on the radiographic film. This method was known as tomography.

Later in 1959, William Oldendorf, a UCLA neurologist and senior medical investigator at the West Los Angeles Veterans Administration hospital, conceived an idea for "scanning a head through a transmitted beam of X-rays, and being able to reconstruct the radiodensity patterns of a plane through the head" after watching an automated apparatus built to reject frost-bitten fruit by detecting dehydrated portions. In 1961, he built a prototype in which an X-ray source and a mechanically coupled detector rotated around the object to be imaged. By

reconstructing the image, this instrument could get an X-ray picture of a nail surrounded by a circle of other nails, which made it impossible to X-ray from any single angle. [5]

He described the basic concept later used by Allan McLeod Cormack to develop the mathematics behind computerized tomography. In October, 1963 Oldendorf received a U.S. patent for a "radiant energy apparatus for investigating selected areas of interior objects obscured by dense material". Oldendorf shared the 1975 Lasker award with Hounsfield for that discovery [6].

This technique leads to visualize objects in a tridimensional view and their internal parts without neither destroying nor cutting them. Computed Tomography was born, indeed, for medical purpose and many advanced studies leads to several generation of CT scanner. Moreover, in the 80's advanced microfocus x-ray computed tomography (CT) based on the same principles as medical CT have been developed, but with more attention regarded to the pixel resolution and the accuracy up to micro dimension.

The first industrial use of CT is dated on 1978 in the Non Destructive Technique field (NDT) with a medical CT system. In this occasion helicopter rotors have been scanned [6].

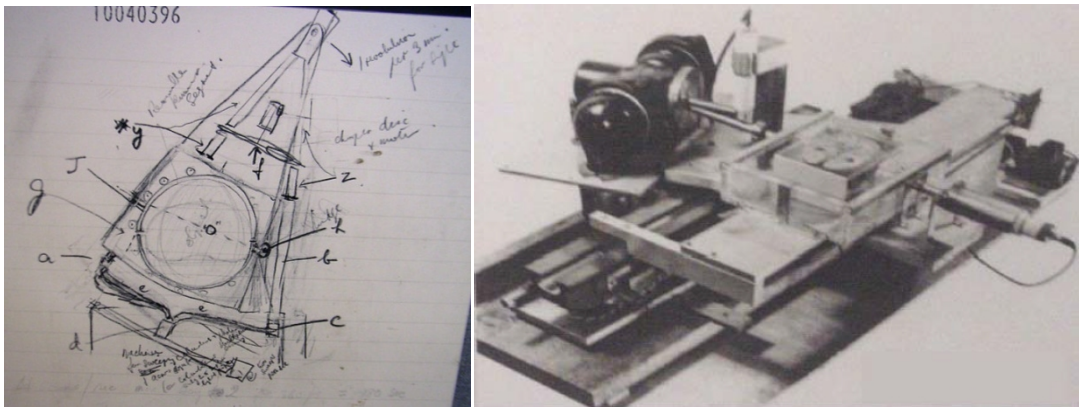

Fig. 1.3: The first X-ray computerized tomography, raw scheme (left) and photo (right) [7]

The first CT dimensional metrology measurement with an industrial CT system was performed in 1991 and it revealed a poor accuracy (around 0.1 mm). Only recently (in 2005) the first dedicated CT system for dimensional metrology purpose was created. This represented the first step from which many several companies started producing CT system for dimensional metrology [8].

2. CT for clinical, material analysis and industrial applications

It was on October 1971 when Godfrey Hounsfield and Jamie Ambrose positioned a patient inside a new machine in the basement of Atkinson Morley Hospital in UK [9].

Since its introduction in the 1970s, CT has become an important tool in medical imaging that uses x-rays to create cross-sectional pictures of the body. It has more recently been used for preventive medicine or screening for disease, as a complete and very effective diagnostic method.

Fig. 2.1: Modern medical CT Scanner [source: Adam]

Comparing to 2D radiography, CT reveals many advantages, such as [10]:

- Possibility of isolating the investigated part (area of interest) by software elaboration;
- Possibility of analyzing several tissues also different density;
- The nowadays high resolution leads to improvements in diagnostic, related to better both spatial and density resolution (see Fig.2.2).

Anyway humans are not the sole beneficiaries of CT invention. Over the years CT scanners have been used to scan trees, animals, industrial parts [3].

Indeed over the past decades, modern experimental methods for microstructural analysis such as SEM imaging have lead to great advances. However, the lack of access to three-dimensional (3D) information represents the main limitation of SEM and other 2D imaging techniques.

7. 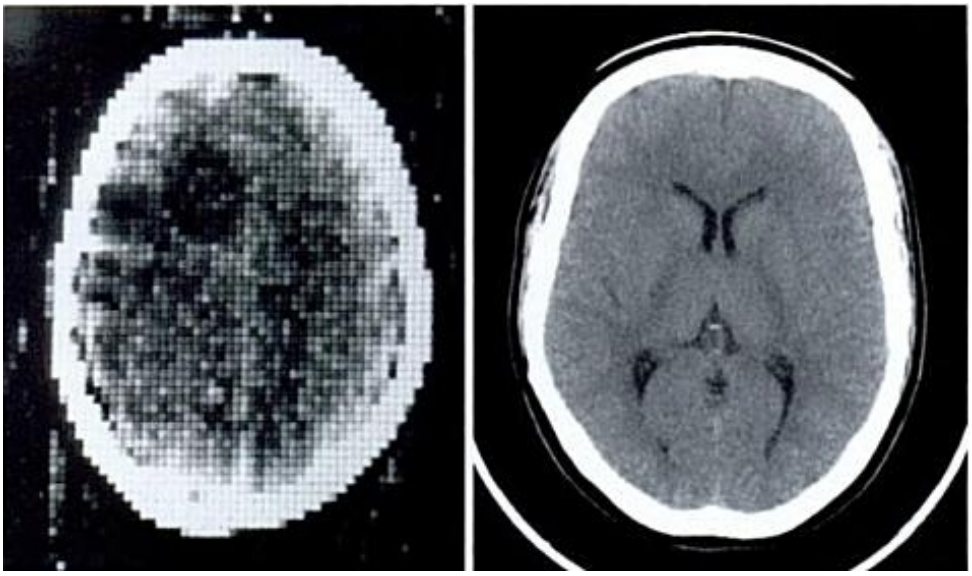

Fig 2.2: Comparison of CT head images from one of the first CT scanners (left) and a 2005 one (right) [3]

The development of non-destructive techniques for the 3D microstructural investigation of materials has become necessary. Nowadays X-ray computed micro-tomography (X-μCT) provides a totally non-invasive tool to investigate in a three-dimensional way the inner structure of materials, with a spatial resolution reaching the sub-μm level when the most advanced systems are employed. X-μCT allows reconstructing 3D maps of the variations of the X-ray linear attenuation coefficient (μ) within a sample without perturbing its structure [11].

CT found many applications in several industrial fields both for small and micro parts (chips, electronic components etc.) and for big ones (i.e. turbine blades) [12].

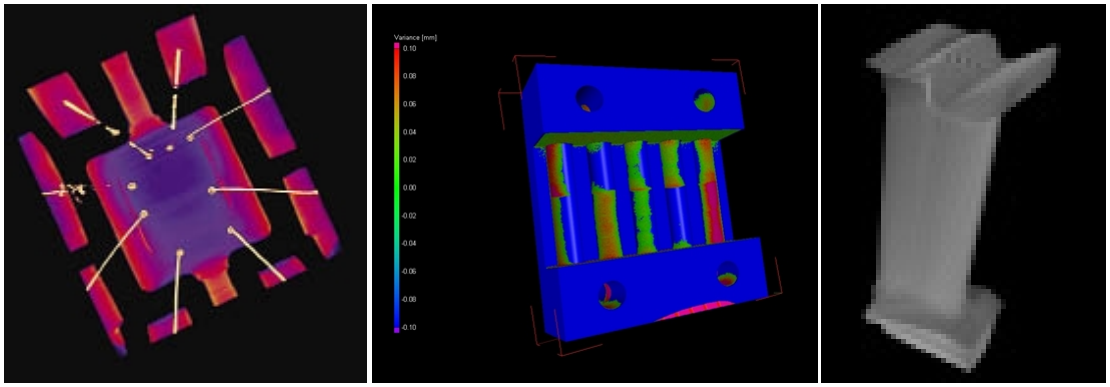

Fig.2.3:a) Integrated circuitmeasured by CT Source: North Star Imaging .b) CAD Comparison between CT and CAD model and c)turbine blade CT reconstruction Source: Hadland technologies

CT is used for several applications, and some examples of them are here following described. High-resolution industrial computed tomography is applied in material application for inspecting materials, composites, sintered materials and ceramics but also to analyze geological or biological samples. Materials distribution, voids and cracks are visualized three-dimensionally at microscopic resolution [13], see Fig. 2.4 (left).

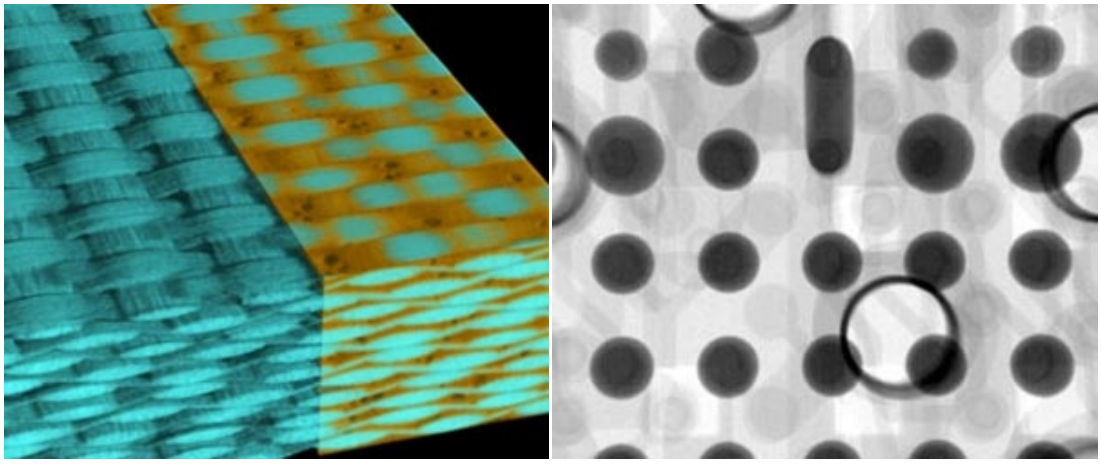

Fig 2.4: Examples of applications in Material Sciences (left) and Electronics (right) [13]

Moreover since electronic components are becoming increasingly miniaturized, CT technology provides the means necessary to inspect such components. See Fig. 2.4 (right)

Typical inspection tasks include [13]:

- Inspection of bond wires and bonding areas;
- Void analysis of conductive and non-conductive die bonds;
- Inspection of flip-chip solder joints in processor cases;
- Analysis of discrete components such as capacitors and inductors [13].

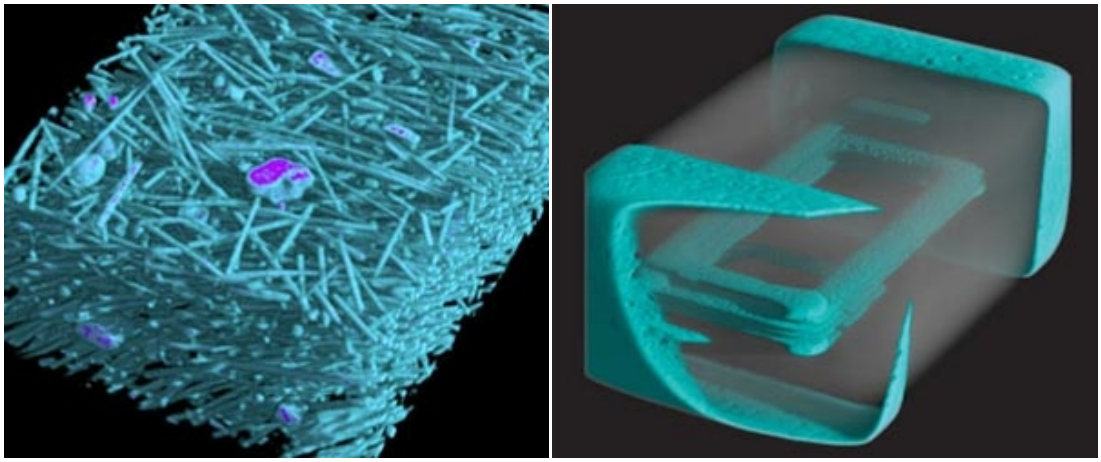

Fig 2.5: Composite materials (left) and casting/welding inspection (right)

In addition CT technology is used in plastics engineering (see Fig. 2.5 (right)) to optimize the casting and spraying process by detecting contraction cavities, blisters, weld lines and cracks, and to analyze flaws. Indeed industrial X-ray computed tomography provides three-dimensional images of object characteristics such as grain-flow patterns and filler distribution as well as of low-contrast defects [13].

Radiographic non-destructive testing seems to be very useful in detecting flaws in castings and welds. The combination of microfocus X-ray technology and industrial X-ray computed tomography enables defect detectability in the micrometer range and provides three-dimensional images of low-contrast defects, see Fig. 2.5 (left) [13].

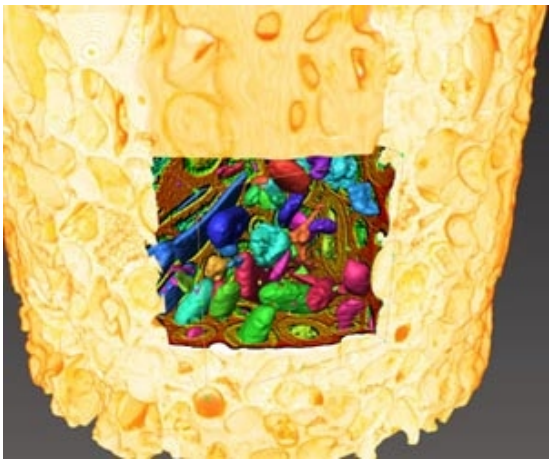

Fig.2.6: Example of application of CT in Geology sciences

Computed tomography is also widely applied in inspecting geological samples, for example in the exploration for new resources. Special designed industrial CT-systems provide three-dimensional images at microscopic resolution of rock samples, binders, cements and cavities and help identify certain sample characteristics such as size and location of voids in oil-bearing rock, see Fig. 2.6 [13].

2.1 The Evolution of CT technology

Over the last 40 years Computed Tomography evolved into more accurate and qualified systems. The typology of CT scanners is subdivided into at least 4 different generations [3].

The early scanners belong to the first generation of CT (see Fig.2.7 left), where only one pencil beam is measured at a time. The x-ray source collimates to a narrow beam and it is translated together with the detector linearly in order to acquire individual measurements.

After the linear measurements, both the x-ray tube and the detector are rotated 1 deg to the next angular position, ready to acquire the next set of measurements, circa 160.

The CT scanner of the first generation were very promising but the data acquisition was particularly slow and the patient was supposed to be exposed to the x-ray for a long time. [14]. The previous disadvantage was very challenging and a new scanner was designed and developed: the so called second-generation scanner. As shown in Fig. 2.7 (right), the scanner translates and rotates, but the number of rotation steps is reduced thanks to the multiple pencil beams. Moreover multiple detectors have been used. This configuration leads to multiple angle acquisition at each position and to a reduced scanning time (under 20 seconds) [3][14].

In the 80's the third-generation scanners were produced. They are made with many detector cells located on an arc concentric to the x-ray source that is fixed, the detectors stay stationary to each other while the system rotates around the patient (see Fig. 2.8, left) [3]. Of course, the exposing time has been drastically reduced.

The fourth-generation scanners (Fig. 2.8, right) have been developed in order to make the x-ray source irradiate the detectors in a fan-shaped x-ray beam at any instant. The difference between the third generation and fourth one is that the fourth-generation system uses a stationary circular array of detectors and only the source moves. The view is made by obtaining successive absorption measurements of a single detector at successive positions of the x-ray source. These scanners combine the artifact resistance of second-generation systems with the speed of third-generation units, but they can be more complex and costly than first-, second-, or third-generation machines, they require that the object fit within the fan of X-rays, and they are more susceptible to scattered radiation [15].

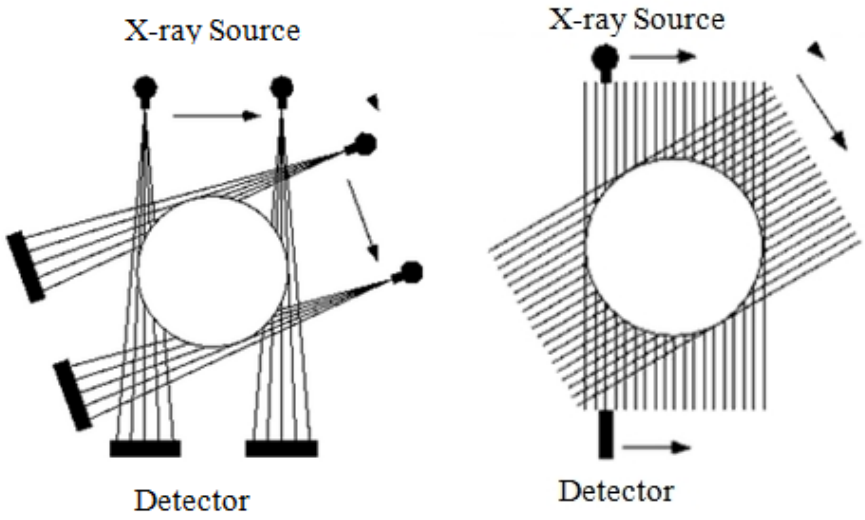

Fig 2.7: First- (left) and Second (right) -generation CT scanners scheme [16]

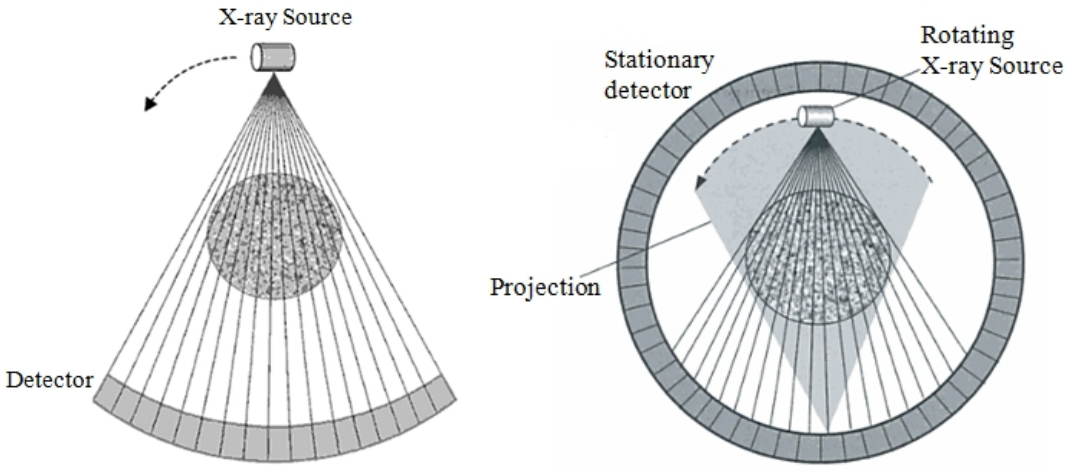

Fig. 2.8: Third (left)- and fourth(right)- generation CT scanners scheme[3]

3. CT for Dimensional Metrology

3.1 What is CT?

According to VDI/VDE 2630-1.1 "Computed Tomography" is defined as the imaging method in which the object is irradiated with X-rays or gamma rays and mathematical algorithms are used to create a cross-sectional image or a sequence of such images [17].

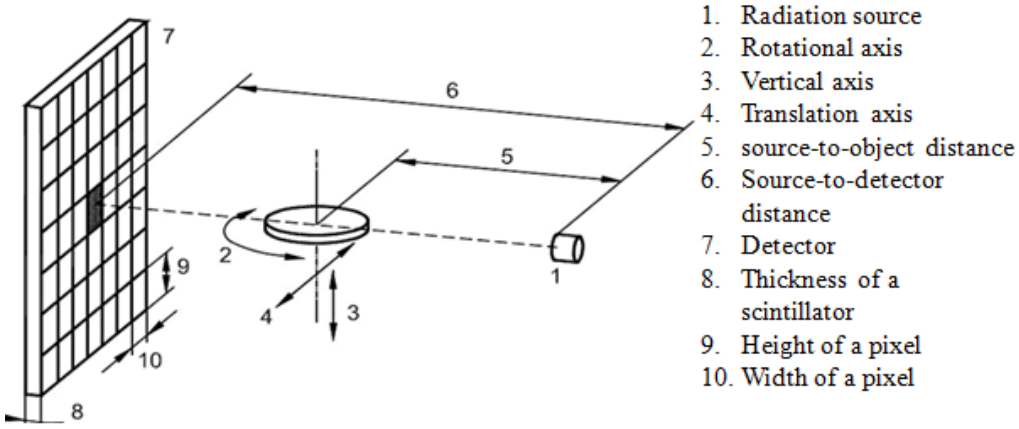

Fig.3.1: Scheme of a CT system [17]

In details a CT system is mainly composed by the following parts, see Fig. 3.1:

1. Radiation Source or x-ray source (object 1 in Fig. 3.1);
2. Rotary Table;
3. Detector (object 7 in Fig. 3.1);
4. Kinematic systems;
5. Software.

3.1.1 X-ray source

The x-ray tube is one of the most important components of a CT system, since it supplies the necessary x-ray photons to perform the scanning [3]. Although the size and appearance of the x-ray tube have changed significantly since its invention by Roentgen in 1895, the fundamental principle of x-ray generation have not changed [18]. The basic components of an x-ray tube are a cathode and an anode (see Fig. 3.2). The radiation source (see Fig. 3.2) is an x-ray vacuum tube. It is made by an electron beam gun with a cathode filament that emits electrons. Then an anode accelerates the electrons beam that are further deflected and focused onto a target. Electrons are decelerated and their energy is converted 99% in heat and 1% in x-rays.

The production of X-rays is caused by two different processes.

The first method a produced a so-called characteristic X-radiation, when the electron interacts with an inner-shell electron of the target. This kind of X-rays results when the interaction is sufficiently strong so as to ionize the target atom by total removal of the inner-shell electron. The appearing hole will be filled with an outer-shell electron. The transition of

an orbital electron from an outer-shell to an inner-shell is accompanied by the emission of an X-ray photon, with energy equal to the difference in the binding energies of the orbital electrons involved. Obviously, this kind of radiation is material dependent. The production of heat and characteristic X-rays both involves interactions between the accelerated electrons and the electrons of the target material.

Another type of interaction in which the electron can lose its kinetic energy delivers the second process of X-ray production, caused by the interaction of the electron with the nucleus of a target atom. As the colliding electron passes by the nucleus of an anode atom, it is slowed down and deviated in its course, leaving with reduced kinetic energy in a different direction. This loss in kinetic energy reappears as an X-ray photon. These types of X-rays are called Bremsstrahlung, where “Bremse" is the German name for slowing down. The amount of kinetic energy that is lost in this way can vary from zero to the total incident energy. While the characteristic radiation results in a discrete X-ray spectrum of characteristic peaks, the bremsstrahlung provides a continuous spectrum, which has a maximum at approximately one-third of the maximum photon energy. The number of X- rays emitted decreases rapidly at very low photon energies [1].

Moreover the size of the x-ray spot is important in the CT measurement. The smaller the spot, the sharpest is the image. [8]

The smallest achievable spot is less 1 μm diameter and it is called nanofocus spot. The CT systems manufacturers quote the focal spot size with a nominal value related to a specific energy setting. Indeed the focal spot depends upon the voltage (normally in kV) and the current (μA), and the higher the power the larger the focal spot will become [19]. Concerning the power of the industrial x-ray tube, the maximum used voltage is around 450 kV [8].

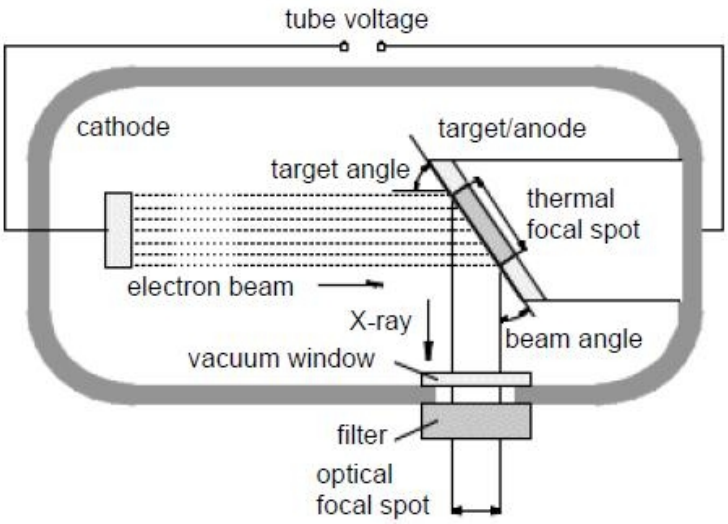

Fig. 3.2: Scheme of an x-ray tube [17]

3.1.2 The Detector

The detector can be defined as the component that records the radiation [17]. Its purpose is to convert the incident x-ray flux into an electrical signal that can be handled by conventional electronic processing technique [19]. After passing through the object, the X-rays are detected by the detector system. The ideal detector for X-ray imaging should detect every incident photon of the complete band of X-ray energies and its response should be linear over a large range of intensities. Furthermore, if the device is designed for digital readout, the time for readout, digitization, and data storage has to be short. In the early days of X-ray radiography, photographic films were used. However, with respect to computed tomography applications, a digital storage of information is favorable. Photographic films have the main disadvantage of a delayed readout and the fact that they have to be erased and reloaded into a cassette before they can be used again. Presently, charge-coupled device (CCD) cameras are most often applied in a microfocus computed tomography set-up. As these are most sensitive to visible light, and since they may get damaged by the radiation, a scintillator is employed to convert the X-rays into light photons. Because of the difference in size between the light emitting material and the CCD chip, a scaling- down medium, such as fibre optics or optical lenses, is used [1].

It is called also as “x-ray sensor” and it is available as [20]:

- Linear sensor, that is related to the fan beam configuration (see paragraph 3.1.3) and that would be perfect in terms of synchronized movement of the x-ray source and the detector and of section plane through the object that is always perpendicular to the rotary axis. On the other hand, each section plane needs to be captured individually in every rotary position;
- Area sensor, that captures several section planes of the object at once. On the other hand, the captured object section plane, except for the center one, are not perpendicular to the rotary axis and this leads to measurements errors. Of course, the smaller the cone angle, the better the results.

The last part of the detection system consists of a charge-coupled device or CCD camera, where photons incident on the surface of the device generate electron-hole pairs in the silicon substrate. The electrons are confined into square adjacent pixels by potential wells generated by a conductive gate structure located on top of the substrate. Each pixel has a set of three gates, which are used to shift the charge contained in each potential well to an on-chip output amplifier. [1]

3.1.3. Different CT systems configurations

Relating to the x-ray source, the CT systems can be divided in three groups [21]:

1. Fan beam scanning mode wherein each CT projection is built from a set of ray paths emanating from a point source but considered to be diverging in only one dimension, thereby forming a 'fan', see Fig. 3.3 (top);

2. Cone Beam: scanning mode wherein each CT projection is built from a set of ray paths emanating from a point source and diverging in two dimensions, thereby forming a cone, see Fig.3.3 (middle);

3. Parallel Beam scanning mode wherein each CT projection (2.12) is built from a set of parallel ray paths, see Fig. 3.3 (down).

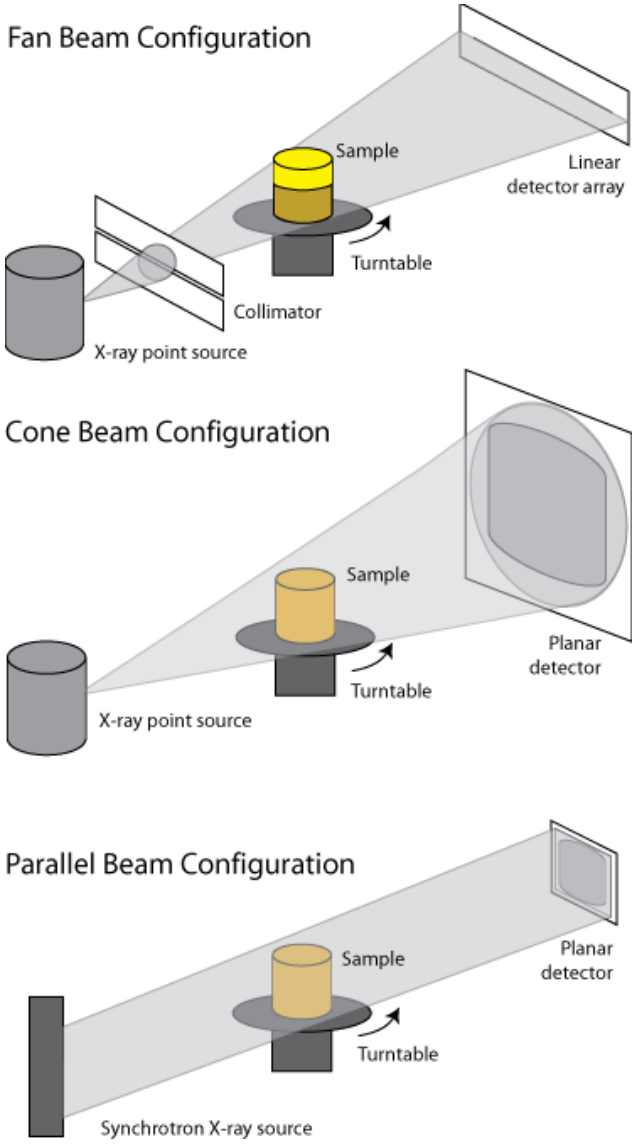

Fig. 3.3: Different CT Systems configuration [22]

The parallel beam is related to large synchrotron radiation facilities that are also used to generate x-rays for CT applications [23]. Synchrotron radiation offers unique x-ray beam properties, such as [8]:

- High intensity of x-ray energies;
- High brilliance energies due to the low angular dispersion of the beam;
- Quasi parallel beam;
- No image magnification, typical of cone beam systems;
- No beam hardening effects due to a monochromatic x-ray beams.

3.1.4 The Rotary Table and kinematic system

In medical CT scanner, the x-ray tubes and the detector rotate around the patient, while the object is translated horizontally through the space between tube and detector. The industrial CT scanners and in particular the ones for dimensional metrology measurements have fixed both x-ray tube and detector, whereas the object rotates in the beam path [8]. The properties of the rotary axis affect greatly the accuracy of measurement results [20]. In a cone beam configuration, the basic axes are the following:

1. A rotary table for step wise or continuous rotation of the workpiece

2. A horizontal translation axis for positioning the rotary table with the measuring object between the x-ray source and the detector. This axis is very important in the calculation of the magnification. When the magnification is high, the object is closer to the x-ray source and better image resolution is achieved, whereas blurred images are obtained (See Fig. 3.5). As shown in Fig. 3.4 the FOD is the distance between the source and the object, whereas the FDD is the distance between the x-ray source and the detector. The imaging magnification is obtained by the following formula [8]:

$$M = \frac{FDD}{FOD} \quad (2)$$

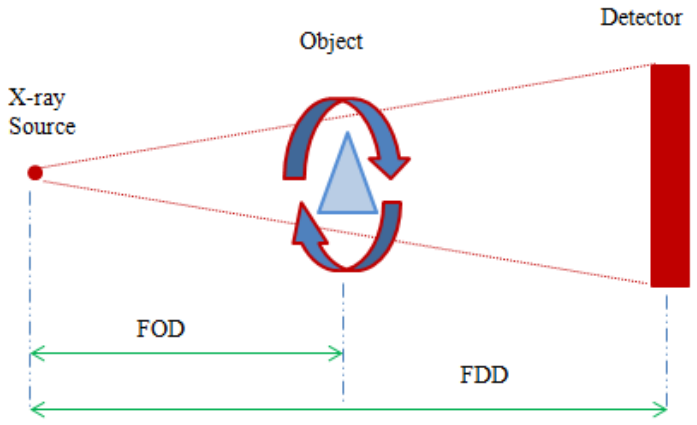

Fig. 3.4.: Distances between Source-Object-Detector [13]

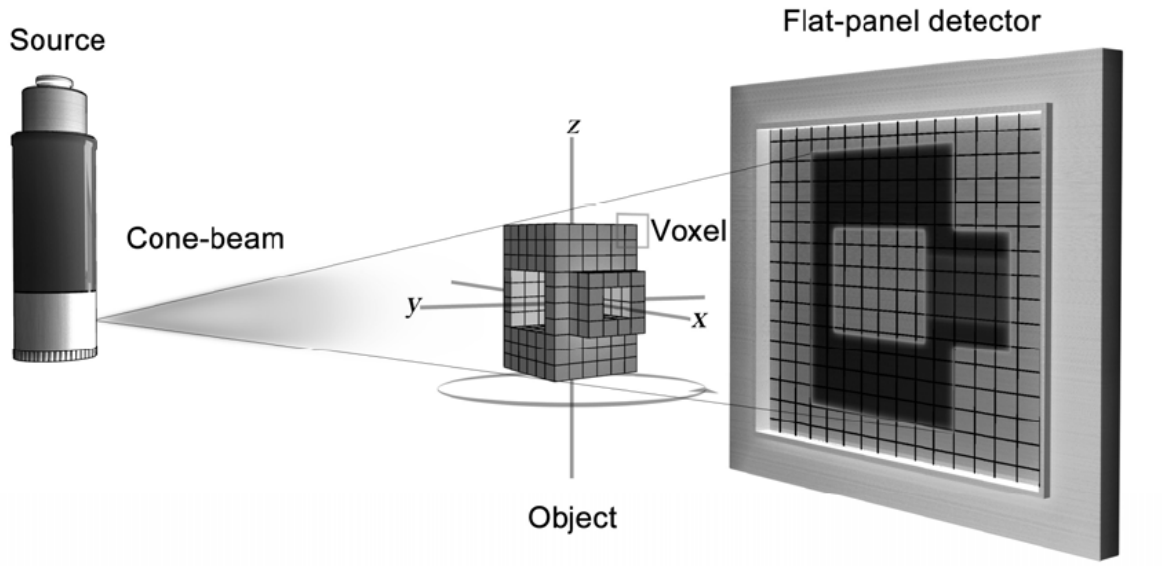

Fig 3.5.: Kinematic Axes in a cone beam CT system configuration[24]

3.1.5 The software

Apart from the CT hardware, software reveals to be vital in two levels of a CT measurement. First the reconstruction that is usually done by filtered back-projection that is based on the Linear Integral Transformation, mathematical model created by Radon in 1917. The Radon model expresses the absorption of x-rays when passing through an object with varying linear attenuation coefficient μ as following [8]:

$$I = I_0 \, e^{-\int \mu(x) dx} \qquad (4)$$

Which refers to the Beer-Lambert law that expresses the exponential attenuation of electromagnetic radiation with initial density I_0 travelling a distance x in an absorbing medium μ [8]:

$$I(x) = I_0 \cdot e^{-\mu x} \qquad (5)$$

The input for the reconstruction process are the "gray value profiles" that represent the intensity trend along the pixels located on one line of the detector [8].The data resulting from reconstruction consists of volumetric elements (voxels) where each of them represents a specific gray value which is proportional to the acquired radiation intensity. In few words the voxels are the 3D equivalent of the 2D pixels [25]. Finally it is important to highlight that when using a cone beam configuration, the reconstruction should take into account that the

voxels do not stay in the same horizontal projection plane while the part rotates. In this case the reconstruction is based on the Feldkamp algorithm [26] that is an approximate formula for cone beam reconstruction [3].
Second important software step is the one for dimensional analysis that are typical only for dimensional metrology measurements since these software allow to extract geometrical features and to calculate geometrical data (see also 3.4 paragraph of chapter 1) [8].

3.2 Dimensional Metrology Developments

According to VIM (International Vocabulary of Metrology), Metrology (from Ancient Greek μέτρον *métron* (measure) and logos (study of)) is the science of measurement [27].

It was 20th May 1875 when the meter was created as the international standard for the length unit by the international convention. After this, the typical dimensional measurement devices used in industry for mass production (around 1900) where manual devices, such as calipers and micrometers,e used to determine one and two dimensional features (diameters, distances etc.). Through the developments of optical and electronic components (RC-filters, inductive displacement sensors etc.), the instruments improved their accuracy and resolution [25]. With the advent of personal computer, it became possible to run measurements completely automatic and the first CMMs were introduced in response to the need for faster and more flexible measuring tools as machining became more complex through the use of numerically controlled machine tools [29]. In the 1950s conventional Coordinate Measuring Machines (CMMs) were developed equipped with tactile probes that mechanically contact the workpiece surface [30]. Today tactile coordinate metrology is well established and accepted by international standards, so all new developments are compared and referenced to it [25]. In the following years the developments achieved were focused on extending the degree of information about an object and on reducing costs and time of measuring. For these reason optical 3D measurements (i.e. fringe projection system or with light interferometer) complemented or replaced the tactile methods, since optical systems showed the following advantages [31]:

- Speed method: it is possible to acquire more data in less time;
- No contact technique: suitable for delicate/plastic objects;
- Good for in-line measurements.

Comparing tactile and optical techniques in production metrology, it is possible to find complementary properties. Soft coatings that should not be touched and thin membranes or cantilevers pose problems for tactile techniques but not for the optical ones. Optical techniques have limitations measuring steep surface slopes, specularly reflecting or transparent or black materials. For ceramics and plastics, light is not reflected from surface but remitted from a volume below the surface, thus causing erroneous optical measures. All of this is not a problem for touch probes (see Fig. 3.6). In the recent years, considering the advantages and disadvantages of different sensor types, the trend for CMM manufacturers goes towards multi-sensor machines, in which mechanical and different optical sensors are combined to measure in a common coordinate system [29].

Around 2000 Computed Tomography started to be used more and more for dimensional metrology applications, in particular after the developing of X-Ray tubes with focal spots of few micrometers. [32]

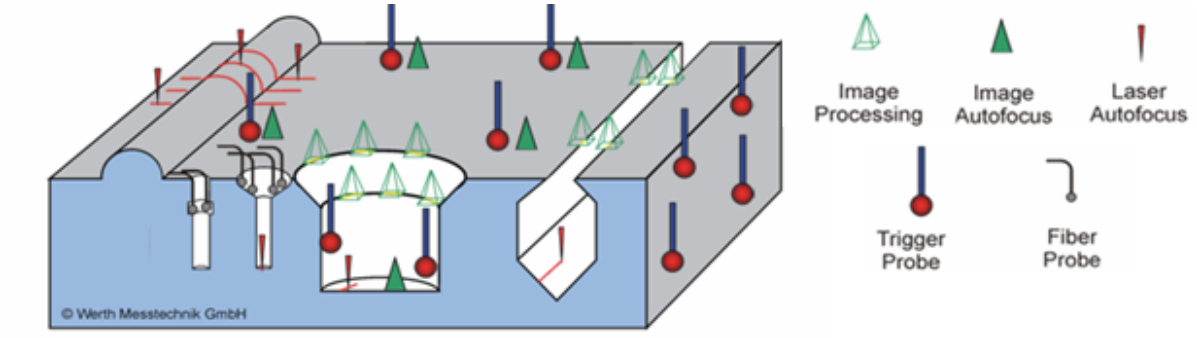

Fig.3.6: Application of tactile and optical sensors by a multisensor CMM [33]

In conclusion, dimensional metrology has seen steady developments from being a tactile coordinate measurement technique to machine vision-based non-contact optical techniques with the advancement in computers and digital technology [31].

However, they are suitable only for specimens where measurement features are accessible. A touch probe based coordinate measurement method relies on acquiring a few sample points across a measurement surface and then establishing an ideal geometrical feature based on the measured points. It is also possible to obtain the dimensional information of multiple features in a single setting of the test object with the development of coordinate measuring machines (CMMs) [34].

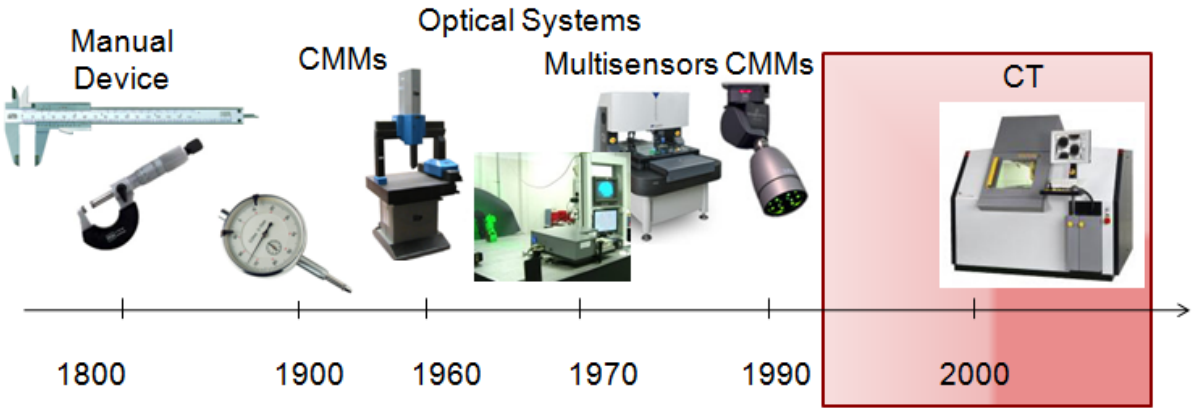

Fig. 3.7: Development of measuring devices

3.3 Computed Tomography for Dimensional Metrology Purpose

Over the last years, computed tomography with conventional x-ray sources has evolved from an imaging method in medicine to a well established technology for industrial applications and in particular for dimensional metrology measurements [35].

CT is not only a simple investigation method but also a measuring principle capable of providing accurate geometrical information [36]. CT acts as coordinate measuring machine and shows both many advantages and many disadvantages [37].

The main advantages can be summarized as following [37]:

- It is a non-destructive technique;
- There is the possibility to determine outer and inner geometries;
- It is possible to achieve a very high point density in a relative short time;
- The user can control simultaneously material and geometrical characteristics.

On the other hand, several limitations are present, e.g. [8]:

- Complex and numerous influence quantities occur;
- Complete standards are not yet available;
- Measurements are typically not traceable since the uncertainty is difficult to evaluate.

Due to the previous CT disadvantages, CT systems are still not completely recognized as reference measuring instruments with well known metrological performances (see paragraph 3.4) [38].

CT offers new possibilities for coordinate measurements as it is possible to acquire a volumetric model of the entire workpiece with a single measurement and a CAD comparison between nominal and actual features is possible [25].

3.4 Traceability and Uncertainty

Due to the advantages of CT technique, CT scanners may be used as Coordinate Measuring Systems performing dimensional and geometrical measurements [39]. Indeed in the recent years, specific CT systems for metrological applications have been developed [40], also integrated on multisensors CMMs [41]. As already said in paragraph 3.3, some drawbacks occur. In particular, at present, CT measuring systems are affected by complex and numerous influence factors that make the uncertainty difficult to evaluate and that limit the traceability of CT measurements [39].

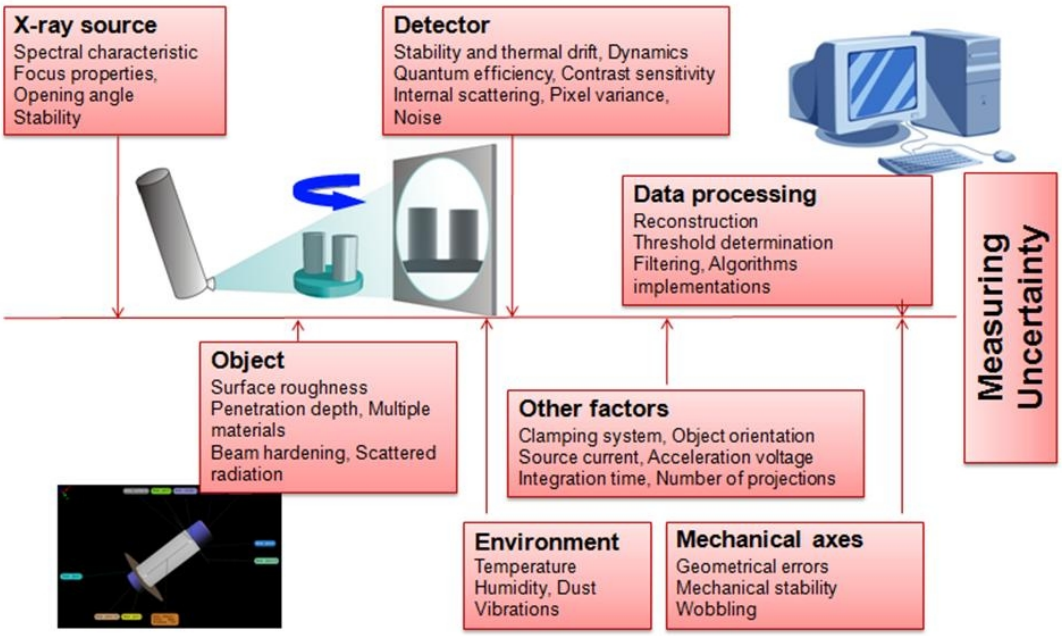

Fig. 3.9: Adapted Ishikawa diagram

This is particularly relevant, since an important condition for high quality industrial production is the availability of reliable measurements [42]. Moreover, for dimensional purpose, the traceability of the measurements is an important subject, since all results have to relate to the international system of units, the length unit meter [25]. Due to the complex influence factors, nowadays not all the components that influence a CT

measurement can be easily quantified. At the state of the art, analytic uncertainty budgeting are proposed, but they revealed to be not valid for this purpose [39].

The already traditional proposed methods are [43]:

- GUM (ISO/IEC Guide 98-3:2008/ JCGM 100:2008), requires model;
- Simulation: Suppl. 1 to GUM (JCGM 101:2008), VDI/VDE 2617-7;
- empirical assessment: ISO/TS 14253-2 ;
- ISO 15530-3 use of calibrated work pieces.

The last one seems to be a good solution is the uncertainty evaluation through the substitution method that has been adapted from ISO/TS 15530-3 [44].

The substitution method is under discussion in terms of definition of the main formula. At the present the ISO formula for the uncertainty budget is proposed as following:

$$U = k\sqrt{u_{cal}^2 + u_p^2 + u_w^2} + |b| \qquad (6)$$

Where U is the expanded uncertainty, k is a correcting factor (=2), u_{cal} , u_p , u_w are the combined uncertainties (related to the calibration, the procedure and the workpiece) and b represents the systematic errors.

As shown in the formula (6) GUM [44] describes the way in which the systematic errors have to be taken into account. The GUM assumes that the result of a measurement has been corrected for all recognized significant systematic effects.

If, contrary to the recommendations of the GUM, the uncorrected estimate y'= y + b is given, the estimate of the not corrected systematic error b has to be taken into account, when calculating the measurement uncertainty associated with y'.

The National metrology institute of Germany (PTB) proposed a new reformulation of the uncertainty definition as following [43] [45]:

This uncertainty is calculated as following (7):

$$U = k\sqrt{u_{cal}^2 + u_p^2 + u_w^2 + b^2} \qquad (7)$$

In the formula (7) the systematic errors b is placed under the square root.

This "diatribe" is not yet completely solved there is no universally accepted agreement.

Since the substitution method is based on the use of calibrated workpieces, traceability of measurements can be established by the comparison between calibrated results obtained by traditional CMM measurements and CT ones (See Fig. 3.10)[39]. This method is considered

the most suitable one, since due to the extensive interaction between the x-ray and the workpiece during the CT measurements, the influence of the workpiece itself is particularly important for estimating the measurement uncertainty [20].

Currently a rewriting of the ISO 15530-3 is in progress as the 2004 does not treat systematic errors in a GUM conformant way [46].

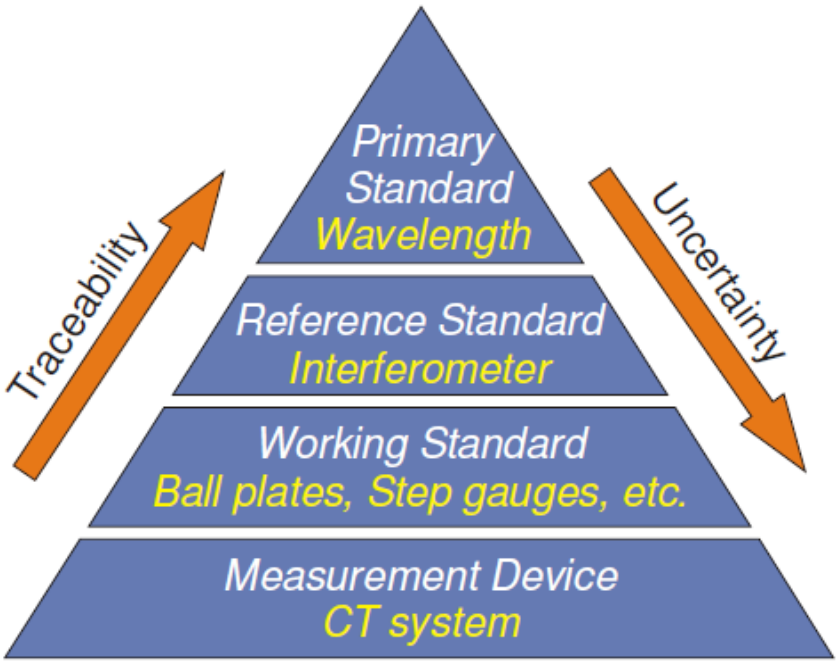

Fig .3.10: Traceability [43]

Concerning the complex and numerous influence factors, it is relevant to report that since a CT dimensional measurement is made of several steps, it contributes to the measurement uncertainty [8], as summarized in Fig. 3.11.

This is called as CT process chain for dimensional metrology starts with the proper CT measurement of the investigated object that generates the surface data, raw 2D x-ray acquired projection images over 360 or 180 degrees.

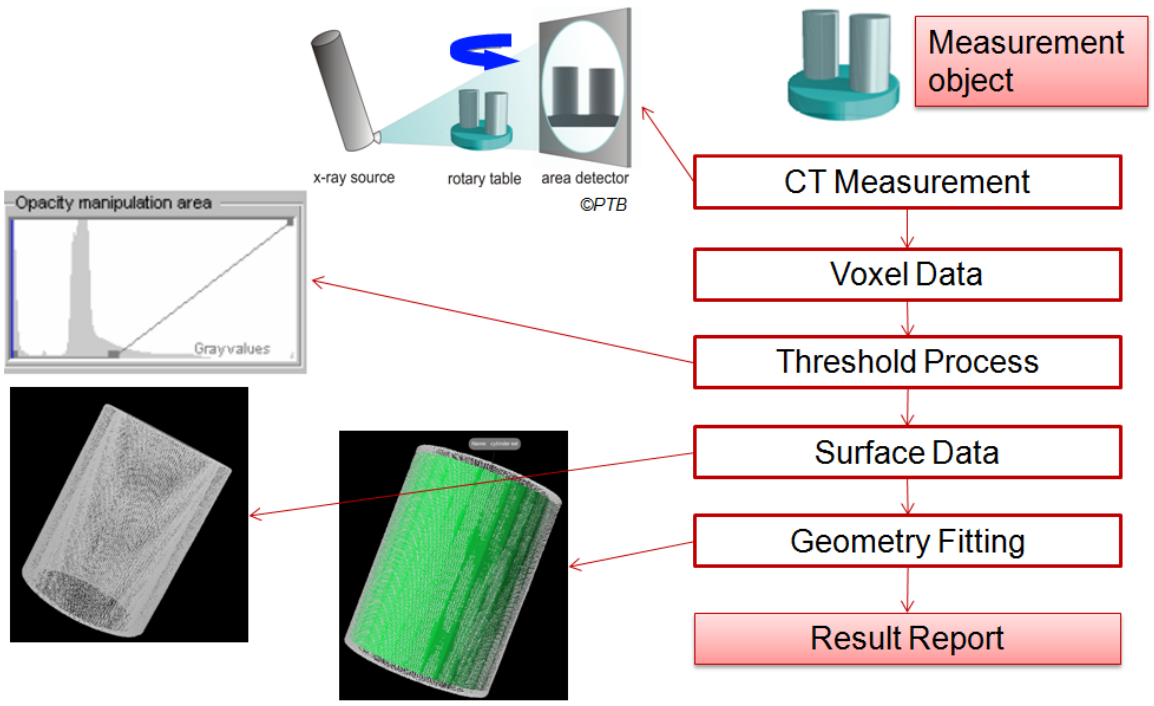

Fig 3.11: CT dimensional measurement process

Through a back-projection reconstruction a volumetric model is obtained in terms of voxel data, where the voxel (volumetric pixel) represents the attenuation coefficient for x-rays at the appropriate location in the volume. If the scanned object is made by only one material, the volume ideally has only two peak gray scale distribution (air and material) see Fig. 3.12. Today many different methods for this volumetric models estimation exist. The simplest is the calculation of the ISO50% threshold that is defined via the histogram of the all grey values represented in the volumetric model. The peak of 100% is the material one and the 0% is the background noise. The 50% peak is the one used for the surfaces extraction [25]. This method, also called as global threshold determination, seems to be very easy and fast but it reveals to be suitable only with very uniform materials. Another method is under investigation and it seems to achieve better accuracy in results. It is called local adaptive thresholds and instead of setting a fixed, single value for the whole data, the voxels surrounding and the current voxel are evaluated and for each voxel the threshold is chosen dynamically via the maximum of the gray value gradient [25].

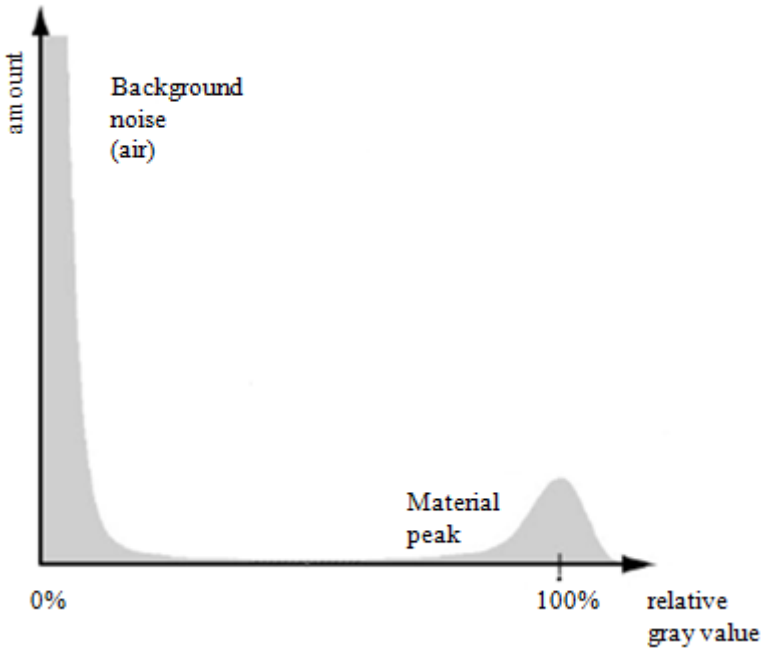

Fig. 3.12: Two peaks gray values

Finally after reconstruction, the surface data is extracted from the volumetric data set in order to evaluate the CT measurements data with standard tools known and adopted from tactile coordinate metrology. The extracted surface can be stored as point cloud or a polygon mesh (STL) and then it is analyzed with industrial software tools. So a complete 3D object is then loaded into 3D software like for example Polyworks Inspector or GOM Inspection [35][25]. These software packages permit to convert points and coordinates generated by the previous steps into features or fitted ones that are already known from the conventional CMMS software, such as cylinders, planes etc. After the previous step, through software the object is investigated and measured following the procedures adopted from the conventional metrology. This last step is still remaining one of the critical steps in achieving accurate and traceable CT measurements, since the CT procedures are still not well defined and standardized [8].

4. Conclusion

Since the development of x-ray CT and its success in medical applications, it became not only a powerful tool in medical and material sciences and NDT application but it was adopted in dimensional metrology in the recent years. CT is a very promising technique and it is under investigation by many researcher centers and universities. In particular the way toward a traceable Computed Tomography for Dimensional Metrology could be the one concerning the developing and defining reference standards for specification testing and for evaluating the uncertainty of measurement. Moreover the influence factors should be deeply investigated and understood in order to correct them in the right way [43].

These solutions can be summarized as following:

- Develop of procedures and related objects in order to correct the measurement errors and to achieve the traceability;
- Adapt methods from coordinate metrology to CT.

The previous sentences will make possible the metrological performance verification of CT systems and the enhancement of accuracy, as described in Chapters 2 and 3.

Chapter 2

Metrological Performance Verification of CT Systems:

State of the art and

Newly developed procedures

In Chapter 2 the state-of-the-art metrological performance verification procedures for CT dimensional measuring systems are presented and discussed. Moreover, new approaches and reference standards for CT systems' performance verification are described.

1. Introduction

Computed Tomography is rather new in the dimensional metrology field and many research projects are currently focused on establishing this technology in manufacturing metrology by determination of the task-specific measurement uncertainty and improving the quality of CT measurement data. The different steps to measure geometrical measurands, shown in Fig.1.1, contributes to the measurement uncertainty of CT. Up to now there are no universally accepted guidelines in order to ensure the traceability of CT measurements respectively to be able to indicate a task-specific measurement uncertainty [47]. Moreover, as already anticipated in Chapter 1, the lack of standardization implies difficulties in testing and comparison of actual metrological performances.

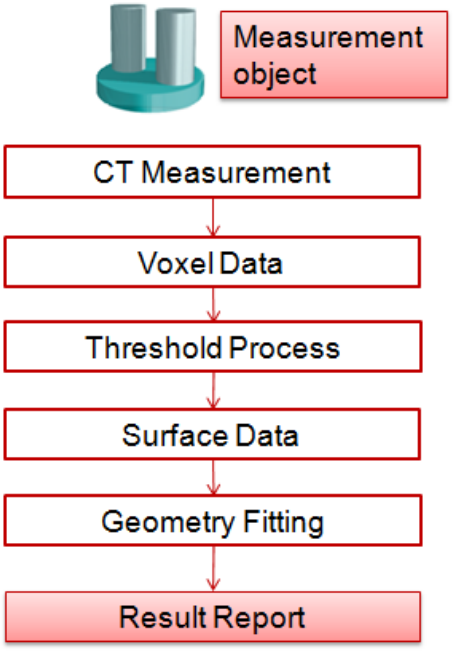

Fig. 1.1: Dimensional measurement with CT procedure scheme

In order to make CT fully recognized as a dimensional measuring technology, several research institutes are working in developing procedures for metrological performance

verification and they are presented in the first part of Chapter 2. The second part, from paragraph 6, will deal with new approaches and reference standards for CT systems' metrological performance verification.

2. Procedures from the American Society for Testing and Materials

ASTM International, formerly known as the American Society for Testing and Materials (ASTM), is a globally recognized leader in the development and delivery of international voluntary consensus standards.

Fig. 2.1: ASTM International Logo

ASTM was formed in 1898 by chemists and engineers from the Pennsylvania Railroad. At the time of its establishment, the organization was known as the American Section of the International Association for Testing and Materials. Charles B. Dudley, Ph.D., a chemist with the Pennsylvania Railroad, was the driving force behind the formation of the Society. In 2001, the Society became known as ASTM International. TM members deliver the test methods, specifications, guides, and practices that support industries and governments worldwide [48].

ASTM International published several standard guides related to Computed Tomography when developing standards in the field of Nondestructive Testing.

In details, the following standards are dedicated to Computed Tomography:

- E 1441-00: Standard Guide for Computed Tomography (CT) Imaging [15];
- E 1570 -00: Standard Practice for Computed Tomographic (CT) Examination [49];
- E 1672 -01: Standard Guide for Computed Tomography (CT) System Selection [50];
- E 1695 -01: Standard Test Method for Measurement of Computed Tomography (CT) System Performance [51];
- E 1935 -03: Standard Test Method for Calibrating and Measuring CT Density [52].

In particular the standard E 1570-00 describes procedures for performing Computed Tomography measurements. This national standard may be used for review by system operators, or to prescribe operating procedures for new or routine test objects.

In order to examine the performance of a CT system, all the influencing parameters must be determined and monitored regularly to ensure consistent results. An accurate CT system performance verification can be made utilizing a test object under the actual operating conditions. The test object, also known as test phantom, must be reliably detected or measured. The test phantom should be designed to provide a reliable indication of the CT system's capabilities. For this reason the phantom are categorized in 5 different types in order to analyze different features, as shown in Table 2.1. In particular, in order to register the geometrical accuracy the proposed phantoms are hollow cylinders or matrix of calibrated holes.

Table 2.1: The test phantom categories [49]

Phantom Type	Detectable Features
Resolution	Holes, Squares, Line pairs, Edges
Contrast	Signal-to-noise ration in a uniform material, Small density variation, Various solids
Slice Thickness	Pyramids, Cones, Columnar row of beads, Slanted sheet, Spiral slits
Geometric Accuracy	Hollow cylinders, Matrix of calibrated holes, Simulated Object
Artifacts	Uniform density test object

In practical terms, the performance measurement methods are a matter of agreement between the purchaser and supplier of the CT system.

The performance verification tests should be standardized and repeated at specified intervals in order to minimize any possibility of time dependent performance variations.

The scan parameters should be registered in order to make measurements with examination objects with the same conditions.

In addition, standard E 1695-01 provides further methods for the evaluation of CT systems performance. It is important to report two specific definitions that are fundamental in order to understand the standard. The word "phantom" is related to an item being used to quantify CT system performance, whereas "examination object" is a specimen being subjected to CT measurements. The proposed test is based on the examination of the CT image of a uniform disk of material. This test will be further discussed in Chapter 5 in relation to the spatial resolution analysis. However some information is definitely interesting for performance verification tests.

The national standard indentified two main factors that affect the quality of a CT image as the geometrical unsharpness and the random noise. The first limits the spatial resolution, i.e. the ability to image fine structural detail in an object, whereas the second one limits the contrast sensitivity, i.e. the ability to detect the presence or absence of feature in an object. As already announced in standard E 1570-00, the disk phantom is a cylinder of uniform material. The diameter if the disk shall be such that the reconstructed image of the disk occupies a significant fraction of the image matrix, as shown in Table 2.2.

Table 2.2: Suggested measurement parameters [51]

Image Matrix Size (pixels)	Disk Image Diameter (pixels)	Number of Fit points
256	235	11
512	470	21
1024	940	41

In Fig. 2.2 the Disk Phantom is schematically represented. The material shall be such that the phantom approximates the attenuation range of the examination object. The thickness of the disk shall be greater than the slice thickness used to inspect the examination object. Finally the surface texture roughness of the curved surface shall not compromise the measurement of geometrical unsharpness. The ratios between slice and disk thickness are only through Fig. 2.2 described.

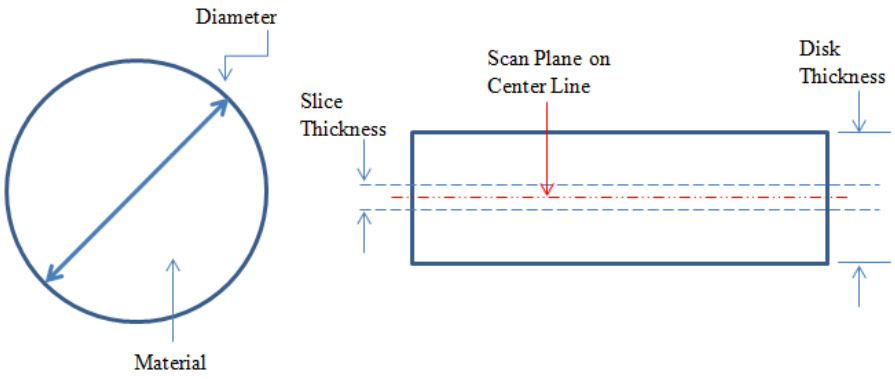

Fig. 2.2: Disk Phantom [51]

Anyhow, the design of the disk phantom is a matter of agreement between the purchaser and the supplier. Concerning the measurement procedures, the phantom is supposed to be mounted on the CT system with the orientation of the axis of the revolution of the disk normal to the scan plane. No information is provided for any software elaboration or reconstruction procedures. The interpretation of results will be discussed in Chapter 5 since they are focused on resolution.

3. Procedures from British Standards International

BSI, British Standards International is a leading provider of standardization to the public and private sector. Covering a wide range of industry sectors as well as governments, consumers, employees and society overall, to make sure that British, European and international standards are useful, relevant and authoritative. [53]

Fig. 3.1: BSI International Logo

Since its foundation in 1901 as the Engineering Standards Committee, BSI Group has grown into a leading global business services organization providing standards-based solutions in more than 150 countries. It is an independent, private, non-profit distributing company which helps organizations in improving their quality and performance, in reducing their risk, etc. In the field of Nondestructive testing, the national BSI group produced a standard related to Computed Tomography that is published as BS EN 16016-1:2011. This is a European

Standard and it exists in three official versions (English, French and German), in Chapter 2 the English one has been consulted.

The document EN 16016 has been prepared by Technical Committee CEN/TC 138 "Non-destructive testing" and it consists of the following parts [21]:

- BS EN 16016-1:2011, Non destructive testing - Radiation methods - Computed tomography - Part 1: Terminology [21];
- BS EN 16016-2:2011, Non destructive testing - Radiation methods - Computed tomography - Part 2: Principle, equipment and samples [19];
- BS EN 16016-3:2011, Non destructive testing - Radiation methods - Computed tomography - Part 3: Operation and interpretation [54];
- BS EN 16016-4:2011, Non destructive testing - Radiation methods - Computed tomography - Part 4: Qualification [55].

BS EN 16016-3 describes the performance verification in terms of dimensional testing. Since the measurement of geometric features using is an indirect procedure, i.e. the dimensional measurement takes place in or is derived from CT images, it is important to monitor two variables in order to achieve accurate measurements, as following [54]:

1. The voxel size;
2. The threshold value process;
3. Adjustment of geometrically primitive bodies;
4. Generation of geometric data.

3.1 Determination of voxel size

The accurate image scale or voxel size must be determined through the measurement of a suitable calibration standard or using reference geometry at the object. The procedure consists in the comparison of the magnification specified by the CT system M (related to the voxel) with the magnification M* (related to the calculated voxel) calculated by using the reference object. The reference object could be a kind of dumbbell, as shown in Fig. 3.2, where the measurement of the centre distances (pre calibrated) of two spheres may give the correct actual voxel size [54].

Fig. 3.2: Reference object (dumbbell)

3.2 Threshold value

The threshold value process is fundamental in the definition of the boundary surfaces and it strongly depends on the material of the measuring object and the x-ray settings.

One method is called "ISO 50" and it is suitable for objects made by homogeneous materials, since it is a global method and only one threshold value (grey value) is used for the extraction of the whole surface.

The threshold can, if necessary, be determined locally in order to give different grey values to the surfaces when different materials are present. This method, since it is more complicated, is more time consuming, but on the other hand, it is more tolerant towards contrast variations and artefact influences [54].

The local method is not described in details, only the principles are explained.

3.3 Adjustment of geometrically primitive bodies

In CT dimensional measurements it is possible to fit geometric reference elements (e.g. planes, cylinders, spheres etc.) to the acquired data using dedicated software and procedures. In this way, several thousand measured points are fitted and the results are more statistically corrected and the influence of the user is reduced.

3.4 Generation of geometric data

From the voxels and the calibrated grey value threshold triangular models or point clouds can be extracted. In particular some standard extracted formats can be stl- or ascii format.

The geometric quality of the generated extracted model depends entirely on the number an d the position of the vertices and on how good the triangle or the point cloud reproduce the actual course of the material surface. [54]

3.5 Performance Testing

It is recommended to document the process of performance verification and to respect the specifications that are shared between the purchaser and the supplier of a CT system. It is not practical to evaluate the "absolute performance" of a CT system and such an evaluation shall always be performed within the context of the parts tested. Moreover a list of parameters is presented divided in acquisition (e.g. voltage, focal spot size, detector type, number of projection, operator experience etc.) and reconstruction (e.g. algorithm, software, filters, operator experience, etc.) parameters.

3.6 Qualification of dimensional testing

The standard BS EN 16016-4 goes more in details in relation to the qualification of the CT dimensional measurements. In particular it is explained that the test object influences on the accuracy of the measurement and in order to estimate the degree of accuracy it is important to monitor the following parameters:

- Spatial resolution that will be discussed in Chapter 5;
- X-ray penetration of the test object (material, maximal wall thickness, contrast resolution);
- 3D component data (i.e. voxel size, extraction method, processing steps).

The proposed method for estimating the degree of accuracy of a CT system is supposed to provide the accuracy for the whole measurement chain [55], see Fig. 1.1.

A reference part is measured and by comparing the measurement data, statements can be made on the degree of accuracy. If it is not possible reference bodies (e.g. spheres or dumbbells) can be used in order to investigate on the accuracy of the system.

The CT system is declared as a high quality system, when it provides stable and reproducible results.

4. Procedures from VDI Guidelines (and ISO draft standards)

VDI is the Association of German Engineers (Verein Deutscher Ingenieure) that plays a relevant role in the international standardization. The first VDI guideline was already published in 1884. The document on examination of steam boilers and engineses was issued for the first time as part of the scientific journal of the Associatin of German Engineers on

October 1884 and has been the launch of VDI Guidelines as integral part of the German technical-economic infrastructure.

Fig. 4.1: VDI Logo

Today, approximately 190 guidelines based on the latest technical developments are produced by the VDI's technical divisions per year. That way the VDI has systematically built up set of technical regulations, which today contains more than 1.800 valid VDI Guidelines extensively covering the broad field of technology. Today's topics range from securing loads on road vehicles to testing of optical fibers up to biomimetics and monitoring of the consequences of genetically modified organisms [56].

VDI elaborated national guidelines about Computed Tomography for dimensional metrology purpose starting from ISO 10360-2 and -8 related to acceptance and reverification tests respectively for CMMs and CMMs with optical sensors [57] [58]. VDI tried to create a standard concerning acceptance and reverification tests suitable for Computed Tomography systems. Concerning CT they published are summarized in Table 4.1:

Table 4.1: VDI/VDE Guidelines related to Computed Tomography [56]

Name	Title	Date
VDI/VDE 2617-13; VDI/VDE 2630-1.3	VDI/VDE 2617-13: Accuracy of CMMs: Characteristics and their testing. Guideline for the application of DIN EN ISO 10360 for CMMs with CT sensors. VDI/VDE 2630-1.3: Computed Tomography in dimensional measurements.	2011-12
VDI/VDE 2630-1.1	Computed Tomography in dimensional measurement: Basics and definitions	2009-07
VDI/VDE 2630-1.2	Computed Tomography in dimensional measurement: Influencing variables on measurement results and recommendations for computed tomography dimensional measurements	2010-11
VDI/VDE 2630-1.4	Computed Tomography in dimensional metrology: Measurement procedure and comparability	2010-06

4.1 ISO Working Draft 10360-11 (derived from VDI/VDE 2617-13)

ISO is the International Organization for Standardization, the world's largest developer and publisher of International Standards.

ISO is a network of the national standards institutes of 162 countries, one member per country, with a Central Secretariat in Geneva, Switzerland, that coordinates the system.

Fig. 4.2: ISO Logo

ISO is a non-governmental organization that forms a bridge between the public and private sectors. On the one hand, many of its member institutes are part of the governmental structure of their countries, or are mandated by their government. On the other hand, other members have their roots uniquely in the private sector, having been set up by national partnerships of industry associations [59].

As already said the guidelines displayed in Table 4.1 are only national, but they have been fundamental in the elaboration of the first draft international standard on dimensional CT testing. In particular the VDI/VDE 2617-13 [60] has been an important source of inspiration for the working draft ISO 10360-11 on Computed Tomography [61]. Only recently the standard has been approved as working draft, and before it was called New Working Item Proposal on CT. In particular this WD specifies the acceptance test for verifying the performance of coordinate measuring devices with sensors using the principle of X-ray computed tomography [61]. The proposed method looks very similar to the ISO 10360-2 and -8, and this is intentionally decided since the aim of this WD is to achieve comparability with the characteristics of coordinate measuring devices with tactile and with optical sensors [61].

The length measurement errors and probing errors when using CT sensors in this WD proposed together with the investigation of influence of material and geometry of the measuring object.

An acceptance test is used to determine if the coordinate measuring device with CT sensors maintains the limits for the characteristics specified by the manufacturer, in terms of Maximum Permissible Error (MPE) [61] [57].

4.1.1 Probing Error

According to ISO 10360, the probing error is well calculated using spheres as test specimens and it is divided in two types of probing error as following:

1. Probing error for form (PF), defined as the span of the radial deviations of measurement points from the calculated fitted sphere, as following

$$PF = R_{max} - R_{min} \quad (1)$$

- Probing error of size (PS), defined as the difference between the spheres' measured diameter D_a and the calibrated diameter D_r, as following:

$$PS = (D_a - D_r) \quad (2)$$

In Fig. 4.3 the definition of Probing Error is visually explained.

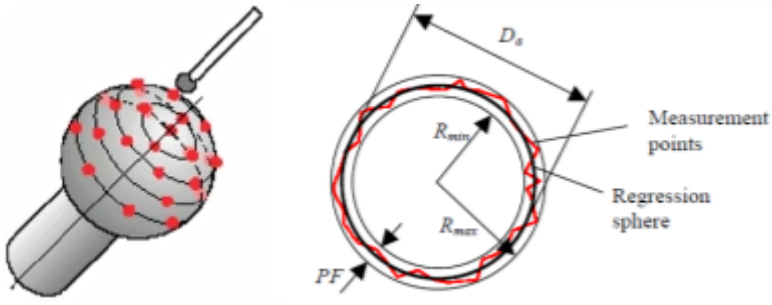

Fig. 4.3: Definition of metrological characteristic values: (left) Sphere sketched with tactile measurement points on it. In the case of CT, not only 25 points should be used but much more; (right) Illustration of characteristic value probing error form PF. The calibrated diameter is not shown in this figure [35].

4.1.2 Length measurement error

Accordingly to ISO 10360, this error characterizes the behavior of the entire system within the total measurement volume. This error results from the superposition of various individual errors e.g. systematic scaling errors as well as random errors. For determination of E material standards such as ball bars having two or more spheres can be used. The distances between the central points of all spheres on the bar have to be calibrated, similar to the suggested dumbbell in BS EN 16016-3 [54]. The value E is determined as deviation of the measured distance (L_a) between two spheres from the calibrated distance (L_r) [35] [61]:

$$E = L_a - L_r \quad (3)$$

The sphere fitting is performed using linear least square method. Using ball bars or other similar artifacts, probing errors should also be considered, since systematic errors in the surface position are automatically compensated in the sphere fitting procedure and have a little influence on the center position [35] [61].

4.1.3 Material and Geometry dependent effects

In a CT measurement the workpiece plays an important role, in particular its material and geometry influence the measurements and contribute to the errors. Indeed ISO WD 10360-11 deals with appropriate tests for the analysis of material and geometry effects.

Two methods are proposed:

1. Measuring a calibrated workpiece with the CMM and comparing the results with reference values assessed with approved methods.

2. Measuring a suitable test specimen with the CMM and comparing the results with reference values assessed with approved methods. A dedicated test specimen, called stepped cylinder is in this standard briefly described, as shown in Fig. 4.4.

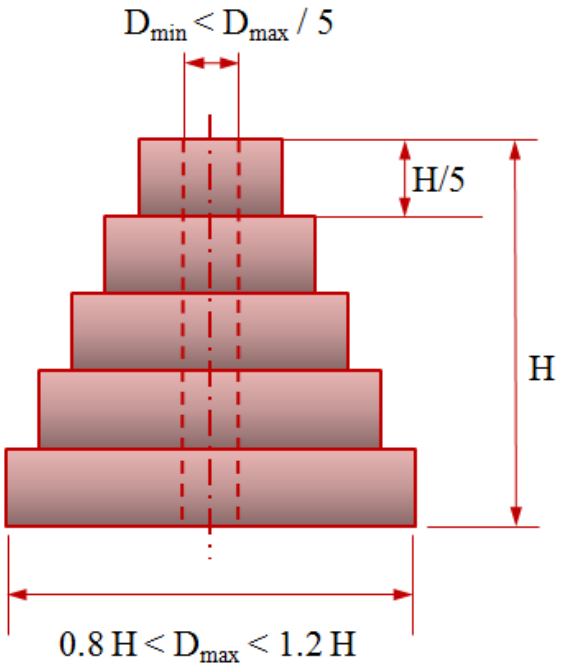

Fig.4.4: Test specimen for determining geometry- dependent errors.

The material of the test specimen should be decided as the same or similar material of the measuring workpiece. Three characteristics are required to be evaluated, following the least squares (Gaussian) fitting:

1. GF that is calculated as the range of the radial errors of the fitted circle;
2. GS that states the error of a measured internal or external diameter D_a and the calibrated D_r;
3. GG that specifies the straightness of the axis of the drilled hole.

The stepped cylinder is recommended to be measured at least with different inclinations at the same magnification.

Finally, the structural resolution (see Table 4.2) will be discussed further, in Chapter 5.

Table 4.2: Summary of ISO WD 10360-11 (under discussion)*

Characteristic	**Length error**	**Probing error**	**Material- and geometry effects**	**Structural Resolution**
Name	E	PF, PS	GF, GS, GG	D_g
Formula	$E= L_a- L_r$	$PF=R_{max}-R_{min}$ $PS= (D_a-D_r)$	$GF= R_{max}-R_{min}$ $GS= (D_a-D_r)$ ~~GG~~	---
Test specimen	Length standard	Reference Spheres	Step Cylinder	Small Spheres *

5. Other reference standards available at state of the art

As already explained, national and international institutes are trying to achieve well accepted procedures for the metrological performance verification of CT systems. In addition many researchers and many metrological institutes are providing their investigated procedures and related objects also in order to contribute to the developments of international guidelines and standards. In this subchapter some proposed procedures and calibrated objects are presented, whereas sub chapters 6.1, 6.2 and 6.3 will show the procedures for metrological performance and related objects provided by the Laboratory of Industrial and Geometrical Metrology of the University of Padova as part of this PhD Thesis.

Different test or reference objects have been proposed for CT CMMs. These metrological standards often aim at different purpose and have different advantages and limitations [8].

The proposed items at the state of the art can be subdivided in 3 categories:

1. Items from conventional and optical CMMs tradition;
2. Items from optical CMMs experience;
3. New items pretty dedicated for computed tomography verification.

As items derived from CMMs tradition, there are reference spheres, like ball bars or assemblies of ruby or cercamic spheres as proposed by Trapet and University of Padova (see Fig. 5.1-left) and Zeiss (see Fig. 5.1-right), QFM and PTB (see Fig. 5.2).

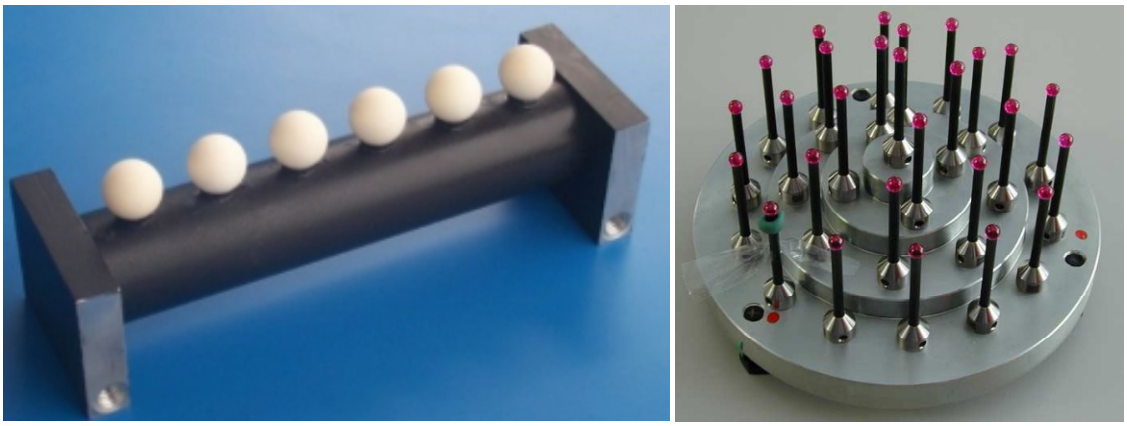

Fig. 5.1: (left) Optical Ball Beam with mat spheres [62], (right) 27 ruby spheres [63]

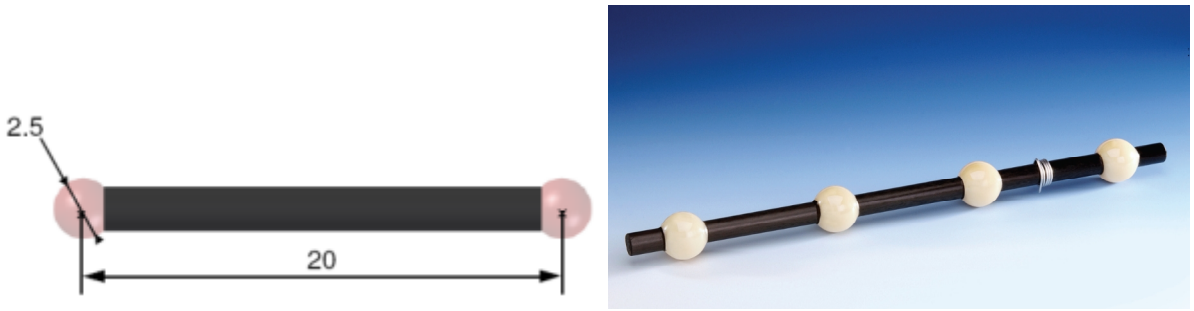

Fig.5.2: (left) QFM ball bar, values in mm [64], (right) PTB ball bar with ceramic spheres [65]

Schulze et al. [66] investigated on the influence on dimensional measurements of multimaterials object measured with micro-CT. They proposed a micro tetrahedron made up with 3 ruby spheres and one silicon sphere of 0,5 mm diameters as shown in Fig. 5.3

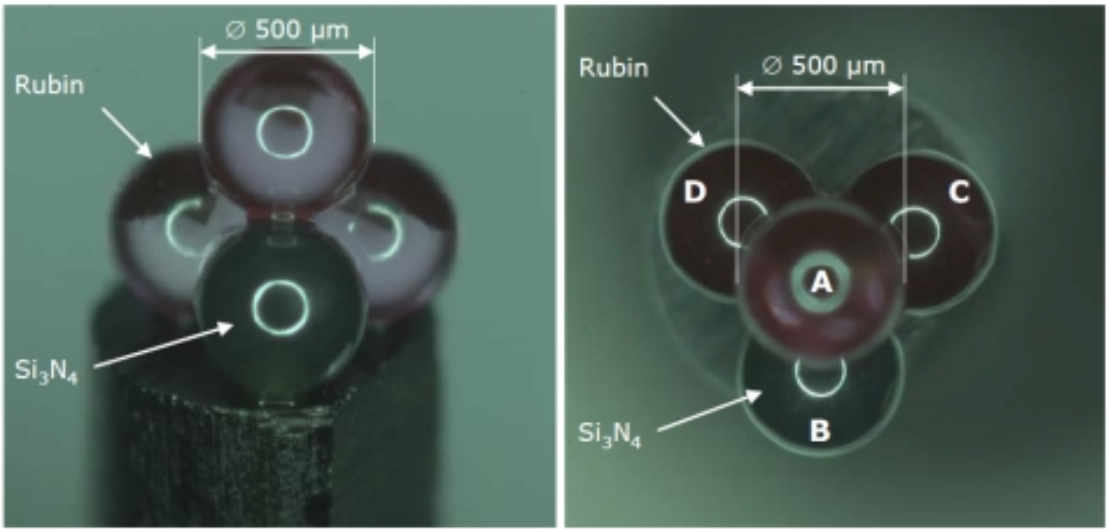

Fig. 5.3: Micro tetrahedron: Front view (left) and top view (right)

These items allow point-to-point distance measurement and are well suited for calibration of CT scale factors, because the measurements of the positions of the spheres are not influenced by threshold value determination, beam hardening and so on [8].

Anyway these items do not allow the setting of correct threshold values and the comparability between other common workpieces, since they have different materials [8].
Other reference items developed for CT testing are the ones related to plane and parallel surfaces such as end gauges, prismatic standards. For example the University of Leuven proposed the multimaterial step gauges and Cactus step gauge (see sub chapter 5.4) [70].
They are suitable for the investigation of accuracy obtained in point-to-point (or face-to-face) length measurements. They may be critical in assessing the barreling effect since it deforms the flat surfaces.
As items derived from optical CMM experiences, PTB proposed a type 2D hole plate that reveals to be suitable for 2D flat panel detectors, further a 3D calotte cube has been proposed, more details are going to be shown in Chapter 4 (see Fig. 5.4) [67]. DTU (Denmark) used the miniature replica step gauge as shown in Fig. 5.5 [68].

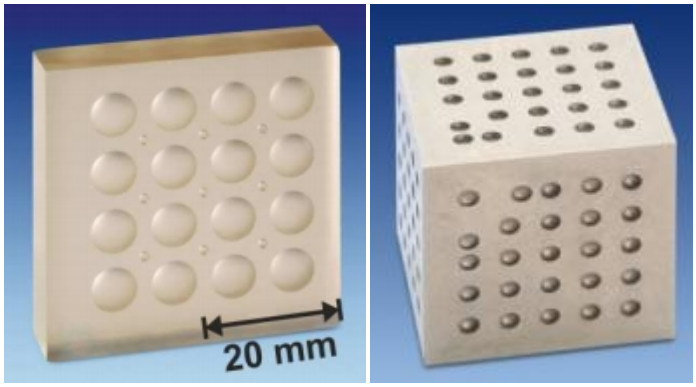

Fig 5.4: Zerodur 2D calotte plate and PTB calotte Cube [67]

Fig.5.5: Miniature replica step gauge [68]

During the last years, many reference items have been proposed as reference for CT measurement, first of all the one already shown in VDI/VDE 2617-13 or in ISO WD 10360-11, called Step Cylinder. Some research centers already used a step cylinder, as for example Nardelli et al. that used the calibrated item made of polyoxymethylene plastic to investigate the extraction operation in a CT dimensional measurement [69], see Fig. 5.6.

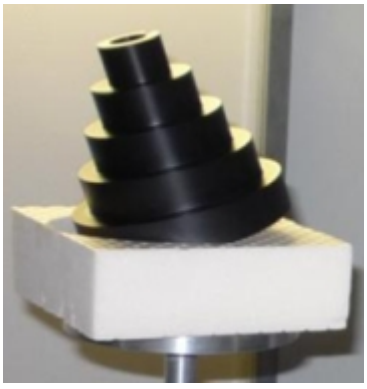

Fig. 5.6: Step Cylinder set up [69]

But other solutions have been proposed or are under developments, some of them are shown in the following subchapters.

5.1 "Fiber Gauge" for testing micro-CT system

Carmignato et al. [23] investigated on the dimensional performance of a micro-CT system that is becoming more and more promising for the possibility of non-destructively measuring of geometrical micro features. They discussed the lack of standardization methods for micro-CT systems and proceeded with test procedure based on the use of a newly developed micro reference standard.

They designed and developed a novel reference standard, called "Fiber Gauge" see Fig. 5.7 and 5.8, that has been fabricated using fiber optic technology, with glass fibers mounted into a multi-holes ferrule.

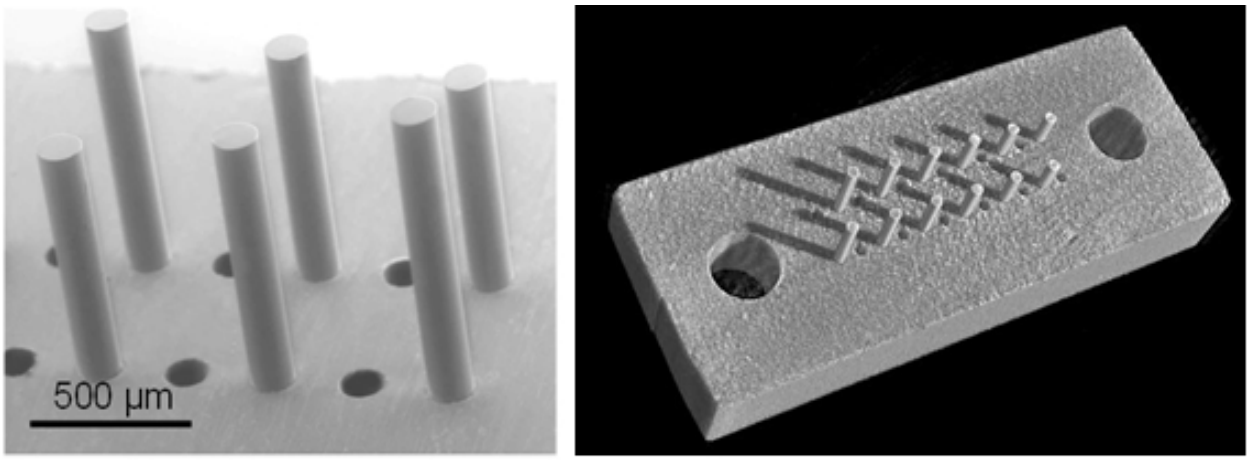

Fig. 5.7: Reference standard developed for testing micro-CT systems: the "fiber gauge". (left) Detail SEM image of the reference standard, (right) Volume rendering obtained from a micro-CT scan

Moreover it includes 12 fibers and 12 holes with nominal diameters equal to 125 µm, whereas the fibers' lengths have nominal values in a range from 350 to 700 µm.

Fig. 5.8: Picture of "Fiber Gauge"

"Fiber Gauge" permits to test the error of indication for size measurements using a reference calibrated lengths, and to evaluate the optimal threshold value by the simultaneous

measurement of internal and external features. Indeed Carmignato et al. observed that the diameters are strongly dependent on the chosen threshold value, since when the threshold value increases, dimension of inner features increases, while the outer ones decrease, as shown in diagram 5.1.

Diagram 5.1: Influence of threshold value on measured diameters of cylindrical features

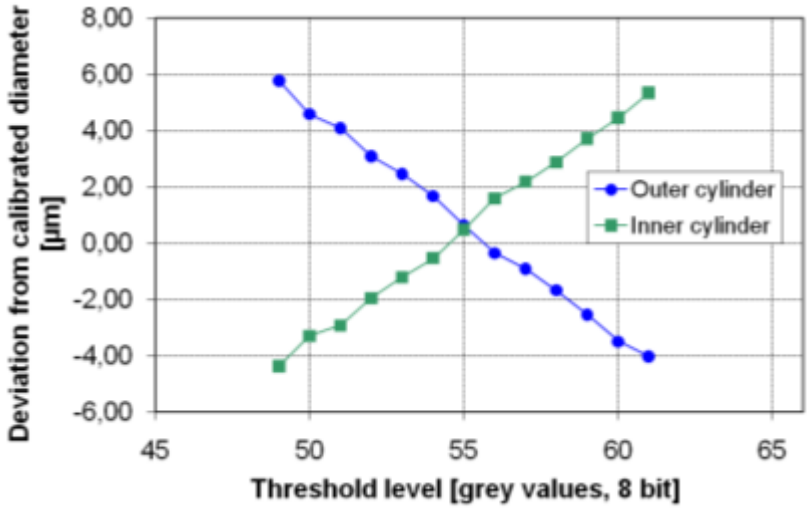

Moreover "Fiber Gauge" leads to the correction of systematic errors, in particular of systematic scale errors that revealed to be not stable over a long time period. For this reason Carmignato et al. suggested to measure always a calibrated item together with the measuring item in order to find out the scale correction [23].

5.2 Dismountable freeform reference standard

As shown in this Chapter, many reference standards have been created and used in order to verify CT measurement and to correct any kind of systematic errors. But all of these items have a common drawback: their features are not similar to industrial workpieces and no free form parts are present. For this reason Bartscher et al. [46] work on a dismountable freeform reference standard made from a cast miniaturized aluminum cylinder head. It can be dismounted in four segments, with fixed reference geometries, see Fig. 5.9.

Fig. 5.9: One A1 segment dismountable freeform reference standard developed by PTB [46]

The reference standard embodies complex freeform surfaces which are a challenging measurement task for CT. In particular segment 1A1, that has been deeply investigated, has been created with three raw unpolished ZTA (Zirconia Toughened Alumina) spheres with a diameter of 6.1 mm. The item has been CT measured with two different CT systems and calibrated with conventional CMMs machines and confoncal measurement systems. After that the output has been investigated in VG Studio Max 2.1 and the scaling factor has been corrected using a 5 reference spheres. The surface determination has been conducted using adaptive threshold method and finally a comparison between CT data and reference values (CMM) has been obtained with GOM Inspect software. The results showed high correlation between tactile data and CT data from both the two different systems and this is a good indication for a valid surface determination, see diagrams 5.2 and Fig. 5.10.

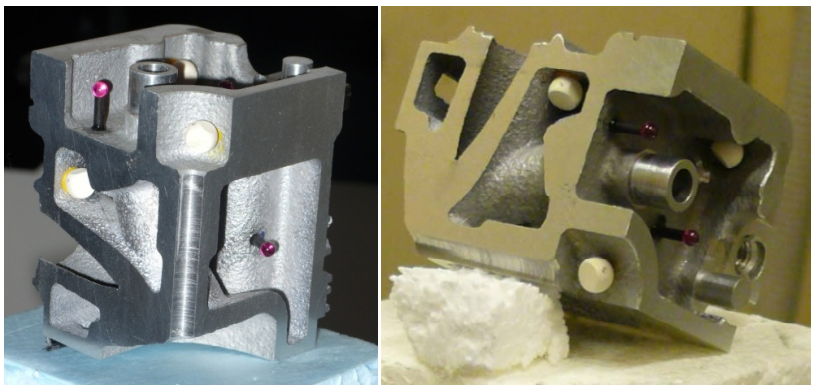

Fig. 5.10: (left) PTB setup, (right) BAM setup [46]

Diagram 5.2: CT-CMM measurements comparisons from two different CT systems [46]

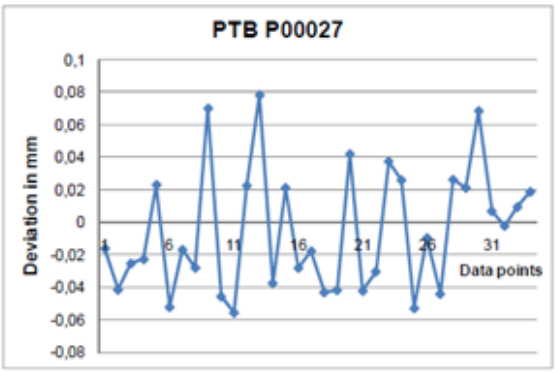

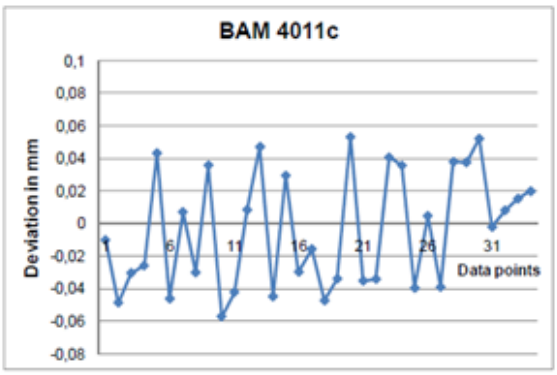

This item reveals to be a very promising object since it will lead to analysis of the influence of surface roughness and workpiece topology. Further investigations are under developing [46].

5.3 Cactus Step Gauge

Kiekens et al. [70] investigated on the influence of the power setting (voltage and current) on the accuracy and repeatability of dimensional CT measurements. Normally the setting of the x-ray source is defined as following: the voltage must be sufficient to penetrate the workpiece in each orientation and the current is chosen in order to maximize the contrast of the images without saturating. Anyhow the real final selection of these settings is strongly dependent on user preferences and experience.

Kiekens et al. proposed a “Cactus step gauge” that is an aluminium cube (45x45x45 mm) with parallel through groves in the shape of a cactus. The planes are numbered from 1 to 8 and divided in six different zones from A to F. The distance between two successive planes is 5 mm nominal. Moreover the measured features reported on in this paper are horizontal distances between the planes in zone D, see Fig. 5.11.

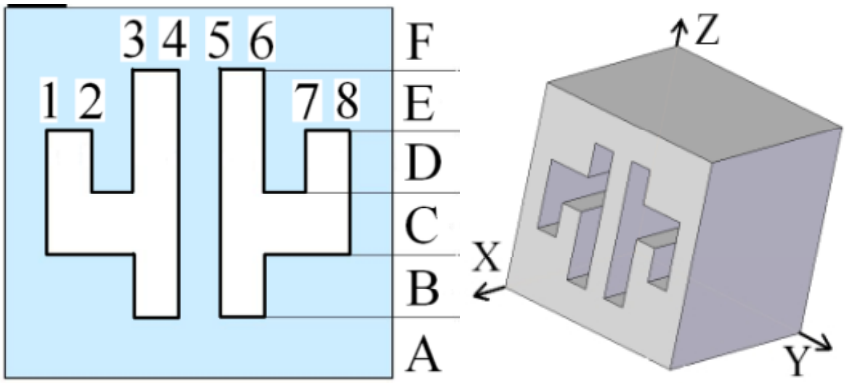

Fig. 5.11: Front view (left) and 3D model (right) of the cactus step gauge [70]

The "Cactus step gauge" has been measured with 13 different power settings. First results have been analyzed after minimizing the rescale factor with the average of the distances 1-7 and 2-8. The rescale factor RS is obtained as following:

$$RS = \frac{Ref_{a,b}}{CT_{a,b}} \quad (4)$$

In formula 4) $CT_{a,b}$ represents the edge independent distance on the voxel model whereas $Ref_{a,b}$ represents the reference value for distance measured with CMMs.
So in the specific case the formula can be re-written as:

$$RS = \frac{Ref_{1,7}}{CT_{1,7}} \quad (5) \quad RS = \frac{Ref_{2,8}}{CT_{2,8}} \quad (6)$$

Diagram 5.3 shows that the deviations are dependent on the voltage and current settings used, since higher settings imply larger deviations.

Diagram 5.3 Deviations between the rescaled CT values and the CMM reference values when varying the power settings [70]

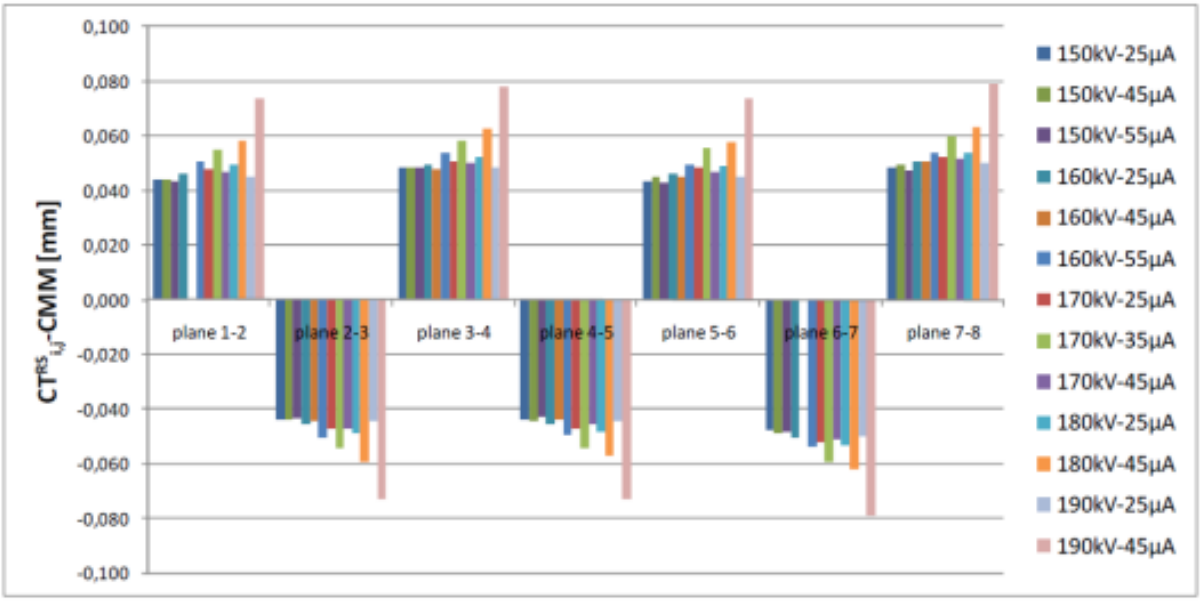

From Diagram 4.3 an edge offset error can be appreciated, maybe due to the differences in width of the air gaps (too wide) and the walls (too thin). The results have been corrected using the distance 4-5 as a setting-dependent correction term as following:

$$CT_{i,j}^{Corr} = CT_{i,j}^{RS} \pm (Ref_{4,5} - CT_{4,5}^{RS}) \quad (7)$$

Formula 7) has been applied to each couple of planes where $CT_{i,j}^{RS}$ is the rescaled distance between plane i and j, whereas $CT_{i,j}^{Corr}$ is the value after edge correction. After this correction, a new diagram (4.4) has been plotted, where there are no significant differences between the results obtained with different settings. This leads Kiekens et al. to the conclusion that after a reliable edge correction method, the setting dependency seems to be eliminated [70].

Diagram 5.4: Deviations between the edge corrected CT values and the CMM reference values when varying the power settings[70]

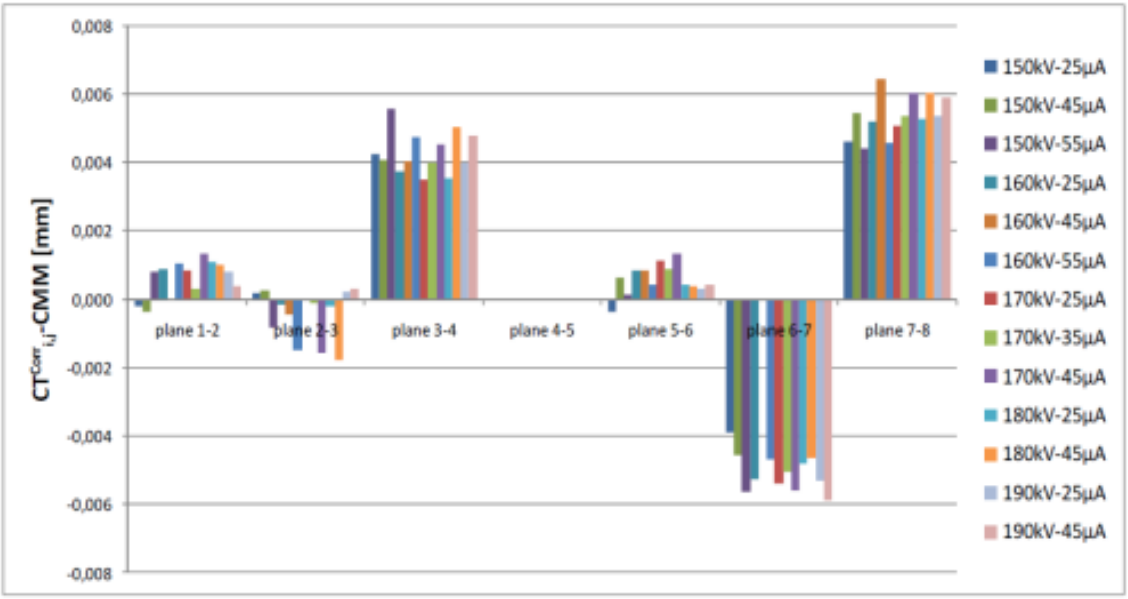

6. Developed Procedures at University of Padova

In the previous part of Chapter 2, the state of the art related to the performance verification for dimensional metrology was discussed. In details some important national and international standards have been described together with alternative solutions. Further developments and investigations conducted by the Laboratory of Industrial and Geometrical Metrology of University of Padova are further proposed in sub chapters 6.1, 6.2 and 6.3.

6.1 Metrological Performance of CT with Synchrotron Light Source at Elettra

In collaboration with Elettra Synchrotron (Syrmep Beam line) the *Laboratory of Industrial and Geometrical Metrology* of University of Padova (DIMEG) developed a new measurement procedures that has been investigated Synchrotron light source CT.

The Syrmep Beam Line uses as source one of the 24 bending magnet of Elettra Synchrotron ring, where the electrons beam orbits. The ring energy is typically around 2 or 2.4 GeV and the ring current is respectively 300 or 1140 mA. The electrons beam, when orbiting, is deviating by the Syrmep bending magnet that has a curve radius of 5.5 m. The light beam is sent to the optical room, or the optic hutch, where the X-ray beam is prepared (energy selection, geometry definition and intensity modulation) for the specific application (see 6.1.3 for the schematic representation of the Syrmep beam line).

The optical elements are inserted between a couple of beryllium windows: the first one divides the beamline from the storage ring, the second one separates the vacuum propagating part of the beam with the air propagating one. The lower energy components of the beam are cut traversing the first beryllium thickness. Furthermore, a thick block of tungsten, the so called beam stopper, controlled by a pneumatic piston, can be inserted into the beam to prevent the beam reaching the experimental hutch [71].

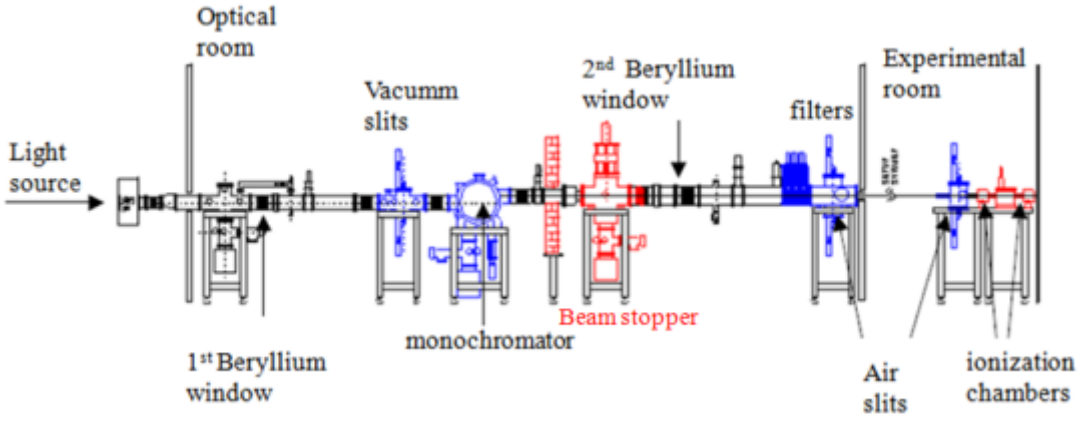

Fig.6.1: The Syrmep beam line layout [71]

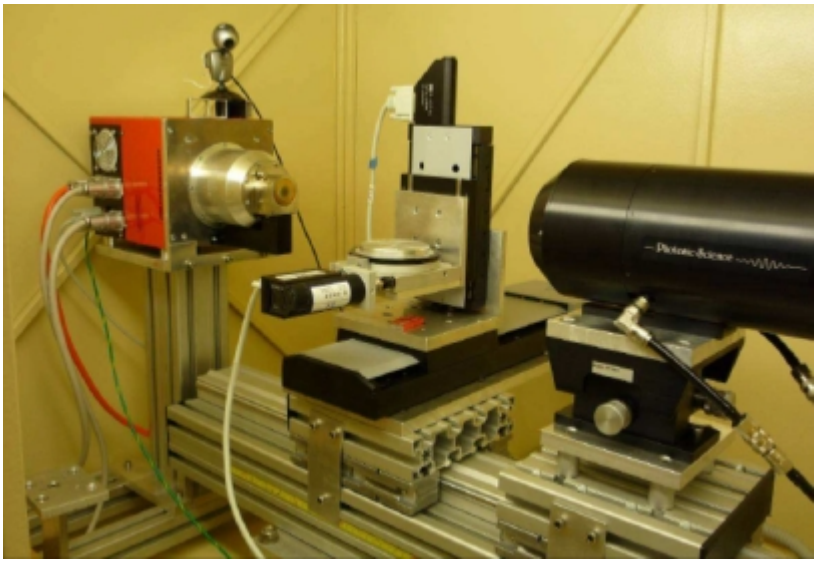

Fig.6.2:: Experimental Room

The polychromatic beam of the ring reaches the monochromator and it is possible to select the energy in a range between 8.3 keV and 35 keV. The monochromatic radiation meets a filters system that reduces the intensity of the radiation. Finally the selected beam is conducted to the experimental room where there are the ionization chamber (to continuously measuring the incoming photon flux), the sample holder, endowed with 4 degrees of freedom and the turn-table on the top, and the detectors for image acquisition [71].

The collaboration with Syremp beam line has been included in an accepted proposal (number 20090159) that give to The Laboratory of Industrial and Geometrical Metrology the opportunity to investigate the performance of CT measurements using synchrotron light source. Recently the using of synchrotron radiation facilities to generate x-rays for CT application, including research for dimensional measurements is becoming very interesting and seems to be pretty promising [8]. Indeed CT systems using synchrotron radiation offer unique x-ray beam properties such as:

- X-ray energies with very high flux;
- X-ray energies with a high brilliance due to the low angular dispersion of the beam;
- The quasi parallel beam eliminates common problem associated to cone or fan beams configuration (e.g. image magnification problems);
- Monochromatic x-ray beam avoids the problems due to the beam hardening, typical of cone beam CT systems.

These properties lead to the improvement of edge detection and the consequent measurement accuracy [8].

6.1.1 Glass Tubes Item

A designed object used as reference standard has been developed and calibrated by *Laboratory of Industrial and Geometrical Metrology* of DIMEG department: "Glass Tubes" (Fig.6.3). It is made by five borosilicate glass cylinders with different lengths supported by a carbon fiber frame, whereas the inner and outer diameters are equal. The internal diameters measure 1.54 mm and the external ones 1.89 mm, whereas the tubes' lengths are in mm: 3.74 - 3.28 -2.77 -2.16 -1.49 [72]. The small dimensions of Glass Tubes have been decided in order to make this item measurable by CT using synchrotron radiation, since the field of view, is reduced comparing to the industrial CT scanner.

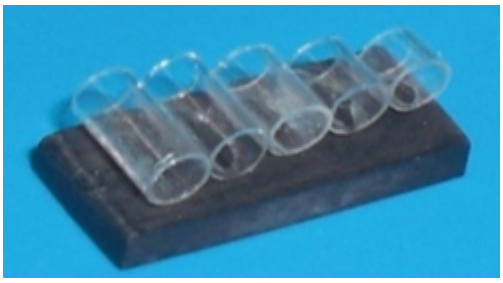

Fig. 6.3: Glass Tubes' picture

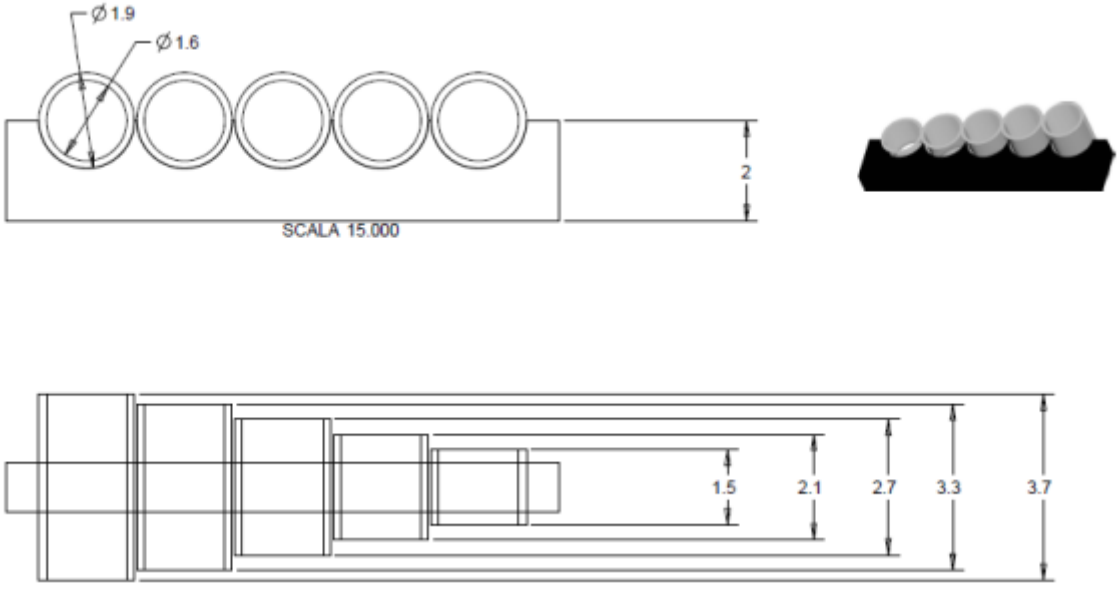

Fig. 6.4: Glass Tubes' Design

"Glass Tubes" has been calibrated at *Laboratory of Industrial and Geometrical Metrology*. Length and diameters of each tube have been calibrated using a multisensor CMM (Werth HA Video Check IP 400, with video, tactile and laser sensors) and a tactile CMM (Zeiss Prismo Vast 7, with scanning head) at University of Padova - DIMEG.

Calibration measurements have been repeated several times, showing good dimensional stability of the developed standard. Parallelism between flat faces and their perpendicularity with the cylinders axis have been found below 2.5 μm. Roundness of internal and external cylinders is below 2 μm.

The flatness of the final cylinders extremities has been calibrated using White Light Interferometry (WLI) at CIVEN Association Laboratory in Marghera (VE), showing form errors below 2 μm.

6.1.2 Measurement Methods

From 3rd to 5th of September 2009, "Glass-Tubes" has been measured under six different conditions concerning the measurement methods, number of projections and rotational amplitude. In particular three alternative procedures have been used in order to estimate the best result and they are detailed shown in Table 6.1. One method has been called "Average measurement" Method. Each projection is scanned three times and an average between the three slices is calculated. As shown in Table 6.1, the acquisition time is definitely longer than the others.

Table 6.1: CT Measurements details at Syrmep Beamline

Measurement Name	Projections	keV	Rot. Speed [deg/s]	Acquisition time	Amplitude rot. [deg]	STEP [deg]	t_{exp} [s]
Average	1440	25	4	10 h, 25'	180	0,125	8,2
21 keV	1800	21	4	1 h, 25'	180	0,100	2,2
27 keV	1800	27	4	6 h, 20'	180	0,100	12,0
540°	1440	25	2	9 h, 10'	540	0,125	7,5
1440 proj.	1440	25	4	3 h, 20'	180	0,125	7,5
Continuous	1450	25	0,018	2 h, 45'	190	---	7,0

"21 keV measurement", as the name suggests, has been performed at 21 keV energy, one of the lowest energy for Syrmep Beam Line; whereas "27 keV measurement" has been set at 27 keV energy. These two method required different time of exposition as shown in Table 6.1.
Moreover "540° measurement" has been conducted in order to evaluate measurements over the traditional 180° or 360° methods. The object rotated for 540 degree and obviously the measurement has been one of the longest.
"1440 proj. measurement" has been performed at 25 keV energy and decreasing the number of projections from 1800 to 1440.
Finally, "Continuous measurement" has been carried out in order to measure without any step of the rotary table. The resulting measurement is a continuous rotation of "Glass Tubes" for 190°.

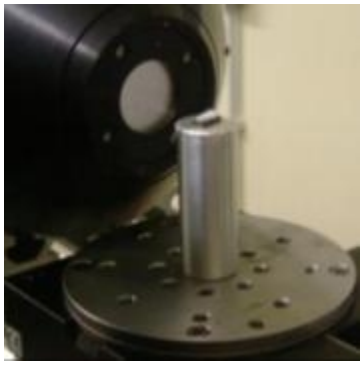

Fig. 6.5: "Glass Tubes" under CT measurement with Synchrotron radiation

6.1.3 Results Analysis

The analyses were focused on the investigation of threshold value determination with global method and of scaling factor correction. These analyses and their results are here following described.
The threshold value is a critical parameter for accurate image segmentation. It converts a grey value image into a binary one. Its determination contributes to the correction of a systematic deviation in CT measurements. It has been evaluated on "Glass Tubes" by the simultaneous measurement of inner and outer diameters, because their dimensions depend on changing threshold in the opposite way [39].
The optimum threshold value, when using global threshold value determination, can be considered as the background grey value that minimizes the differences between calibrated

and measured diameters. When increasing the threshold value, the inner features increase while the outer ones decrease. The optimum value is the crossing point between inner and outer gap lines, as shown in Fig. 6.6 and in Table 6.2 and 6.3.

Table 6.2: Tube 1 Example of optimum threshold value determination

Tube 1 (nominal 3.7 mm diameter) Measurement "Continuous"(Gauss)						
Threshold value	**Inner Diam (Ref) mm**	**Outer Diam (Ref) mm**	**Inner Diam mm**	**Outer Diam mm**	**Deviation Inner Diameter µm**	**Deviation Outer Diameter µm**
156	1.5422	1.896	1.5413	1.92906	-0.898	33.059
158			1.54501	1.92531	2.8078	29.3064
160			1.54851	1.92163	6.3052	25.6328
162			1.55189	1.91826	9.6918	22.2642
164			1.55528	1.91475	13.0778	18.7484
166			1.55866	1.91131	16.4624	15.313
168			1.56219	1.90768	19.9868	11.6814
170			1.56599	1.90389	23.7894	7.8922
optimum						
165.57			1.55787	1.91203	15.6744	16.0272

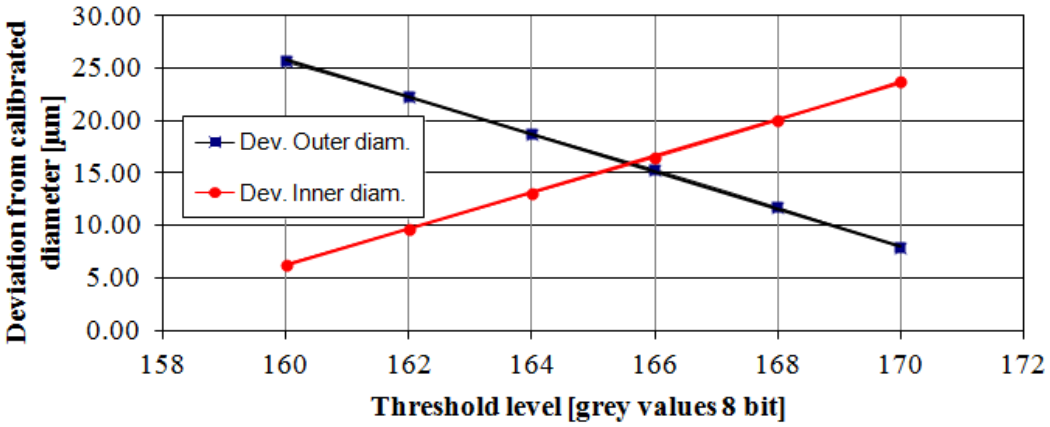

Fig. 6.6: Tube 1 Example of optimum threshold value determination

Table 6.3: Threshold Summary

Measurement	**NL Diffusion**	**Median**	**Gauss**	**Average**
Average	191.98	193.04	190.66	**191.89**
21 keV	162.13	162.64	160.87	**161.88**

27 keV	165.47	165.81	164.26	**165.18**
540°	148.99	149.75	147.9	**148.88**
1440 proj.	188.69	189.08	187.1	**188.29**
Continuous	166.59	167.27	165.57	**166.48**

Moreover a systematic scaling error, called scaling factor k, in all space directions can be observed in any CT systems. In order to correct scaling factors of synchrotron computed tomography set up, "Glass Tubes" has been used as calibrated reference object.

The influence of the threshold value has been estimated as linear; therefore the measured diameters are correlated to the set threshold value in a line equation as following (8) and (9):

$$D_{meas,inner}(T_{value}) = m_{inner} * T_{value} + q_{inner} \qquad (8)$$

$$D_{meas,outer}(T_{value}) = m_{outer} * T_{value} + q_{outer} \qquad (9)$$

, where T_{value} is the set Threshold grey values, m_{inner} and m_{outer} are the angular coefficients of the lines.

From (8) and (9) the lines equations for the deviations between calibrated values and measured ones can be obtained as following (10) and (11):

$$D_{meas,inner}(T_{value}) - D_{cal,inner} \qquad (10)$$

$$D_{meas,outer}(T_{value}) - D_{cal,outer} \qquad (11)$$

In order to determine the scaling factor k, the equation of the lines that nullifies the deviations between calibrated and measured values must be figured out, as following (12) and (13):

$$k * D_{meas,inner}(T_{value}) - D_{cal,inner} \qquad (12)$$

$$k * D_{meas,outer}(T_{value}) - D_{cal,outer} \qquad (13)$$

Fig. 6.7 shows how to interpret the above equation graphically.

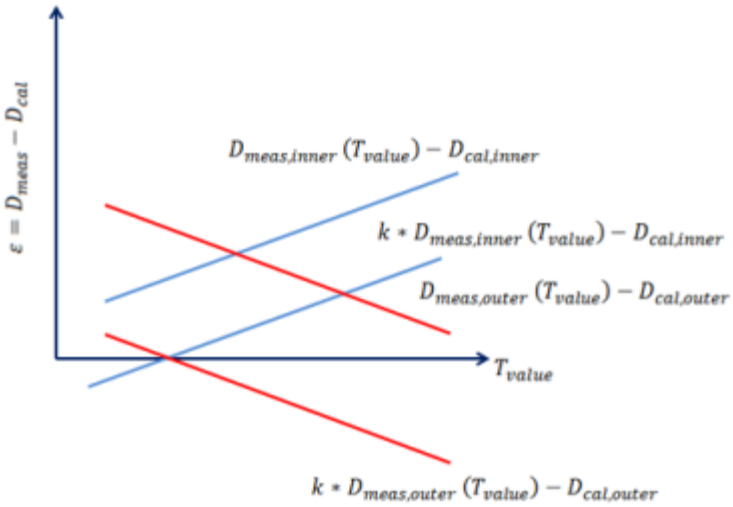

Fig.6.7: Schematic representation for calculation of k scaling factor

Consequently from (12) and (13), k is obtained when the lines are equal to zero, as following (14):

$$k * D_{meas,inner}(T_{value}) - D_{cal,inner} = k * D_{meas,outer}(T_{value}) - D_{cal,outer} = 0 \quad (14)$$

From equations (8) and (9), k is obtained as following (15):

$$k = \frac{D_{cal,inner} - \left(\frac{m_{inner}}{m_{outer}}\right) * D_{cal,outer}}{q_{inner} - q_{outer} * (m_{inner}/m_{outer})} \quad (15)$$

Starting from equation (15), the scaling factor has been calculated for each measurement as shown in Table 6.4 where the results related to tube 1 (nominal length 3.7 mm).

Table 6.4: Summary of k scaling factor values

Measurement	NL Diffusion	Median	Gauss	Average
Average	0.9908	0.9909	0.9907	0.9908
21 keV	0.991	0.9911	0.9909	0.991
27 keV	0.9908	0.9909	0.9907	0.9908
540°	0.9909	0.991	0.9908	0.9909
1440 proj.	0.9907	0.9908	0.9907	0.9907
Continuous	0.9909	0.991	0.9908	0.9909

6.2 Olympic Gauge and Pan Flute Gauge

Starting from *Glass Tubes*, another reference item, called *Olympic Gauge,* has been designed from a concept by Carmignato at *Laboratory of Industrial and Geometrical Metrology of University of Padova* [73].

The standard is made with five precise borosilicate glass cylindrical tubes of different lengths (nominal lengths equal to *Glass Tubes*) supported by a carbon fibre frame. The five tubes are arranged similarly to the Olympic rings' configuration, as shown in Figure 6.8.

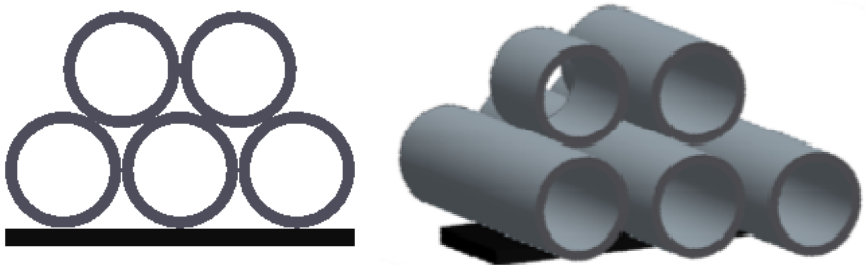

Fig. 6.8: Schematic representation of the newly developed reference standard: (left) frontal view and (right) axonometric view.

Consequently, a new reference object according to the *Olympic Gauge* concept, but with different tubes' arrangement and dimensions, has been developed and calibrated *by Laboratory of Industrial and Geometrical Metrology* of University of Padova. The reference item has been called *Pan Flute Gauge* and it has been created for the first international interlaboratory comparison on CT systems for dimensional metrology, named "CT Audit" (more details in Chapter 4). *Pan Flute Gauge* consists of five borosilicate glass tubes supported by a carbon fibre frame The five tubes have same nominal diameters (inner diameter: 1.5 mm ca.; outer diameter: 1.9 mm ca.), but different lengths (ranging from 2.5 to 12.5 mm). As shown in Figure 6.9, the five tubes are designated with five different names. Starting from the longest one, the five tubes are named respectively: Tube 1, Tube 2, Tube 3, Tube 4 and Tube 5. Nominal lengths of the tubes are given in Figure 6.10.

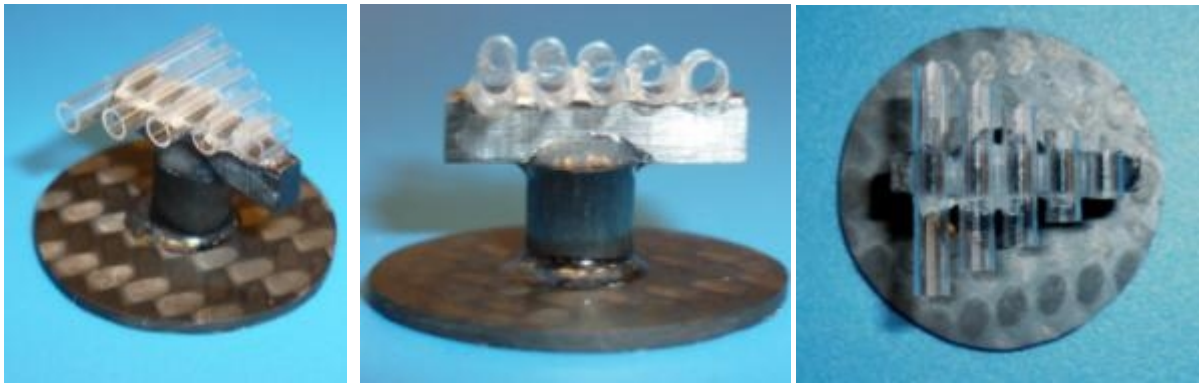

Fig.6.9: Pictures of Pan Flute Gauge, Axonometric view (left), side view (middle), top view (right)

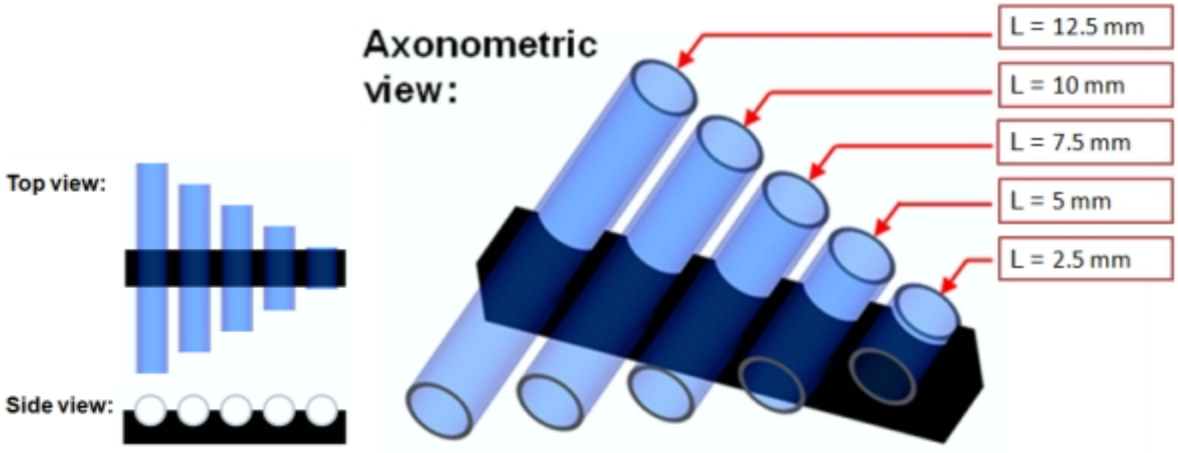

Fig. 6.10: Schematic representation of Pan Flute Gauge

Pan Flute Gauge has been created suitable for metrological performance verification of CT systems. Indeed it allows verification of measurements on both internal and external features, giving the possibility of setting an optimal threshold value that minimize the deviations of inner and outer diameters from the reference values as shown in Fig. 6.11.

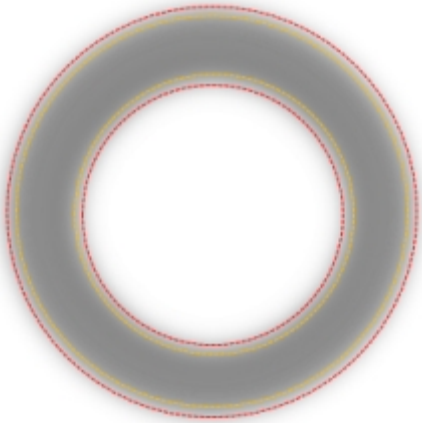

Fig.6.12: Threshold value trade for inner and outer geometries

Furthermore, including five different lengths, it allows testing five bidirectional length errors, similarly to the procedure described in ISO 10360-2:2009 for determining errors of indication for size measurements.

Each glass cylinder has been manufactured by cutting precise borosilicate capillary tubes using the so called scribe-and-break technique. After cutting, the five cylinders have been ground in both extremities with an automatic grinding and polishing machine. The flatness of the final cylinders extremities has been calibrated using White Light Interferometry (WLI), showing form errors below 2 µm, as illustrated in Fig. 6.13.

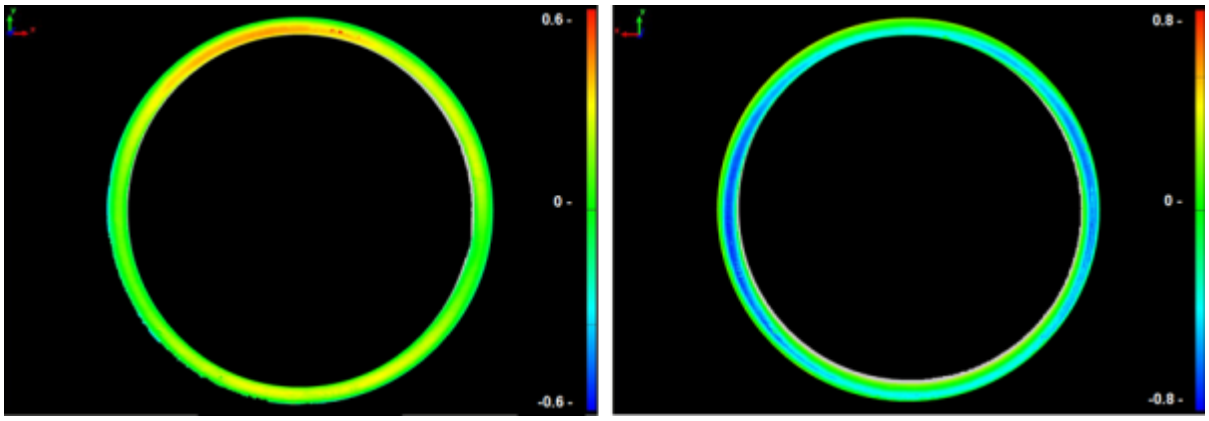

Figure 6.13: WLI measurement [µm] concerning Tube 3 faces extremities.

The high dimensional stability of *Pan Flute Gauge* was verified and confirmed through two CMM calibrations (Zeiss Prismo Vast 7, with scanning head) one in March 2010 and the other one in March 2011, showing deviations within the calibration uncertainty.

Fig.6.14: Pan Flute Gauge set up for CMM calibrations

The stability is documented in Diagram 2.1, which reports the absolute value of the En numbers comparing the calibrations in March 2010 and 2011. The En number is calculated using the following equation (16).

$$E_n = \frac{X_1 - X_2}{\sqrt{U_1^2 + U_2^2}} \quad (16)$$

Where X_1 is related to the first calibration in March 2010 and X_2 is the second calibration in March 2011, whereas U_1 and U_2 are the related uncertainties [74].

According to [74], if |En|<1 then there is good correspondence between the two calibrations, otherwise the correspondence is unsatisfactory. As visible in Fig. 6.15, the En number is always below the unit for all the calibrated characteristics of *Pan Flute Gauge* (inner and outer diameters, lengths), which confirms the good dimensional stability of the item. Further information is available on [78].

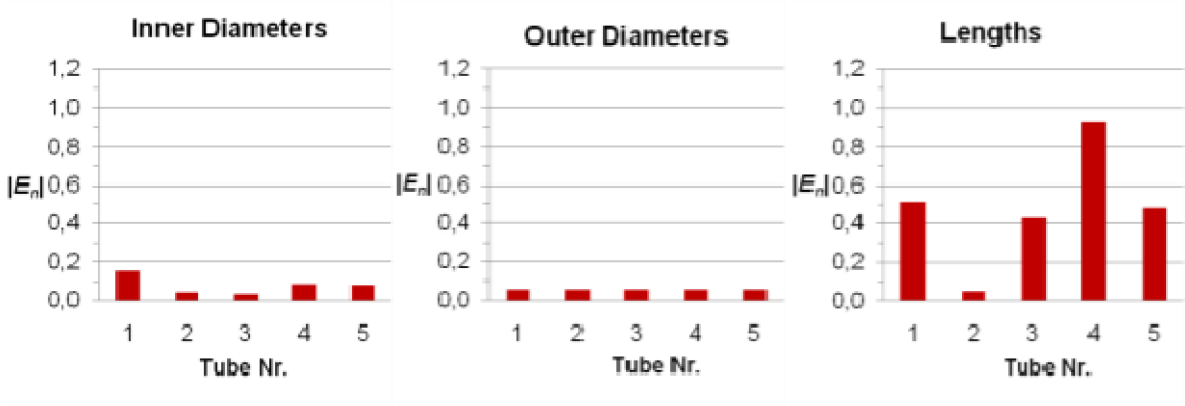

Fig. 6.15: E_n number for inner and outer diameters and lengths of Pan Flute Gauge

6.3 CT Tetrahedron

A second developed item is called CT Tetrahedron. It was developed by the *Laboratory of Industrial and Geometrical Metrology*, University of Padova, from concept by Carmignato. It consists of four ruby spheres supported by a carbon fibre frame (see Fig. 6.16 and 6.17). The four spheres centres are ideally positioned on the vertexes of a tetrahedron with nominal side length of 25 mm. The frame is made with carbon fibre bars with diameter of 2 mm. As shown in Figure 6.17, the four spheres are designated with four different names. Starting from the base of the carbon fibre frame, the four spheres nominal diameter are 5 mm; 4 mm, 4 mm 3 mm.

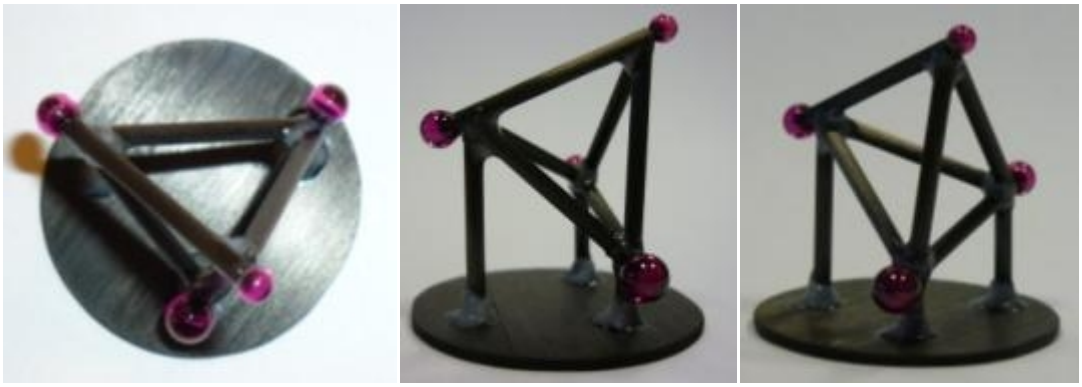

Fig. 6.16: Pictures of CT Tetrahedron, top view (left), side views (middle and left)

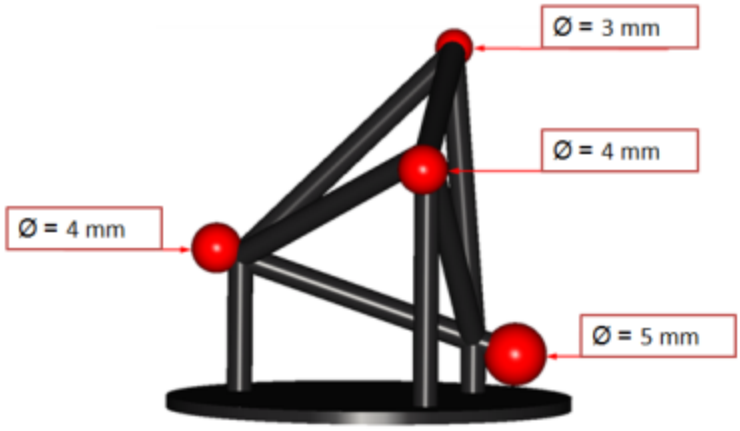

Fig. 6.17: Schematic view of CT Tetrahedron

CT Tetrahedron has been created suitable for metrological performance verification and accuracy of CT systems. Indeed it is possible to evaluated the characteristic "Form Error" with the measuring of the four ruby spheres according to the definition of the characteristic "Probing error of form" (PF) given in the working draft ISO 10360-11 [61] and the draft VDI/VDE 2617-13 [60], where PF is defined as the span of the radial deviations of the measurement points from the calculated fitted sphere, as shown in Fig.6.18.

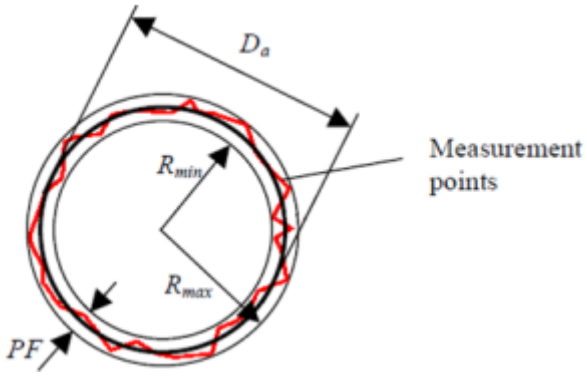

Fig. 6.18: Illustration of characteristic value probing error form PF [35]

Furthermore, the evaluation of distances between spheres centers on *CT Tetrahedron* allows evaluating unidirectional length measurement errors that are not influenced by the threshold values, since the distances between spheres centers do not change with the threshold value as shown in Fig. 6.19.

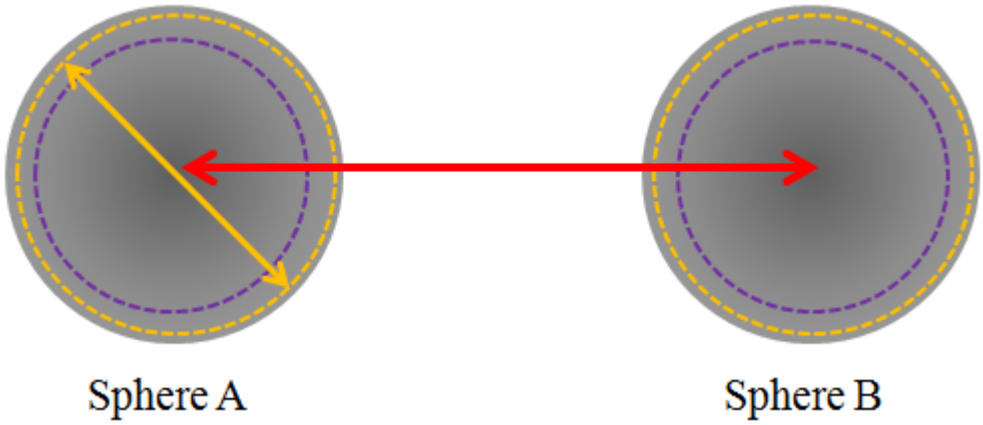

Fig. 6.19: Unidirectional lengths, not influenced by the Threshold values [70]

Moreover it is possible to evaluate the diameters of spheres on *CT Tetrahedron* and measuring bidirectional measurement errors, since the diameters are strongly influenced by the threshold values.
Finally the four spheres are intentionally positioned at different heights, in order to avoid the overlapping of them during the CT measurement when rotating on the rotary table.

The high dimensional stability of *CT Tetrahedron* was verified and confirmed through two CMM calibrations (Zeiss Prismo Vast 7, with scanning head) one in March 2010 and the other one in March 2011, showing deviations within the calibration uncertainty.

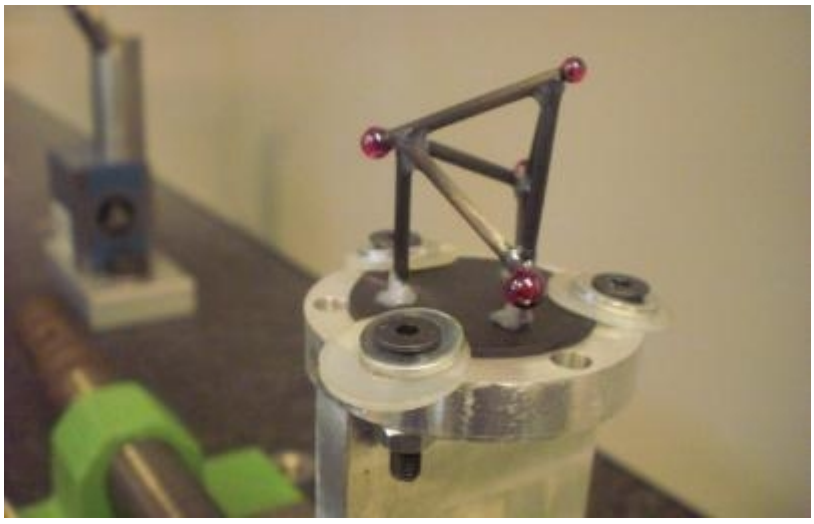

Fig. 6.20: Dedicated set up for CMM calibration

CT Tetrahedron has been fixed on a dedicated support as shown in Fig. 6.20 in order to calibrate it at different inclination and to evaluate the item from different positions, giving easier possibilities of access for the mechanical probe as shown in Fig. 6.21.

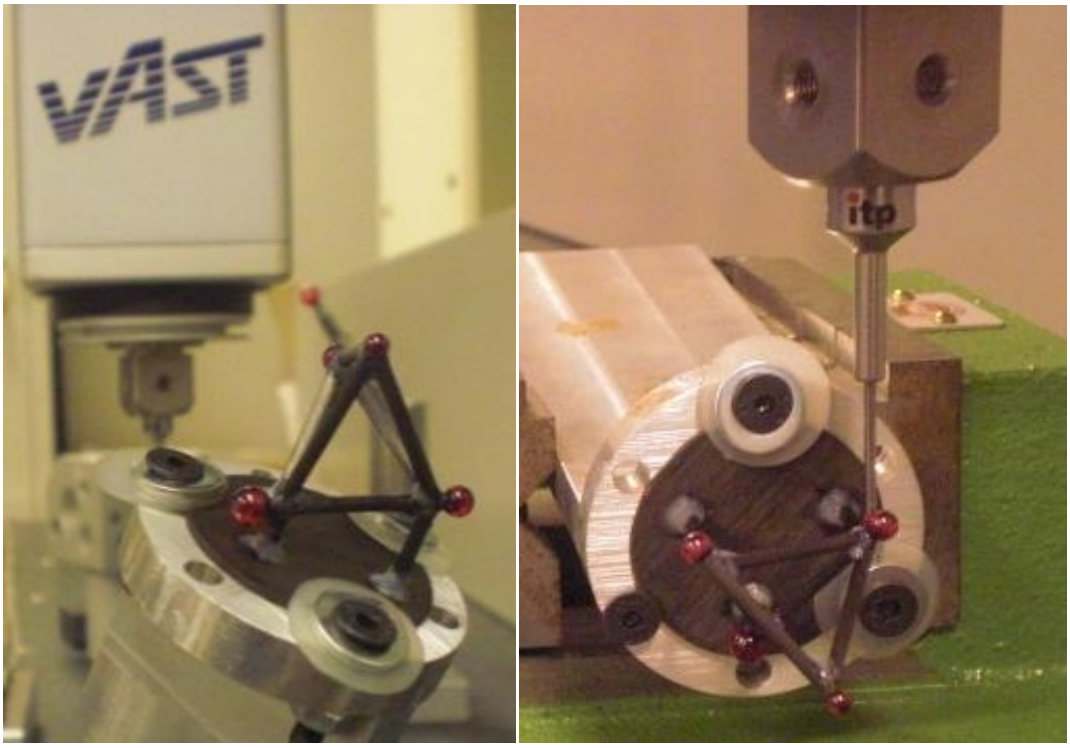

Fig. 6.21: Different inclination for CMM Calibration

The stability is documented in Diagrams 3.1, which reports the absolute value of the En numbers comparing the calibrations in March 2010 and 2011. The En number is calculated using the following equation (16).

$$E_n = \frac{X_1 - X_2}{\sqrt{U_1^2 + U_2^2}} \quad (16)$$

Where X_1 is related to the first calibration in March 2010 and X_2 is the second calibration in March 2011, whereas U_1 and U_2 are the related uncertainties [74].

According to [74], if |En|<1 then there is good correspondence between the two calibrations, otherwise the correspondence is unsatisfactory. As visible in Fig. 6.22, the En number is always below the unit for all the calibrated characteristics of *CT Tetrahedron* (spheres distances, diameters and form errors), which confirms the good dimensional stability of the item. Further information is available on [78].

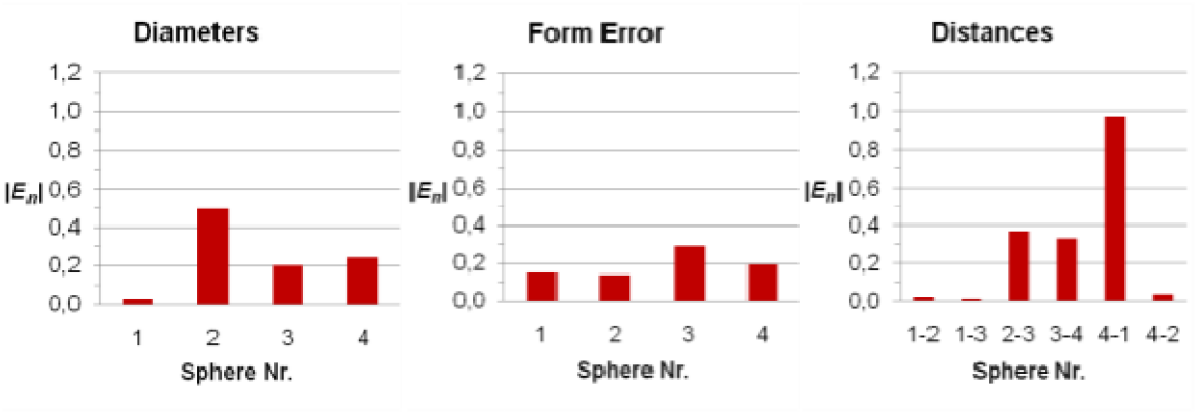

Fig. 6.22: E_n number for spheres diameters, form error and distances between the centers related to CT Tetrahedron

7. Conclusions

Chapter 2 described the state of the art related to the metrological performance verification of CT systems. In details some important national and international standards have been described together with alternative solutions coming from international research centres and universities. The development of procedures and reference items is still under discussion and no universally accepted procedures have been agreed. In the second part of the chapter, the procedures for metrological performance and related objects provided by the *Laboratory of Industrial and Geometrical Metrology* of the University of Padova have been described. In particular *Pan Flute Gauge*, *CT Tetrahedron* have been designed, created and calibrated in order to analyze CT systems metrological characteristics such as:

- The optimal threshold value;
- Size error for unidirectional and bidirectional distances measurements;
- Form error.

These calibrated items revealed to be pretty relevant and they have been used, as reference items for the first international intercomparison on CT Systems for dimensional metrology (CT Audit); further details concerning the CT Audit project are presented in Chapter 4.

Chapter 3

Tactile and CT Investigation on PTB Tetrahedron

In Chapter 3, the experience at PTB (National Metrology Institute of Germany) is presented with the description of PTB Tetrahedron and related investigations of its stability, calibration procedures and CT measurement results.

1. PTB Tetrahedron

From August to November 2010 a training period has been held at PTB (Physikalisch-Technische Bundesanstalt), the National Metrology Institute of Germany in Braunschweig.

PTB is analysing the dimensional measurement properties of industrial computed tomography systems. The creation of appropriate reference standards is definitively important. In particular the sphere seems to be the best geometric feature in order to characterise CT systems because it is relatively easy to create and it is full of information (form error, diameter, origin coordinates…). Topic of this investigation is to study the capability of CT to measure form using features with a known and calibrated form deviation.

Two similar reference standards have been created by PTB. They consist of 4 spheres each made from ceramics forming a tetrahedron and mounted on a CFRP rod, as shown in Figure 1. They are made of two different materials and two different surfaces (see table 1.1 and Fig. 1.1, 1.2 and 1.3).

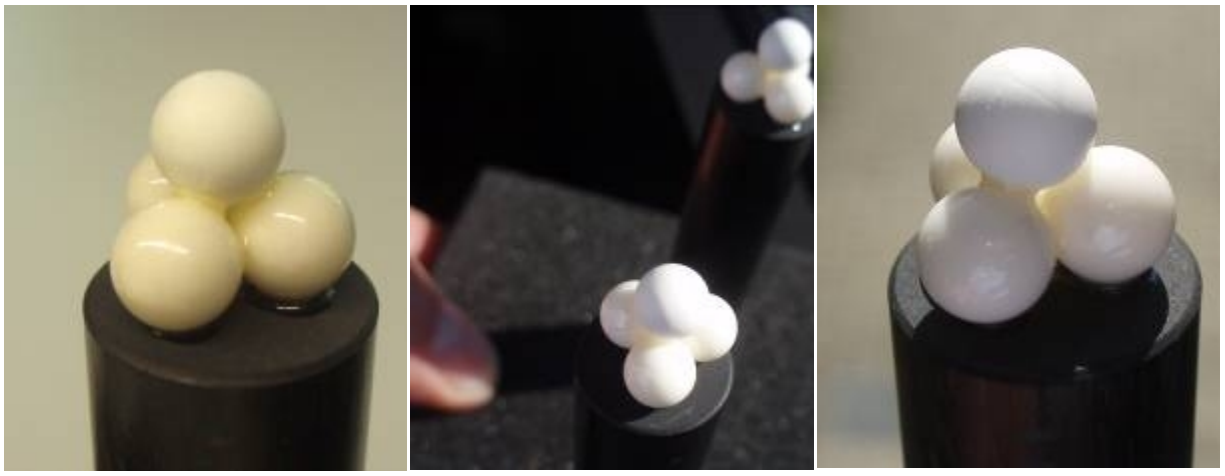

Fig. 1.1 (a,b,c): Tetrahedron Pictures

In details, the top sphere is different from the lower ones as shown in table 1.1.

Table 1.1: Tetrahedron details

	Top Sphere (A)	Lower Spheres (3) (B,C,D)
Material	Ceramic mixture ZTA (Zirconia Toughened Aluminumoxyd) (86% Al2O3 + 14% ZrO2)	Ceramic (Al2O3)
Nominal Diameter	6 mm	6 mm
Maximal Form Deviation	0,15 mm	0,001 mm

The two tetrahedrons have been investigated with a microscope in order to underline the different surfaces and to document eventual defects.

As shown in Figures 4.2 and 4.3, it is confirmed the raw surface of the top sphere, in particular a ring pattern has been observed. The lower spheres are quite good, even if the glue is sometimes too much and it covers a little bit of surfaces.

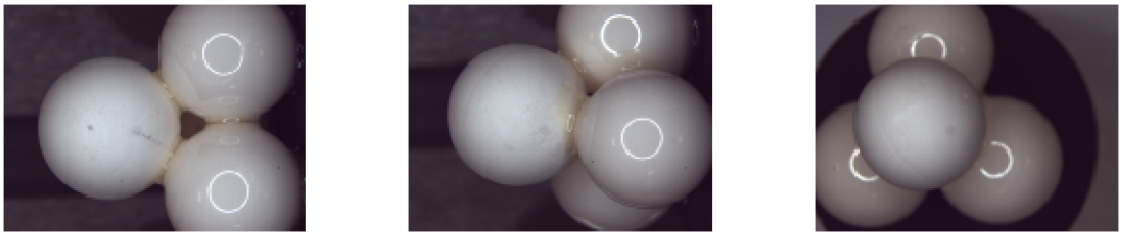

Fig. 1.2: Microscope pictures of Tetrahedron 1

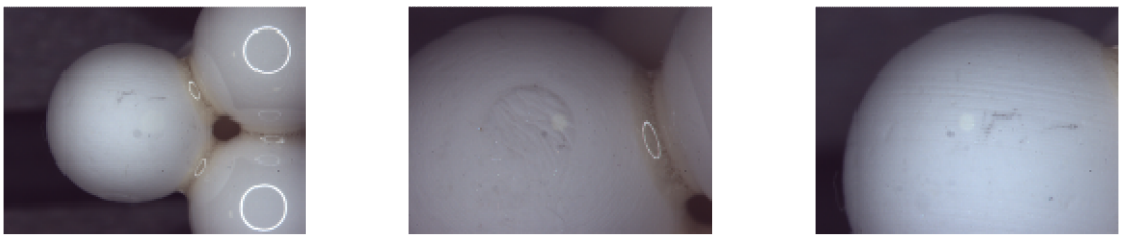

Fig. 1.3: Microscope pictures of Tetrahedron 2

1.1 Objectives

The main objective of this work consists in investigating the capability of CT to measure form. Due to the high error form of the top sphere, Tetrahedrons 1 and 2 have been considered suitable to characterize errors and effects of CT.

Since CT measurements have the advantage of acquiring thousands of points in a short time, a proper tactile CMM calibration of several thousands of points has been desired. This leads to a long time measurement and the concerning increasing of the CMM´s drift.
For this reason a drift compensated tactile measurement is an important part of this work. Moreover the CT data elaboration should be analyzed and the scale error should be corrected.

2. Tactile Measurements

The calibration of the reference standards is an important part of the work; in particular one objective of the CMM measurements is to assess the raw ceramic sphere (the top one) with a high point density in single point measurements modus, and the other spheres with an adapted lower point density. The desired points´ number for the top sphere is of the order of several thousand points. The tactile machine is a Zeiss UPMC 1200 Carat CMM with the software Calypso 5.0 and a tactile probing system.

2.1 Drift Correction

The accuracy of a CMM is affected by many error sources as well as:

- Kinematic errors;
- Thermo-mechanical errors (drift);
- Loads;
- Dynamic forces;
- Motion control and control software.

Special attention has been dedicated to the drift of Carat CMM. Error sources are due to the presence of internal and external heat/cold sources in CMMs and the very often significant expansion coefficients and coefficient differences of machine part materials [75].
Measurement of several thousand single points with the Carat CMM can be more than eight hours long. Long measurements lead to consider the possible drift of a CMM machine, due to the temperature deviations and the machine itself. The drift of Carat CMM had been already calculated with a value of 0.5µm/hour. But in order to correct the CMM drift it is important to validate:

- If the drift is linear or not;
- What happens with smaller probes of the order of 0.8 mm in diameter;

- If the tetrahedron fixing is stable.

With a dedicated program tetrahedron 1 has been measured for 26 hours, repeating 38 times the alignment on a reference sphere (see Figure 2.1).

In detail:

Table 2.1: Reference sphere details

	Reference Sphere
Nominal Diameter	6,3504 mm
Nominal Form deviation	0,0005 mm

Fig. 2.1: Reference Sphere (called "E sphere")

The probing system has the following parameters:

- Radius of probing element= 0,4003 mm;
- Specified Standard Deviation = 0,0001 mm;
- Orientation: -z direction.

The alignment of the tetrahedron has been fixed as following described (Y kinematics is assumed as X CMM):

- xy plane (primary) : plane created by the three lower spheres centres (called B,C,D);
- x axis (secondary): line created by two lower spheres centres (called D,B);
- origin (zero point): centre of reference sphere (called E).

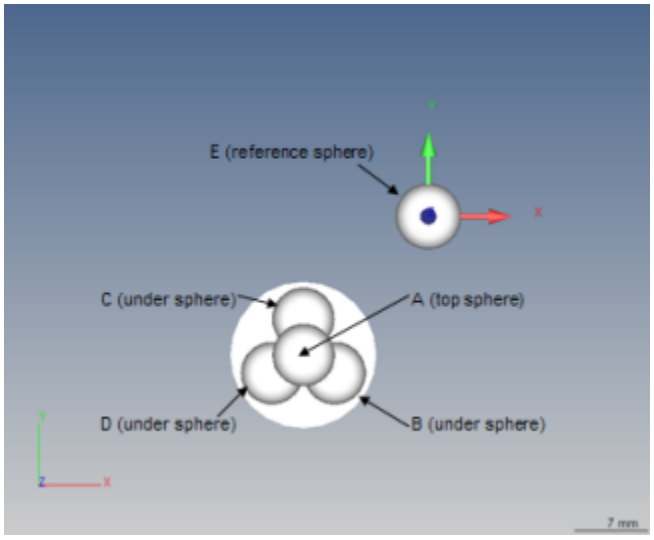

Fig. 2.2: Alignment description (Drift Investigation)

Between two alignments 400 (always the same) points have been taken, so in total 15200 points have been recorded. In detail:

- Sphere A : 200 points;
- Sphere B : 50 points;
- Sphere C : 50 points;
- Sphere D : 50 points;
- Sphere E : 50 points.

The number of points has been decided in order to keep the ratio 1:1 between number of points on sphere A and on BCD-E spheres as following:

N° points (A)= N° points (B)+ N° points (C)+ N° points (D)+ N° points (E)

200=50+50+50+50

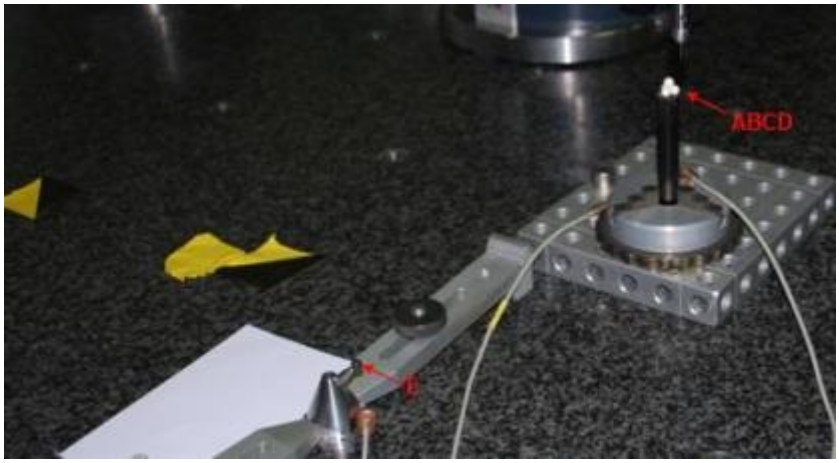

Fig.2.3: Measurement setup for drift investigation

The measured features are:

- Origin of each sphere;
- Distances between the spheres;
- Single point coordinates saved in ASCII files.

Each value has been re-called in Machine Coordinate System in order to make the final comparison possible. As shown in the diagrams from 2.1 to 2.15, the measurement deviations reveals to be always under 0,8 μm. The first measurements should not be taken in account and they are highlighted. Indeed they are considered as test measurements, because the temperature was not completely stable. In order to document everything, all the measurements are shown. The useful measurements can be considered from the third replication to the 38^{th}: in total 36 replications and circa 24 hours.

The diagrams from 2.1 to 2.15 present the deviations in 26 hours (38 replications) concerning the centre coordinates for each sphere (E-A-B-C-D) and the distances between the spheres (EA-EB-EC-ED-BA-BC-BD-CA-CD-DA).

It is clear from the diagrams that drift occurs and that its trend is not linear. In particular there is smaller drift in y axis (x kinematic).

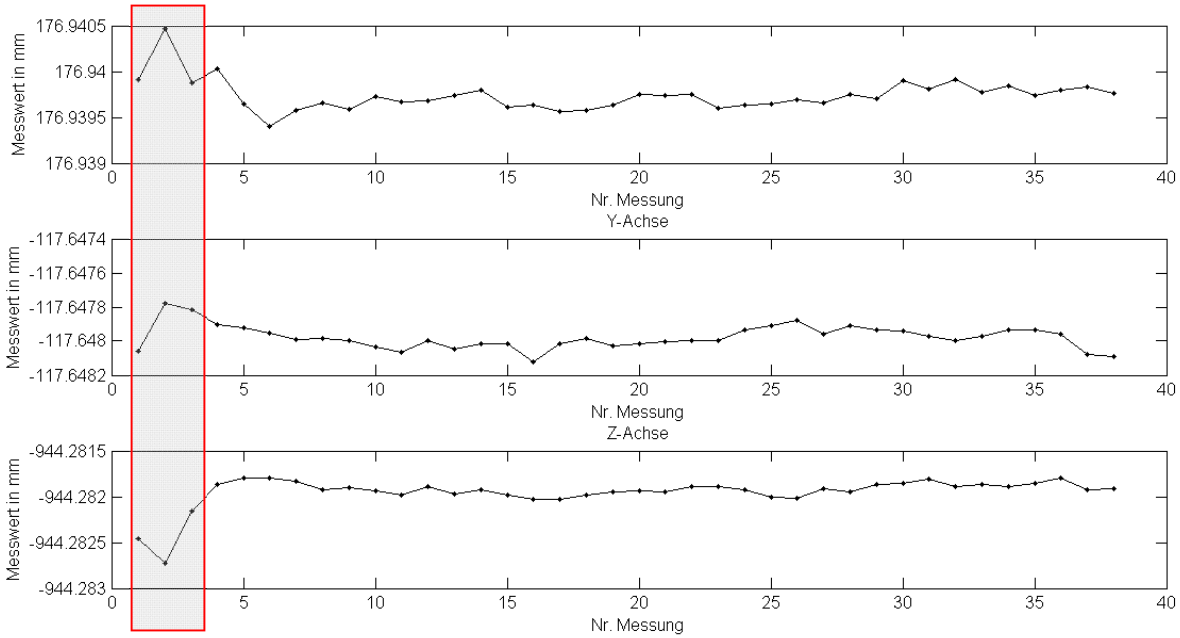

Diagram 2.1: x,y,z centre coordinates(Sphere A) during drift investigation, "Nr. Messung" is the number of measurement and "Messwert in mm" is the measured value in mm related to X,Y,Z axes

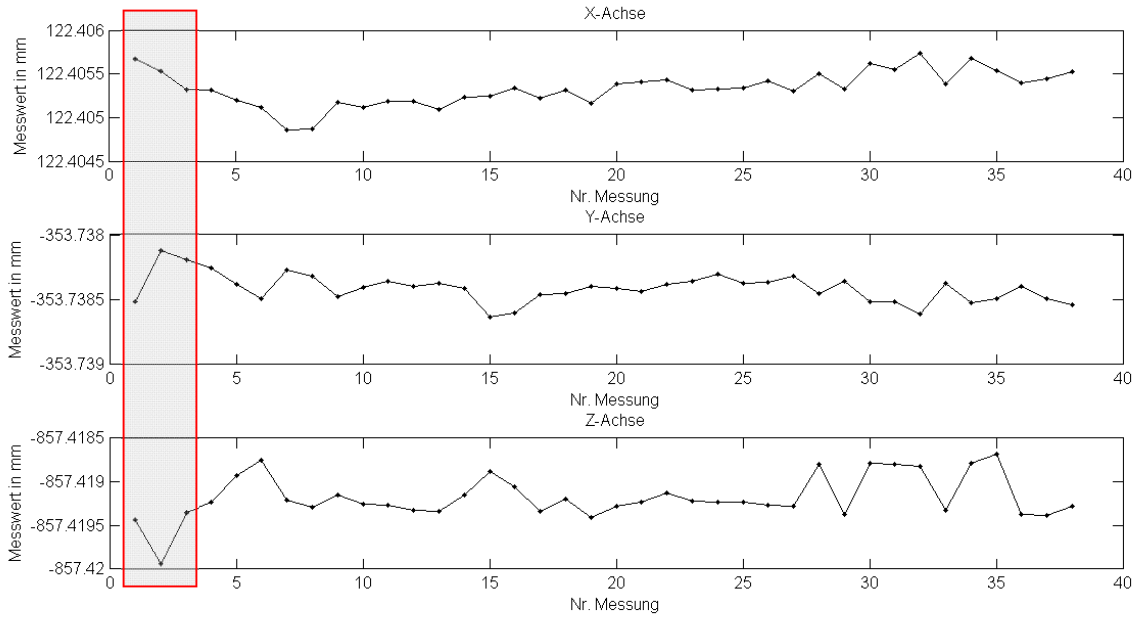

Diagram 2.2: Sphere B x,y,z centre coordinates values

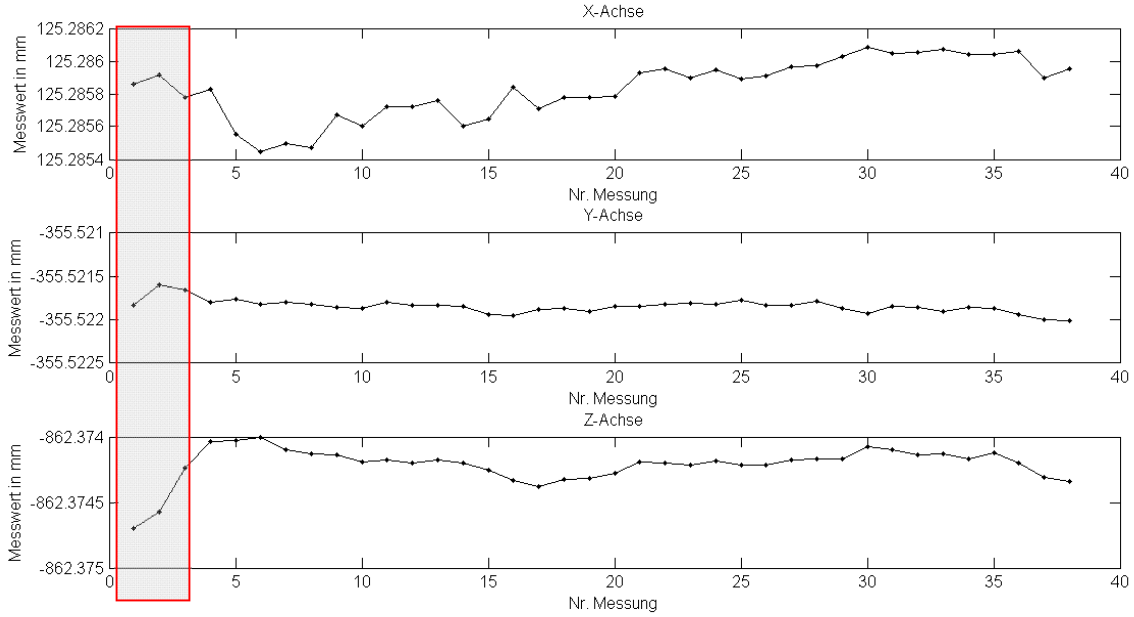

Diagram 2.3: Sphere C x,y,z centre coordinates values

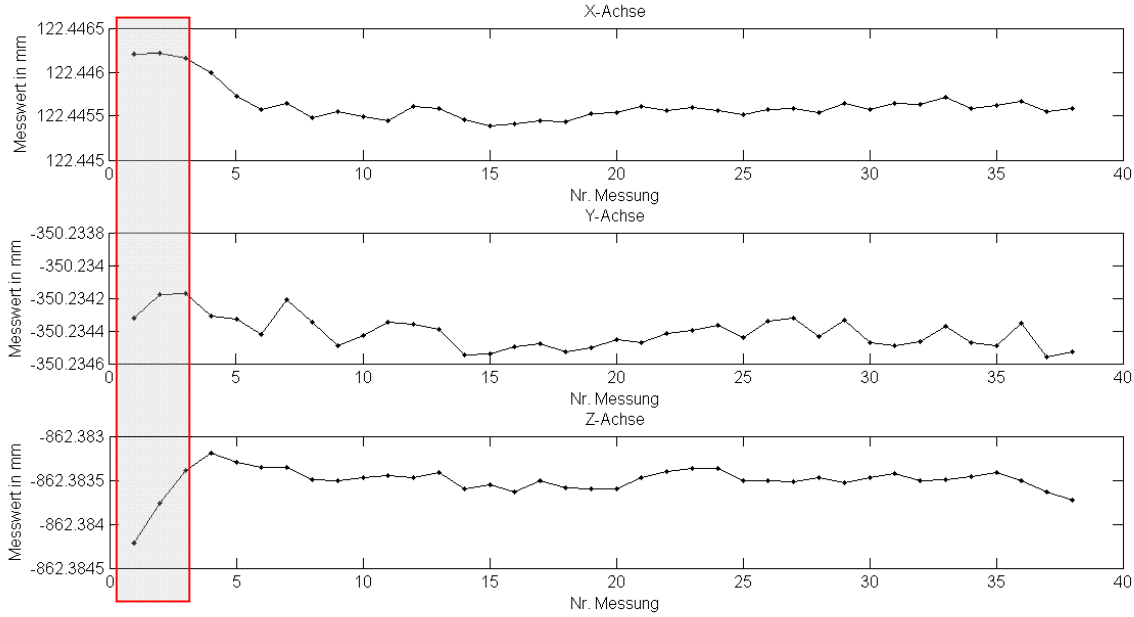

Diagram 2.4: Sphere D x,y,z centre coordinates values

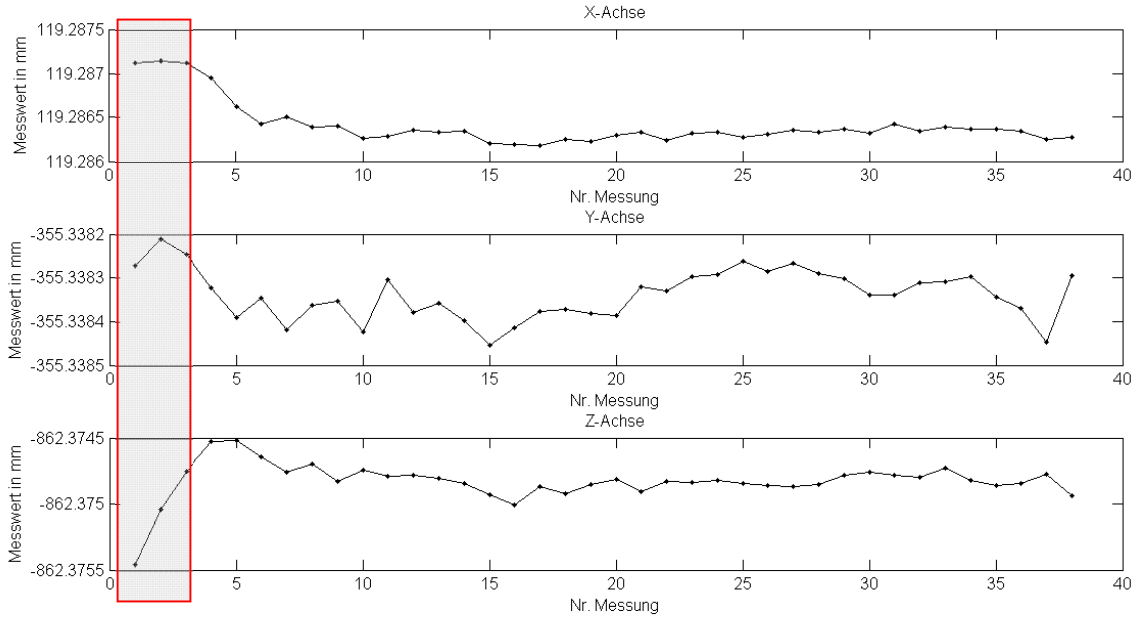

Diagram 2.5: Sphere E x,y,z centre coordinates values

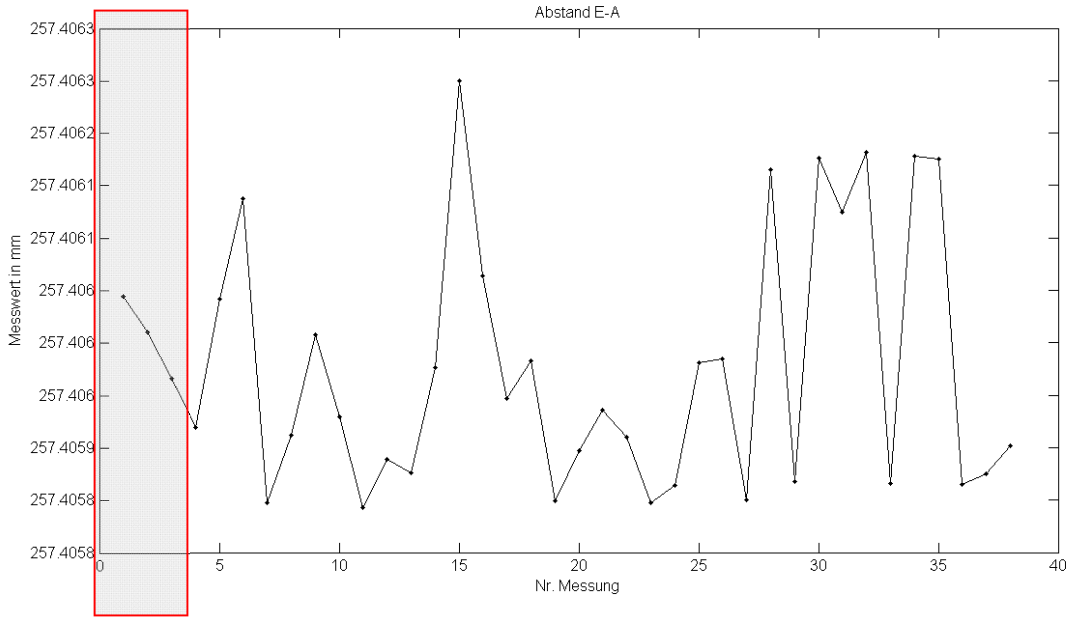

Diagram 2.6: Distance between E-A spheres

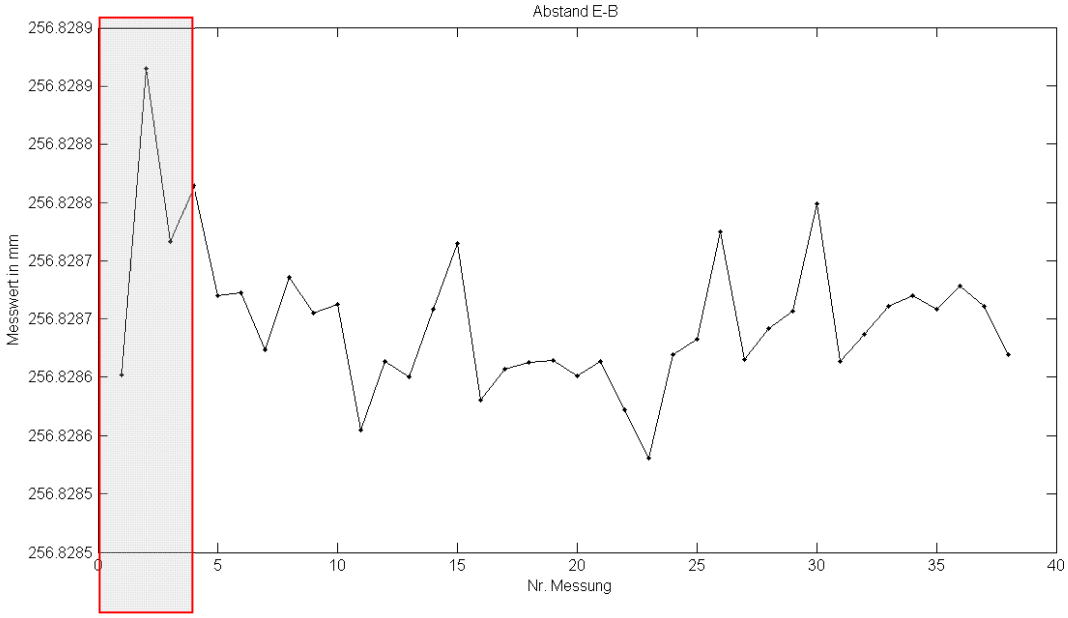

Diagram 2.7: Distance between E-B spheres

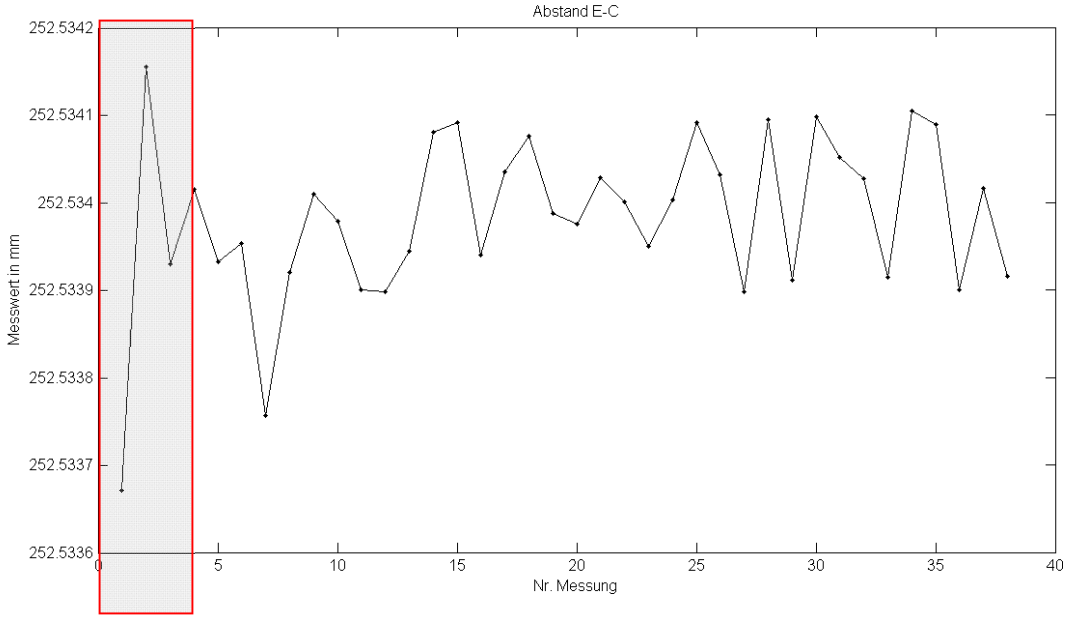

Diagram 2.8: Distance between E-C spheres

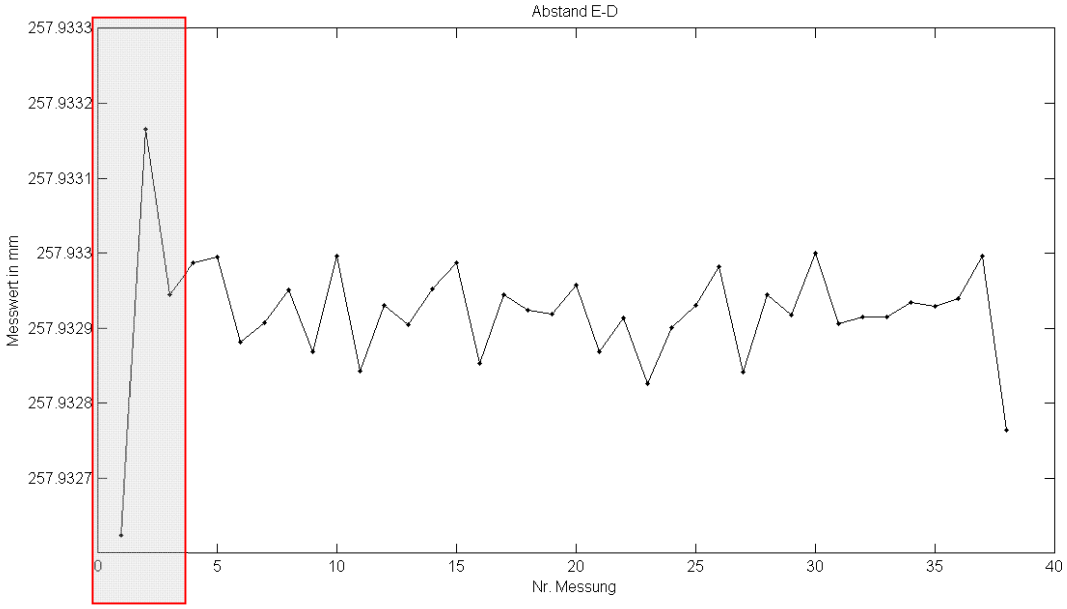

Diagram 2.9: Distance between E-D spheres

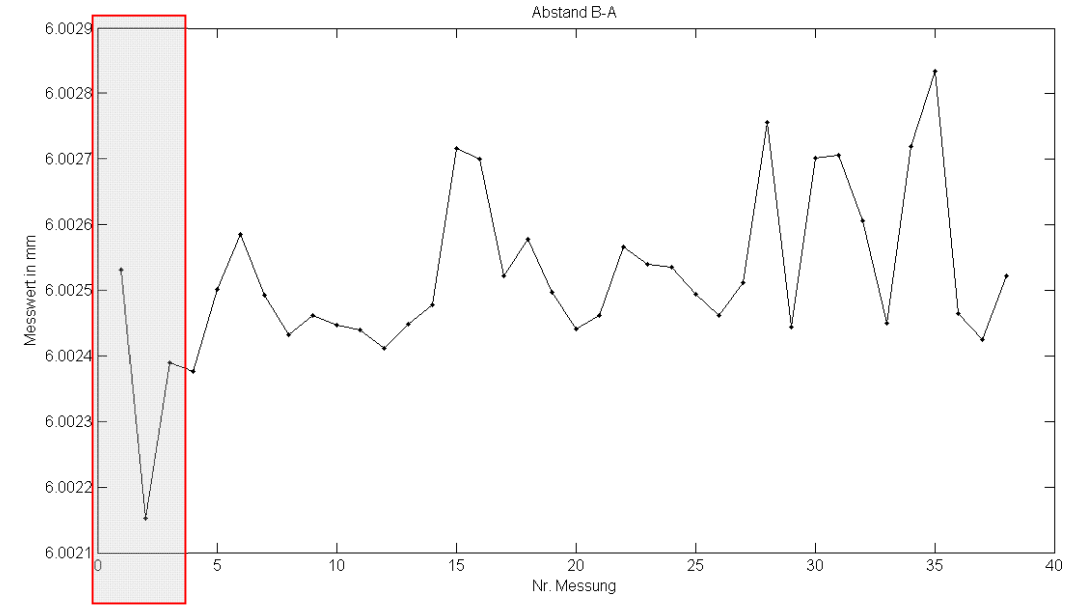

Diagram 2.10: Distance between B-A spheres

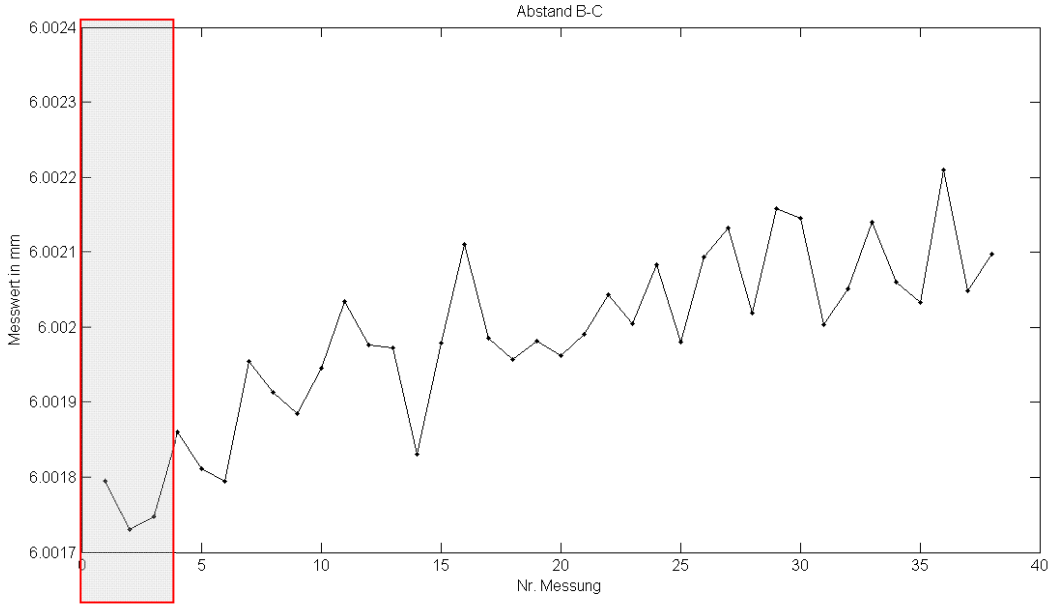

Diagram 2.11: Distance between B-C spheres

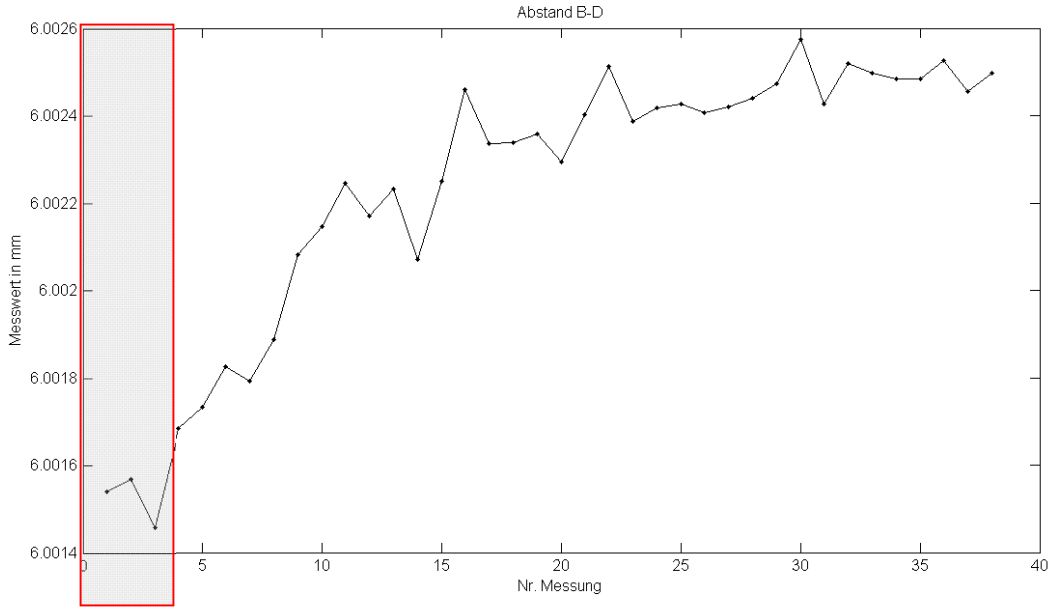

Diagram 2.12: Distance between B-D spheres

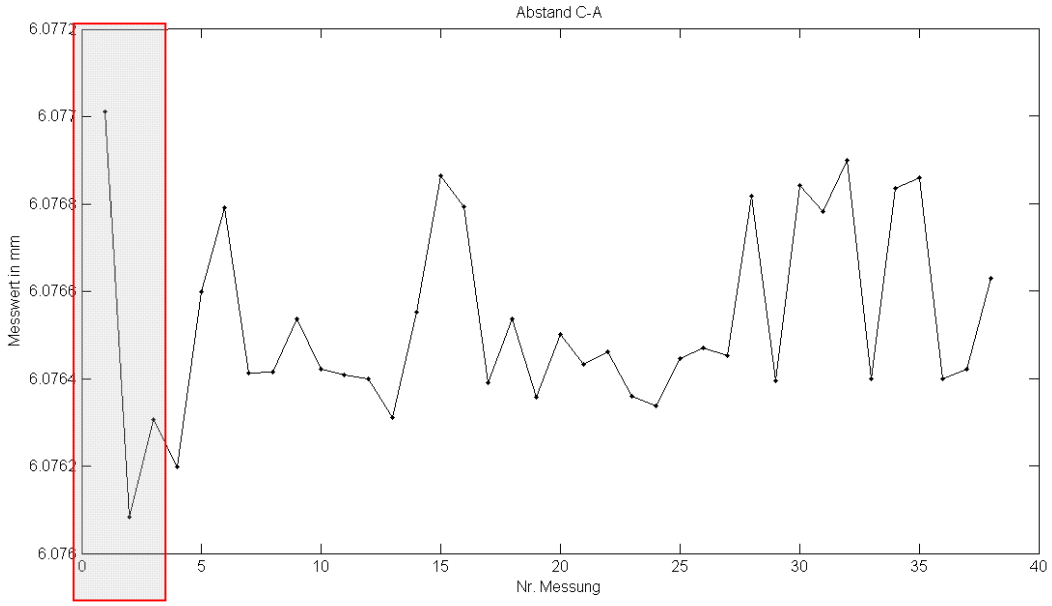

Diagram 2.13: Distance between C-A spheres

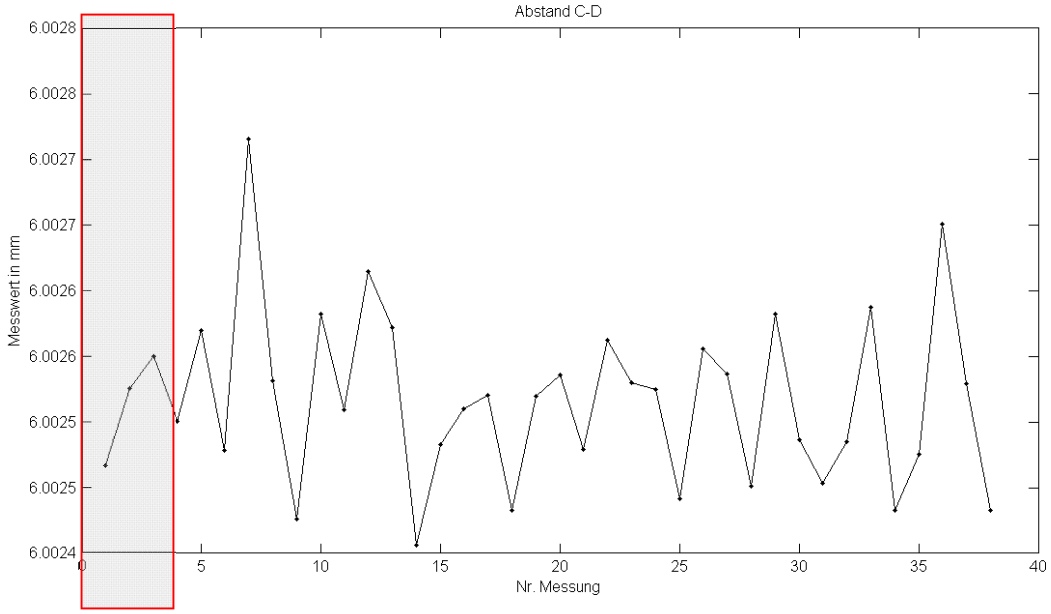

Diagram 2.14: Distance between C-D spheres

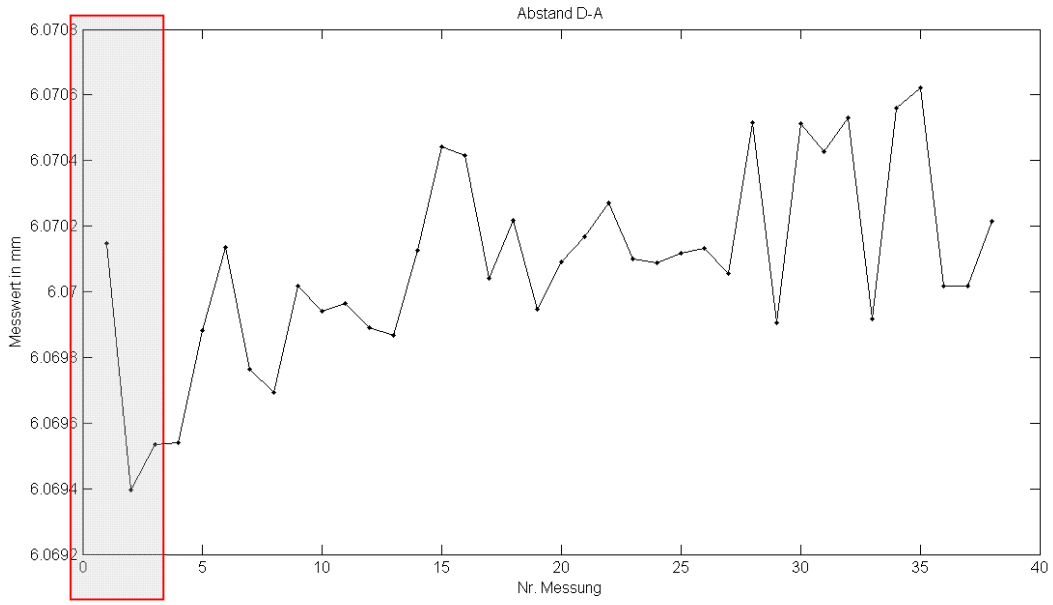

Diagram 2.15: Distance between D-A spheres

The temperature from 15:50 of 11 October to 17:20 of 12 October has been quite constant. In particular, there were 5 temperature sensors:

- T1 and T2 for the air conditioning control;
- T3 for the temperature of the reference sphere;
- T4 and T5 for the temperature of the workpiece (Tetrahedron).

The temperature has been recorded each 5 minutes for 26 hours as shown in diagram 2.16.

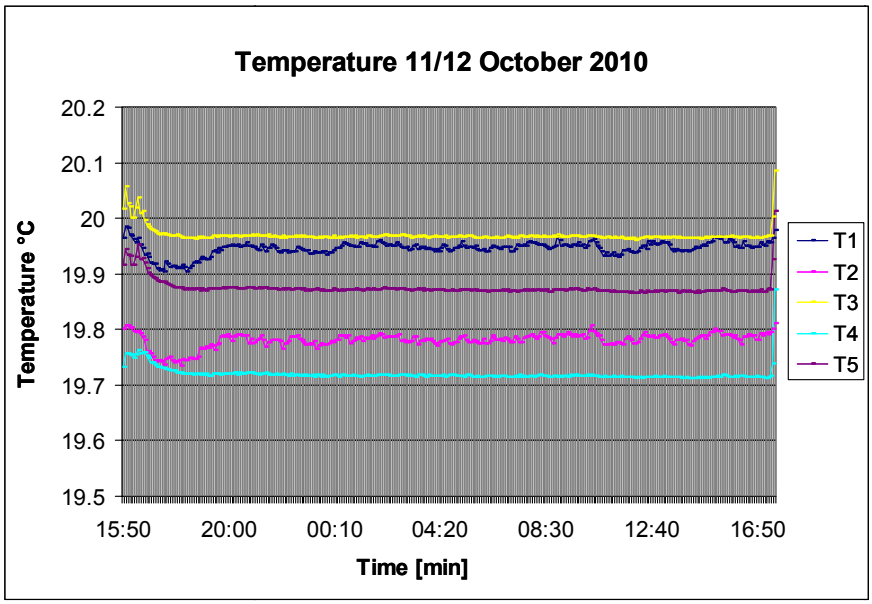

Diagram 2.16: Temperature 11/12 October 2010

The drift analysis leads to some conclusions:

- Drift value is quite small (no more than 0,8 µm in 26 hours);
- Drift is not linear, there is no trend;
- Temperature has been quite constant in 24 hours.

For example, as shown in the diagram 2.17, it is clear that at the beginning there is a bigger shift that becomes smaller and smaller with the time. After measurement number 17 the drift of sphere D is smaller for x, y, and z.

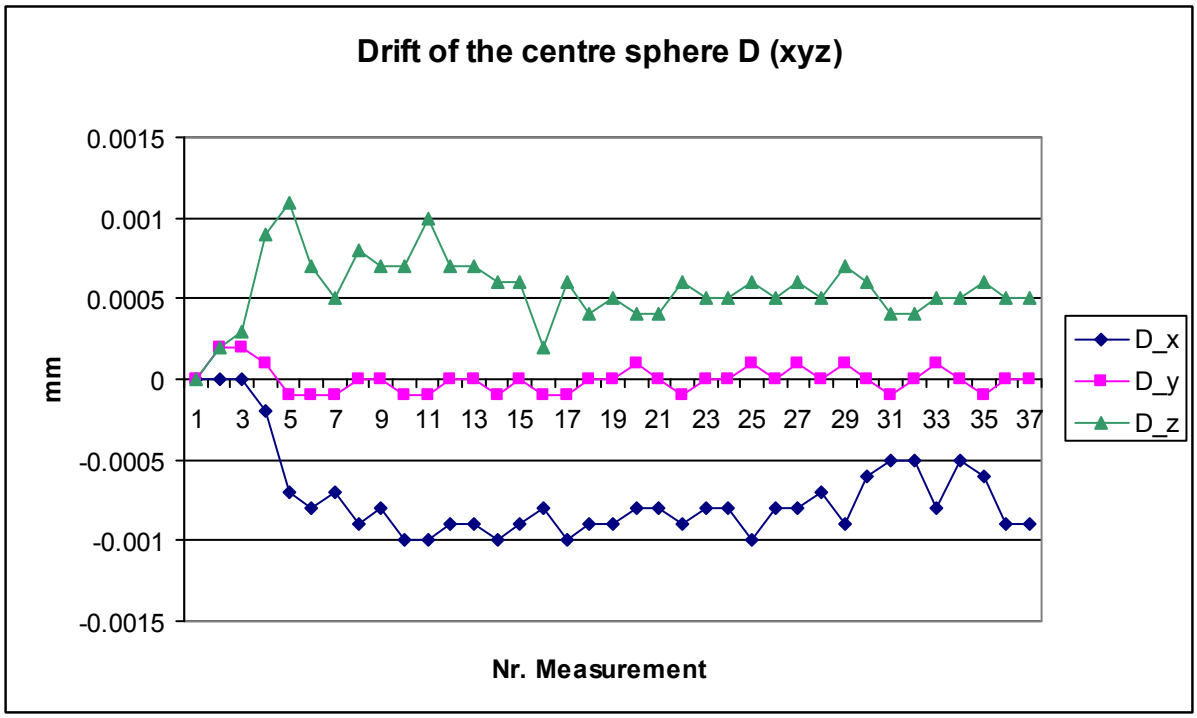

Diagram 2.17: Centre Coordinates x, y z of sphere D, absolute drift

These conclusions are really important in order to create an accurate and complete program for evaluating the form of the top sphere with several thousand points.

2.2 Definitive Program

From the drift investigation, the following parameters have been decided for a complete and definitive program:

- 3000 points on the top sphere (A);
- Almost 160 points on each lower sphere (B-C-D);

- Alignment has been repeated after each 300 points on the top sphere;
- Total time measurement of 8 hours circa (7h 38min for Tetrahedron 1 and 7h 31min for the second one);
- Data to be saved in local coordinate system (object).

2.2.1 Tetrahedron 1

Tetrahedron 1 has been measured for 7 hours and 38 minutes on 27th of October 2010.
The object has been fixed as shown in Figure 2.4.

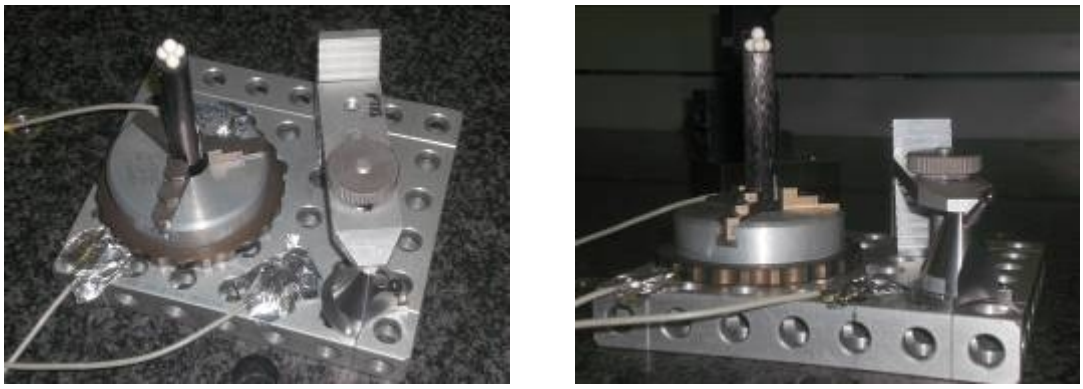

Fig. 2.4: Measurement setup of definitive program

The alignment has been decided as described in the following:

- xy axes (primary) : plane created by the three centres of lower spheres (called B,C,D);
- x axis (secondary): line created by two centres of lower spheres (called D,B);
- origin (zero point): centre of one of the lower sphere (the one called D).

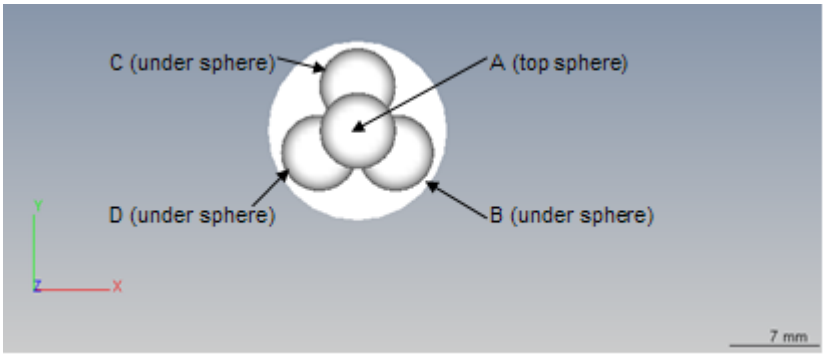

Fig. 2.5: Alignment description (Definitive program)

Figure 2.6 shows the 3000 measured tactile points on the top sphere (A). As already said, every 300 points the alignment has been repeated measuring the lower spheres, in order to minimize the drift error of the machine.

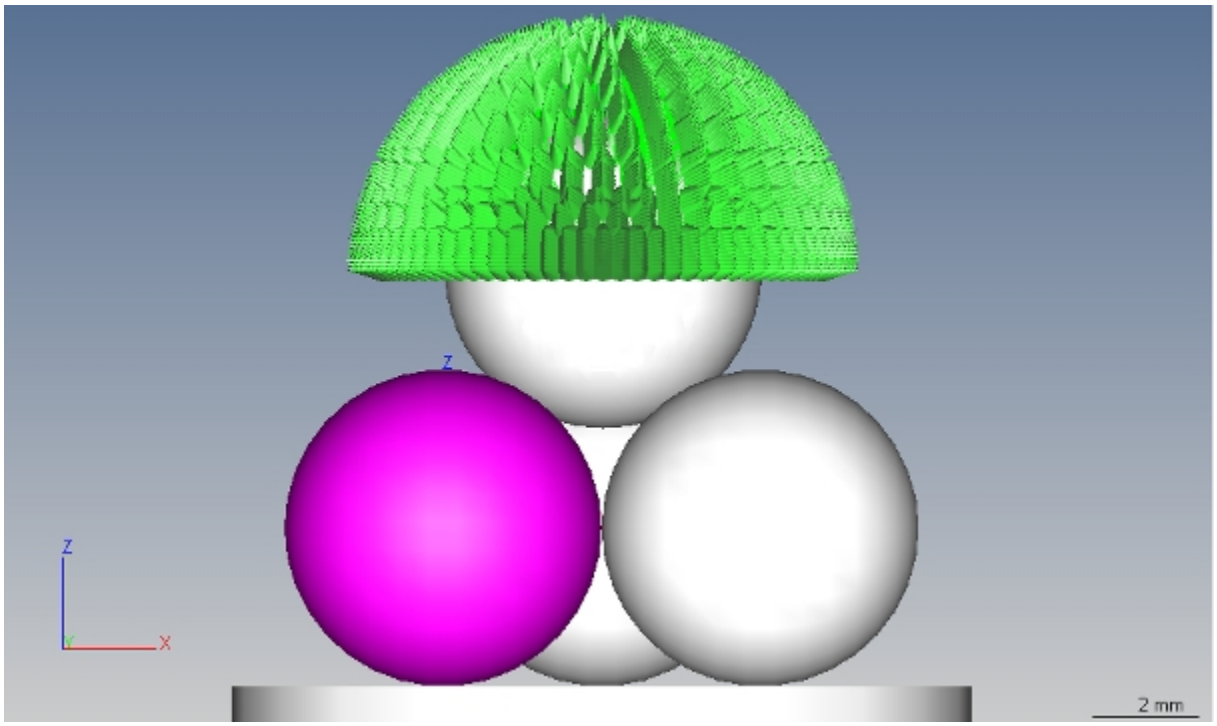

Fig. 2.6: 3000 measured points on sphere A (Calypso)

The alignment has been re-adjusted 10 times (circa each 45 minutes) and the diagram 2.18 shows how much the origin coordinates (in sphere D) have changed during the measurements. Moreover the diagram 2.19 plots the z values for the lower three spheres (BCD) that should be always stable in zero.

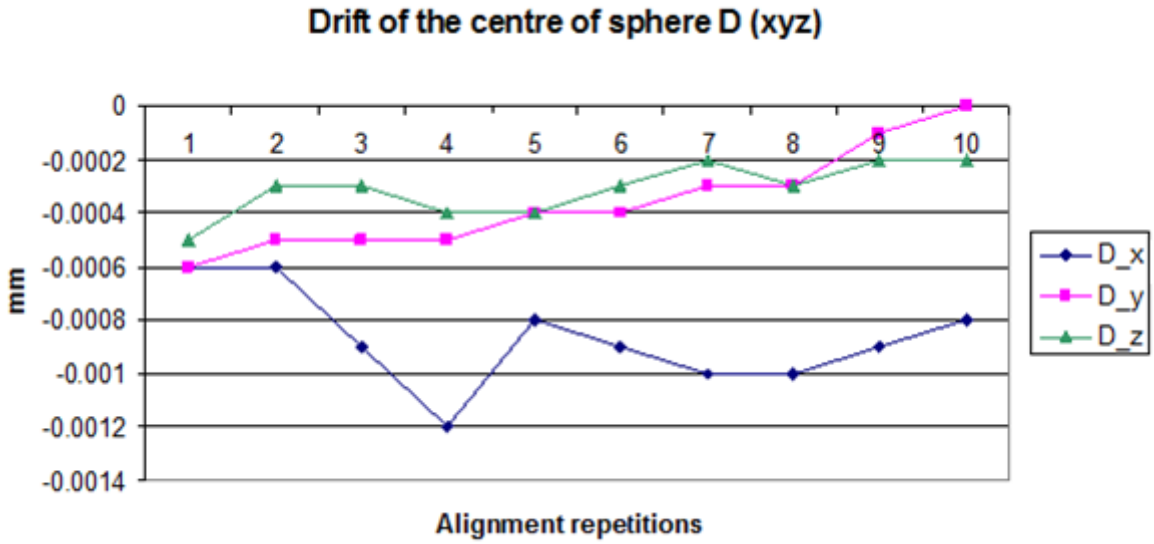

Diagram 2.18: Center coordinates x,y,z of sphere D (absolute drift)

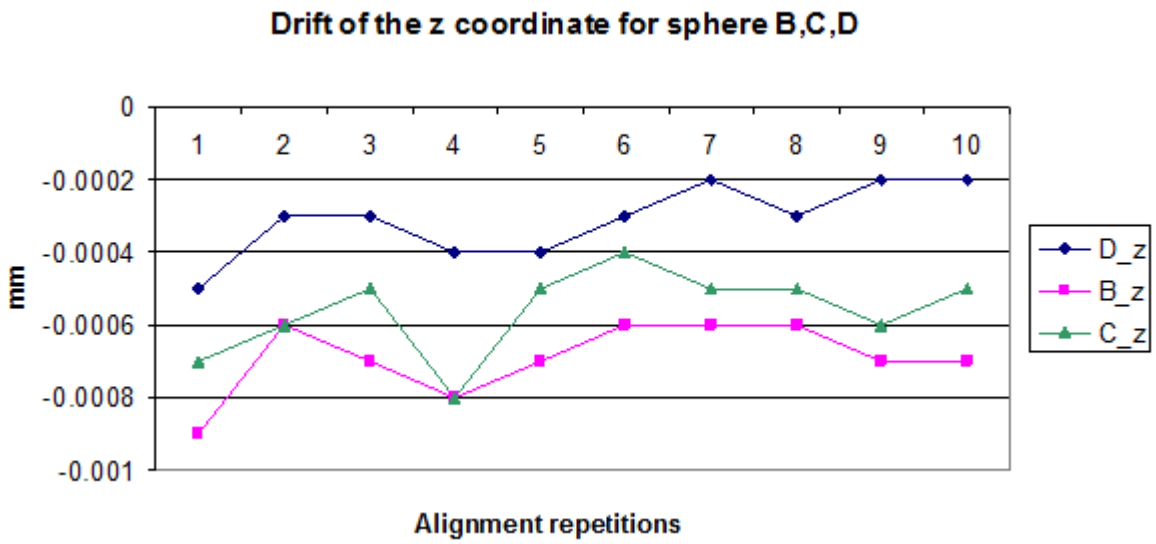

Diagram 2.19: z coordinate for BCD spheres

The z coordinates for spheres B,C,D created the alignment plane XY; its variation in seconds of grade is displayed in diagram 2.20, whereas diagram 2.21 shows the deviation of the x direction.

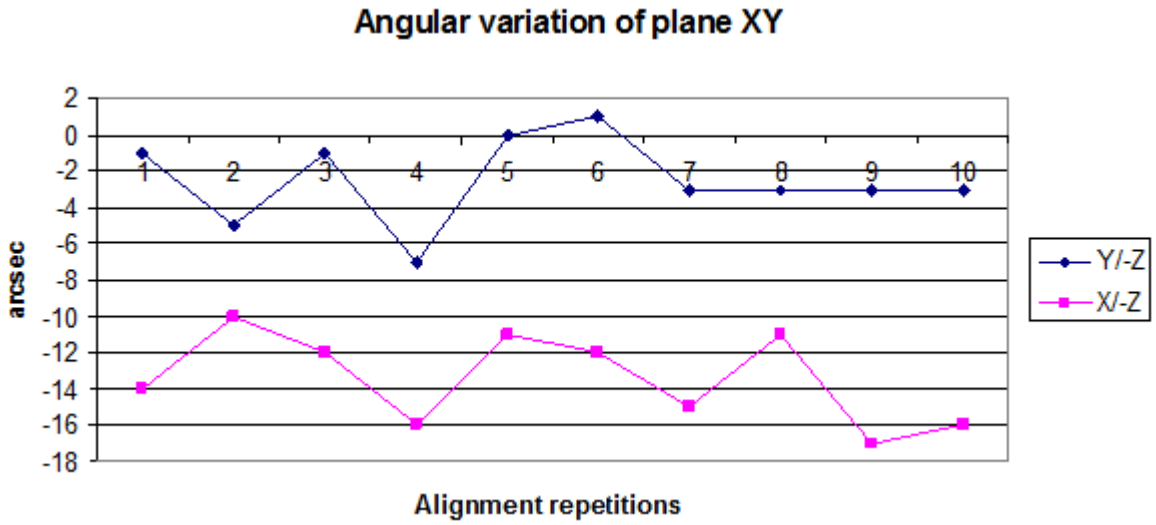

Diagram 2.20: Angular variation of plane XY

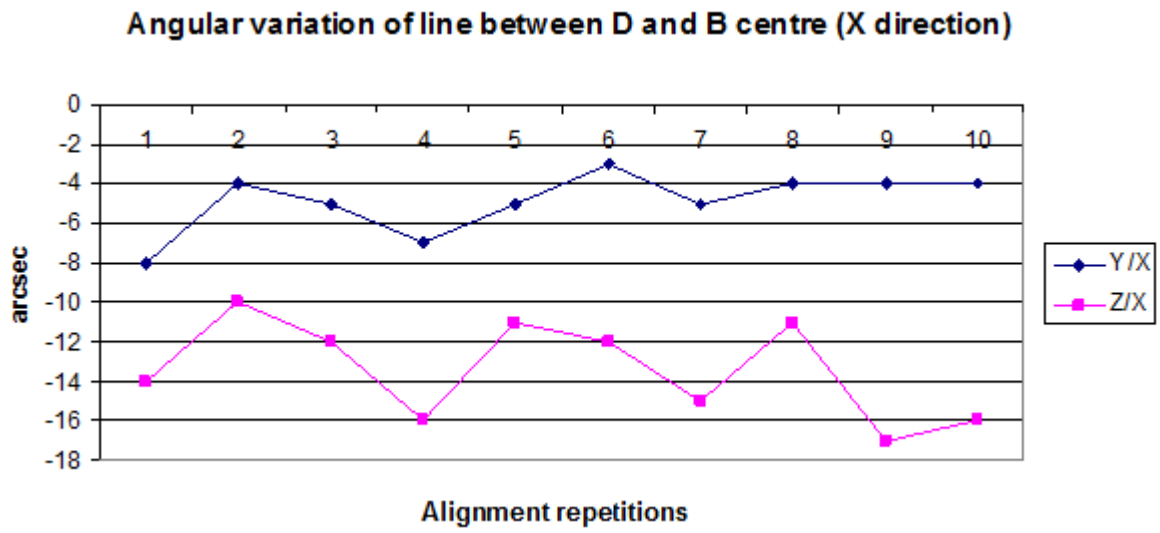

Diagram 2.21: Angular variation of line between D and B centre

In diagram 2.22 the temperature data are displayed.

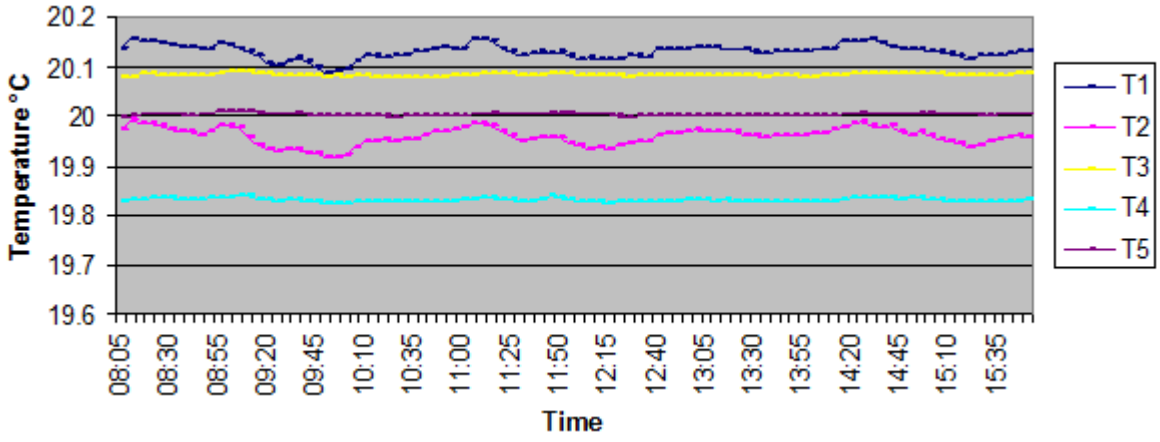

Diagram 2.22: Temperature of 27th October 2010

The tactile points of A sphere (in ASCII format) have been analyzed with the software "CloudFit" (PTB). In detail, figures 2.7-2.9 show very clearly how big the form deviation of the top sphere is.

Table 2.2: Cloud fit output Tetrahedron 1

Tetrahedron 1	
Xc	3.06912 mm
Yc	1.68585 mm
Zc	4.95898 mm

Diameter	6.08672 mm
Min. Dev.	-0.06784 mm
Max. Dev.	0.02715 mm
Form Dev. (Gauss)	0.09499 mm

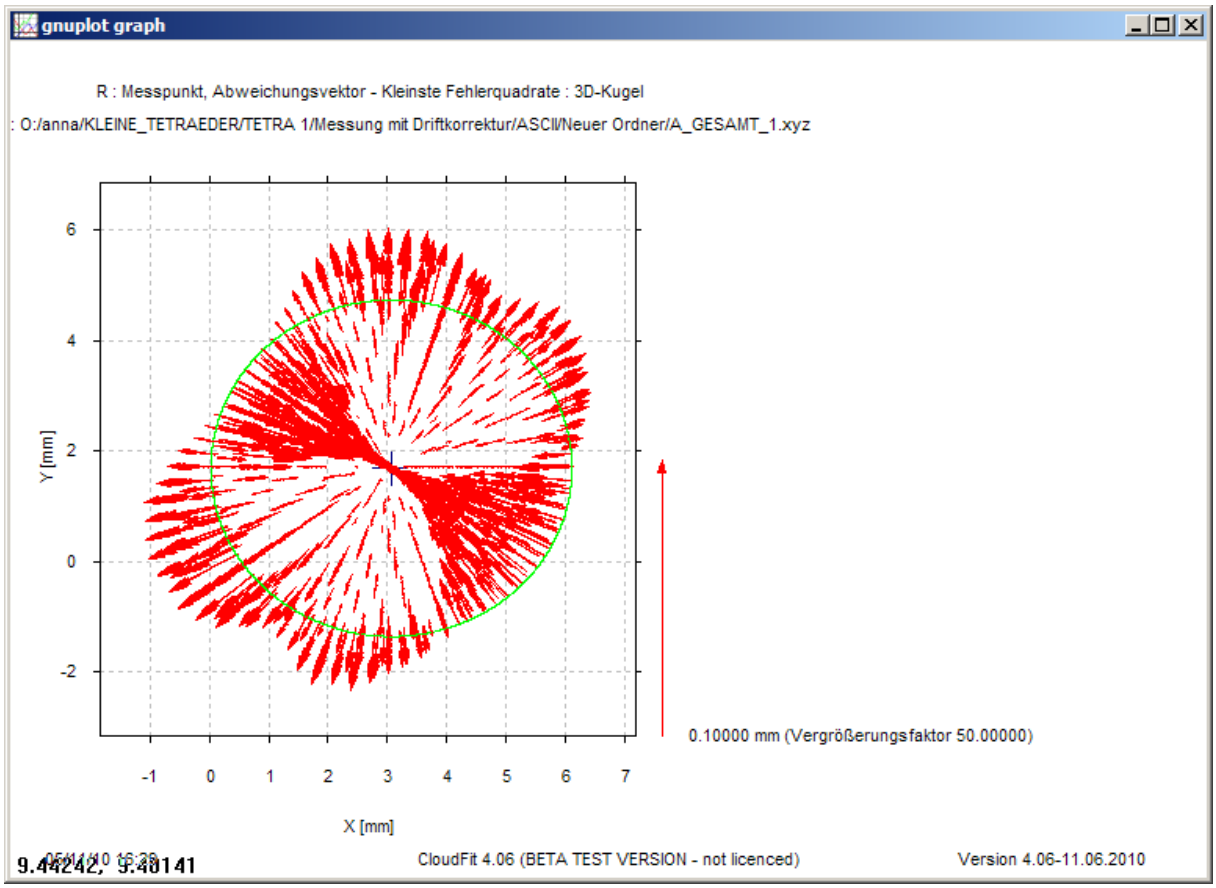

Fig. 2.7: Sphere A (Cloud fit)

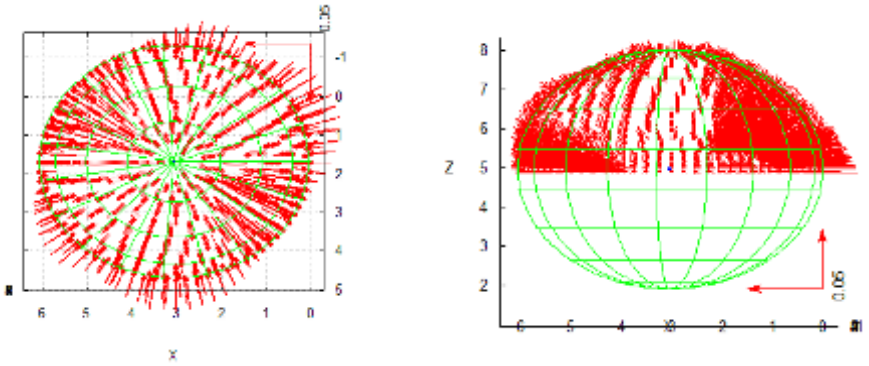

Fig. 2.8: Sphere A (Cloud fit)

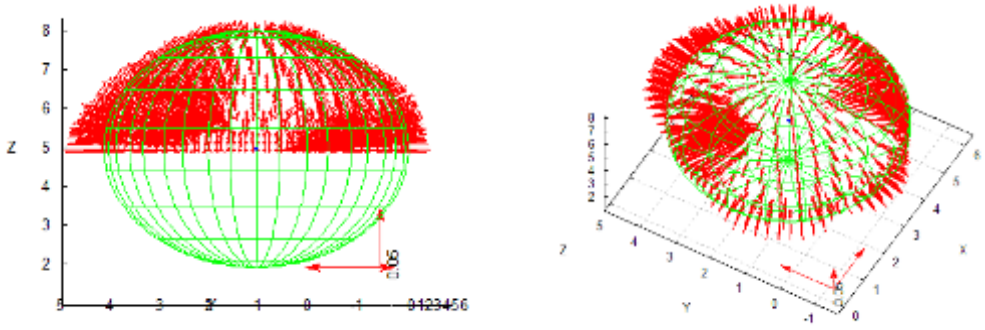

Fig. 2.9: Sphere A (Cloud fit)

2.2.2 Drift Investigation

The analysis of the drift can be conducted again with the definitive measurements in order to confirm and to control the drift of the machine and the workpiece. Each ca. 45 minutes the alignment has been repeated and recorded by the software Calypso. The investigation of the variation of the centre coordinates the xy plane and the x direction lead to further considerations about drift, especially in comparison with the drift results of the previous Calypso program.

In table 2.3 the incremental and maximal deviation from the null is shown for the centre of sphere D.

It is important to underline that the total drift for each single coordinate (divided for time interval of 8 hours) is comparable to the drift from the drift program (divided 26 hours), see table 2.4.

Table 2.3: Alignment deviation (definitive program)

	Incremental [mm]	**Maximal [mm]**	**/8 hours [mm]**
Dx	-0.0087	-0.0012	-0.0010875
Dy	-0.0036	-0.0006	-0.00045
Dz	-0.0031	-0.0005	-0.0003875

Table 2.4: Alignment deviation (Drift program)

D_x [mm]	**D_y [mm]**	**D_z [mm]**
0	0	0
0	0.0002	0.0002
0	0.0002	0.0003
-0.0002	0.0001	0.0009
-0.0007	-1E-04	0.0011
-0.0008	-1E-04	0.0007
-0.0007	-1E-04	0.0005
-0.0009	0	0.0008
-0.0008	0	0.0007
-0.001	-1E-04	0.0007
-0.001	-1E-04	0.001
-0.0009	0	0.0007
-0.0009	0	0.0007
-0.001	-1E-04	0.0006

-0.0009	0	0.0006
-0.0008	-1E-04	0.0002
-0.001	-1E-04	0.0006
-0.0009	0	0.0004
-0.0009	0	0.0005
-0.0008	0.0001	0.0004
-0.0008	0	0.0004
-0.0009	-1E-04	0.0006
-0.0008	0	0.0005
-0.0008	0	0.0005
-0.001	0.0001	0.0006
-0.0008	0	0.0005
-0.0008	0.0001	0.0006
-0.0007	0	0.0005
-0.0009	0.0001	0.0007
-0.0006	0	0.0006
-0.0005	-1E-04	0.0004
-0.0005	0	0.0004
-0.0008	0.0001	0.0005
-0.0005	0	0.0005

	-0.0006	-1E-04	0.0006
	-0.0009	0	0.0005
	-0.0009	0	0.0005
	-0.027	-1E-04	0.0205
/26 hours	-0.00103846	-3.84615E-06	0.00078846

2.2.3 Additional measurement with F25

Tetrahedron 1 has been measured also with Zeiss F25. 5000 points have been taken for ten times, and the results are shown in tables 2.5 and 2.6. Before each measurement repetition, the alignment (as already shown for Carat UPMC 1200) has been recalled.

Table 2.5: F25 measurement results for Top Sphere

	Mean (10 measurements)	**Std. Dev.**
	mm	µm
x-Pos	-1.6844699	0.119
y-Pos	3.0738388	0.344
z-Pos	4.9596869	0.136
Radius	3.042717	0.009
Form Deviation (minimum zone)	0.1032253	0.080

Table 2.6: F25 vs Carat

Diameter F25	6.085434	mm
Diameter Carat	6.086700	mm
Difference F25 - Carat	-1.266	µm

The measurements have been analyzed with CloudFit as shown in figures 2.10-2.13.

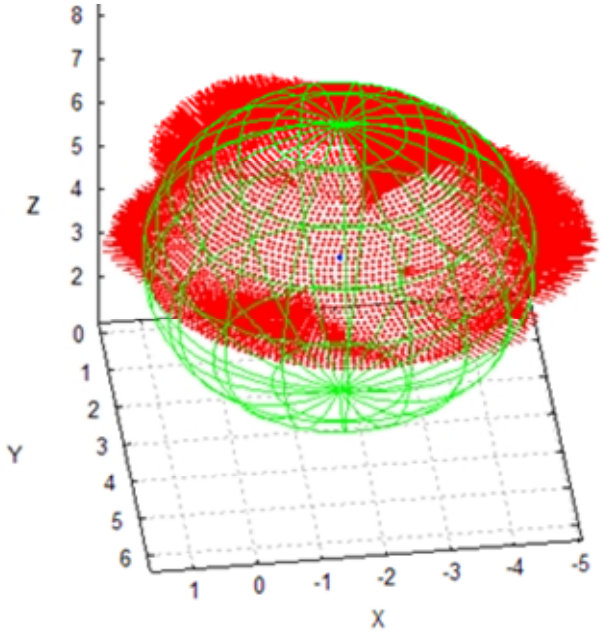

Fig. 2.10: Sphere A_F25 (Cloud fit)

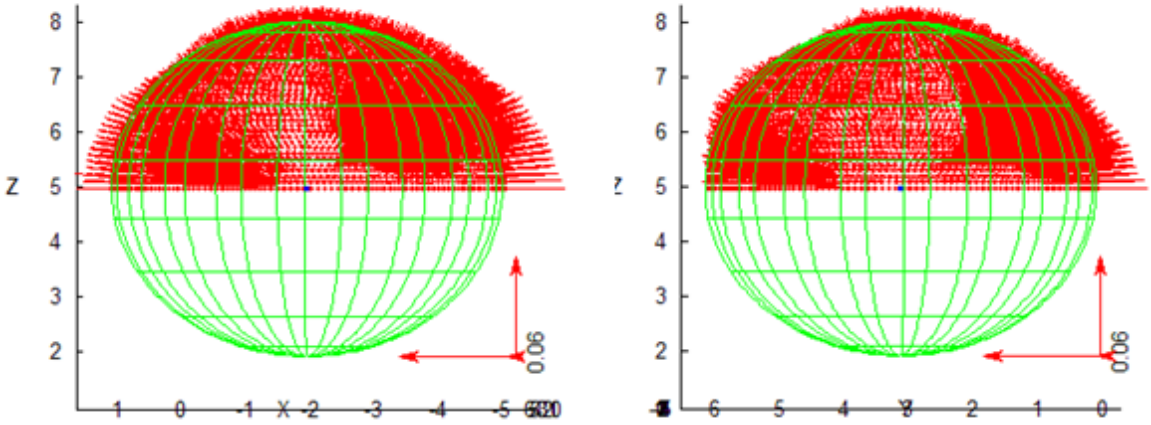

Fig. 2.11: Sphere A_F25 (Cloud fit)

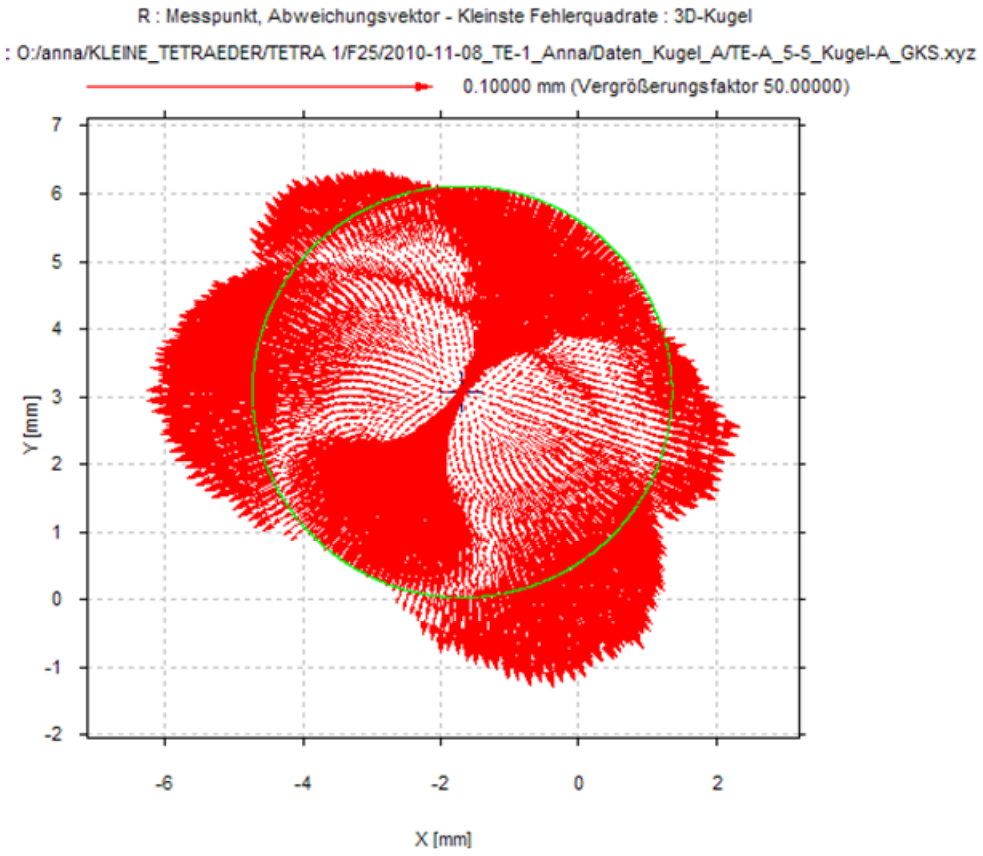

Fig. 2.12: Sphere A_F25 (Cloud fit)

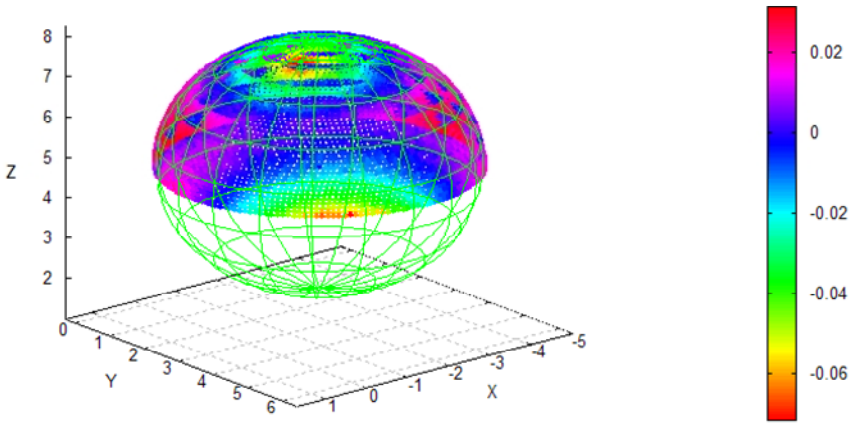

Fig. 2.13: Sphere A_F25 (Cloud fit)

2.2.4 Tetrahedron 2

The measuring procedure of Tetrahedron 2 is the same as the one of Tetrahedron 1.

Tetrahedron 2 has been measured with the Zeiss Carat machine for 7 hours and 31 minutes on 28th of October 2010.

The object has been fixed as shown in figure 2.14.

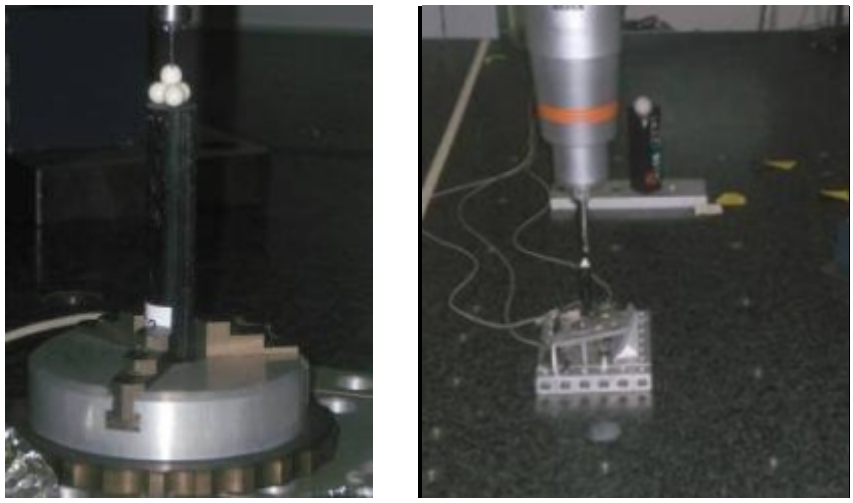

Fig. 2.14: Thetrahedron 2 measurements

Figure 2.15 shows the 3000 measured tactile points on the top sphere (A).

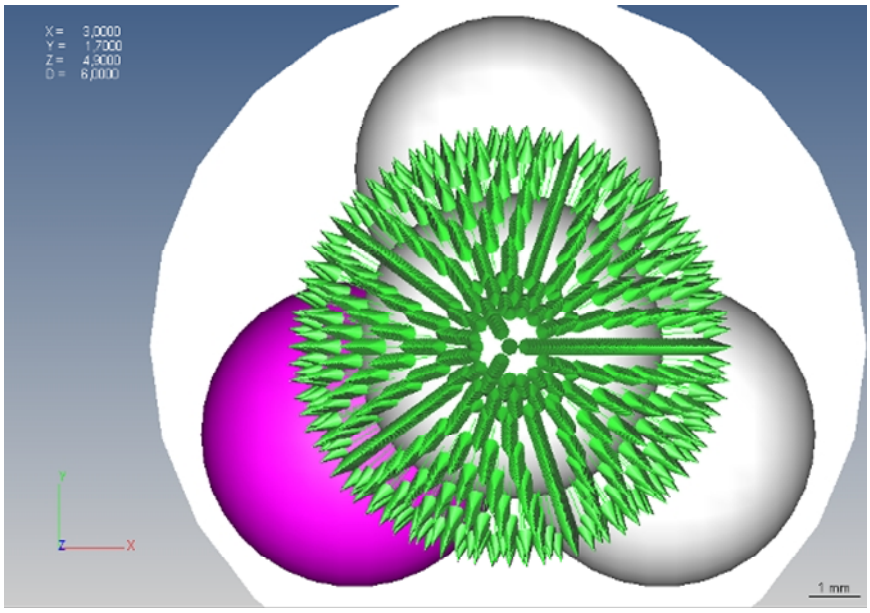

Fig. 2.15: 3000 points sphere A (Calypso)

In diagram 2.23 the temperature data are displayed.

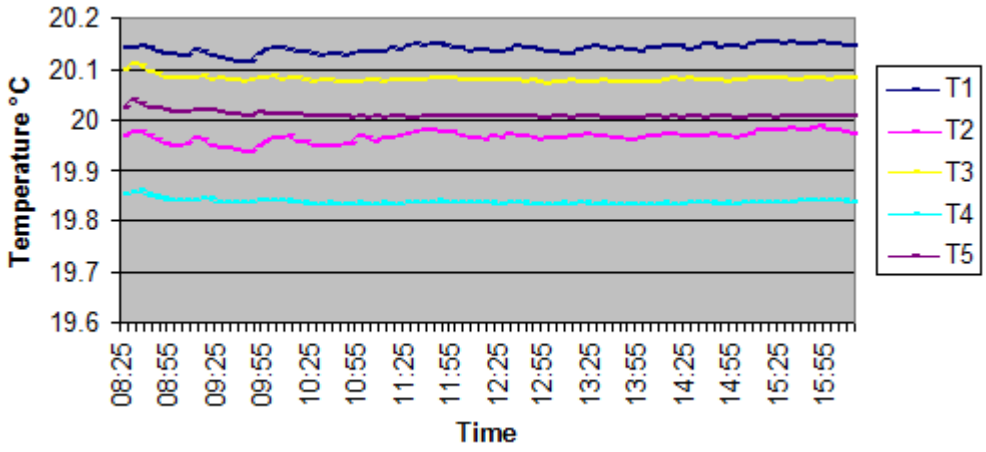

Diagram 2.23: Temperature of 28th October 2010

The tactile points of sphere A (in ASCII format) have been analyzed with the software "CloudFit" (PTB). In detail, figure 2.15-2.17 shows very clearly how big the form deviation of the top sphere is.

Table 2.7: Cloud fit output Tetrahedron 3

Tetrahedron 2	
Xc	2.98257 mm
Yc	1.74833 mm
Zc	5.00275 mm
Diameter	6.04798 mm
Min. Dev.	-0.08553 mm
Max. Dev.	0.04556 mm
Form Dev. (Gauss)	0.13109 mm

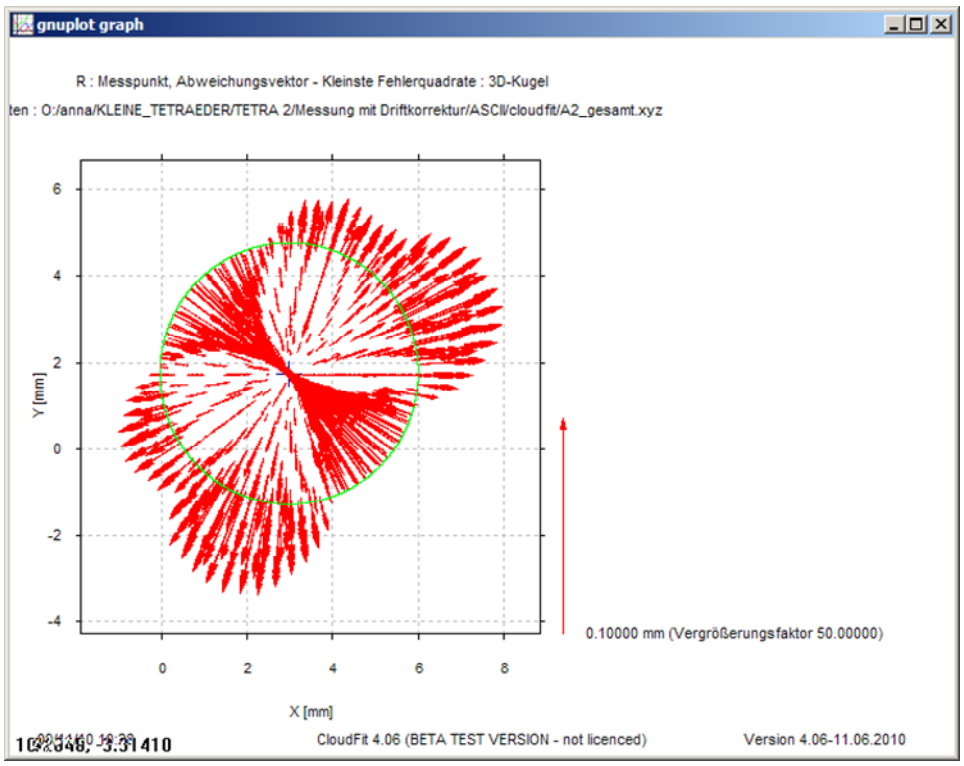

Fig. 2.15: Sphere A_2 (Cloud fit)

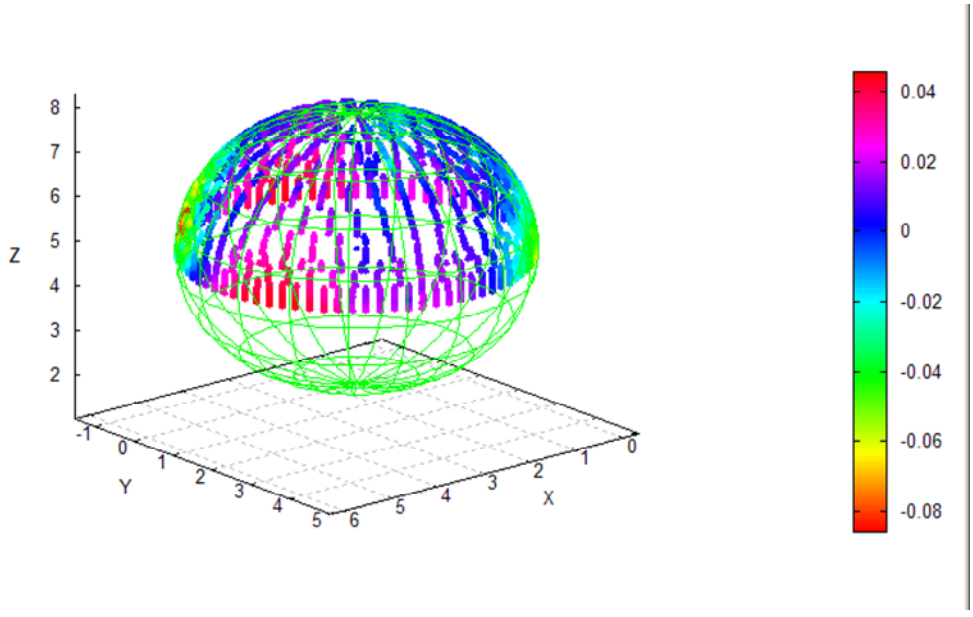

Fig. 2.16: Sphere A_2 (Cloud fit)

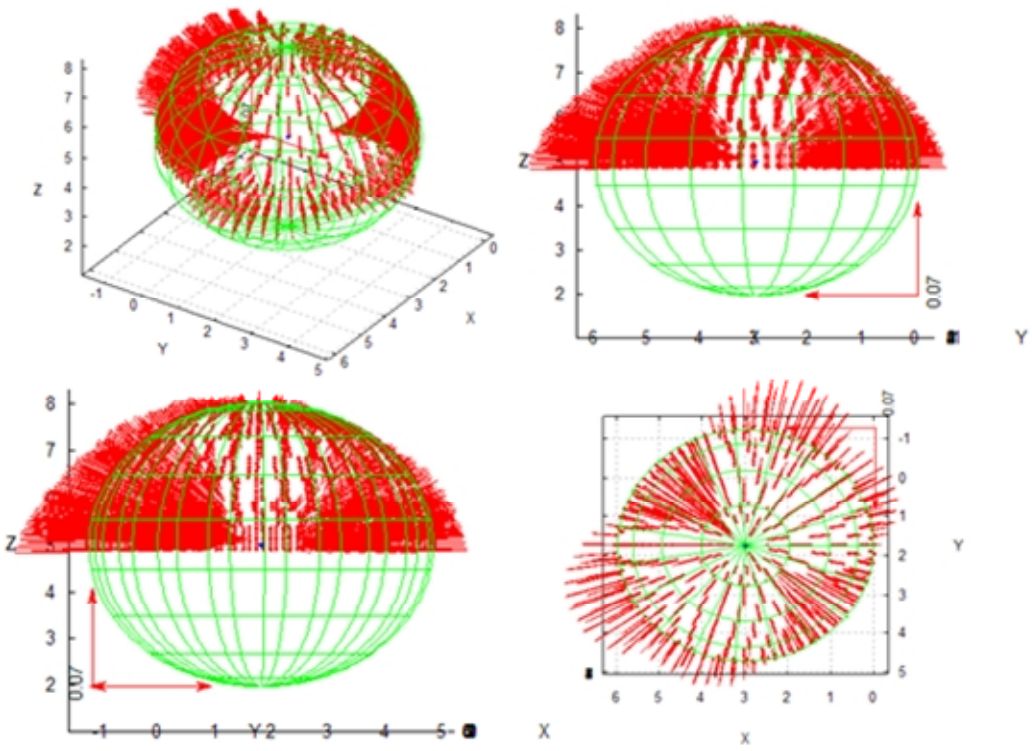

Fig. 2.17: Sphere A_2 (Cloud fit)

3. VCMM

The VCMM [76] (Virtual coordinate measuring machine) offers the opportunity of calculating the task-specific measurement uncertainty. The VCMM determines the measurement uncertainty by Monte Carlo Simulation. This method complies with the principles laid down by national and international standards for the uncertainty calculation (GUM) and the VDI/VDE Guideline 2617-7.

The VCMM is completely integrated into the operating and evaluation software of the CMM (calypso 5.0). It takes all influences producing effects on the measurement task into consideration and links all deviations in order to determine the task-specific measurement uncertainty.

For the calculation of the deviation, the VCMM needs information about the CMM, the workpiece and the environment as:

- Systematic deviations of the slideways;

- Uncertainties due to calibration;
- Thermal deformation of the slideways;
- Thermal expansion of the scales;
- Drift occurring in the course of the measurement;
- Uncertainties of the stylus calibration;
- Thermal expansion of the workpiece;
- Roughness of workpiece surfaces.

The figure 3.1 shows the VCMM procedure.

In the protocols all the uncertainties are shown in the column "Messunsicherheit". The uncertainties values are:

- always under 1,5 µm concerning centre points of the spheres and their diameters;
- always under 3 µm concerning the form deviations.

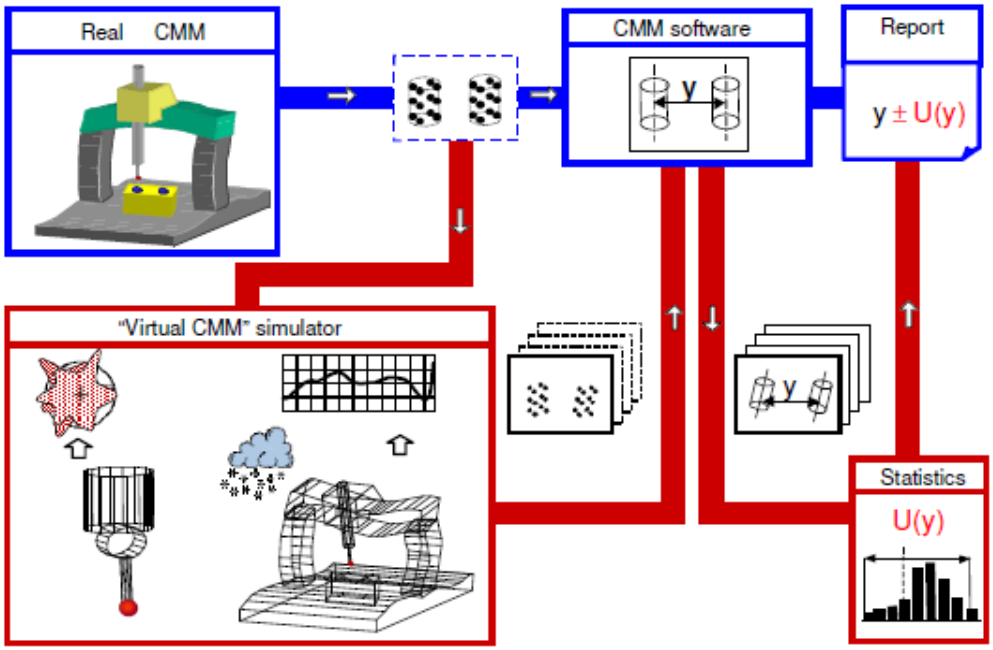

Fig. 3.1: VCMM procedure

4. CT Measurements

The CT measurements have been taken by BAM (Federal Institute for Materials Research and Testing) in Berlin between August and September 2010. Figures 4.1 and 4.2 show the CT measurement set up.

Table 4.1: CT System Details (BAM)

Source	µFocus, 225 kV
Detector System	2048 Pixel x 2048 Pixel
Magnification	up to 40:1
Max Object Size	180 mm
Spatial Resolution	10 µm
Contrast Resolution	from 1% to 5%

- Tetrahedron 1 (1st September 2010) - Name: 4044a.bd

Voxel size : 0.00968 mm

Angle increment : 0.2 grad

Exposure time : 4.0 s

Distance Source-Detector : 1152.9399 mm

Distance Source-Object: 55.8023 mm

Voltage : 80 kV

Current : 100 µA

Start : 1.9.10//10:36

Stop : 1.9.10//12:36

Pre filter : 0,25 mm Cu

- Tetrahedron 2 (25th August 2010) - Name: 4033a.bd

Voxel size: 0.00793 mm

Angle increment : 0.2 grad

Start angle : 0.00 grad

Exposure time : 4 s

Distance Source-Detector : 1152.9399mm

Distance Source-Object : 45.5411 mm

Voltage : 80 kV

Current : 100 µA

Start : 25.8.10//15:27

Stop : 25.8.10//17:28

Pre filter : 0,25mm Cu

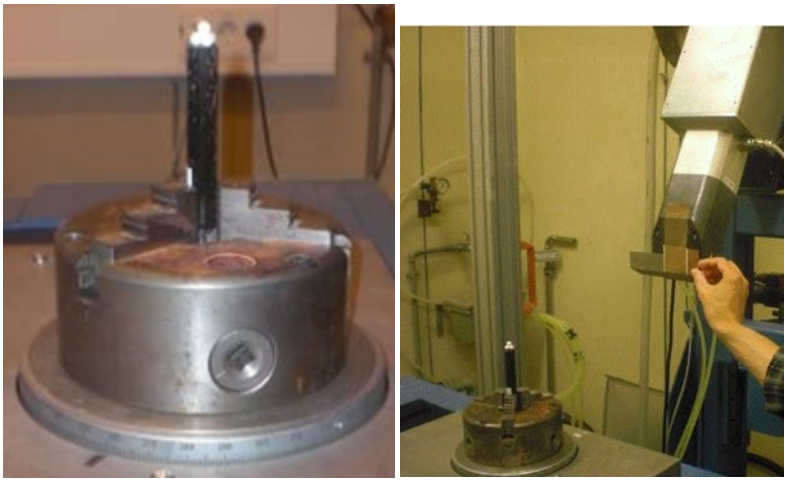

Fig. 4.1: (left) Fixing of Tetrahedron 1 during CT measurement, (right) pre filter 0,25mm Cu

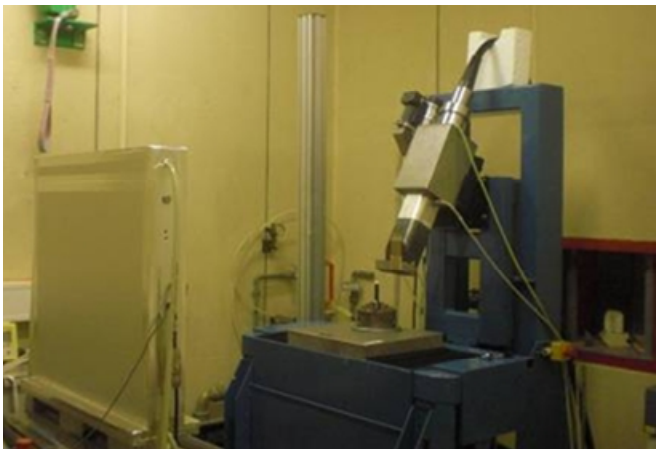

Fig. 4.2: CT measurement set up

Both measurements scale factor has been corrected using a reference object (Rubin star probe see Fig. 4.3).

Fig. 4.3: Rubin star probe

This object has been measured after each CT measurement, keeping the similar distances Source-Object-Detector and same energies.

Here following adjusted volume resolutions determined with reference object are reported:

- (Tetrahedron 1) 0.009779 → 0.00968 mm;
- (Tetrahedron 2) 0.008044 → 0.00793 mm.

In the software VG Studio Max it is possible to calculate the distances between spheres. In order to correct the scale error more accurately, the distances between the lower spheres (BCD) have been compared with the tactile distances. When a systematic error in the difference between these spheres distances is found, the voxel is corrected as following:

Voxel size (origin) / (ct distance*tactile distance) = voxel size (new)

Tetrahedron 1: in table 4.2 the column "CT-tactile" shows that there is no systematic deviation. For this reason the voxel size has been kept as 0.00968 mm. Whereas there is a systematic error in Tetrahedron 2, as shown in table 4.3 and the voxel size has been corrected to 0,00796 mm.

Table 4.2: calculation of eventual systematic error Tetrahedron 1

				Voxel size
Name	**CT**	**tactile**	**CT tactile**	**0.00968**
Distance B-C	6.00244	6.00187684	0.00056316	0.009679092
Distance B-D	6.002301	6.0025	-0.000199	0.009680321
Distance C-D	6.003752	6.00231347	0.00143853	0.009677681
				New Voxel size
			Average	0.009679031

Table 4.3: calculation of eventual systematic error Tetrahedron 2

				Voxel size
Name	**CT**	**tactile**	**CT tactile**	**0.00793**
Distance B-C	5.983208	6.00270628	-0.0194982	0.007955843
Distance B-D	5.982886	6.0015	-0.018614	0.007954672
Distance C-D	5.98347	6.00245633	-0.0189863	0.007955163
				New Voxel size
			Average	0.007955

4.1 VG Studio Max 2.1.1 and ATOS

The raw CT Data from BAM measurement (.bd files) have been imported in VG Studio Max 2.1.1 software (VG Version 4.0.0). This software is applied for:

- building up a STL file for the further nominal/actual comparison (CT against Tactile measurements);
- make the correct alignment;
- correct the scaling factor (residual), calculating the distances between the centres of the lower spheres (B,C,D);
- volume rendering → calibrate objects with a proper gray value;
- consider only what is going to be measured → Region Of Interest.

4.1.1 Extraction Methods in VG Studio Max

In order to evaluate the best extraction method (Trade-off between Speeds, quality of extraction…), the following 5 methods on the sphere A extraction have been investigated:

1. Fast;
2. Normal;
3. Precise;
4. Super Precise;
5. Quick.

In particular, Fast and Normal seem to be really fast comparing the others, but the comparisons between the extracted surface (actual) and the volume in VGStudio (nominal) show better results with Precise, Super Precise and Quick extraction. The deviations from the sphere A surface are shown in figures from 4.4 to 4.8. The Fast and Normal extraction deviations are of the order of circa 5 µm, whereas of 2.5 µm for Precise, Super Precise and Quick ones.

In table 4.4, all the investigated parameters have been displayed. The deviation in table 4.4 is related to the difference between the extracted surface and the volume in VGStudio format.

Table 4.4: Investigated parameters of the 5 different extraction methods

	Time	**Deviation**
Fast	8'	5 µm
Normal	10'	5 µm
Precise	1 h	2.5 µm
Super Precise	1 h 15'	2.5 µm
Quick	30'	2.5 µm

For these reasons Quick Extraction has been used for this work.

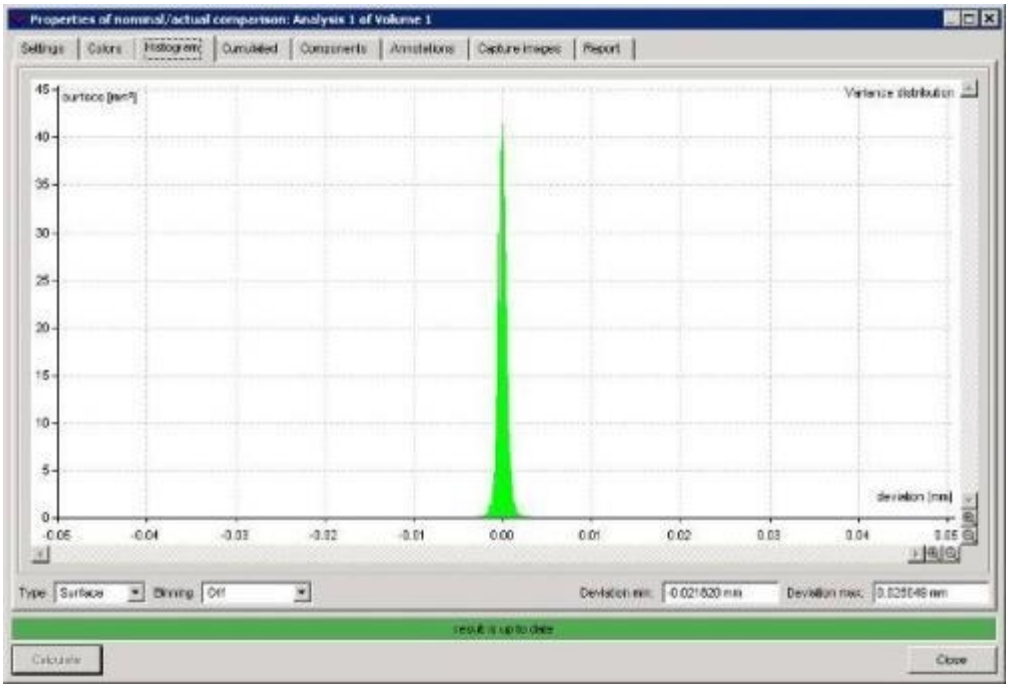

Fig. 4. 4: Fast extraction deviations

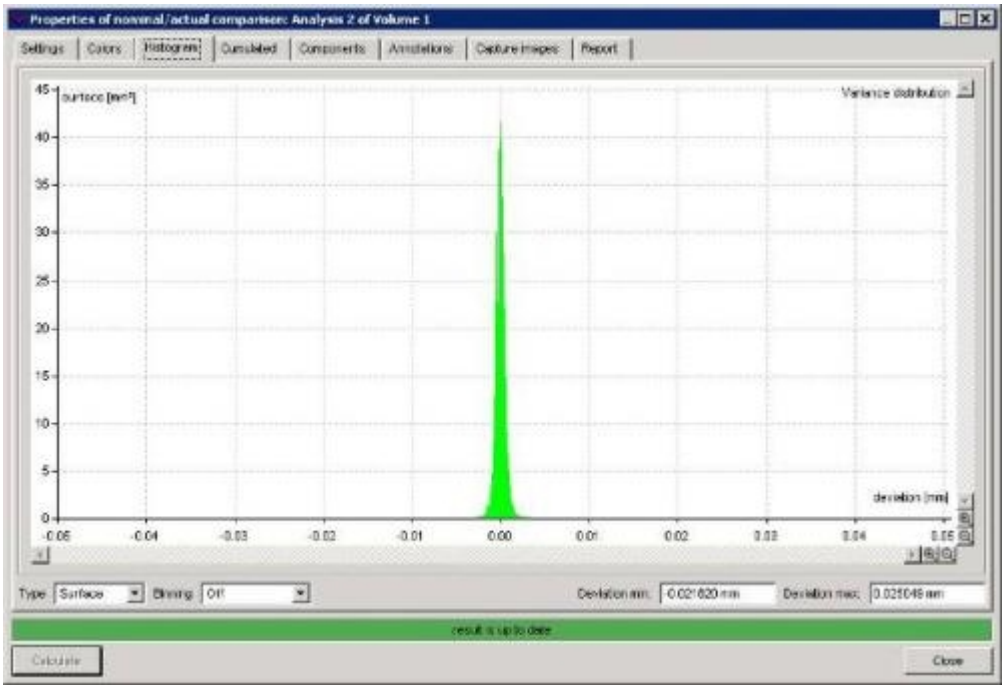

Fig. 4. 5: Normal extraction deviations

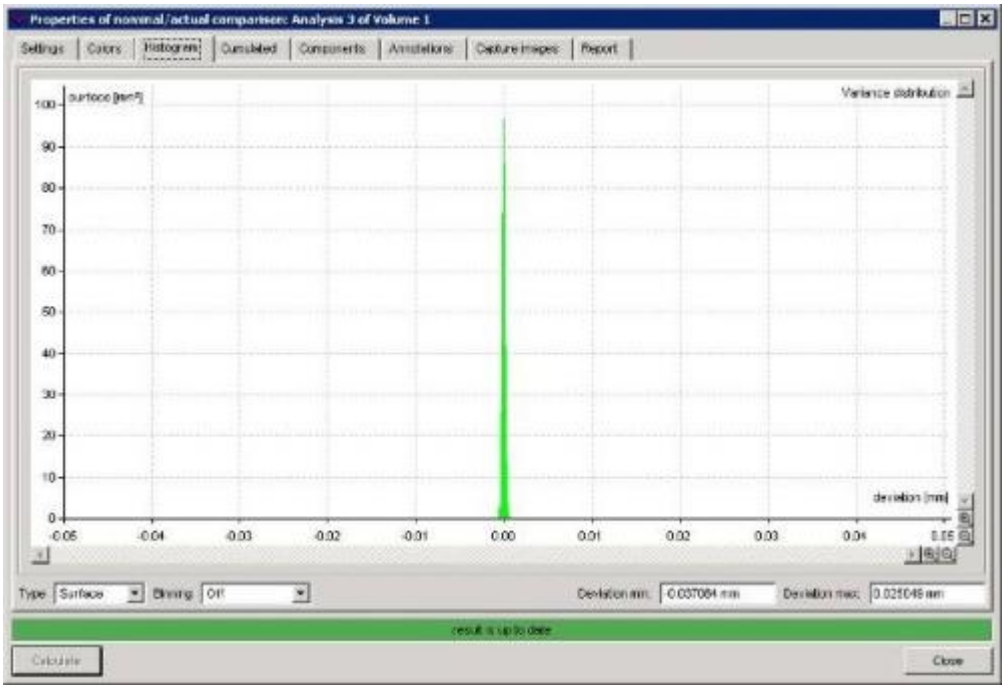

Fig. 4. 6: Precise extraction deviations

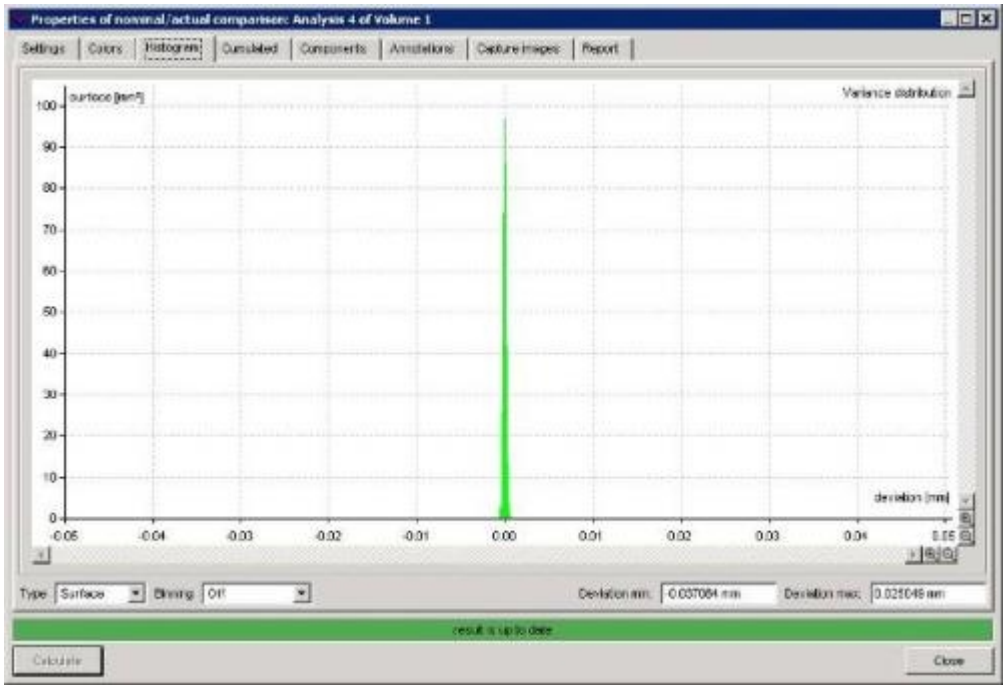

Fig. 4. 7: Super Precise extraction deviations

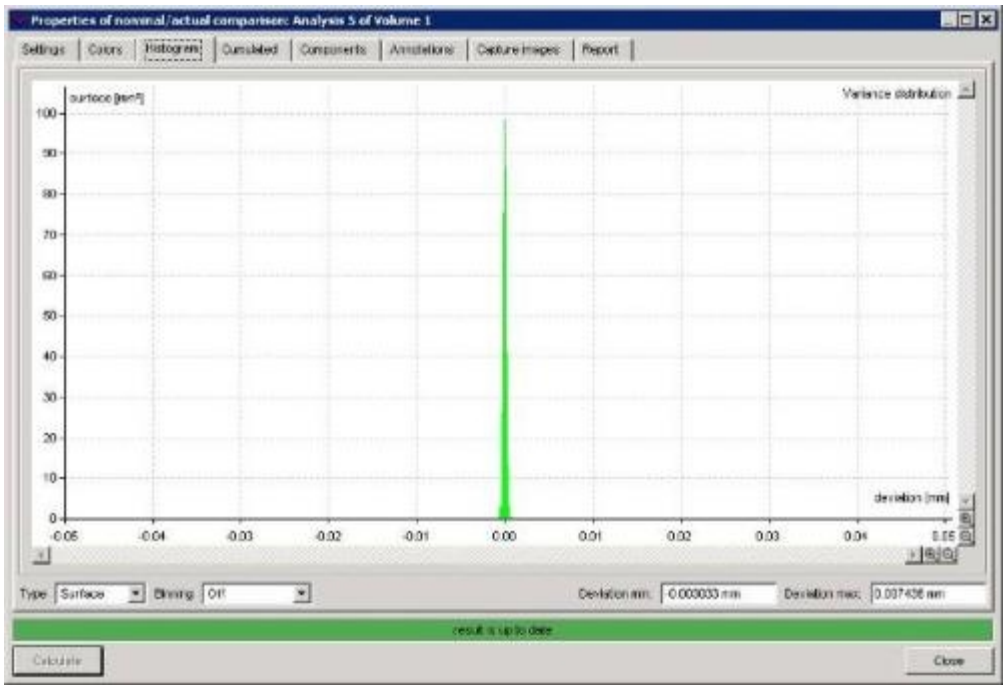

Fig. 4. 8: Quick extraction deviations

4.1.2 "Soll-Ist Vergleich" = Nominal-Actual Comparison

With the support of the software ATOS (v6.2.0.), a direct comparison between CT Data and Tactile Data has been carried out for both Tetrahedrons.

In this work the proper Nominal/Actual comparison is not carried out, because the normal components of each point were needed.

The CT Data have been set as nominal and the tactile measurements as actual.

This leads to a comparison not in the proper way, but still the difference is not so relevant for bodies like sphere A due to the low curvature changes.

The ASCII (Tactile Data) and the STL files for each Tetrahedron have been uploaded. The first important step lies in fixing the alignment correctly, in particular in checking that:

- D sphere (0,0,0) both in CT Data and tactile Data;
- B sphere (x,0,0) both in CT Data and tactile Data;
- C sphere (x,y,0) both in CT Data and tactile Data.

As shown in figure 4. 9.

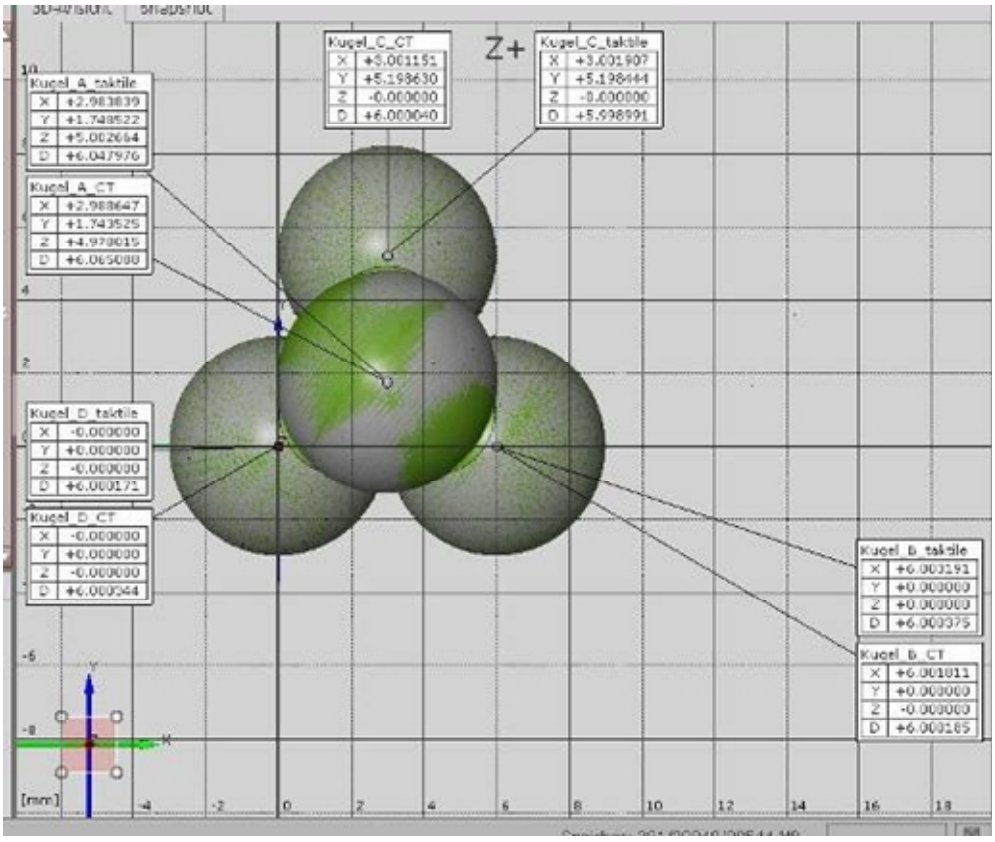

Fig. 4.9: Alignment in ATOS (CT and tactile data)

Once the objects are correctly fixed, the direct comparison can be carried out.

The figures 4.10 and 4.11 show the Nominal/Actual comparison. In particular it is important to pay attention to the histogram at the right side of each figure. Here the deviations from the CT Data have been shown.

Respectively, Tetrahedron 1 has a deviation between -0,001 and 0,007 mm, Tetrahedron 2 between 0 and 0,009 mm. The form deviations of the top spheres are bigger than the deviations of the CT measurements from the tactile reference measurements. Moreover the range of deviation is in order of the voxel size. See table 4.5.

Table 4.5: Nominal/Actual considerations, where the "Reference Tactile – CT" is related to the actual/nominal comparison obtained by ATOS software

Sphere A	Tetrahedron 1	Tetrahedron 2
Tactile form deviation (minimum zone criteria)	0.0894 mm	0.12 mm
Computed tomography form deviation	0.14615 mm	0.14721 mm
CT measurement voxel size	0.00968 mm	0.00796
Reference Tactile - CT (ATOS diagram)	0.008 mm	0.009

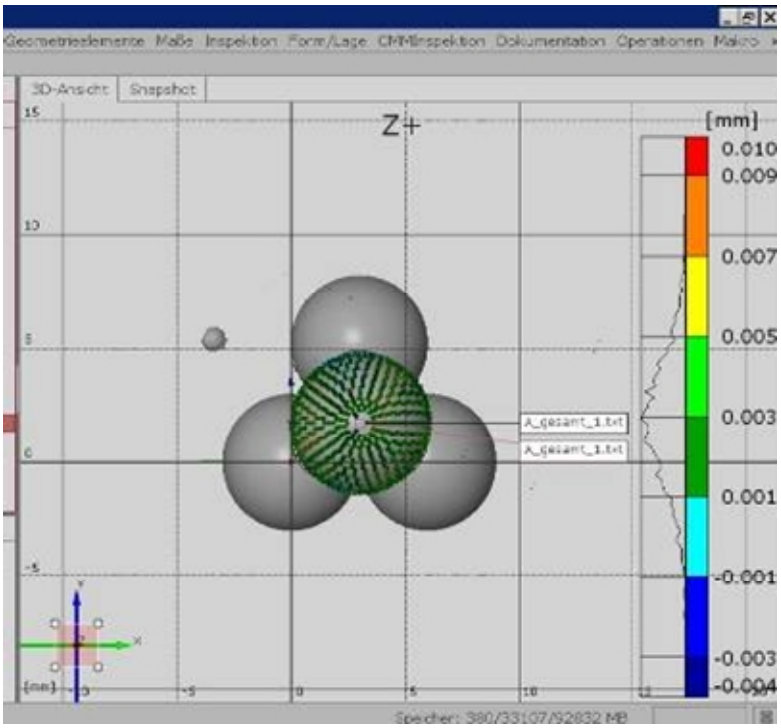

Fig. 4.10: Nominal/Actual comparison Tetrahedron 1

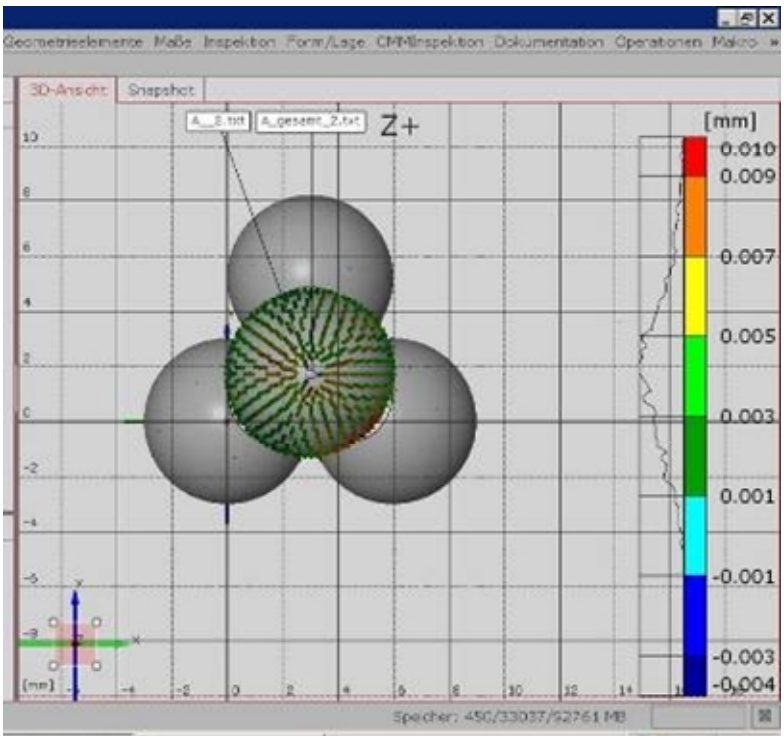

Fig. 4.11: Nominal/Actual comparison Tetrahedron 1

4.1.3 Considerations about the Nominal/Actual comparison

From figures 4.10 and 4.11 one can infer that something strange in the diagrams occured, because there is a Gaussian trend but the middle point is shifted from zero. In details it is set at 0,003 mm (Tetrahedron 1) and at 0,004 mm (Tetrahedron 2).

This deviation can be caused by:

1. Tactile measurements;
2. CT measurements (scale factors);
3. Software VG Studio : surface extractions and threshold values determination;
4. Object (form and material).

The tactile measurements with UPMC 1200 Carat have been compared with the measurements with F25 Machine (see paragraph 5) and they both show the same trend in the nominal/actual comparison between the tactile and the CT measurement. For this reason, the tactile measurements should not take a big influence on the shift in the comparison diagram.

Moreover the voxel size and the scale factor have been verified by BAM in Berlin using a calibrated 5-rubin-spheres object and further with the measurements of the distances between the lower spheres (BCD) of the tetrahedrons.

This shift can be caused by the software VG Studio and the object, in particular the threshold values determination (static or adaptive) and the high free form of the top sphere (A).
The surface determination (the definition of the material boundary) can be obtained by different methods. In this work it has been calculated firstly in an advanced mode (local threshold using region of interest) considering single and multiple material options.
The material boundary is defined by locally adapted gray values, depending on the surrounding voxels. It is a very useful approach when the measuring object is flawed and the beam hardening occurs. Considering a single material option or multi material, the systematic shift in the nominal/actual comparison is not avoided as shown in figure 4.12.
Here following a series of different extracted surfaces have been uploaded and nominal/actual compared. Each surface has been calibrated with an adaptive threshold in order to show that there is no difference between them; in particular they show the same behaviour in terms of shift, as plotted in Figure 4.12. In details in Fig. 4.12 the maximum of a Gaussian distribution is collocated at 0.003 mm for each extracted surface, in order Single Material Calibration, Multimaterial Calibration at three different threshold values (respectively 150-110 and 168 only as start values) and single material calibration with F25 tactile data.

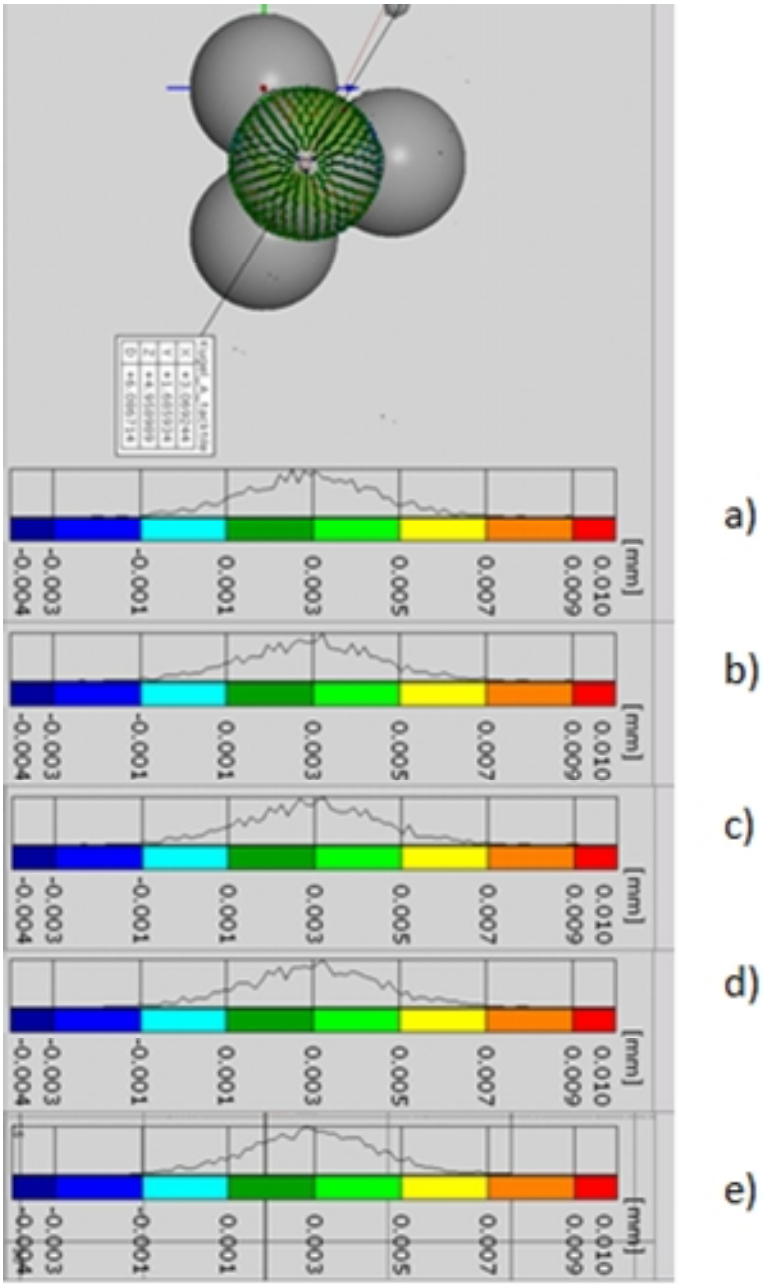

Fig. 4.12: Nominal/Actual comparison in order: a) Single Material calibration (Carat Tactile Data), Multimaterial calibrations b),c) and d) (threshold values 150, 110,168 only as start value) (Carat Tactile Data), and Single material with F25 tactile data e).

The lower three spheres do not have any "shift problem" as shown in figures 4.13. But they are almost perfect spheres.

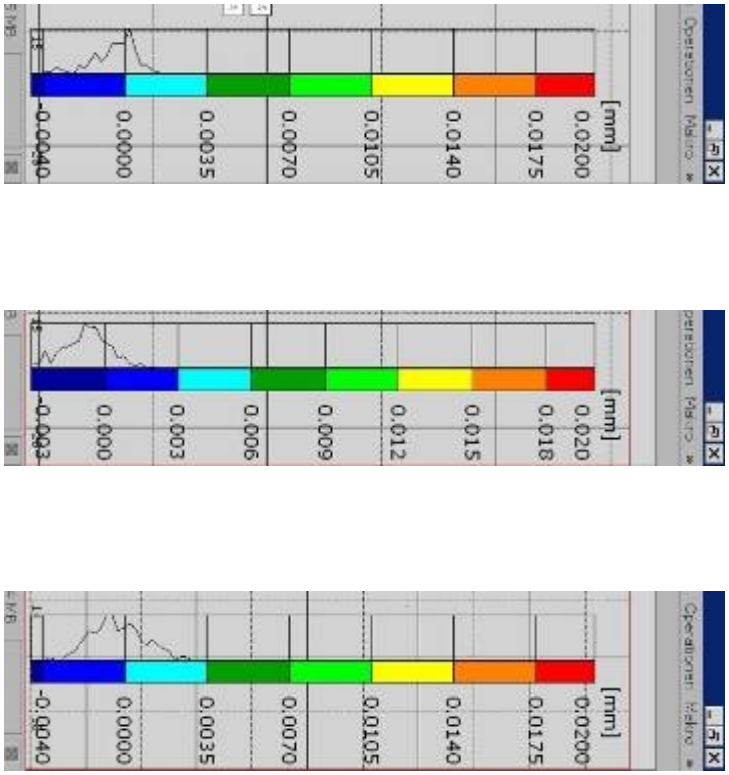

Fig. 2.13: Lower sphere Nominal/Actual comparison sphere (in order) B, C, D of Tetrahedron 1

A qualitative approach has been conducted on the investigation of the top sphere in VG Studio.

The surface of the top sphere has been static calibrated (ISO 50) with different threshold values as following:

85, 90, 95, 105, 106, 115, 125, 130

Each different gray value, a sphere has been fitted in order to obtain a complete fitting of the sphere (see table 4.6 and Figure 4.14) and its diameter.

Table 4.6: fitting parameters (VG Studio Max)

Fitting Sphere in VG Studio Max	
Fit Method	Least Squares
Auto fit point	On
Step Width [mm]	0.005
Max. Points	100000

Fit Point filter options	On
Search distance [mm]	0.1
Max. gradient [deg]	45
Edge Void [mm]	0.001
Iterations	4
Auto expand	On

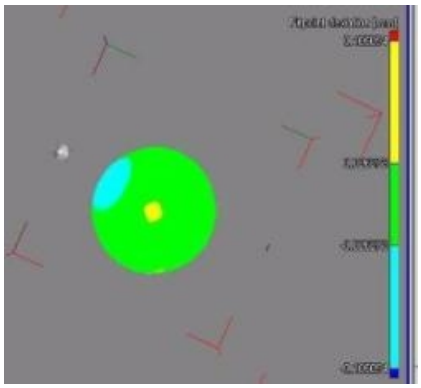

Fig. 4.14: Fitted Sphere in VG studio

Finally the diameter has been compared to the one calculated from the tactile measurements. (See diagram 4.1 and table 4.7). In particular it is shown that each 3 µm correspond ca. 5 gray values.

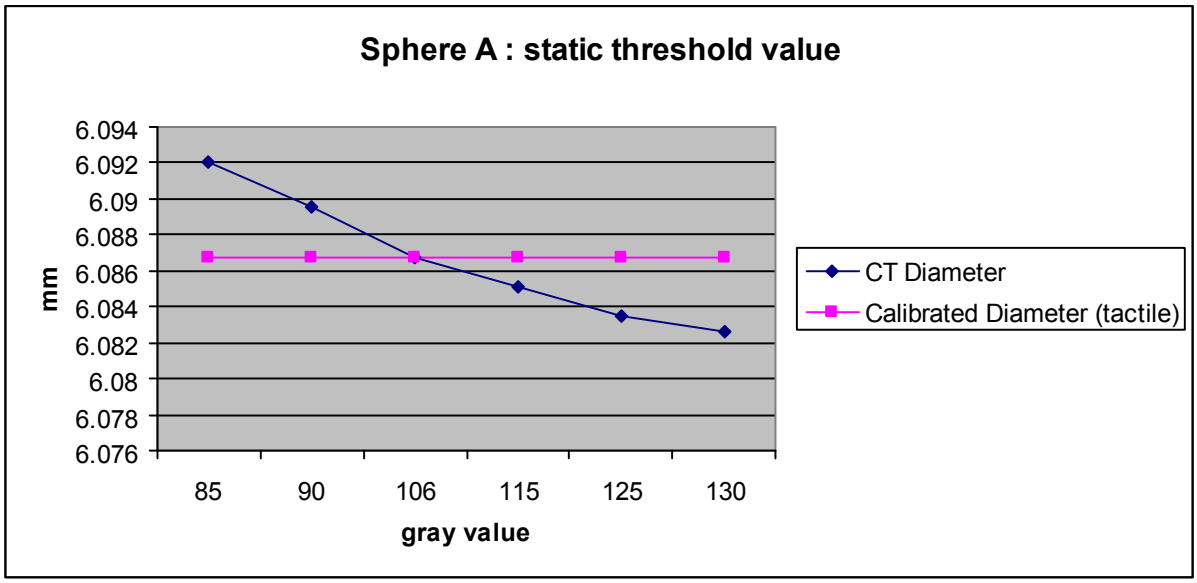

Diagram 4.1: Different threshold values of Sphere A

Table 4.7: Static threshold values

CT Diameter [mm]	CT - Tactile [mm]	Threshold value
6.092002	0.0052	85
6.089598	0.0028	90
6.086894	0.0002	105
6.086722	8E-06	106
6.085162	-0.0015	115
6.083434	-0.0032	125
6.082572	-0.0041	130
Tactile Diameter [mm]	6.0867	

In detail, the threshold value around 106 has been calculated as the best for the sphere A.
It is important to underline that the CT diameter has been calculated with circa 60000 points whereas the tactile diameter with "only" 3000 points.
Moreover the extractions of these ISO surfaces have been uploaded in ATOS in order to make a nominal/actual comparison. The comparison between the results in VG Studio and in ATOS is not commensurable because the methods are completely different. In ATOS the nominal/actual comparison is conducted with the matching points to points, whereas in VG Studio it was points to surface (CT).
One can infer anyway that also in ATOS comparison there is a trend in the diagrams (see figure 4.16) that is similar to VG Studio. It seems to be opposite, but in ATOS the comparison is Reference Tactile minus CT, whereas in VG Studio it is CT minus Reference Tactile.

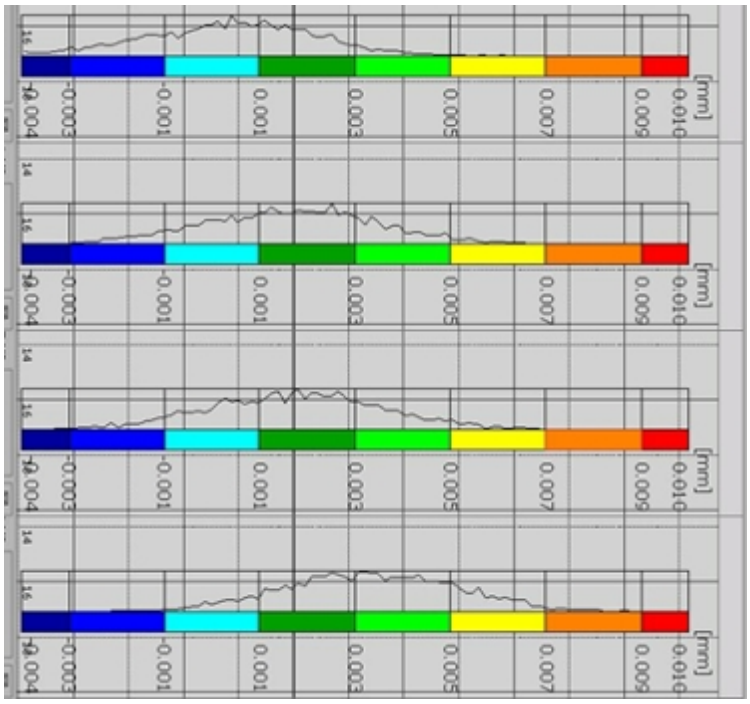

Fig.4.16: Nominal/Actual comparison with Static Threshold values of 90-105-105-125

5. Conclusion

This work is about the investigation of a new type of calibrated object for CT measurements: tetrahedron made of 4 spheres. Its main and new important characteristics are:

1. The Top sphere that, with its high error form, leads to the studying of CT capability in form measurements;
2. Good quality of the lower spheres that is fundamental in order to correct the scale error and to fix a proper alignment of the object both in tactile (reference) and in CT measurements.

Two similar tetrahedrons have been prepared and investigated.

CT measurements have an important advantage: thousands of points are acquired in a relative short time. More than 3000 points have been taken for the tactile calibration of sphere A (high form deviation), in order to make a meaningful comparison between CT and reference measurements (tactile ones).

The reference measurements have been carried out with a Zeiss machine (UPMC 1200 Carat) and its drift has been deeply investigated. The drift is not bigger than 1 µm in 26 hours, but it is not linear. For this reason drift should be compensated constantly during the measurement,

especially when it takes a long time. Since the measurements of 3000 points extend to more than 7 hours, a dedicated program with the repeating of the alignment has been crucial.
The two top spheres (in Tetrahedron 1 and 2) show form errors of:
Tetrahedron 1→ 0.0894 mm (minimum zone method)
Tetrahedron 2→ 0.1200 mm (minimum zone method)
The CT measurements have been carried out by BAM facilities and the Data elaboration has been conducted with the support of VG Studio Max and ATOS.
In detail the CT data have been imported in VG Studio and elaborated in order to extract a surface and to make a proper nominal/actual comparison between tactile and CT data in ATOS. VG Studio Max offers different extraction methods. In particular 5 of them have been investigated and compared. Concerning the time and the quality (in terms of deviation from the original surface) of extraction, the best extraction method was "Quick extraction".
Once extracted, the stl file has been imported together with the tactile (ASCII file) data in ATOS. In ATOS it is possible to fix as nominal only CAD Data. For this reason the CT data have been set as nominal and the tactile as actual. The nominal/actual comparison is shown by diagrams as the subtraction of CT from the tactile reference. The deviations between CT Data und tactile data are smaller than the voxel size (ca. 8 μm and 10 μm respectively for Tetrahedron 1 and 2). The form error of top sphere A is bigger than the difference between tactile and CT data. This is a confirmation of the goodness of CT measurements. See table 5.1.

Table 5.1

A Sphere	**Tetrahedron 1**	**Tetrahedron 2**
Tactile form deviation (minimum zone criteria)	0.0894 mm	0.12 mm
Computed tomography form deviation	0.1462 mm	0.1472 mm
CT measurement voxel size	0.00968 mm	0.00796
Reference Tactile - CT (ATOS diagram)	0.008 mm	0.009

Anyway measuring form with CT systems is still a research topic. For this reason many other further works are suggested. First of all more tactile points should be taken in order to get a proper comparison concerning form, for example 5000 points should be good as shown in the tactile measurements with F25, because the sphere is measured closer to a scanning method. However this leads to longer tactile measurements.

Finally an estimation of single point uncertainty of the tactile CMM measurements is missing, whereas the uncertainty has been calculated with the VCMM for the following features: diameters, centre of spheres and error deviations.

Further CT measurements on the same tetrahedrons in order to keep under control the repeatability of the CT technique.

The nominal/actual comparison in ATOS should be further studied in order to get a proper comparison. Setting CT measurement as nominal is neither completely wrong nor completely right.

Moreover working with two different softwares (VG Studio and ATOS) causes an increasing possibility of errors and of course an also increasing uncertainty. It would be very interesting to carry out the elaboration of CT Data and the nominal/actual comparison only in VG Studio.

Chapter 4

First International Intercomparison on CT Systems for Dimensional Metrology

Chapter 4 introduces to the First International Intercomparison on CT Systems for dimensional metrology. An extract from the official CT Audit project's report of 323 pages is presented.

1. Introduction

As already described in Chapter 1, recently Computed Tomography Technique has been identified as a very promising technique in the metrology field due to important advantages respect to tactile and optical coordinate measuring machines (CMMs) and other measuring systems. The main advantages are [8]:

- Ability to measure as well the inner as the outer geometry of objects without disassembling or destroy it;
- Possibility to acquire a high point density in a relative short time;
- Non contact inspection.

On the other hand, several limitations are present, e.g. [8]:

- Complex and numerous influence quantities occur;
- Complete standards are not yet available;
- Measurements are typically not traceable since the uncertainty is difficult to evaluate.

Moreover as discussed in Chapter 2, due to the previous CT disadvantages, CT systems are still not completely recognized as reference measuring instruments with well known metrological performances. An interlaboratory comparison may be an indispensable means to establish the effectiveness and comparability of measurement methods and to validate uncertainty claims [74]. For this reason, the University of Padova organized the first international intercomparison of CT systems for dimensional metrology [38].

Fig 1.1:. CT Audit project logo

At end of the project an exhaustive report has been written and shared with all the Participants, part of this report is adapted in this Chapter [78].

2. CT Audit Project

CT Audit project is the first international intercomparison of CT Systems for dimensional metrology purposes and it involved many institutes, research centers and metrological laboratories in Europe, Asia and America.

The main objectives and benefits of the *CT Audit* project have been to deepen the knowledge on CT dimensional metrology and to spread information on available reference geometrical standards and procedures for metrological verification of CT systems.

The Participants gained many benefits from the *CT Audit* Project. First of all they received calibrated geometrical standards and procedures for testing their CT Systems. They had the possibility to evaluate their measurement's results by comparing them to reference calibrated values and to results of other laboratories. Moreover they could validate their measurement and uncertainty evaluation methods. Finally, all Participants are now establishing an international network of laboratories using CT Systems for dimensional metrology; this network can be the basis for promoting further international initiatives in the field of industrial CT. Part of the CT Audit project network had the chance to discuss together in a dedicated workshop at University of Padova on 26th of October 2011, see Fig. 2.1. Moreover the CT Audit established network will contribute also to a new society, called "Society for Tomography", that is going to develop and that will cover a wide range of applications in the non-medical domain, hardware and software research, scanning techniques, standardization and calibration, imaging etc. The Society for Tomography has been ideally created during the CT Audit project during the discussions of both GeoX 2010 in New Orleans (USA) and 3D IMS 2010 in Hourtin (France) by Jacobs Patrick of Ghent University [79].

Fig. 2.1: Part of the CT Audit international network

2.1 CT Audit project organization and running

The project was organized and coordinated by the *Laboratory of Industrial and Geometrical Metrology*, University of Padova, Italy, and it was self-financed by the organizing Laboratory and all Participants took part in the intercomparison with no funding to the University of Padova.

The intercomparison involves 15 companies and laboratories form different Countries around the world, with a total of 15 CT systems, see world map in Fig. 2.2. Names of participating organizations are listed in alphabetical order, for general information only, in Table 1. The confidentiality of results is ensured by associating an anonymous identification code to each Participant. Only the specific Participant and the Coordinator know the association with the identification code.

A website was built for distributing information and measurement procedures (www.gest.unipd.it/ct-audit) [80]. The time scheduling of the project has been divided in 5 phases, as schematically described in Fig. 2.3.

The project was born in September 2009 and the end can be set on 26th of October 2011, when officially all the Participants had the possibility to meet each other and to discuss results in a dedicated Workshop hold on at University of Padova (DIMEG Department). Anyway the proper circulation of the four items was carried out in one year from March 2010 and March 2011.

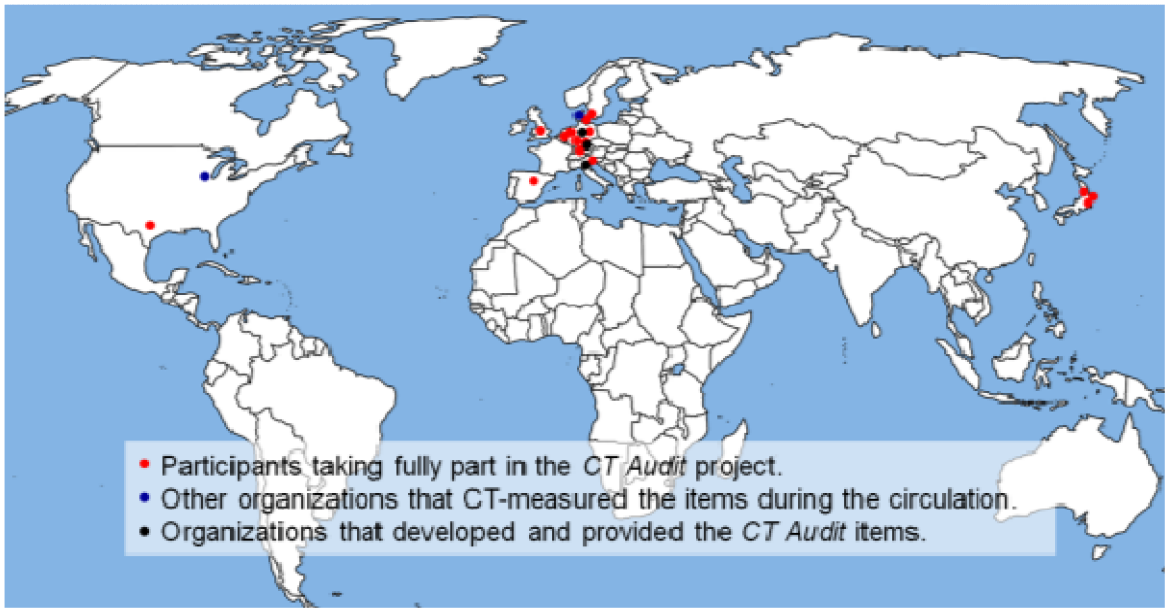

Fig. 2.2: Distribution of Participants on the world map

Project phases	2009				2010												2011					
	9	10	11	12	1	2	3	4	5	6	7	8	9	10	11	12	1	2	3	4	5	6
Plan, Participants definition																						
Reference items calibration																						
Circulation																						
Analysis of results																						
Reporting and dissemination																						

Fig. 2.3: CT Audit Project Schedule

3. General considerations on CT Audit items

The four calibrated items were chosen in order to represent a variety of dimensions, geometries and materials; they were designed and manufactured suitably for metrological performance verification of CT systems.

The four items were sent within a dedicated suitcase, in Fig. 3.1, from one Participant to the next one in a sequential participation scheme [74].

Fig.3.1: The CT Audit suitcase: closed and ready to departure (left), opened (right)

Moreover the items were protected in thin plastic sealed boxes in order to reduce the risk of damages, to limit contamination and to avoid measurements with other sensors. The sealed cylindrical boxes are made of polyethylene, with wall thickness of 0.8 mm circa. Participants were asked to measure the items without opening the sealed boxes. The four Items are shown in Fig.3.2. Item 1, which is called "CT Tetrahedron", consists of four calibrated ruby spheres on a carbon fiber frame. Item 2 is called "Pan Flute Gauge"; it is composed of five calibrated glass tubes of different lengths. Both items 1 and 2 were developed by University of Padova,

Italy. Item 3 is the "Calotte Cube", which consists of 75 spherical calottes on three sides of a titanium hollow cube. This item is provided by Physikalisch-Technische Bundesanstalt, Germany.

Finally, item 4 is the "QFM Cylinder", consisting of a titanium cylinder and a ball plate with five sapphire balls. This item is provided by QFM − University Erlangen-Nuremberg, Germany [38].

Fig.3.2: Items protected by sealed boxes: in order from left to right, item 1,2,3, and 4

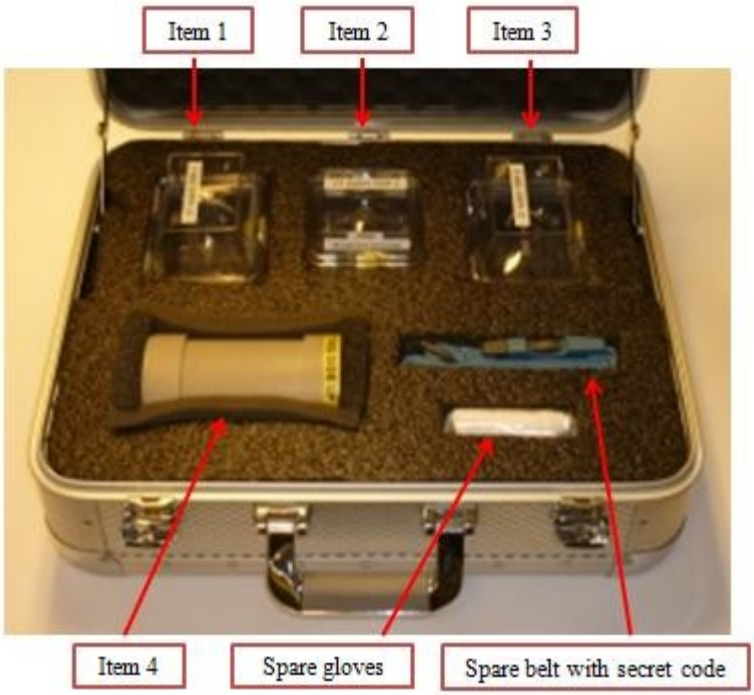

Fig. 3.4: Contents of CT audit Suitcase

The dimensional stability of the four items has been checked through CMM's calibrations before and after the circulation, as following described in sub chapters 4.3 and 4.4 of Chapter 4.

The four calibrated objects are sent to the Participants during the circulation together with detailed measurement procedures. In particular for each item, a dedicated measurement procedure has been sent to the Participants. In these documents the four items are presented and detailed instructions are described, how to:

1. Position of each item on the CT system table;
2. Extract the points from CT data;
3. Associate ideal geometric elements to the extracted points;
4. Define the reference coordinate system;
5. Evaluate the measurement results;
6. Report the measurement results.

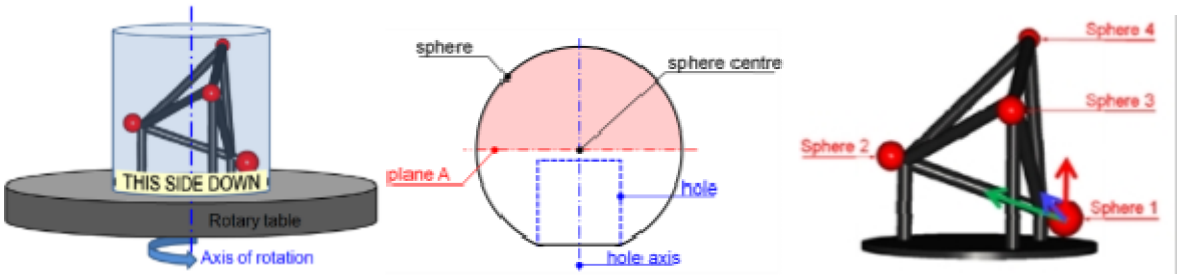

Fig. 3.5: Measurement instructions for item 1: (left) positioning on the rotary table, (center) associating of ideal gemoetric elements to the extracted points, (right) defining the reference coordinated system

Moreover the Participants received, together with the measurement procedures, also other important sheets to fill in concerning the summary of activities, the receipt and dispatch forms, and the results form for each items.

4. CT Audit items descriptions and related results

The four items are here following further detailing presented and for each items are discussed some important results.

The items have been used to compare different Participants CT system performance. For this reason, the Participants received at the end of the project the results in relation to the other Participants but also personal analyses of the results. Here following the results related to the single items are presented in terms of deviations charts, histograms and plots.

The deviation charts compare the results of all Participants with the reference values that correspond to the calibration results of each CT Audit items. The charts (see for example

Fig.4.2) report the Participants code numbers that are confidential in the horizontal axis and the on the vertical one the deviations from reference value in μm. Two red dashed lines are placed side by side on the horizontal axis and it represents the expanded uncertainties of the reference values. Sometimes the reference values have different uncertainties, so the dashed red line represents only the maximum uncertainty of the reference values. Moreover the colored dots correspond to the deviations of the measurement values given by the Participants, different color and shape are related to different features measured by the same Participant. Finally the vertical error bars on the colored dot represented the expanded uncertainty as stated by the Participant.

In addition, the histograms are used to report the E_n numbers used to correlate the results given by the Participants together with the stated uncertainty to the reference values obtained by the CMM calibration and the related uncertainty. E_n number, as already described in Chapter 2-6.2, is defined as [74]:

$$E_n = \frac{X_{lab} - X_{ref}}{\sqrt{U_{lab}^2 + U_{ref2}^2}} \qquad (1)$$

where X_{lab} is the results given by the Participant, and X_{ref} the reference value. U_{lab} and U_{ref} are the uncertainties related respectively to the Participant's results and to the reference calibrated value.

E_n number expresses the validity of the expanded uncertainty estimate associated with each result [81]. If E_n number is less than the unity in absolute value, then there is a good correspondence between the Participant's results and the reference value, otherwise the agreement between them is unsatisfactory.

The histograms (see for example Fig. 4.4) report the E_n numbers in intervals of 0.5 in the horizontal axis. On the vertical axis the frequency of occurrence of measurement results belonging to specific intervals of E_n number is displayed.

Together with deviations charts and En histogram, other additional plots are used to analyze the results. Since they are related only to single items, they are presented further, when necessary.

4.1 Item 1: CT Tetrahedron

CT Tetrahedron (Fig.4.1) has been already presented in Chapter 2-6.3. It is also called Item 1 in the CT Audit project.

The high dimensional stability of Item 1 has been confirmed through CMM calibrations before and after the circulation, showing deviations within the calibration uncertainty.

Fig. 4.1: Item 1 picture

The Participants were asked to measure the following characteristics from CT data collected on the four spheres of Item 1:

- Diameters of spheres;
- Form errors, defined according to the definition of the characteristic "Probing error of form" (PF) given in the draft ISO 10360-11 [61] and VDI/VDE 2617-13 [60], where PF is defined as the span of the radial deviations of the measurement points from the calculated fitted sphere. For this reason, the evaluation of the "Form error" by the CT Audit Participants can be regarded also as an indication of their characteristic PF according to state-of-the-art guidelines for CT systems' testing;
- Coordinates of spheres' centres;
- Distances between spheres' centres.

Concerning the requested features to be measured, interesting results have been achieved. First of all the Participants' deviations for diameter measurements had a mean of absolute values of 18.1 μm that is definitely lower that the Participants' deviations for form error measurements that is 34.7 μm, as shown in Fig 4.2 and 4.3. The better abilities of the Participants in measuring Diameters than Form Errors can also be appreciated in the E_n histograms as shown Fig. 4.4. From the histogram shown in Fig. 4.5 an overestimation of the Form Error is documented for all the Participants results, and this will be confirmed also by Item 3 results (4.4.3). Moreover for CT measuring systems, form measurements are more problematic than size measurement is connected to the fact that form measurements are more affected by the influence of scatter and noise of CT data, while size measurements (like sphere's diameter) is the result of a fitting that eliminates the influence of outliers.

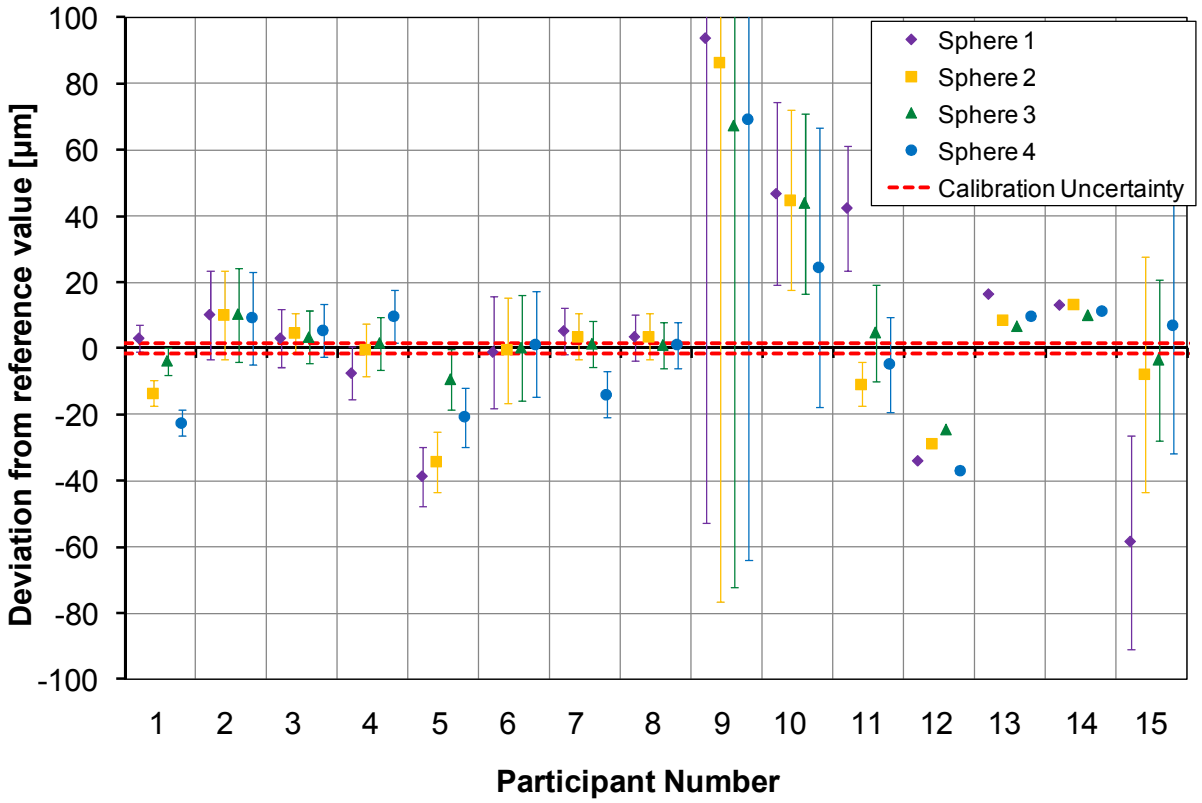

Fig. 4.2: Deviations charts for Diameters' measurements results

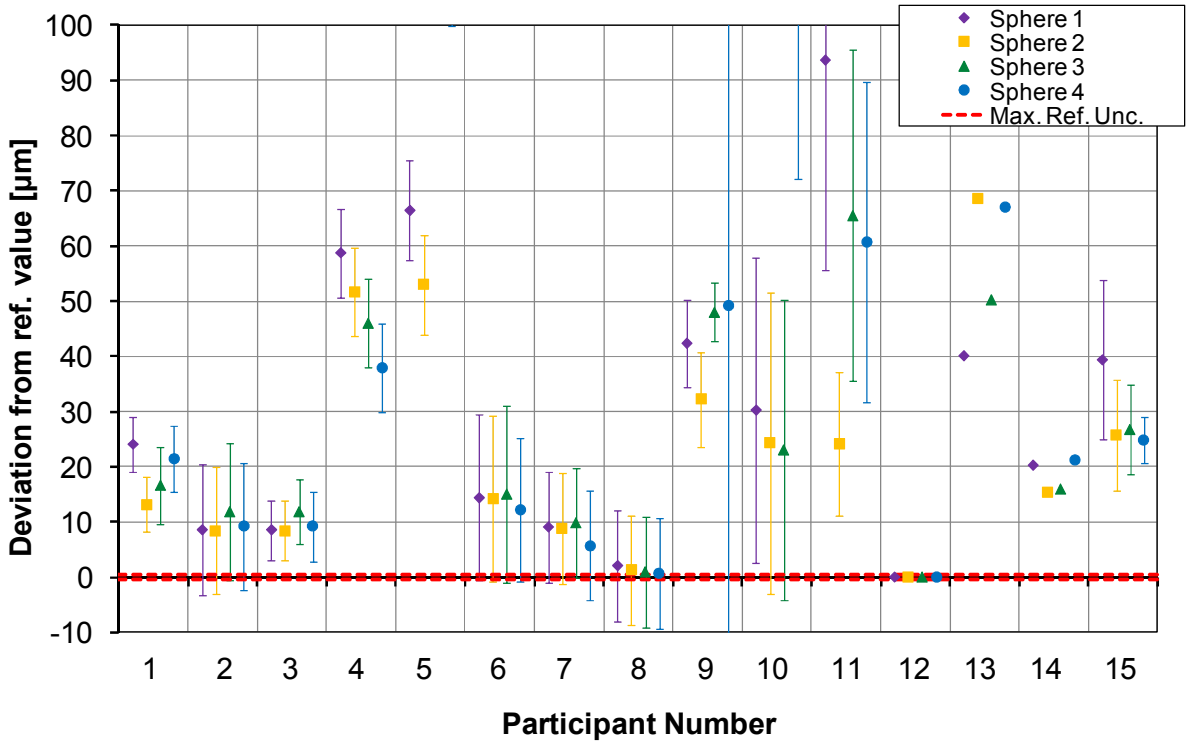

Fig.4.3: Deviations charts for Form Errors' measurements results

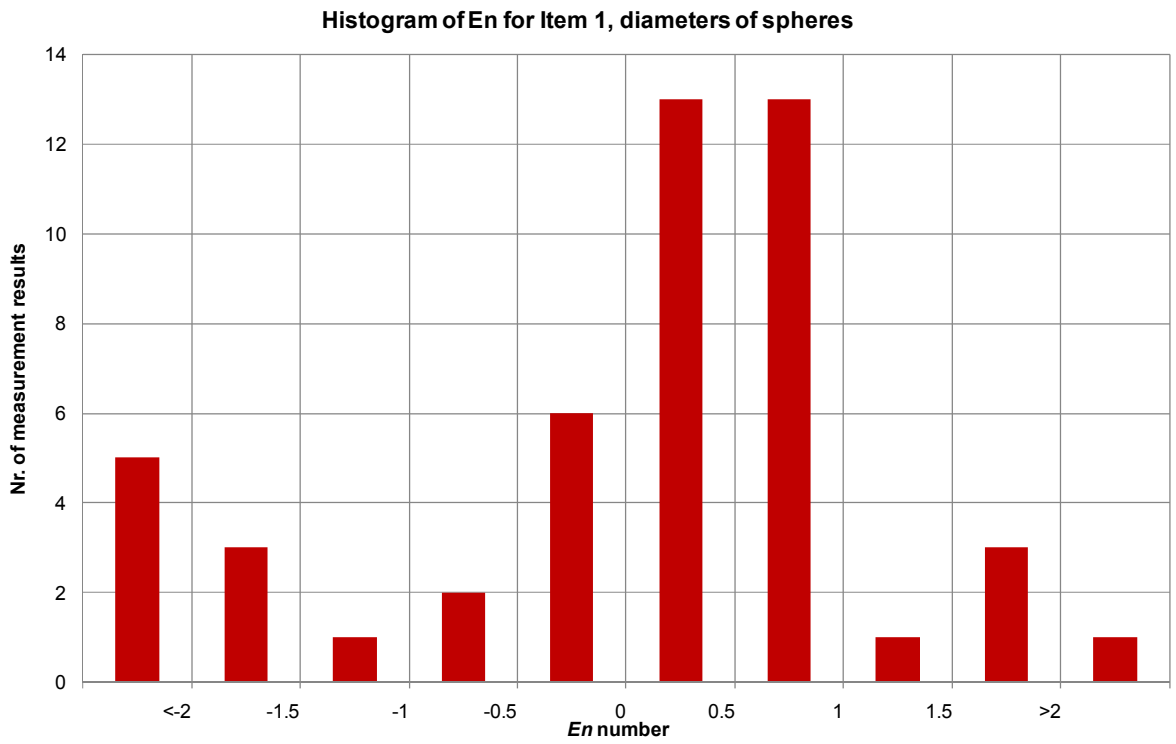

Fig. 4.4: Histograms for Diameters' measurements results

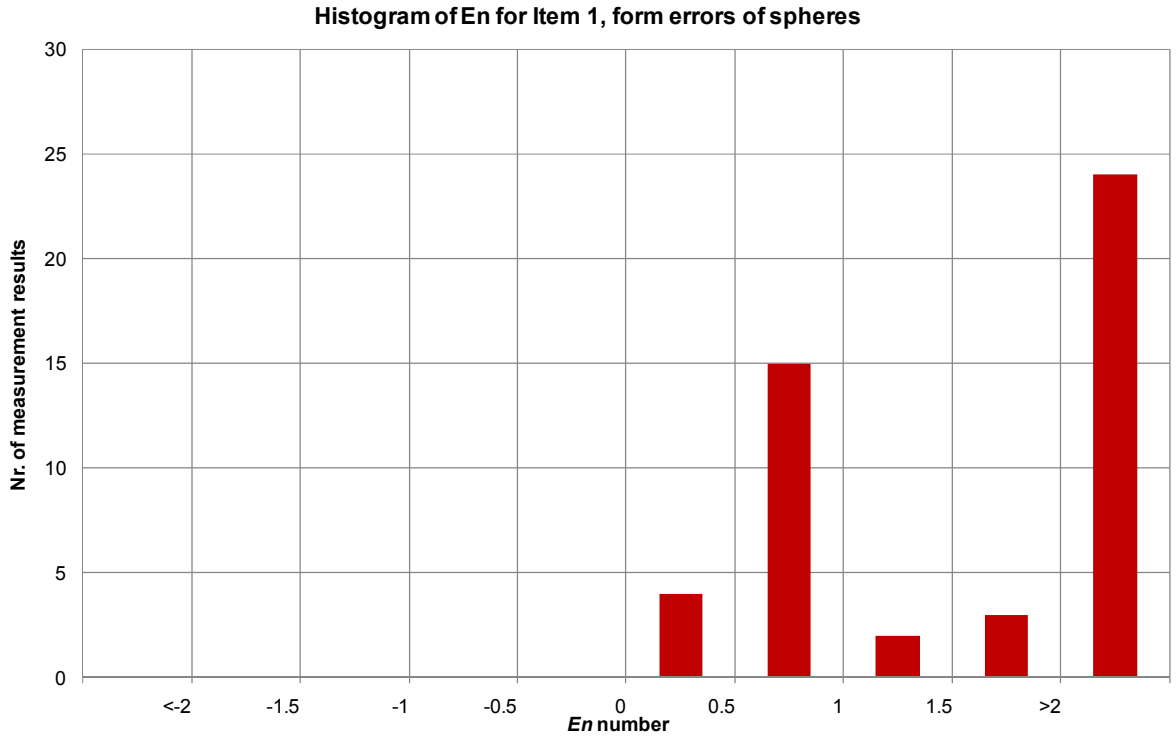

Fig.4.5: Histograms charts for Diameters' measurements results

4.2 Item 2: Pan Flute Gauge

Pan Flute Gauge (Fig. 4.6) has been already presented in Chapter 2-6.2. It is also called Item 2 in the CT Audit project.

The high dimensional stability of Item 2 has been confirmed through CMM calibrations before and after the circulation, showing deviations within the calibration uncertainty.

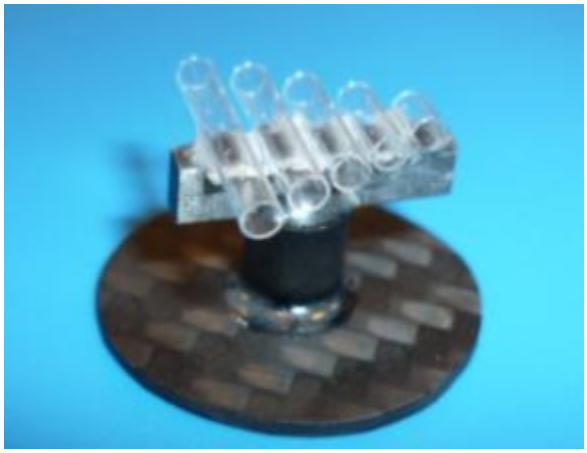

Fig. 4.6: Item 2 picture

The Participants were asked to measure the following characteristics from CT data collected on the five tubes of Item 2:

- Inner diameters;
- Outer diameters;
- Lengths.

Concerning the requested features to be measured, interesting results have been achieved.

The Participants reveal good abilities in measuring lengths, obtaining a mean of deviations from all Participants, lower than the ones obtained in Item 1 (4.4.1), that is 10.4 µm, as shown in Fig. 4.7.

Moreover, a very interesting result trend has been observed: the deviations of inner and outer diameters from the calibrated values have a systematic "mirror distribution" as shown in Fig. 4.8.

At the end of the *CT Audit* circulation in March 2011, all the Participants received the calibrated diameters of Item 2 and they were requested to use these values to verify and eventually correct their measurement results. The values were obtained from CMM calibration. In particular, the Participants could use the calibrated internal and external diameters values to correct their systematic errors, including errors due to threshold

determination and scaling factor. Each Participant was free to decide which correction procedure to apply and was asked to send the new lengths' results to the project coordinator. This second part was facultative, and only 6 Participants corrected their values; most of them obtained significant improvement from this correction of systematic errors, see Fig. 4.9 and 4.10.

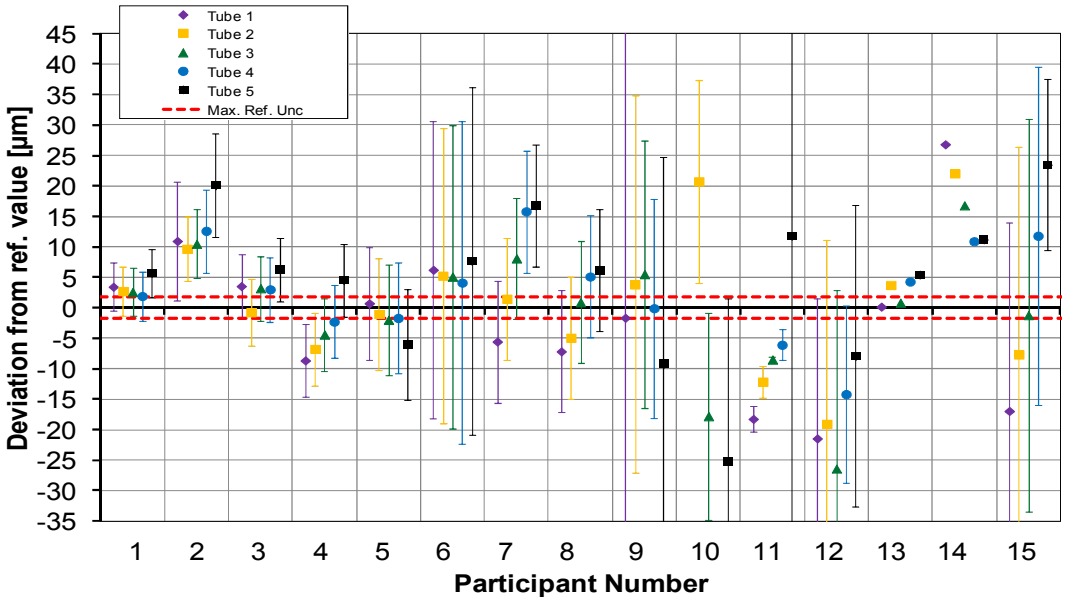

Fig. 4.7: Deviations charts for Lengths measurements results

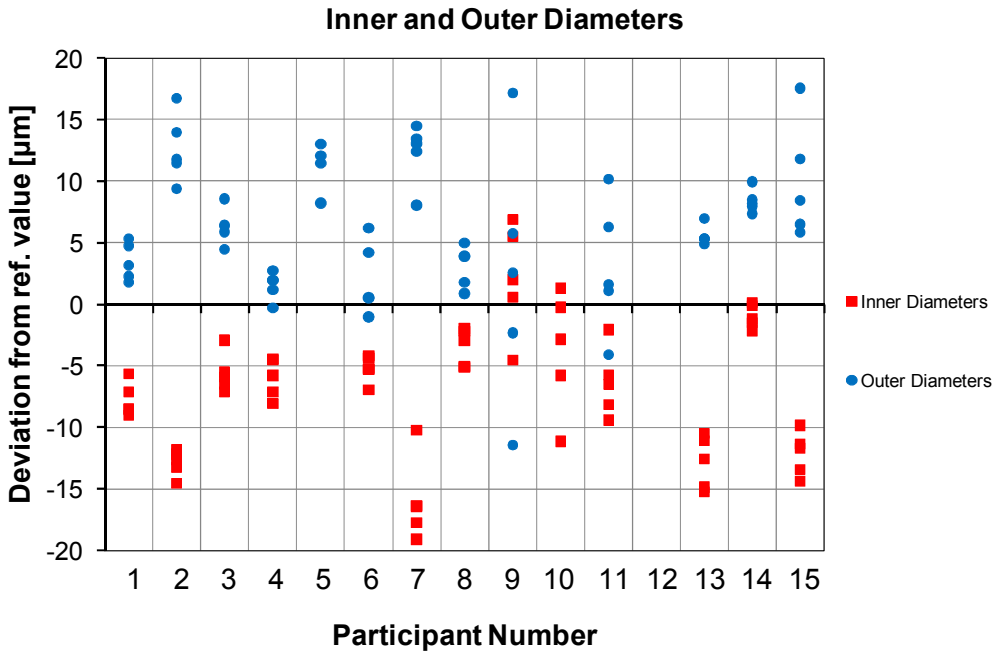

Fig. 4.8: Mirror trend of Inner and Outer Diameters

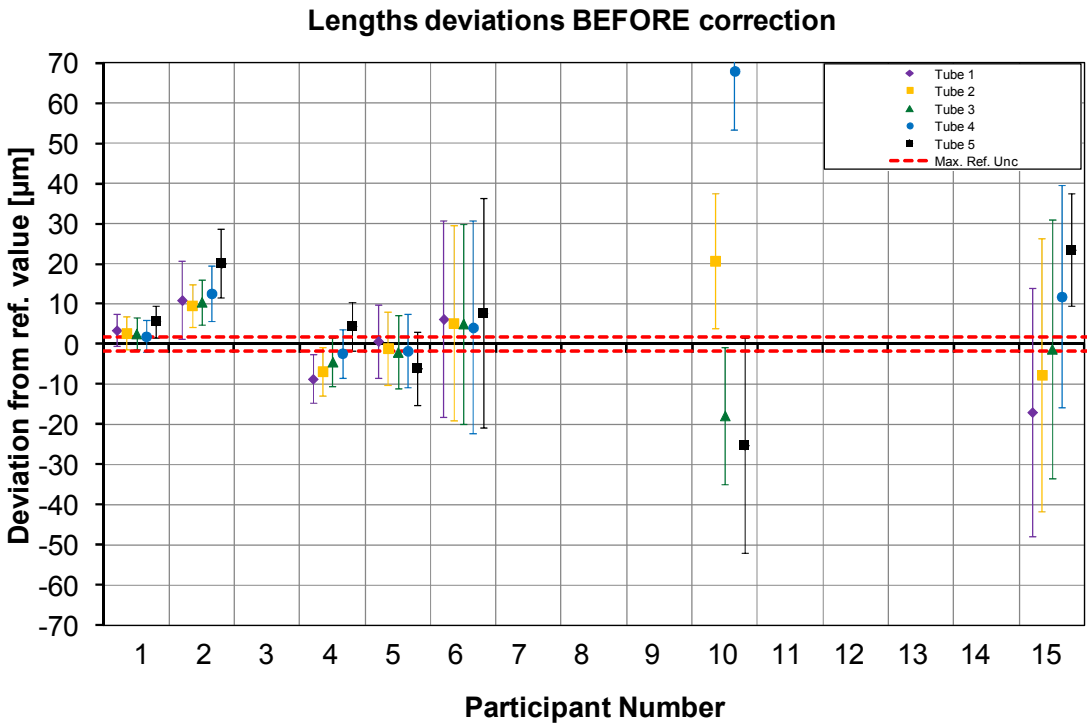

Fig. 4.9: Lengths deviations of Participants Nr. 1, 2, 4, 5, 6, 10 and 15, before systematic errors correction.

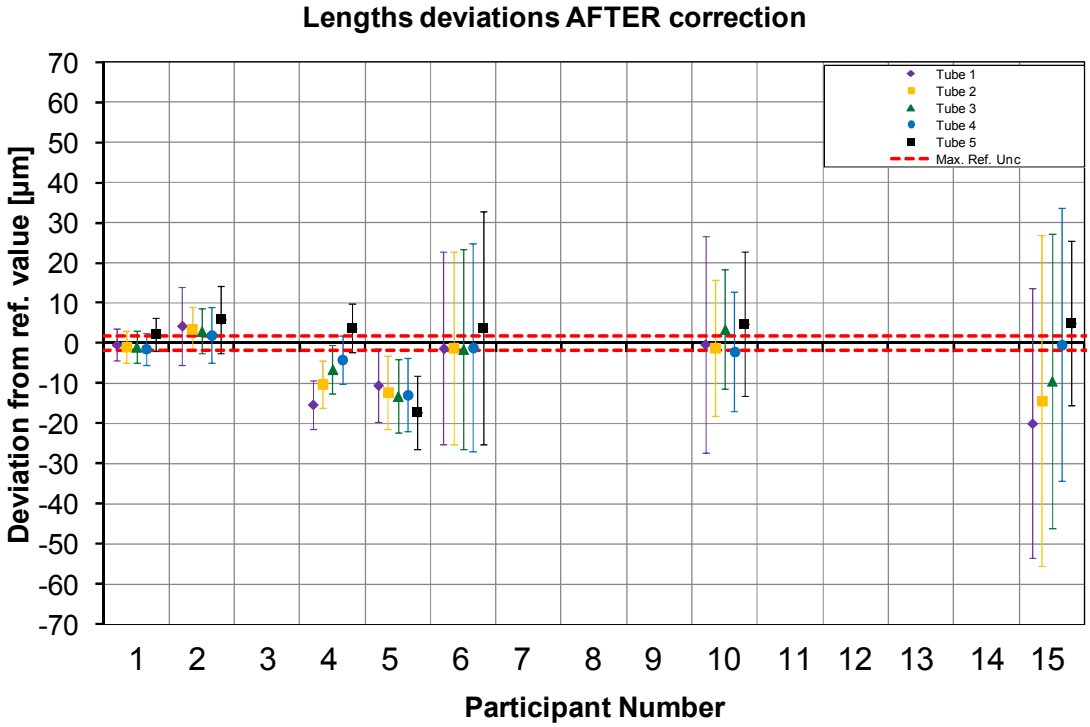

Fig. 4.10: Lengths deviations after systematic errors correction by Participants Nr. 1, 2, 4, 5, 6, 10 and 15.

This particular "mirror trend" reveals to be very interesting and it has been deeply discussed in the CT Audit Workshop on 26th October 2011.

The discussion had lead to some possible conclusions:

- The trend can be due to the thin material of the tubes that can influence the threshold determination, for this reason other similar items have been proposed, with different sizes;
- The material can influence the measurements, so the same item can be created just changing the material;
- The positioning of the item could influence the measurements; since in the suggested positions as shown in Fig. 4.12 (left), the x-rays pass through more material see Fig. 4.11, than in others. So different inclinations should be analyzed as shown in Fig. 4.12 (right).
-

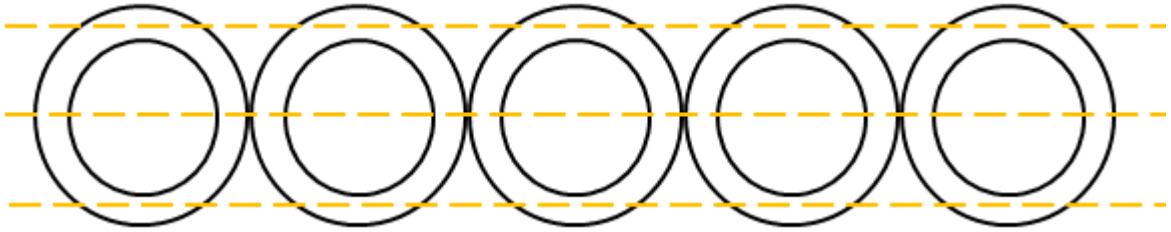

Fig.4.11: x-rays through the material, with the original CT Audit Item 2 orientation

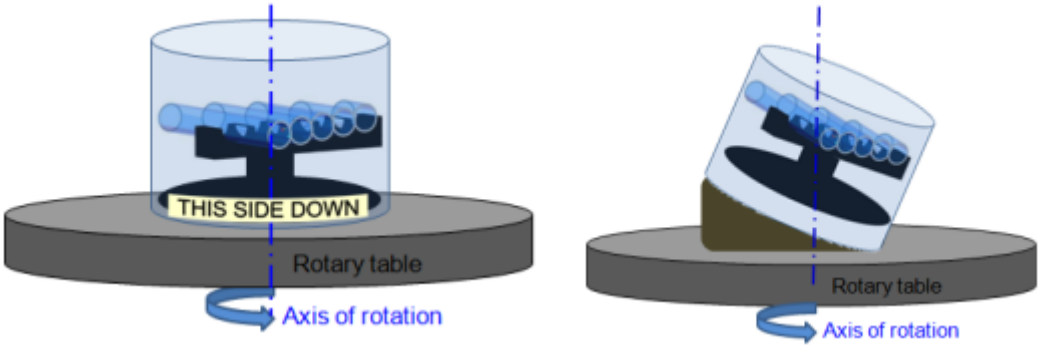

Fig. 4.12: Positioning on the rotary table: (left) CT Audit position, (right) new proposed position

4.3 Item 3: Calotte Cube

Item 3 is called Calotte Cube. It was developed by and belongs to Physikalisch-Technische Bundesanstalt (PTB), Braunschweig and Berlin, Germany. It consists of a hollow titanium

cube, with 75 spherical calottes on three sides of the cube (see Fig. 4.13). The nominal edge length of the cube is 10 mm. As shown in Fig. 4.13, three of the six faces of the cube are provided with a pattern of 5x5 spherical calottes; while only one face 4 is provided with an engraving reproducing the "PTB logo", another one has only three calottes, and one shows a deep stepped cavity (nominal cavity depth = 8.5 mm, front length = 7 mm, front width = 7 mm).

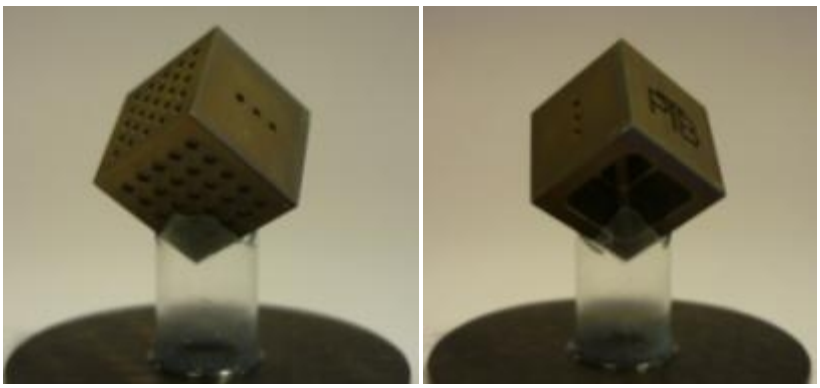

Fig. 4.13: Calotte Cube, front (left) and back (right) view

Item 3 was calibrated with CMM measurements at the calibration laboratory of Feinmess GmbH&Co.KG (accredited by the Accreditation Body of Deutscher Kalibrierdienst – DKD).

The high dimensional stability of Item 3 is well known from literature [82] and was confirmed through CMM calibrations before and after the circulation, showing deviations within the calibration uncertainty. The stability is documented in Fig. from 4.14 to 4.18, which report the absolute value of the E_n numbers comparing the calibrations before and after the circulation. The E_n number is calculated using Equation (1). According to [74], if $|E_n|<1$ then there is good correspondence between the two calibrations, otherwise the correspondence is unsatisfactory. As visible in Fig. from 4.14 to 4.18, the E_n number is always below the unit for all the calibrated characteristics of Item 3, which confirms the good dimensional stability of Item 3.

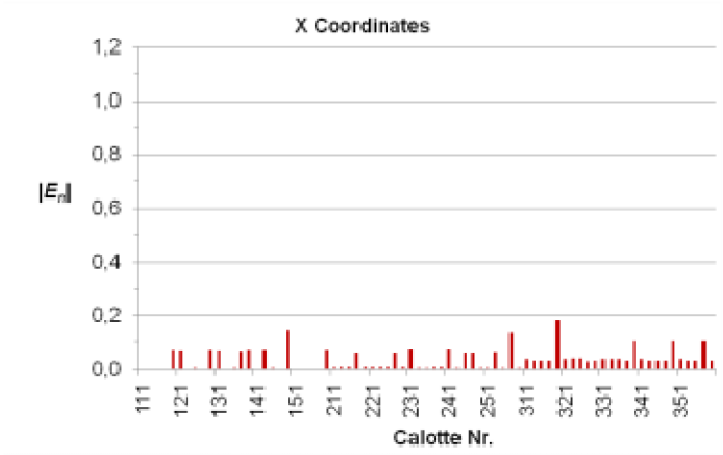

Fig. 4.14: E_n number calculated from the calibrations performed before and after the circulation on Item 3: calibration of X coordinates of calottes' centres.

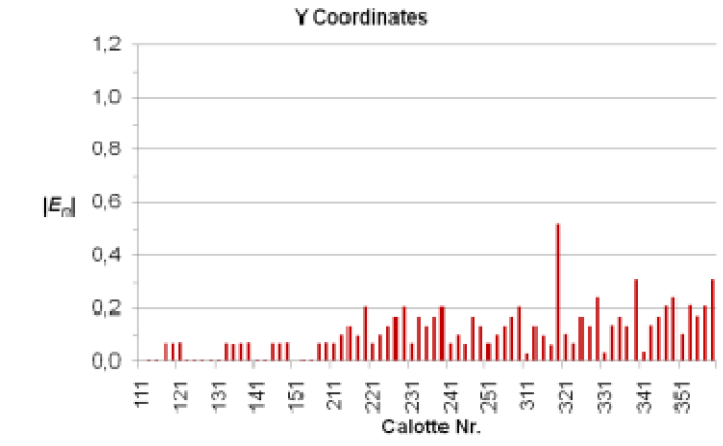

Fig.4.15: E_n number calculated from the calibrations performed before and after the circulation on Item 3: calibration of X coordinates of calottes' centres.

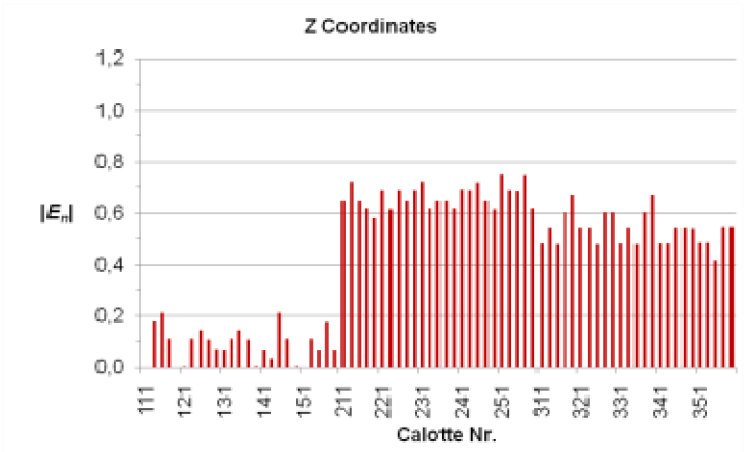

Fig.4.16: E_n number calculated from the calibrations performed before and after the circulation on Item 3: calibration of Z coordinates of calottes' centres.

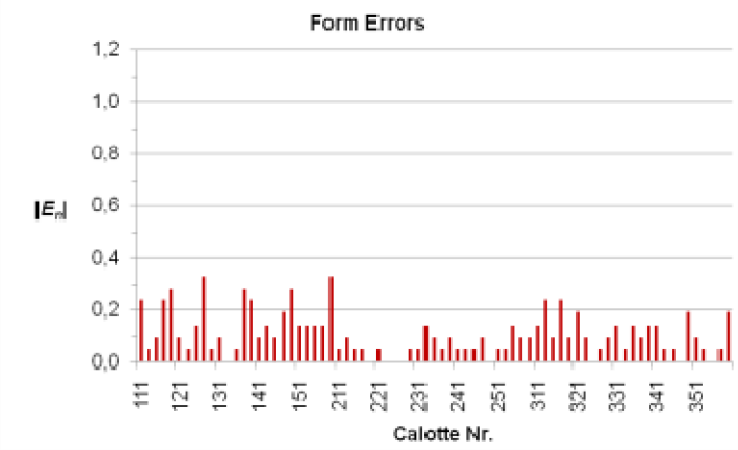

Fig.4.17: E_n number calculated from the calibrations performed before and after the circulation on Item 3: calibration of Form Errors of calottes' centres

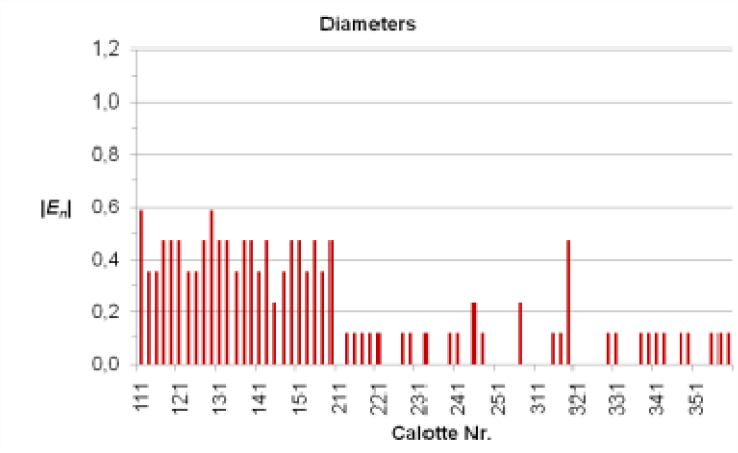

Fig.4.18: E_n number calculated from the calibrations performed before and after the circulation on Item 3: calibration of Diameters of calottes' centres

The Participants were asked to measure the following characteristics from CT data collected on the 75 spherical calottes of Item 3:

- Diameters;
- Form errors;
- Coordinates of centres;
- Distances between centres.

CT measurements of Item 3 yield a large amount of data that is very useful for determining the length measurement errors of the tested CT system: 75 calottes (diameters and form errors) and 2775 distances.

Item 3 is particularly suited for testing the length measurement capabilities of CT systems in various directions. In fact, the large number of calottes allows the identification of a huge number of distances between spheres' centres, oriented in almost any direction. Each distance between spheres' centres allows verification of unidirectional length error.

Fig. 4.19 illustrates how frequently the Participants' measurement results meet or fail to satisfy the proficiency assessment criterion $|E_n| < 1$, for form error, diameter and calottes' distances measurements on Item 3. Fig. 4.19 confirms that form measurements are more problematic than size measurements. Moreover, Fig. 4.19 shows that diameter measurements give larger E_n numbers than calottes' distances measurements; again, this can be explained by the fact that spheres' distances are unidirectional length measurements, while spheres' diameters are not unidirectional and therefore are subject to additional uncertainty components – such as threshold determination errors – that are not properly taken into account by Participants.

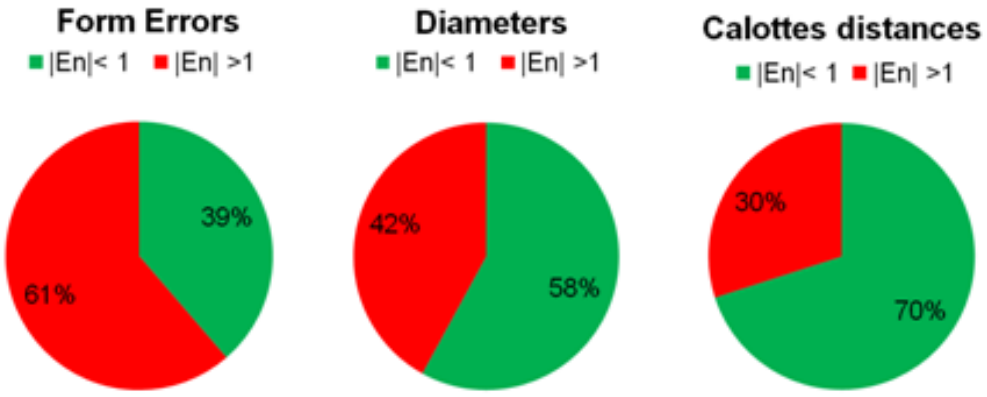

Fig. 4.19: Comparison of E_n numbers for measurements of Form errors, Diameters and Calottes Distances

Measurement results on Item 3 show that there is an overestimation of the form error values measured by all Participants (Fig. 4.20), as already seen for Item 1.

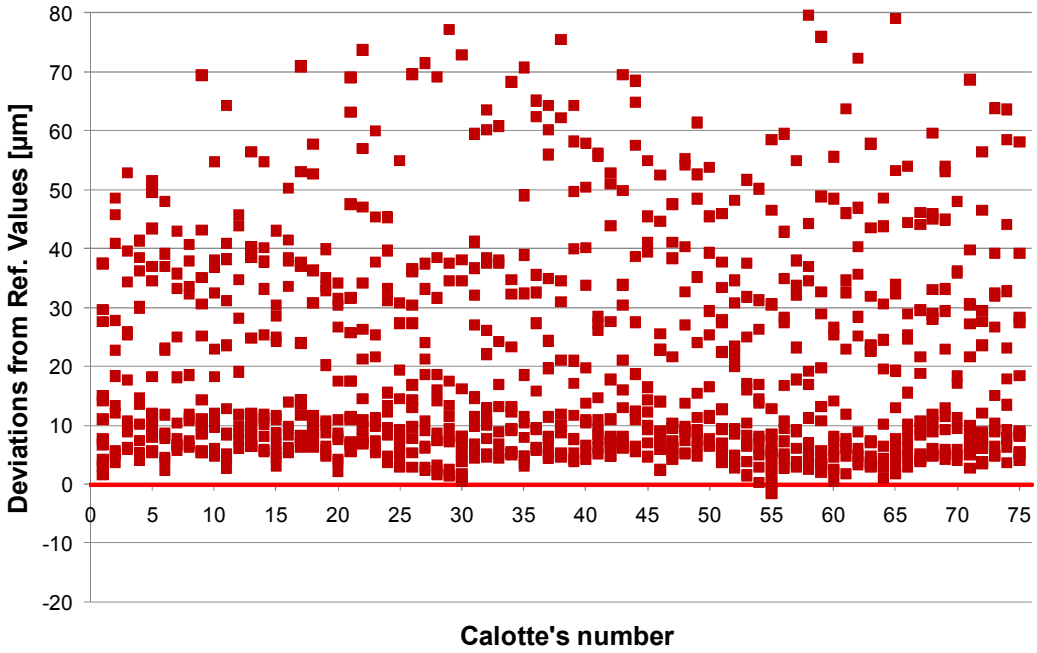

Fig. 4.20: Overestimation of form errors

Moreover each Participant received personal plots (examples in Fig. 4.21 and 4.22) that show the deviations from reference values for the distance measurements between all the centres of calottes of Item 3. For the 75 calottes of Item 3, this means a total of 2775 distances between couples of calottes, ranging from 1.6 to 13.2 mm. The deviations of the 2775 distances are represented by black crosses on the plot. Furthermore, the linear regression line is drawn on the plot. This line can be used by the Participant for determining the correction of scale error. Fig. 4.21 represents the deviations with dedicated attention to the vertical direction distances deviations (parallel to the CT scanner direction), whereas Fig. 4.22 the horizontal ones (to the CT scanner direction).

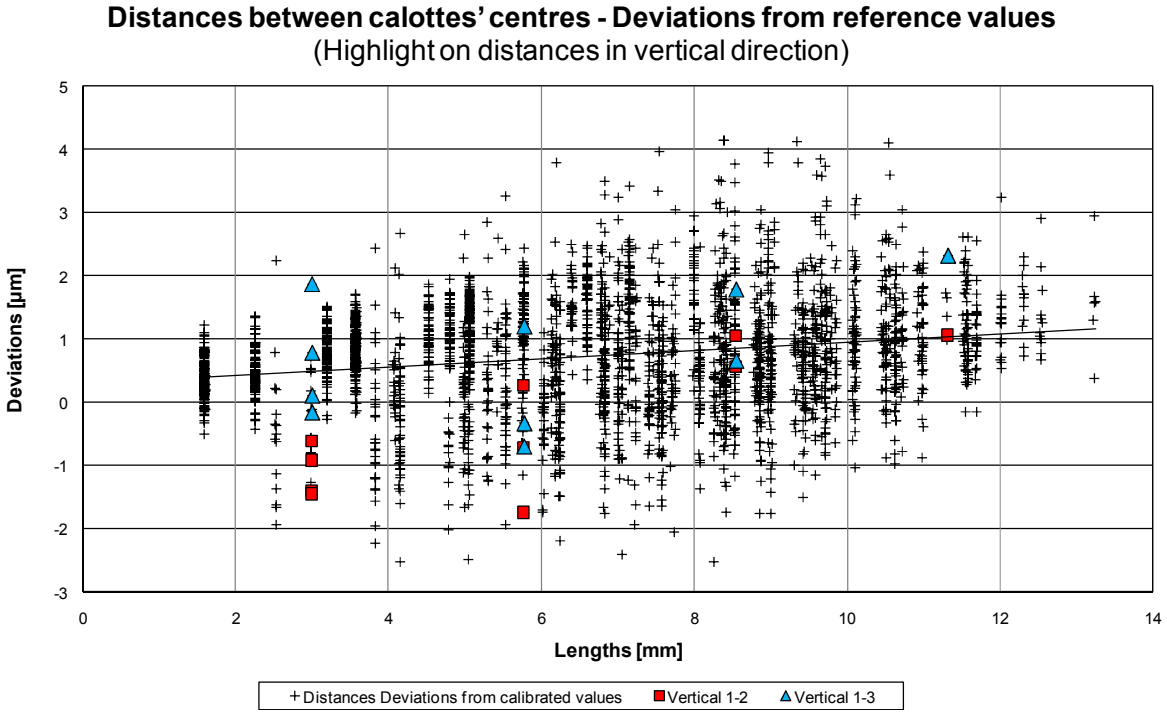

Fig. 4.21: Plot of deviations of distances between calottes with highlighted distances in vertical direction.

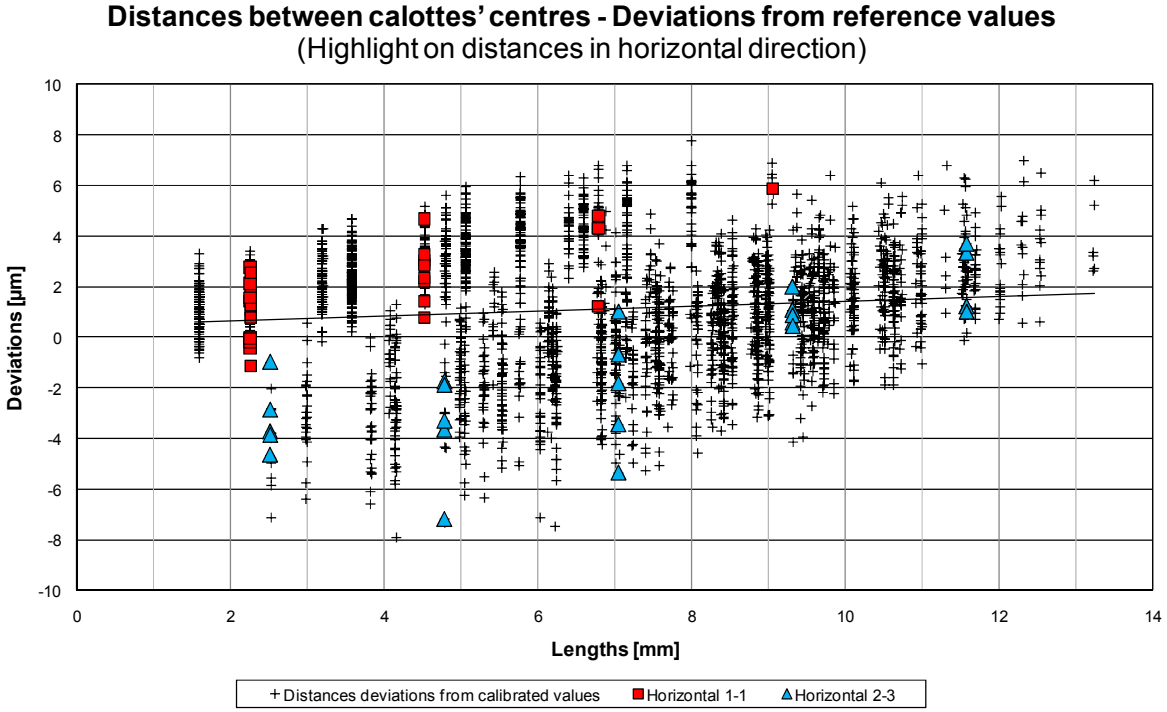

Fig. 4.22: Plot of deviations of distances between calottes with highlighted distances in horizontal direction

4.4 Item 4: QFM Cylinder

Item 4 is called *QFM Cylinder*. It was developed by and belongs to University of Erlangen-Nuremberg - Chair Quality Management and Manufacturing Metrology (QFM), Erlangen, Germany. It consists of a hollow titanium cylinder with a nominal height of 80 mm, a nominal outer diameter of 50 mm and an inner diameter of 40 mm. 28 calotte spheres are embodied on top and bottom and 14 calotte spheres are located on the cylinder barrel. Two symmetrical breakouts contain several micro structures (micro cylinders of radii 0.2-1.3 mm and micro spikes in different sizes). A ball plate carrying five sapphire spheres is clamped into the cylinder. The nominal diameter of the balls is 4 mm, the distances between the balls centres vary from 17 to 42 mm. The item is shown in Fig. 4.22.

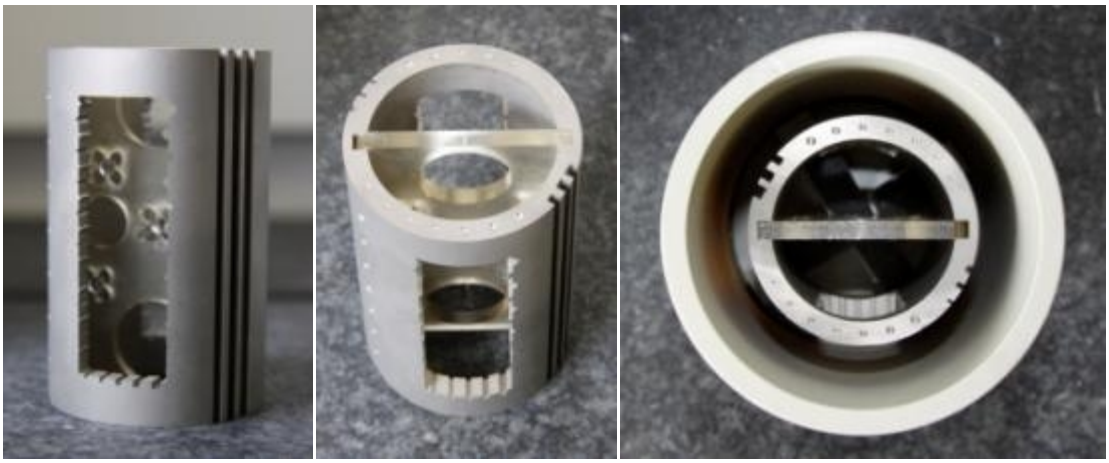

Fig. 4.22: Item 4: Front view (right), traversal view (centre) and top view (left)

The dimensional stability of Item 4 was checked through CMM calibrations before and after the circulation. Different stability results were obtained for the two main parts of the QFM Cylinder: (1) the epoxy ball-plate and (2) the titanium cylinder.

1) The epoxy ball-plate was found to be not sufficiently stable for the purposes of the interlaboratory comparison. For this reason it was decided to exclude the spheres distances of the ball plate from the results of the CT Audit intercomparison.

2) The titanium cylinder is highly stable. This was proven by QFM through specific CMM calibrations of selected geometrical features (including e.g. internal and external diameter of the cylinder) that were executed before and after the circulation, showing deviations within the calibration uncertainty.

The stability of the titanium cylinder is documented in Fig. 4.23, which reports the absolute value of the E_n numbers comparing the calibrations before and after the circulation. The E_n number is calculated using Equation (1). According to [74], if $|E_n|<1$ then there is good correspondence between the two calibrations, otherwise the correspondence is unsatisfactory. As visible in Fig. 4.23, the E_n number is below the unit for both internal and external diameters of Item 4, which confirms the good dimensional stability of the titanium cylinder.

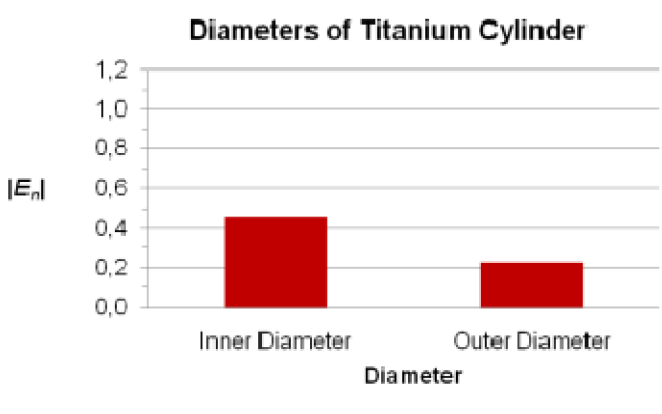

Fig. 4.23: E_n number calculated from the calibrations performed before and after the circulation on Item 4: calibration of diameters of the titanium cylinder

It is worth to notice that Item 4 is particularly rich of geometrical features that allow testing various characteristics of CT systems. It also includes micro-structures of different dimensions that in certain cases can be used for checking the structural resolution.

The Participants were asked to measure the following characteristics from CT data collected on Item 4:

- outer and inner diameter of the titanium cylinder;
- diameters of calotte spheres embodied on top and bottom faces of the cylinder;
- spheres distances of the ball plate;
- diameter of smallest measurable cylindrical micro structure.

Item 4 was found to be the most challenging item to measure, due to its multi material configuration and its size (which was larger than those of the other items). Indeed, only 8 Participants were able to measure Item 4 and the results showed larger deviations from calibrated values, with respect to the other items, as shown in Fig. 4.24.

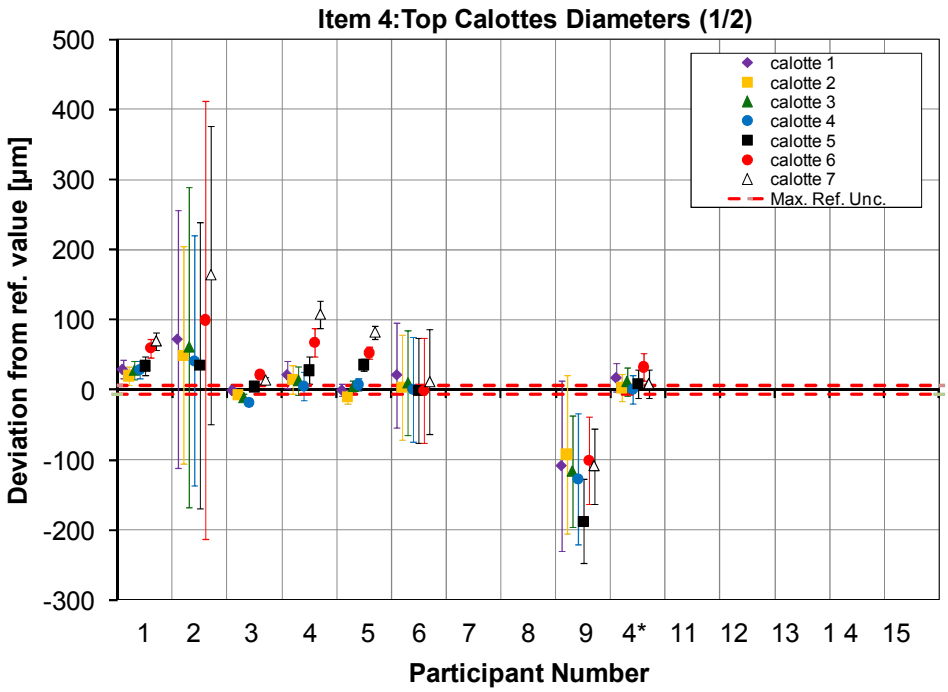

Fig. 4.24: Deviation chart for measurements of top calottes' diameters of Item 4 (calottes 1 to 7). (Note: Participant Nr. 4 represents the second measurement scan provided by Participant Nr. 4)*

Concerning the measurements of the diameter of smallest cylindrical micro-structure, these features have been asked to measure in order to evaluate the metrological structure resolution of the CT Systems. Unfortunately this type of measurement resulted in high variability of results from the Participants, in a range of almost 0.5 mm, see Fig. 4.25. These results cannot be used to evaluate the structural resolution of CT systems. Further studies, at University of Padova, on different methods for determining the structural resolution are discussed in Chapter 5.

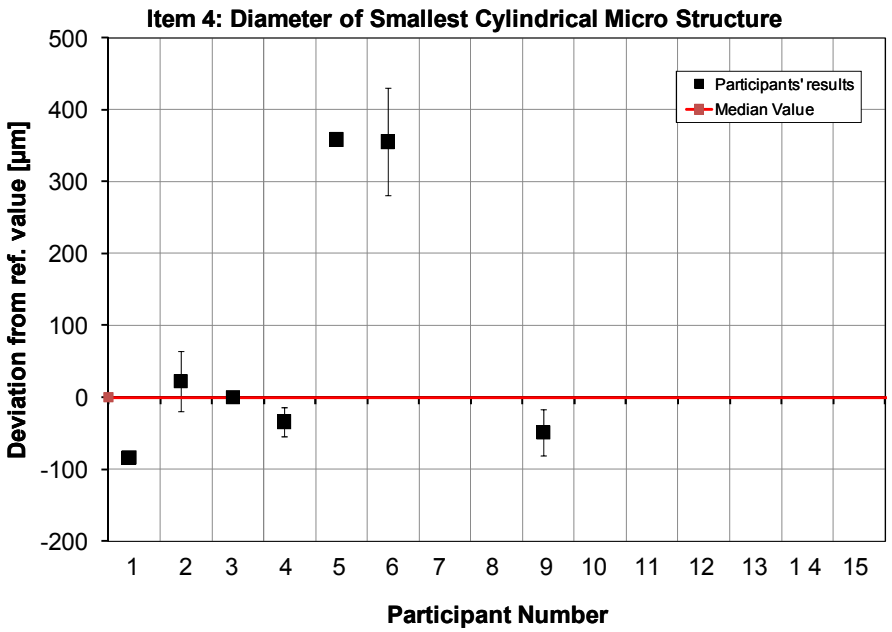

Fig. 4.25: Deviation chart for measurements of the diameter of the smallest cylindrical micro-structure of Item 4. (Note: in this case the reference value is the Participants' median value).

5. General results

Moreover considerations that involved the four items measured by the Participants can be discussed. First of all it is important to underline that the four items were not measured by each Participants, for dimension and material reasons. As shown in Fig. 5.1, only Item 1 and 2 have been measured by all the Participants.

Fig. 5.1: Distribution of Participants that did or did not measure each CT Audit item

Moreover the Participants have difficulties in evaluating the measurement uncertainty appropriately. They were asked both to estimate the uncertainty and to declare which method they used. Fig. 5.2 reports the uncertainty evaluation methods that were used by the Participants, where:

- U_A means uncertainty budget through analytical calculation of uncertainty contributors;
- U_B means evaluation based on the use of similar calibrated items and substitution method;
- U_C means evaluation based on the experience of the Participant on similar measurement tasks;
- U_D means evaluation based on measuring performance specification stated by the CT system manufacturer;
- No U means that the Participant did not state the measurement uncertainties.

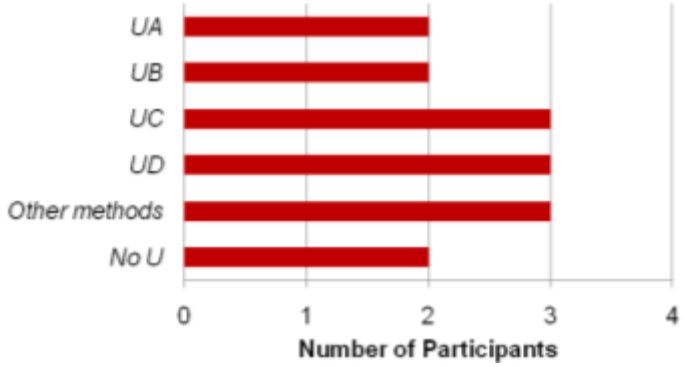

Fig.5.2: Uncertainties evaluation methods used by the Participants

In addition, the lack of standardized procedures, already discussed in Chapter 2, is one of the problems that should be promptly solved by national and international Organizations for standardization, in order to eliminate one of the reasons for current scarce consideration of CT as a valid metrological technique in industry. Indeed, the Participants were also asked to quantify the metrological performance specifications of their CT system, for example reporting the Maximum Permissible Errors (MPE) for length measurements as stated by the CT system's manufacturer, possibly according to a standard procedure. AND only 6 Participants out of 15 were able to declare their MPE, and only 4 of them could state an MPE according to a standard procedure (VDI/VDE 2617-13 [60] in all four cases). This is a confirmation of the insufficient use of standardized testing procedures for metrological CT systems.

Finally, concerning the temperature control and compensation, only one Participant (number six in Fig. 5.3) measured at reference temperature of 20 °C, and only Participants numbers 2 and 3 compensated their measurements results.

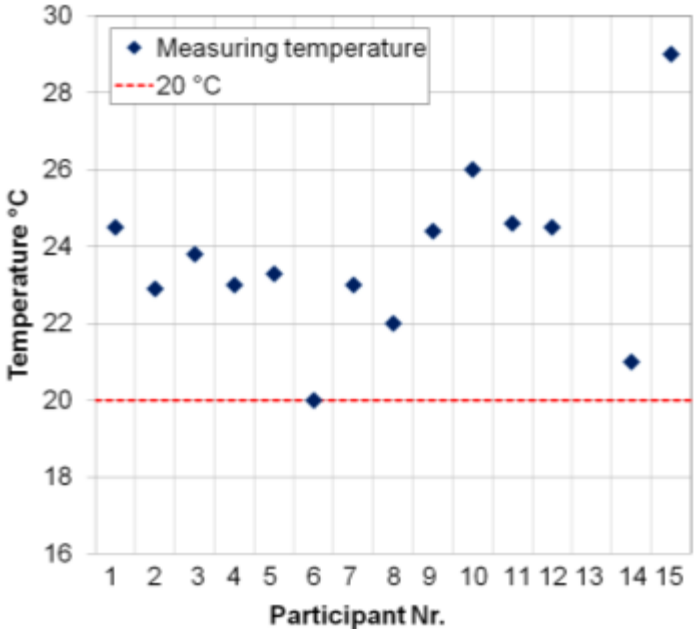

Fig. 5.3: Participants' measuring temperatures: mean temperatures during measurement of the Item 1.

6. Conclusion and further work

The CT Audit project is the first international interlaboratory comparison of CT systems for dimensional metrology, organized by the Laboratory of Industrial and Geometrical Metrology and carried out from September 2009 to June 2011. Four calibrated samples, chosen in order to represent a variety of dimensions, geometries and materials, were sent from one Participant to the next one, in a sequential participation scheme, together with detailed measurement procedures and reporting instructions. The results showed better abilities from the Participants in measuring sizes, such as diameter and distances, than form errors. Results from Item 1 and Item 3 show also that diameter measurements give larger E_n numbers than spheres' distances measurements. This can be explained by the fact that spheres' distances are unidirectional length measurements, while diameters are not unidirectional and therefore are subject to additional uncertainty components – such as threshold determination errors – that are not properly taken into account by Participants.

Moreover an interesting trend has been obtained in the analysis results of Item 2. The deviations from calibrated values of inner and outer diameters have a systematic "mirror distribution": deviations of outer diameters' measurements are always more positive than deviations of inner diameters' measurements. The possible causes of this systematic trend are going to be investigated with all the Participants. Moreover calibrated diameter values of Item 2 after the conclusion of the circulation have been distributed to each Participant, and only six of them corrected their lengths measurements in terms of systematic errors, mainly due to the threshold value determination and the scale error.

Participants have difficulties in evaluating the measurement uncertainty appropriately. This confirms that traceability of dimensional measurements is still a major challenge in CT scanning, even for experienced users.

Finally an important outcome of the CT Audit project is the establishment of an international network of laboratories using CT dimensional measuring systems. This network is an important basis for further international collaborations in the field of metrological verification and uncertainty evaluation of CT systems. Part of the network, had the chance to meet at a workshop for discussing the results of the CT Audit project on 26th of October 2011 in Padova at Dimeg Department.

Chapter 5

Investigation on

Structural Resolution

Metrological structure resolution is investigated in Chapter 5 and an industrial method is proposed for its evaluation.

1. Resolution in CT: concepts and definitions

Resolution is one of the fundamental characteristics that shall be tested when evaluating metrological performances of CT systems. According to VIM (International Vocabulary of Metrology) resolution can be defined as the smallest change in a quantity being measured that causes a perceptible change in the corresponding indication [27]. However since many years resolution of optical and imaging systems has been discussed and many definitions have been proposed.

One of the first definitions of resolution was given by Lord Rayleigh in 1897, with investigations on the limit resolution of some optical instrument such as telescopes and spectroscopes [1]. He proposed the Rayleigh Criterion that consists in the minimum resolvable detail - the imaging process is said to be diffraction-limited when the first diffraction minimum of the image of one source point coincides with the maximum of another [1] [83].

The resolving power of an optical instrument is a measure of its ability to create individual images of objects, as opposed to a single merged image. When looking at two stars in the sky, for example, it is possible to tell that they are two stars if they are separated by a large enough angle. Some stars are so close together they look like one star to the naked eye, but when using a telescope it is possible to identify the two stars as separated.

According to Rayleigh Criterion (see Fig. 1.1) the angular resolution of a lens (or an ideal objective) of diameter D is given by [83]:

$$\theta_{Rayleigh} = 1.2197 \cdot \frac{\lambda}{D} \qquad (1)$$

, where λ is the wavelength of radiation.

A more appropriate and stringent criterion has been further proposed by C. Sparrow (see Fig. 1.1) where the diffraction limit of resolution can be calculated as following [83]:

$$\theta_{Sparrow} = 0.947 \cdot \frac{\lambda}{D} \qquad (2)$$

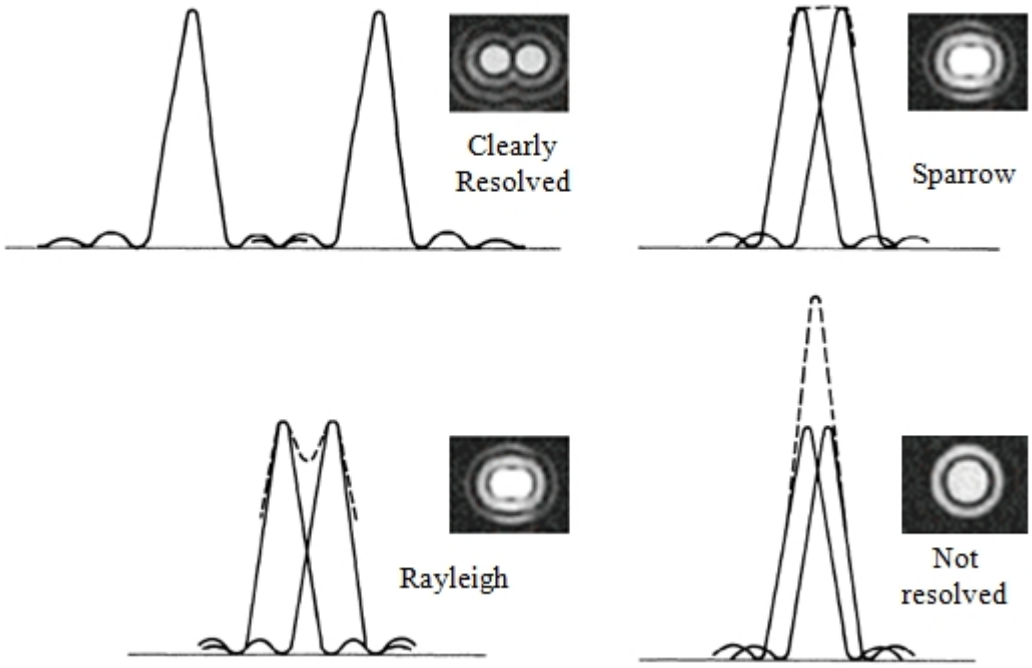

Fig. 1.1: The Rayleigh and Sparrow criteria for overlapping point images [83]

These approaches to the resolution of a measuring system (in this case an optical one) are only the first of many studies, since the resolution reveals to be one of the most important parameter in order to test the quality of measuring device.

1.1 Methods for resolution evaluation

1.1.1 Modulation transfer function

Several methods for measuring the spatial resolution of a CT system are based on measuring the modulation transfer function (MTF), the point spread function (PSF), the line spread function (LSF) or the edge spread function (ESF) and they all rely on the characterization of the imaging system as a linear filter [1].

In terms of point spread function, the resolution of an imaging system can be obtained considering an object consisting of a perfect point source. When plotting the profile through the spot the one-dimensional PSF is obtained as shown in Fig.1.2. The resolution can be defined as the width within which the PSF drops to half the maximal value, called the full width at half maximum (FWHM).

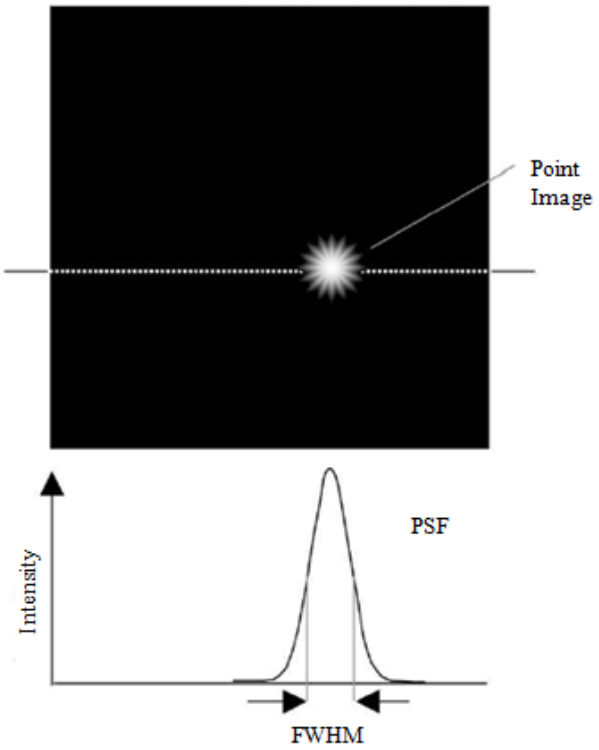

Fig.1.2: The image of a point source and its resulting one-dimensional point spread function. [1].

Similarly to the PSF method, the resolution can be determined in terms of line spread function (LSF) considering the image of an ideal line. The FWHM of these profiles express the resolution at a specific point in a specific direction.

Using edge spread function (ESF) an ideal step function is used to calculated the resolution and the LSF can then be also obtained as the first derivative of the ESF.

Finally [54] the spatial resolution can be obtained by calculating the MTF from the image of a simple cylinder that once its center of mass is determined, profiles through this point are perpendicular to the cylinder edge. The method consists in determining the MTF by computing the amplitude of the Fourier transform of the PSF. The PSF is obtained by calculating the derivative of the cylinder profile. Many non-overlapping profiles can be computed, aligned, concatenated, and smoothed to reduce system and quantization noise on the edge-response function (ERF). PSF or the equivalent LRF, line response function) is estimated by taking the discrete derivative of the ERF and its discrete Fourier transform (FT) is taken to obtain the MTF. The resolution is calculated in correspondence of the first minimum of the MTF (see also Fig. 1.3) [54] [84] [85].

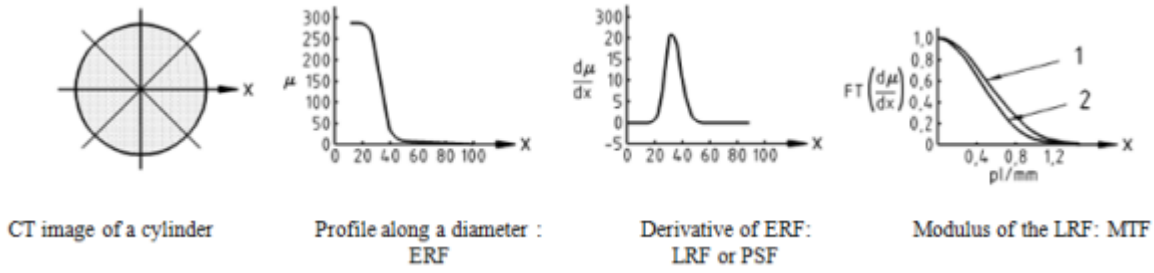

Fig.1.3: Method to obtain the MTF form the image of an homogeneous cylinder adapted from ISO 15708-2 [84][54]

1.1.2 ASTM spatial resolution definition for CT Systems

In particular in Chapter 5 the efforts of defining resolution and in particular the structural one for CT systems are documented. At the state of the art, a unique universally accepted definition is not available.

The American Society for Testing and Materials handle the concept of resolution in particular in the standard ASTM 1695 [51]. In particular it defines the spatial resolution as the ability of a CT system to image fine structural detail in an object. The test object for evaluating the spatial resolution is a disk phantom as already explained in Chapter 2.2. The spatial resolution is then quantified in terms of edge response function (ERF), point spread function (PSF) and modulation transfer function (MTF).

Hsieh J. [3] divided the definition of resolution in three different parts:

1. High contrast spatial resolution that describes the ability of a CT system to resolve objects closed to each other. The spatial resolution is further on divided in:

    a) In-plane spatial resolution (xy plane): it is calculated in terms of line pairs per millimeters (lp/mm), where line pair is a pair of equally sized black white bars. The ability of the CT system consists in resolving different bar patterns under predefined conditions. The in-plane spatial resolution is calculated in terms of MTF, defined as the ration of the output modulation to the input modulation, measuring the response of a system to different frequency. The MTF curve is a flat curve, when the system is an ideal CT scanner. Dedicated phantoms with bar patterns of different spatial frequency have been proposed for testing the spatial resolution in plane, as shown in Fig.1.4. Also by visually inspecting the bar patterns, it is possible to determine the

finest bar pattern (that is the highest spatial frequency) that is just resolvable or barely separable.

b) Cross-plane spatial resolution (z direction): it can be described as the slice sensitivity profile (SSP), that declares the systems response to another function, called Dirac delta function in z.

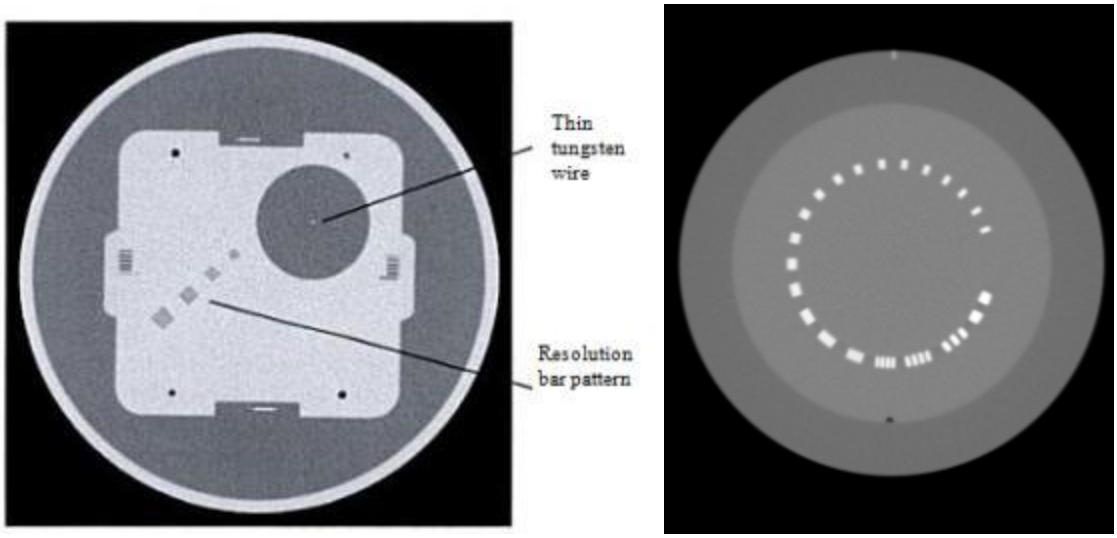

Fig. 1.4: GE performance phantom (left), Catphan phantom (right) [3]

2. Low contrast resolution is the ability of a CT system to differentiate a low contrast object from the surrounding. It is measured with dedicated phantoms with low contrast objects (materials with slightly different attenuation coefficients) of different sizes. It is calculated in terms of low-contrast detectability (LDC).

3. Temporal resolution that is typical for medical CT scanner applications. It consists in the efficacy of any cardiac imaging technology relates to its ability to deliver image detail (as expressed in spatial resolution) in the smallest "window" of time - expressed as temporal resolution, often by a number of milliseconds (ms) [86].

1.1.3 BSI resolution definition for CT Systems

British Standards International (BSI) considers the spatial resolution as an important parameter in order to predict and measure CT system performance and to compare different CT systems. It is directly related to the concept of modulation-transfer function (MTF), that describes the ability of the system to reproduce spatial frequencies [54]. A simple cylinder is proposed as test phantom, the suggested material is the same as the actual test object to be measured.

Moreover spatial resolution is suggested to be measured using test phantom with line pair gauges, as shown in Fig.1.5 and 1.6.

The measurement consists in evaluate the CT system response to the reference object features. The response factor (R) can be defined as:

$$R(i) = \frac{N_B(i) - N_A(i)}{N_C - N_A} \times 100$$

, where N_A, N_B and N_C are respectively the signal inside the holes, the signal between holes and the material signal.

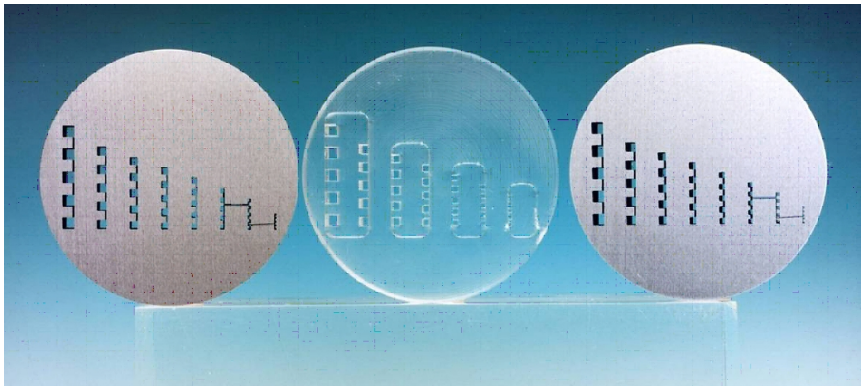

Fig. 1.5: Test phantoms (in aluminium alloy, plexiglass, stainless steel) for spatial resolution measurement using line pair gauges [54]

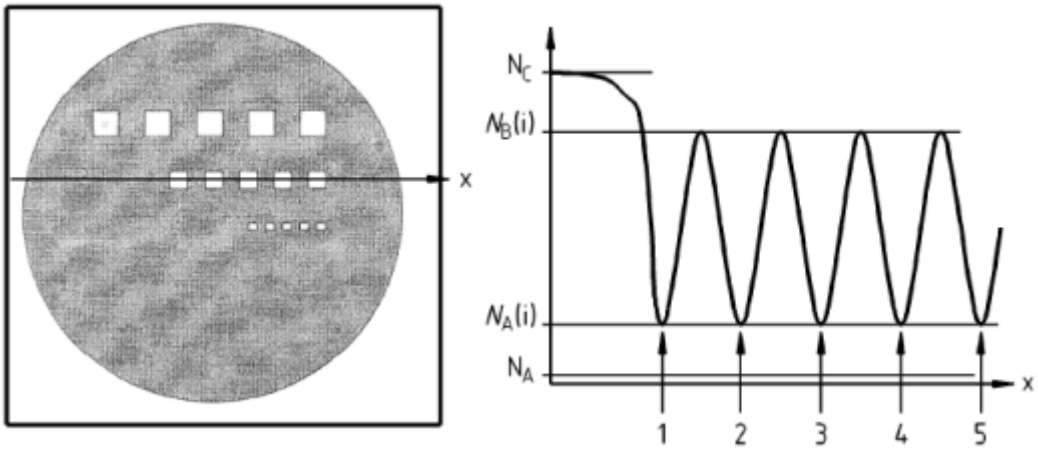

Fig 1.6:. Measurement principle of response factor using line pairs gauge [54]

1.1.4 VDI and ISO resolution definition for CT Systems

The Association of German Engineers (VDI) in the standard VDI/VDE 2630-1.1 (Basic and definitions for computed tomography in dimensional measurement) divides the concept of

resolution in three different definitions, without including a structural resolution, as following described [17]:

- Contrast resolution defined as the property of a CT unit of identifying objects of low contrast comparing to the background;
- Density resolution that is the capability of a CT unit of reproducing objects of low density comparing to the surrounding;
- Spatial resolution that is the property of a CT unit of recognizably reproducing objects very closed to each other as separated from the background.

The definition of structural resolution is not universally accepted and defined, and it is described only in annex A of VDI/VDE 2617-13 [60]. According to VDI/VDE 2617-13, "the structural resolution (also called spatial resolution) describes the size of the smallest structure that can still be measured dimensionally". Moreover the structural resolution for dimensional measurements gives to the users an immediate impression of the range of "good" performance of the CT systems.

From the definitions of VDI, the working draft ISO Standard 10360-11 [61] is developing ISO definitions and approaches in evaluating the structural resolution.

The working draft ISO standard distinguishes between spatial and structural resolution. In particular the structural resolution is called as metrological structure resolution, in order to underline the metrological aspect of this characteristic.

ISO Standard divides resolution in two different definitions that are:

1. Spatial resolution;
2. Metrological structure resolution.

Spatial resolution is defined as the smallest measurable displacement in the measured direction (x,y and z). The evaluation of spatial resolution can be done in the length and probing measurements. A different definition is dedicated for metrological structure resolution, since it describes the size of the smallest structure that is measurable within the maximum permissible error to be specified. Each structure needs to be not only detectable, but also correctly measurable in terms of size and form. The metrological structure resolution shall be distinguish from the metrological structure resolution in the grey scale range of voxels that does not involve the complete dimensional measurement chain but only the threshold value process. Moreover the metrological structure resolution in the grey scale

range of voxels can be evaluated in terms of MTF (modulation transfer function) and it influences of course the metrological structure resolution.

When worsening the metrological structure resolution for dimensional measurements, the probing error for form improves and for this reason the information given by the length and probing error do not provide any evaluation of the resolution.

It is affected by many influence factors that cover the whole dimensional measurement chain, as following:

- Size and shape of the focal spot;
- Voltage and Current;
- Pre-filtering of the X-ray radiation;
- Magnification;
- Pixel of the detector;
- Number of rotary table steps;
- Post processing operations;
- Threshold operations for surface examinations.

A test procedure and a related definition have been proposed. "The metrological structure resolution for dimensional measurements D_g is specified as the diameter of the smallest sphere that can be measured with the manufacturer's specified limits MPE for the from probing error PF and size probing error PS". According to this definition the manufacturer should specify the smallest resolvable sphere for dimensional measurements; the sphere needs to a calibrated in diameter and form error. The diameter of the sphere equals the specified resolution.

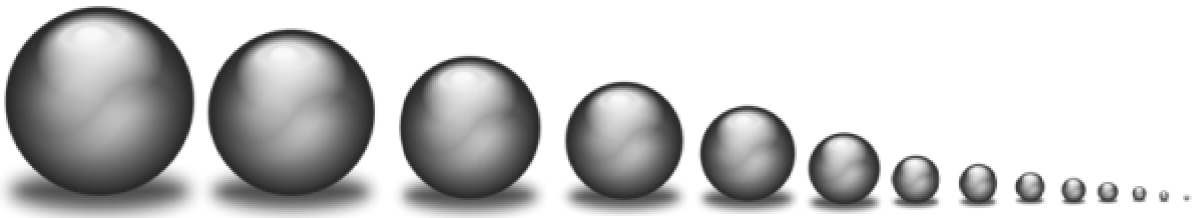

Fig.1.7: ISO standards proposed test procedure

Kruth el al. [8] confirmed the ISO standard definition and they stated that it is vital to cover the entire sequence of a CT measurement while determining the metrological structure resolution.

Contrary, Ralf C. et al. [20] strongly differentiated from ISO resolution definition. In particular they divided resolution in two concepts:

1. Structural (or spatial) resolution
2. Positional (or metrological) resolution

1.1.5 Resolution definitions by R. Christoph (Werth Messtechnik GmbH)

Christoph R.et al. [20] relate the structural resolution to the capability of CT systems to identify small features; in particular it represents the size of the smallest structures that is detectable on the measured object. The structural resolution mainly depends on:

- Size of x-ray spot: the smallest the spot, the better the resolution;
- Current and voltage of the x-ray tube, with low electrical power the resolution improves;
- The accuracy of the rotary table;
- The size of the pixel detector;
- Binning, when it is selected, the resolution get worst;
- The influence of any filter in the reconstruction procedure.

The test phantoms proposed are smallest spheres, cylinders and holes.

On the other hand, they define the positional resolution as the smallest increment that can be practically used when determining the position of a transition point between two materials, or between material and the background.

2. Developed Methods

In order to test the metrological structure resolution of a CT system according to ISO 10360-11, some investigations have been conducted at *Laboratory of Industrial and Geometrical Metrology* in collaboration with DEI Luxor Department (University of Padova), Elettra Synchrotron (Trieste) and Geosciences and Image Department (University of Padova).

2.1 Method using Needle and Hourglass object

As already described, metrological structure resolution for dimensional measurements D_g is defined as “the size of the smallest structure that is measurable with error limits to be specified” [61]. In order to evaluate the metrological structure resolution, the ISO Standard proposed a test procedure (still as draft) where the resolution of CT systems is evaluated

measuring a sphere in terms of PS (size probing error) and PF (form probing error). The metrological structure resolution D_g is the diameter of the smallest sphere that can be measured within the manufacturer's specified limits MPE. This test procedure has been studied and even if is the only one officially proposed, some disadvantages occur. In particular each CT measurement reveals different structure resolution when using different parameters, (such as source-object-detector distance, pixel size) that lead to the necessity of providing many spheres of several dimensions. Moreover the spheres should be ideal spheres even with very small diameters and this causes higher costs of providing and calibrating spheres. Finally the test procedure is too long and slow for industrial applications since the user (or the manufacturer) should measure a number of spheres since the smallest one can be measured.

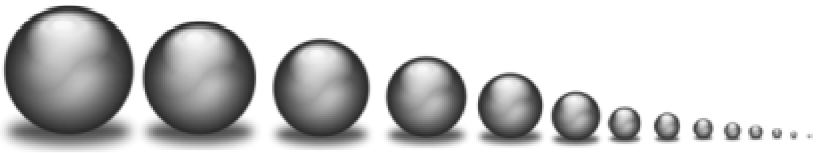

Fig. 2.1: ISO standards proposed test reference object

In order to reduce these limits of the ISO standard test procedure, other test objects have been proposed. The idea by Carmignato consists in measuring only one object in order to test the metrological structure resolution in order to reduce the onerous measurements of many spheres.

The item should be suitable for different setting parameters and so different metrological structure resolution. For these reasons an item with several dimensions in decreasing trend is needed.

One of the first proposed objects is *Needle* (Fig. 2.2). The item shows decreasing dimensions from a point (point A in Fig. 2.2) and reduced tolerances.

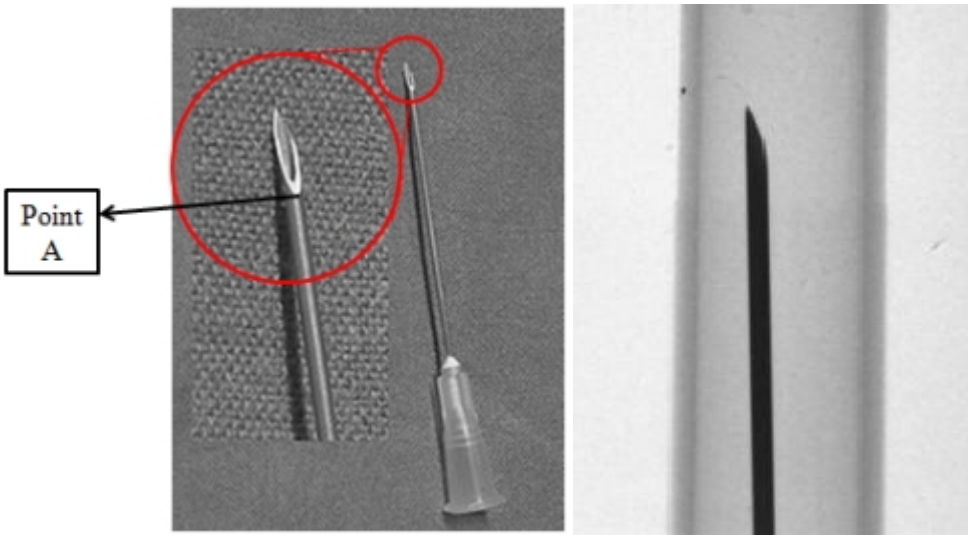

Fig.2.2: Needle object details (left), Needle under CT radiation (right)

The item has been measured at DEI Luxor Department where a self-developed CT scanner is available with the following main characteristics:

- Microfocus x-rays source (voltage from 20 to 90 kV) with 5 Watt power and a focal spot size of 5 μm;
- CDD Detector 1392 x 1040 imaging array with 4.65 x 4.65-μm pixels.

Fig. 2.3: Dei Luxor CT scanner picture

The item reveals not very good results in terms of metrological structure resolution, since the identification of the minimum visible feature was impossible to measure, even if visually the item seems to be pretty interesting.

After this first experiment, another dedicated object has been studied: *Hourglass* (which was developed on a concept by Carmignato).

The procedure for evaluating the structural resolution was based on the idea of making the test procedure as easiest as possible in order to be achievable for industrial applications. For this reason, only one test object should be created and it should contain all the information necessary for the structural resolution evaluation.

The prototype item, called *Hourglass*, is composed by two ceramic spheres of 8 mm nominal diameters. The two ideal spheres are in contact in one point as shown in Fig. 2.4 (right) and they are fixed without any kind of glue at the contact point. A carbon fiber cylinder makes the spheres fixed and in contact as shown in Fig 2.4 (left and right).

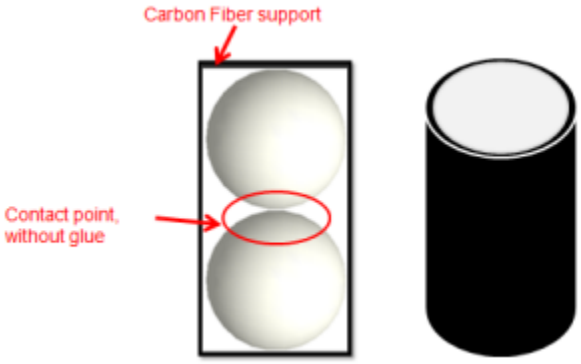

Fig. 2.4: Hourglass design, the two spheres in contact (left) and the carbon fiber cylinder (right)

Hourglass has many infinite features available. These features ideally decrease till zero value, as shown in Fig.2.5.

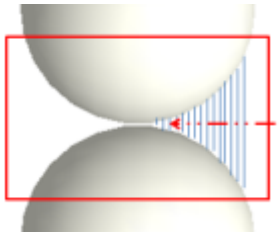

Fig.2.5: Infinite set of measurable distances.

The structural resolution is related to the contact zone of the two spheres. When the contact zone is reduced to an infinitesimal point, it is a condition of optimum structural resolution and it is ideal. With the worsening of structural resolution, the contact zone is supposed to move from the optimal point conditions. As shown in Fig. 2.6 (centre and right) the two spheres are not separated as supposed and the contact zone has become a “cylinder” with a particular height and radius. The limit of the structural resolution can be correlated to the height of the cylinder.

Fig.2.6: Hourglass concept: excellent(left), and poor (centre) metrological structure resolution, and representation of the cylinder contact zone (right)

Following trigonometry rules, the structural resolution related to h can be calculated as:

$$r = R \cdot sen(\alpha) \qquad (3)$$

$$\propto = arcsen(\frac{r}{R}) \qquad (4)$$

$$h = 2 \cdot R \cdot (1 - cos\alpha) \qquad (5)$$

$$h = 2 \cdot R \cdot (1 - \cos(arcsen(\frac{r}{R})) \qquad (6)$$

, where *r* is the cylinder's radius, *R* the spheres' radii, *h* the cylinder's height and *α* the angle formed between the height and radius of the "cylinder", as shown in 2D in Fig. 2.7.

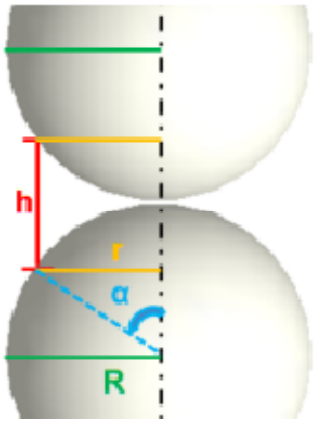

Fig. 2.7: Hourglass: calculations of h, related to structural resolution

The item has been created assembling two ceramic spheres and inserting them in a carbon fiber cylinder. Before composing *Hourglass*, the two spheres have been calibrated and the carbon fiber cylinder has been checked in its faces planarity and perpendicularity to cylinder axis through CMM calibration at *Laboratory of Industrial and Geometrical Metrology* of University of Padova.

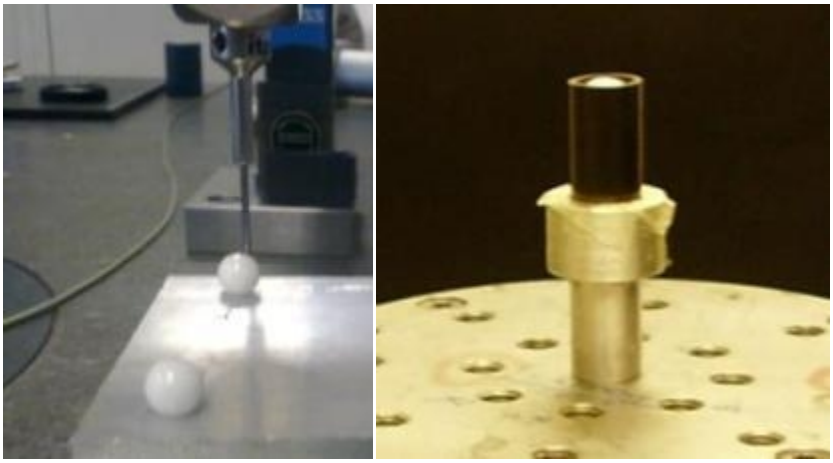

Fig.2.8: Spheres CMM calibration (left) and Hourglass picture (right),

16 ceramic spheres have been calibrated in order to use the more ideal spheres with radii as similar as possible. The selected spheres have a roundness error less than 1 μm and diameter of 8.0022 ± 0.0015 mm.

The item reveals to have the ulterior advantage of being suitable for many CT systems since the contact zone is particularly small and it is possible to isolate only the contact part to evaluate the structural resolution. For this reason, it is also possible to evaluate the structural resolution in different magnification position, such as closed to the x-ray source or to the detector. This is one of the advantages that points out the industrial suitability of *Hourglass*.

3. Experimental Investigation on Hourglass

3.1 First pilot test at Elettra (Trieste) using Synchrotron radiation

First pilot tests have been conducted at Elettra Synchrotron of Trieste (Italy). *Hourglass* has been measured with Synchrotron radiation at Syrmep Beamline (see Chapter 2-6.1 for more details).

The measurement with Synchrotron radiation has been done in order to verify the suitability of *Hourglass* for CT system with small field of view.

The synchrotron coherent beam allows the acquisition of images under Phase Contrast mode. The Phase contrast is a physical effect that is produced by the path-length variations of the X-rays travelling within the sample. This effect enhances the contrast between different materials, also when they exhibit a small absorption with respect to hard X-rays [1]. *Hourglass*

has been scanned three times under three different measurement conditions, as shown in Table.3.1 In details, only one parameter has been changed: the distance between the object and the detector, at 5.5 cm (normal scanning), 20 cm and 40 cm. When increasing the distance between object and detector, phase contrast effect occurs and the contours and edges of the object blur. So the measurement is expected to be less accurate in terms of dimensional measurements, when phase contrast effect happens. For this reason the metrological structure resolution has been supposed to be worst in Phase Contrast mode.

Table 3.1: Hourglass with Synchrotron radiation measurements parameters

	HG	**HG 20**	**HG 40**
Nr. proj	1800 over 180°		
Energy (keV)	26		
Step [°]	0.1		
Exp. Time [sec]	10		
Pixel size [µm]	9		
Distance Object to Detector [cm]	**5.5**	**20**	**40**

The data acquired at Syrmemp beam line have been post processed with the not commercial program *Syrmep Tomo Project* that is based on the filtered back projection method. The volume of Hourglass has been further analyzed in *VG Studio Max 2.1* and a point cloud (.txt file) has been exported and investigated with *Polyworks 10.0 Innovmetric* software. The contact zone between the two spheres reveals to produce a "cylindrical hole" due to structural resolution, and its radius has been calculated as a fitting of points following the Gaussian best fit filter (see Fig.3.1 and 3.2).

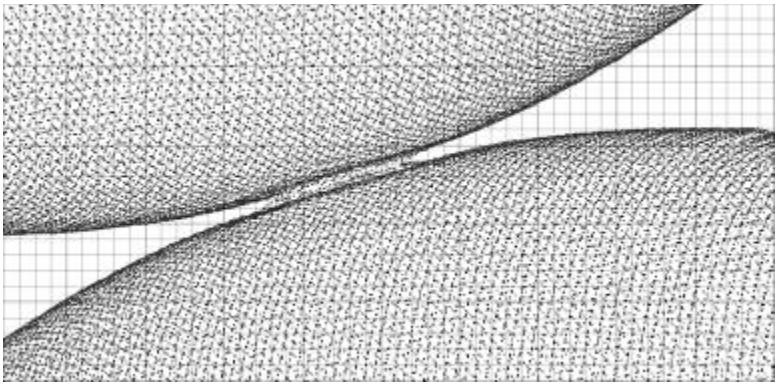

Fig. 3.1: Hourglass Contact zone of the two spheres

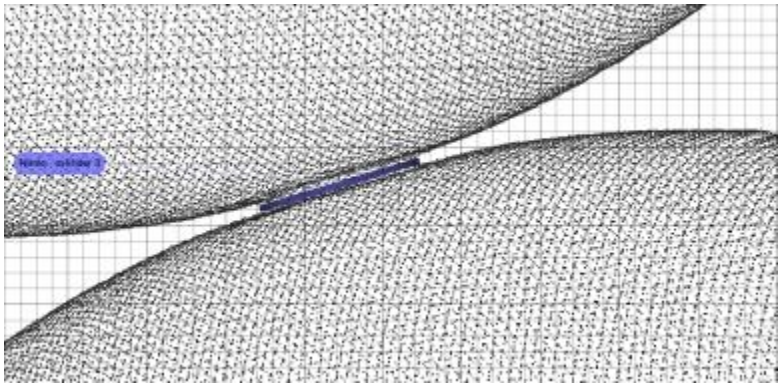

Fig.3.2: Hourglass fitted cylinder in the contact zone of the two spheres

The fitted cylinder radius has been recorded and according to (6) the height of the cylinder has been calculated. In Table 3.2 the results have been reported. The height *h* of the cylinder is supposed to represent the metrological structure resolution of the CT system using synchrotron radiation and as supposed, the height of the cylinder is getting bigger with the increasing of the phase contrast effect. As shown in Table 3.2 when the distance object-to-detector is:

- 5.5 cm, the height of the cylinder is 2.6 μm;
- 20 cm, the height of the cylinder is 3.5 μm;
- 40 cm, the height of the cylinder is 6.4 μm.

Table 3.2: Hourglass results with Synchrotron radiation CT measurements

***Hourglass* at Synchrotron [mm]**			
R	**h**	**r**	**α**
4	**0.0026**	0.10193	0.02549

***Hourglass* at Synchrotron [mm] Object to Detector Dist. 20 cm**			
R	**h**	**r**	**α**
4	**0.00352**	0.11865	0.02967

Hourglass at Syncrotron [mm] Object to Detector Dist. 40 cm			
R	**h**	**r**	**α**
4	**0.00644**	0.16042	0.04011

3.2 Pilot test at Elettra (Trieste) using a micro CT system

Further pilot tests have been conducted at Elettra (Trieste) using a different micro CT system, with cone beam configuration at TOMOLAB station. It (see 3.3) has been realized by collaboration between Elettra and the University of Trieste (Dipartimento di Ingegneria Civile e Ambientale, Unità Clinica Operativa di Clinica Odontostomatologica). It is equipped with a sealed microfocus X-ray tube, which guarantees a focal spot size of 5 microns, in an energy range from 40 up to 130 kV, and a maximum current of 300 microA. A water cooled CCD camera providing a good combination between a large field of view (49.9 mm×33.2 mm) and a small pixel size (12.5×12.5 microns2) is used as detector [71].

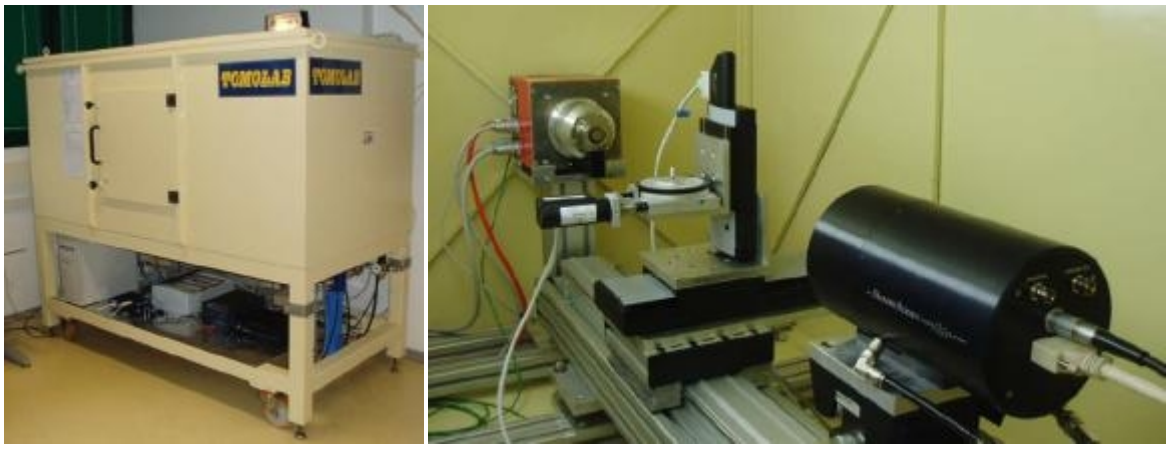

Fig.3.3: TOMOLAB set up, external (left) and internal (right) appearance

More interesting results in terms of industrial applications than the ones obtained with Synchrotron radiation have been achieved with the cone beam CT system. Indeed more influence factors for the evaluation of metrological structure resolution are available, as already explained in 1.1.4 of this chapter. In particular, with Synchrotron CT system it is not possible to act on the magnification, whereas with the Cone beam CT system configuration the distance between source-object-detector has the possibility to be varied resulting in different magnifications. This is clearly shown in Fig.3.4.

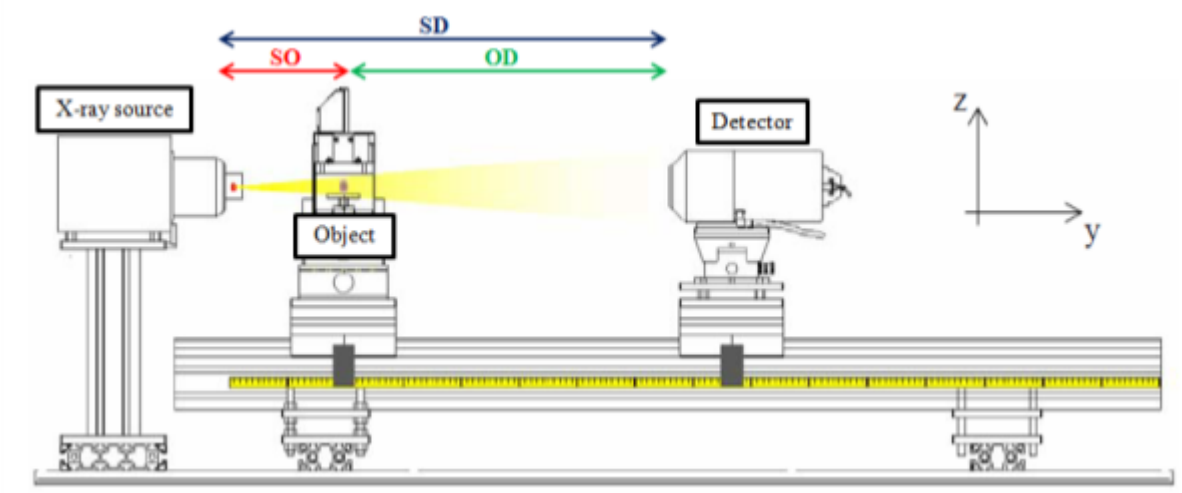

Fig.3.4: Scheme of the instruments inside the Tomolab facility [71]

The magnification is calculated as following:

$$M = \frac{SD}{SO} \qquad (7)$$

, where SD is the source-to-detector distance and SO the source-to-object one *[71]*.

Hourglass has been measured 4 times under three different magnification values. According to 7) the magnification factor *M* has been calculated for four different positions of the objects and related pixel sizes changed as shown in Table 3.3.

Table 3.3: Hourglass at Tomolab CT measurements parameters

11	**M 4**	**M 3**	**M 2.5**	**M 2**
Nr. proj	1200 over 360 °			
Voltage (kV)	100			
Current (µA)	80			
Exp. Time [sec]	5			
Pre-filter	1.5 mm Aluminium			
Pixel size [µm]	**6.181**	**8.325**	**9.978**	**12.524**

As similarly explained in 3.1 the data acquired at Tomolab micro CT system been post processed with COBRA Software that is Exxim's implementation of 3D CT reconstruction using the filtered back-projection algorithm (Feldkamp). The volume of Hourglass has been further analyzed in VG Studio Max 2.1 and a point cloud (.txt file) has been exported and investigated with Polyworks 10.0 Innovmetric software. The contact zone between the two

spheres reveals to be a "cylindrical hole" and its radius has been calculated as a fitting of points following the Gaussian best fit method.

The fitted cylinder radius has been recorded and according to (6) the height of the cylinder has been calculated. In Table 3.4 the results have been reported. As already described in 3.1, the height *h* of the cylinder is supposed to represent the metrological structure resolution of the micro CT system and as supposed, the height of the cylinder is getting smaller with the increasing of magnification and the decreasing of the pixel size. As shown in Table 3.4 when the distance magnification is:

- 4 (pixel size=6.2 μm), the height of the cylinder is 13.8 μm;
- 3 (pixel size=8.3 μm), the height of the cylinder is 15 μm;
- 2.5 (pixel size=9.9 μm), the height of the cylinder is 21.8 μm;
- 2 (pixel size=12.5 μm), the height of the cylinder is 25.5 μm.

Moreover, comparing the results reported here in 3.2 and in 3.1, the more accurate performance of CT system using synchrotron radiation has been confirmed, since the metrological structure resolution is worst, when measuring with the micro CT cone beam system.

Table 3.4: Hourglass results at Tomolab

***Hourglass* at Tomolab [mm] M 4**			
R	**h**	**r**	**α**
4	0.01378	0.23464	0.05869

***Hourglass* at Tomolab [mm] M 3**			
R	**h**	**r**	**α**
4	0.01503	0.24506	0.0613

***Hourglass* at Tomolab [mm] M 2.5**			
R	**h**	**r**	**α**
4	0.02179	0.29504	0.07383

***Hourglass* at Tomolab [mm] M 2**			
R	**h**	**r**	**α**
4	0.0255	0.3191	0.07986

3.3 Measurements by Geosciences and Image Department

Preliminary further experimental tests on *Hourglass* have been conducted in collaboration with Geosciences and Image Department (University of Padova). A SkyScan CT system had been available for its metrological performance investigation and further studies on metrological structure resolution. The CT system is a high resolution micro CT system with cone beam x-ray radiation from 20 to 100 kV with a declared spot size under 8 µm. The detector is a 12 bit cooled CCD fiber optically coupled to a scintillator. The dimensions of the systems are displayed in Fig. 3.5 [87].

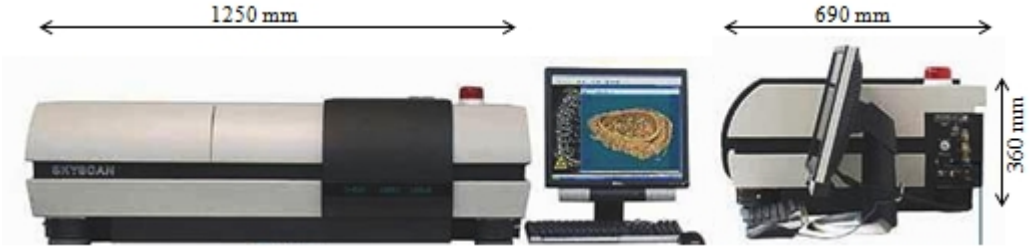

Fig.3.5: SkyScan 1172 pictures and dimensions [87]

3.3.1 CT measurements of Hourglass for determining metrological structure resolution

Similarly to the CT measurements at Elettra, *Hourglass* has been used to test the metrological structure resolution of the SkyScan CT system. The item has been measured under three different magnifications as shown in Table 3.5. One as close as possible to the x-ray source (HG 5.5), one as far as possible from the x-ray source (HG 13.22) and the third one in the middle (HG 9.26).

Table 3.5: Hourglass with SkyScan CT system: measurements parameters

	HG 5.5	**HG 9.26**	**HG 13.22**
Nr. proj	1800 over 180°		
Voltage (kV)	82		
Current (µA)	122		
Pre-filter	0.5 mm Aluminium		
Pixel size [µm]	**5.59**	**9.26**	**13.22**

As similarly explained in 3.1 the data acquired with SkyScan CT system been post processed with the software NRecon 1.6.3.3 version Software provided by SkyScan where the reconstruction is based on the filtered back-projection algorithm (Feldkamp). The volume of

Hourglass has been further analyzed in VG Studio Max 2.1 and a point cloud (.txt file) has been exported and investigated with Polyworks 10.0 Innovmetric software. The contact zone between the two spheres reveals to be a "cylinder" and its radius has been calculated as a fitting of points following the Gaussian best fit filter see Fig. from 3.6 to 3.9.
The fitted cylinder radius has been recorded and according to (6) the height of the cylinder has been calculated. In Table 3.6 the results have been reported. As already described in 3.1, the height *h* of the cylinder is supposed to represent the metrological structure resolution of the micro CT system and as supposed, the height of the cylinder is getting smaller with the increasing of magnification and the decreasing of the pixel size. As shown in Table 3.6 when the pixel is:

- 5.59 µm, the height of the cylinder is 100 µm;
- 9.26 µm, the height of the cylinder is 168.9 µm;
- 13.22 µm, the height of the cylinder is 173.4 µm.

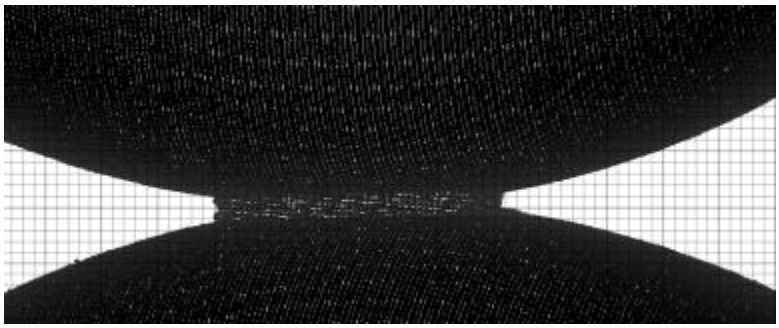

Fig.3.6: HG 5.5 contact zone of the two spheres

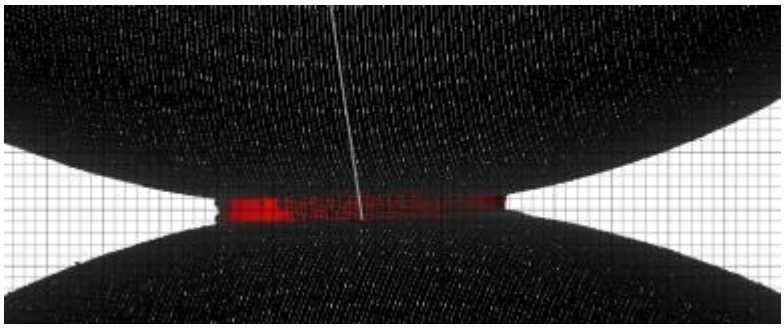

Fig.3.7: HG 5.5 Fitted cylinder in the contact zone of the two spheres

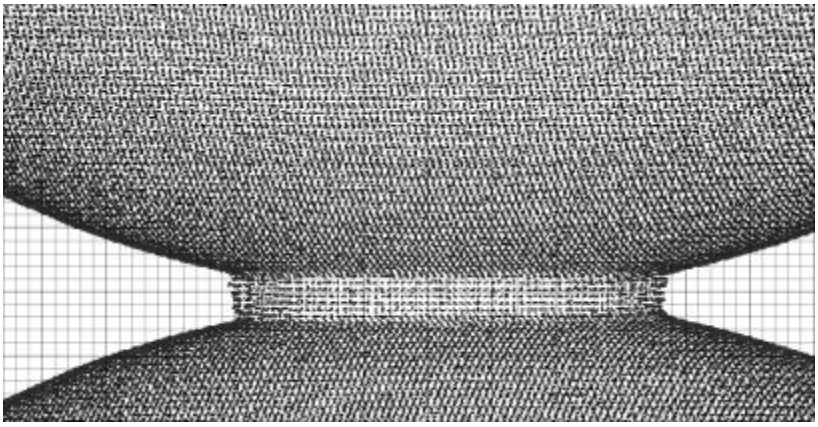

Fig.3.8: HG 13.22 contact zone of the two spheres

Fig. 3.9: HG 13.22 Fitted cylinder in the contact zone of the two spheres

Table 3.6: Hourglass results with SkyScan CT system

***Hourglass* with SkyScan [mm]- 5.5 µm voxel size**			
R	**h**	**r**	**α**
4	0.10004	0.6306	0.1583104

***Hourglass* with SkyScan [mm]- 9.26 µm voxel size**			
R	**h**	**r**	**α**
4	0.16894	0.8177	0.2058763

***Hourglass* with SkyScan [mm]-13.22 µm voxel size**			
R	**h**	**r**	**α**
4	0.1734	0.8283	0.2085842

Comparing the results with the ones obtained with Tomolab CT system, the metrological structure resolution reveals to be definitely worst with SkyScan CT system, even if the used pixel size often has been smaller than in the Tomolab measurements. This is a confirmation that the pixel size is not the only influencing parameter in the metrological structure resolution investigation. For this reason further measurements on *Hourglass* have been conducted with the variation of different parameters, as described in 3.3.2.

3.3.2 Further investigation on *Hourglass* and validation of the Hourglass method

As already anticipated in 3.3.1, the investigation on *Hourglass* should take into account not only the variation of pixel size, but also other influencing parameter in order to follow the definition given by the working draft ISO 10360-11 [61], where the metrological structure resolution is supposed to cover the entire sequence of CT measurements [8].

For this reason the following parameters have been decided to be modified and investigated:

1. Scanning parameter: two different pixels sizes have been selected, in Table3.7 “HG 5.5” and “HG 13.22”, as already done for the previous investigations;
2. Image parameter: the images have used with normal binning and with a binning of 4x4, in Table 3.7 “HG 5.5” resize and “HG 13.22” resize;

Binned data consists in merging pixels in order to reduce data quantity (see Fig. 3.10); in this case it has been done in order to reduce the resolution of the images [20].

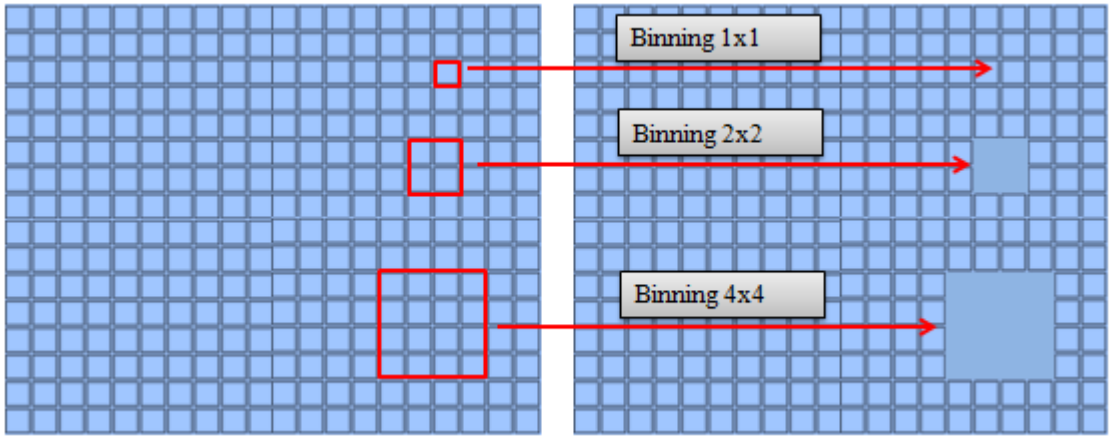

Fig. 3.10: Binning procedure

3. Surface parameter: the 3D volume has been investigated without and with a smoothing filter, in Table 3.7 “HG 5.5 smoothing” and “HG 13.22 smoothing”.

Smoothing acts on the triangle vertexes of a polygonal model (for example .stl file). The smoothing is a filter applied to vertices. A radius value specifies a 3D distance around a vertex for the smoothing filter, see details in Fig. 3.11.

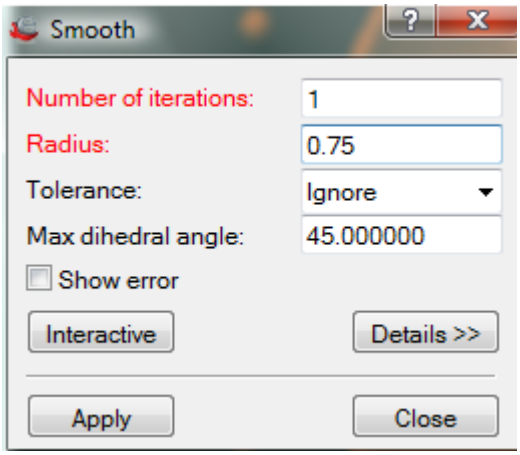

Fig. 3.11: Smoothing filter set up in Polyworks software

Table 3.7: Hourglass with SkyScan CT system: measurements parameters

	HG 5.5	**HG 13.22**	**HG 5.5 resize**	**HG 13.22 resize**	**HG 5.5 smoothing**	**HG 13.22 smoothing**
Nr. proj	1800 over 360 °					
Voltage (kV)	77					
Current (µA)	100					
Pre-filter	0.5 mm Aluminium					
Modified Parameter	Scanning	Scanning	Image	Image	Surface	Surface
Pixel size [µm]	**5.59**	**13.22**	**22.35**	**52.89**	**5.59**	**13.22**

Moreover according to the structure resolution method given by ISO [61] (see 1.1.4), the Hourglass method has been validated. A set of 12 microspheres has been selected and calibrated with optical multisensors CMM (Werth Video Check). They have been calibrated in terms of diameter, as shown in Fig. 3.13, with a range from 575 to 53 µm.

The 12 spheres have been positioned on an adhesive tape from the biggest to the smallest (see Fig.3.14 right) and they have been fixed on the carbon fiber cylinder of *Hourglass* in order measure simultaneously the microspheres and *Hourglass*. The combined item (see Fig. 3.14 left) has been measured with the parameters already described in Table 3.7.

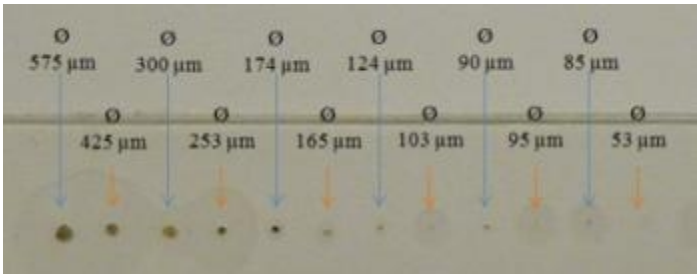

Fig3.13: Micro spheres diameters values

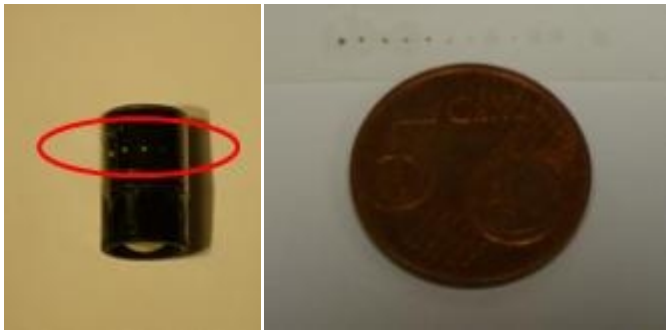

Fig.3.14: Hourglass with microspheres (left), selected microspheres pictures (right)

According to ISO WD 10360-11 [61], when the metrological structure resolution is represented by a height cylinder value, the microspheres with diameter lower than this value should not appear in the 3D volume, see Fig. from 3.16 to 3.17. On the other hand, the microspheres with diameter bigger than this height value should be detectable on the 3D image.

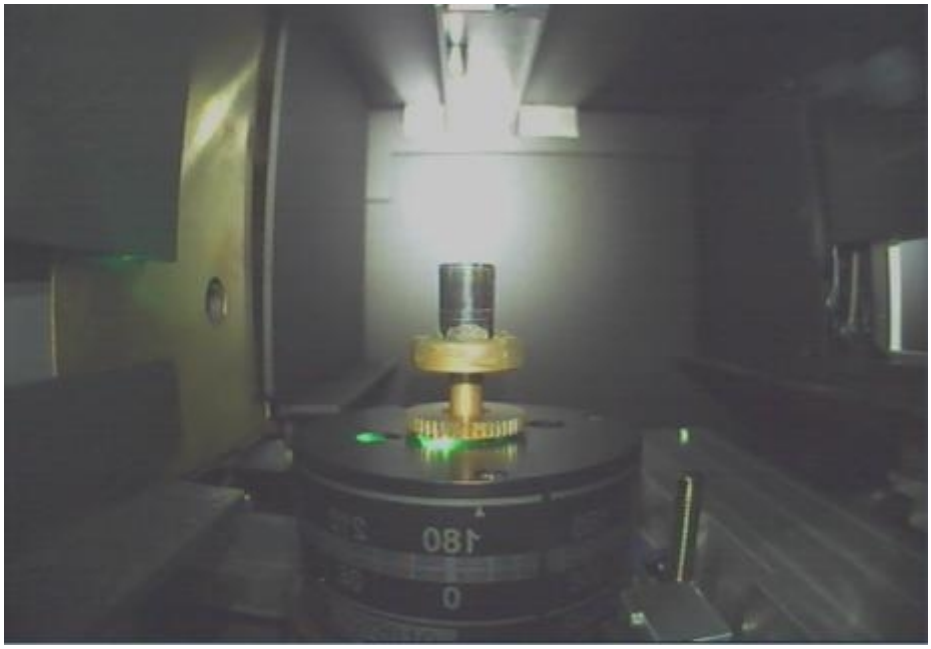

Fig.3.15: Hourglass inside the Skyscan CT system

The metrological structure resolution of SkyScan has been evaluated similarly to the previous tests on *Hourglass* and these results are shown in Table 3.8. The smoothing filters applied in this work were not so much influencing on the results, so stronger further smoothing filters will be tested in future work, looking for more interesting results.

Fig.3.16: HG 5_5 amd HG 5_5 resize point clouds

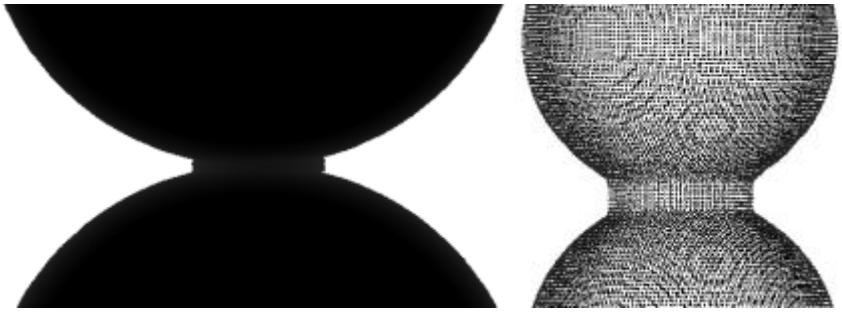

Fig.3.17: HG 13_22 amd HG 13_22 resize point clouds

Table 3.8: Hourglass combined with microspheres results using SkyScan CT system

***Hourglass* with micro spheres at SkyScan [mm]- 5.59 µm voxel size**			
R	**h**	**r**	**α**
4	0.08437	0.5794	0.14536

***Hourglass* with micro spheres at SkyScan [mm]- 13.22 µm voxel size**			
R	**h**	**r**	**α**
4	0.22438	0.9407	0.2374

***Hourglass* with micro spheres at SkyScan [mm]- 5.59 µm voxel size - resize data**			
R	**h**	**r**	**α**
4	0.35708	1.18171	0.2999

***Hourglass* with micro spheres at SkyScan [mm]- 5.59 µm voxel size - resize data**			
R	**h**	**r**	**α**
4	0.08712	0.5887	0.14771

***Hourglass* with micro spheres at SkyScan [mm]- 13.22 µm voxel size - - smoothing**			
R	**h**	**r**	**α**
4	0.22546	0.942939	0.23797

The microspheres have been seen in the 3D volume in relation to the actual calculated metrological structure resolution. In Table 3.9 the results are displayed and with the worsening of the metrological structure resolution, more microspheres disappeared.

Table 3.9: results on combined Hourglass with microspheres [µm]

	Pixel Size	$r_{(cylinder)}$	$h_{(cylinder)}$	µspheres	$D_{min\ µspheres}$
HG 5.5	5.59	579.4	84.37	11	85
HG 13.22	13.22	940.7	224.37	6	165
HG 5.5 resize	22.35	1181.71	357.07	4	253
HG 13.22 resize	52.89	1824.92	881.10	0	--
HG 5.5 smoothing	5.59	588.7	87.12	11	85
HG 13.22 smoothing	13.22	942.939	225.46	6	165

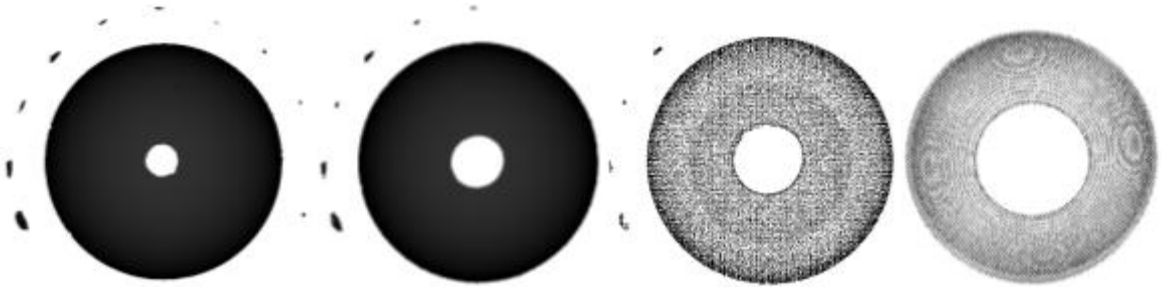

Fig.3.18: HG 5_5 (11 visible microspheres), HG 13_22 (6 visible microspheres), HG 5_5_resize (4 visible spheres), HG 13_22 resize (no visible spheres)

From Table 3.9, it is possible to deduce that the height of the cylinder (h) does not represent the diameter of the smallest visible microsphere, but it is a limit that divides the spheres that are detectable and the ones that are not visible. In other terms, when the diameter of one microsphere $D_{\mu sphere}$ is bigger than the height of the cylinder *h,* the microsphere is fully detectable. Moreover when the diameter of the microsphere has a value similar to the height of the cylinder, the microsphere is getting worst and it is not perfect visible. Finally when the diameter of the microsphere is definitely smaller than the height of the cylinder, the microsphere is not possible to be seen. Following:

$$D_{\mu sphere} > h\,,\ the\ \mu sphere\ is\ visible \qquad (8)$$

$$D_{\mu sphere} \sim h\,,\ the\ \mu sphere\ is\ not\ perfect\ visible \qquad (9)$$

$$D_{\mu sphere} \ll h\,,\ the\ \mu sphere\ is\ not\ visible \qquad (10)$$

From Table and formula (8), (9) and (10), it is possible to deduce a factor *c*, called detectable ratio factor that correlate the minimum diameter of the smallest detectable sphere (D_{min}) and the related height of the cylinder *h*, as following:

$$c = \frac{D_{min}}{h} \qquad (11)$$

According to (11) in Table 3.10 the *c* factor is calculated for each measurement. Further the diameter of the biggest sphere that is not detectable is reported its *c* factor is calculated (*c* factor not detectable). The average between the *c* factors detectable and not detectable is the optimum c factor (c_{opt}), that is 0.68.

Since the set of 12 spheres does not cover the entire possible values of metrological structure resolution, the diameter of the microspheres directly related to the height of the cylinder can be calculated with the c_{opt}. The optimum visible *c* factor has been calculated only taking into account the results on HG with different magnifications and different binning, since the influence of the smoothing filters reveals to be not that much influencing.

*Table 3.10: optimum c factor calculation (c_{opt}) [µm] (where there is * the data are resized)*

	Calculated cylinder h	D_{min} of smallest detectable sphere	*c* factor (detectable)	D of the biggest **not** detectable sphere	*c* factor (not detectable)		D_{min} (real) of the smallest detectable sphere
HG 5_5	84.37	85	1.007	53	0.628		57.4
HG 13_22	224.37	165	0.735	124	0.553		152.7
HG 5_5*	357.07	253	0.709	174	0.487		243.0
HG 13_22*	881.1	--		575	0.653		599.6
			0.709		0.653		
					0.681	c_{opt}	

4. Conclusion and Further Works

Preliminary results have been achieved in the developments of an industrial procedure for evaluating the metrological structure resolution of CT systems. Starting from the definitions given by the international standards [61], a new method has been investigated: Hourglass method. The item, made of two ceramic spheres connected by a carbon fiber cylinder reveals to be pretty useful, when investigating on the contact zone of the two spheres that ideally should be infinitesimal. The contact zone can be correlated to the metrological structure resolution, since the contact zone reveals to be a "cylindrical hole" with different heights when changing different parameters and so achieving different metrological structure resolution. The method has been validated with first experimental measurements, according to the method proposed by the WD ISO Standard [61]. Hourglass has been measured together with 12 microspheres (in a range from 575 to 53 μm). When the height cylinder has a determinate value, the microspheres with diameter lower than this value did not appear in the 3D volume. On the other hand, the microspheres with diameter bigger than this height value are not detectable on the 3D image. After this first validation, the height of the cylinder in the contact zone has been correlated directly to the metrological structure resolution with a optimum *c* factor that has been calculated as 0.68. The height of the cylinder reveals to be a limit that divides the spheres that are detectable and the ones that are not visible.

This procedure preliminary validated the Hourglass concept. Further investigations will be carried on in order to make Hourglass method fully applicable for industrial uses. In particular the spheres reveal to be not perfect in terms of spherical features and they are made of different material from the Hourglass spheres. Moreover, the spheres should cover as much as possible the range of measurements, especially in the upper and lower values. Finally other important parameters should be investigated in order to test all the influencing factors on the metrological structure resolution, such as: the surface filters (further investigations on smoothing and other filters), voltage and current of the x-ray source, the presence of the pre-filtering, the number of rotary step and the threshold operations due to the user [61].

Chapter 6

Conclusions

The main conclusions of the PhD thesis are collected and summarized in Chapter 6.

1. Conclusions

This thesis presented the main results of investigations carried out during the PhD period on accuracy of dimensional measurements using x-ray Computed Tomography systems.
Chapter 1 illustrated the state of the art related to the Computed Tomography used for several applications, with main focus on Dimensional Metrology field.
In particular x-ray CT first developed in medical applications and further it became a powerful tool in material science and NDT applications. In the recent years, CT technique has been adopted in dimensional metrology, due to many advantages over traditional coordinate measuring techniques. The main advantages are [37]:

- The ability to measure as well the inner as the outer geometry of objects without disassembling or destroying them;
- Possibility to acquire a high point density in a relative short time;
- Non contact inspection.

On the other hand, several limitations are present, e.g. [37]:

- Complex and numerous influence quantities occur;
- Complete standardized testing procedures are not yet available;
- Measurements are typically not traceable since their uncertainty is difficult to evaluate.

Due to the CT disadvantages listed above, CT systems are still not completely recognized as reference measuring instruments with metrological performances comparable to other coordinate measuring techniques. Moreover the influence factors should be deeply investigated and understood in order to correct them in the right way and improve measurement accuracy [43].
The metrological performance verification of CT systems and the enhancement of accuracy have been further analyzed in Chapter 2, where the state-of-the-art metrological performance verification procedureswere presented and discussed. Moreover, new approaches and reference standards were described. In addition, the procedures for metrological performance testing and related objects provided by the *Laboratory of Industrial and Geometrical*

Metrology of the University of Padova have been described. In particular *Pan Flute Gauge* and *CT Tetrahedron* have been designed, created and calibrated in order to analyze CT systems metrological performance such as the determination of optimal threshold value, of the size error for unidirectional and bidirectional distances measurements and of form error.
In Chapter 3 the experience at PTB (National Metrology Institute of Germany) from August to November 2010 has been illustrated with the description of the investigated item *PTB Tetrahedron* and related analyses of its stability, calibration procedures and CT measurement results. In details the study the capability of CT to measure form using features with a known and calibrated form deviation has been conducted through the analysis of *PTB Tetrahedron*, characterized by a top sphere with high form error (maximal form deviation 0.15 mm). In particular the quality of CT measurements has been confirmed since the form error of the top sphere resulted bigger than the difference between the tactile reference data and the CT data.
Further on, in Chapter 4 an extract from the official CT Audit project report has been presented. CT Audit project was the First International Intercomparison on CT Systems for dimensional metrology, organized by the *Laboratory of Industrial and Geometrical Metrology* of University of Padova and it has been carried out from September 2009 to June 2011. Four calibrated samples, chosen in order to represent a variety of dimensions, geometries and materials, were sent from one Participant to the next one, in a sequential participation scheme, together with detailed measurement procedures and reporting instructions. The results showed better abilities from the Participants in measuring sizes, such as diameter and distances, than form errors. Results from Item 1 and Item 3 show also that diameter measurements give larger E_n numbers than spheres' distances measurements. This can be explained by the fact that spheres' distances are unidirectional length measurements, while diameters are not unidirectional and therefore are subject to additional uncertainty components – such as threshold determination errors – that are not properly taken into account by Participants. Moreover an interesting trend has been obtained in the analysis results of Item 2. The deviations from calibrated values of inner and outer diameters have a systematic "mirror distribution": deviations of outer diameters' measurements are always more positive than deviations of inner diameters' measurements. The possible causes of this systematic trend are going to be investigated with all the Participants. Moreover calibrated diameter values of Item 2 after the conclusion of the circulation have been distributed to each

Participant, and only six of them corrected their lengths measurements in terms of systematic errors, mainly due to the threshold value determination and the scale error. Participants have difficulties in evaluating the measurement uncertainty appropriately. This confirms that traceability of dimensional measurements is still a major challenge in CT scanning, even for experienced users. A further important outcome of the CT Audit project is the establishment of an international network of laboratories using CT dimensional measuring systems. This network is an important basis for further international collaborations in the field of metrological verification and uncertainty evaluation of CT systems. Part of the network, had the chance to meet at a workshop on 26th of October 2011 in Padova at Dimeg Department, for discussing the results of the CT Audit project.

Finally, Chapter 5 presented preliminary investigations on metrological structure resolution, defined as the size of the smallest structure that can still be measured dimensionally [60]. The state of the art related to the metrological structure resolution has been illustrated and from this investigation came out that a clearly well accepted definition of structure resolution and related metrological verification procedure is not definitely published in standards.

At *Laboratory of Industrial and Geometrical Metrology* of University of Padova, preliminary investigation have been carried out in the developments of an industrial procedure for evaluating the metrological structure resolution of CT systems. Starting from the definitions given by the draft international standards [61], a new method has been investigated: Hourglass method. The Hourglass reference standard, made of two ceramic spheres connected by a carbon fiber cylinder reveals to be pretty useful for determining the structural resolution on the contact zone of the two spheres. The measurement errors visible on the contact zone can be correlated to the metrological structure resolution, since the contact zone is distorted by the CT structure resolution into a “cylindrical hole” with height depending on structure resolution itself. The method has been validated with first experimental measurements, in comparison to the method proposed by the WD ISO Standard [61]. Hourglass has been measured together with 12 microspheres (in a range from 575 to 53 µm). When the height of the “cylindrical hole” has a determinate value, the microspheres with diameter lower than this value did not appear in the 3D volume. On the other hand, the microspheres with diameter bigger than this height value are detectable on the 3D image. After this first validation, the height of the cylinder in the contact zone has been correlated

directly to the metrological structure resolution through a *c* factor that has been calculated as 0.68.This procedure validated the applicability of the Hourglass method, even if further investigations should be carried on in order to make this method fully applicable for industrial uses. Finally other important parameters should be investigated in order to test all the influencing factors on the metrological structure resolution, such as: the surface filters, voltage and current of the x-ray source, the presence of the pre-filtering, the number of rotary steps and the threshold operations performed by the user [61].

References

[1] Van de Casteele E., 2004, Model-based approach for Beam Hardening Correction and Resolution Measurements in Microtomography (PhD Thesis), Universiteit Antwerpen

[2] Wikipedia, http://en.wikipedia.org/wiki/X-ray, as it is on January 2011

[3] Hsieh, J., 2009, Computed Tomography: Principles, Design, Artifacts, and Recent Advances, Second Edition (SPIE Press Book) ISBN: 9780819475336

[4] Bettyann Holtzmann, K., 1996, Naked to the Bone Medical Imaging in the Twentieth Century. Camden, NJ: Rutgers University Press. pp. 19–22. ISBN 0813523583.

[5] Oldendorf, WH., 1961, Isolated flying spot detection of radiodensity discontinuities--displaying the internal structural pattern of a complex object. Ire Trans Biomed Electron, BME-8:68-72.

[6] Oldendorf, WH., 1978, The quest for an image of brain: a brief historical and technical review of brain imaging techniques. Neurology, 517-33.

[7] Hounseld, G.N., 1973, Computerized transverse axial scanning (tomography): Part1. description of system. British Journal of Radiology, 46:1016 1022

[8] Kruth, JP., et al., 2011, Computed Tomography for dimensional metrology. CIRP Annals –Manufacturing Technology (821-842), doi: 10.1016/j.cirp.2011.05.006

[9] Filler, A.G., 2010, The history, development and impact of computed imaging in neurological diagnosis and neurosurgery: CT, MRI, and DTI. The Internet Journal of Neurosurgery, Volume 7 number 1.

[10] Brian, R, Subach, M.D., et. al., 2008, Reliability and accuracy of fine-cut computed tomography scans to determine the status of anterior interbody fusions with metallic cages. Spine J. 2008;8:998–1002

[11] Parisatto, M., 2011, Applications of x-ray tomographic techniques to the study of cement-based materials, PhD Thesis, University of Padova, Padova Digital University Archive, http://paduaresearch.cab.unipd.it/4047/ , as it is on August 2011

[12] Schörner, K., Goldammer, M. , Stephan, J., 2011, Scatter Correction by Modulation of Primary Radiation in Industrial X-ray CT: Beam-hardening Effects and their Correction. DIR

[13] phoenix|x-ray, http://www.ge-mcs.com/en/phoenix-xray, as it is on May 2011

[14] ImPACT, http://www.impactscan.org/slides/impactcourse/basic_principles_of_ct/img24.html, as it is on October 2011

[15] E 1441-00:2000, Standard Guide for Computed Tomography (CT) Imaging. West Conshohocken, PA: ASTM International standard

[16] Department of Geological Sciences, University of Texas at Austin, http://www.ctlab.geo.utexas.edu/overview/index.php, as it is on October 2011

[17] VDI/VDE 2630 - Part 1.1 (2009-07), Computed tomography in dimensional measurement - Basics and definitions. VDI, Duesseldorf, 2009.

[18] Fox, S.H.,1995, "CT tube technology" in Medical CT and Ultrasound: Current Technology and Applications, L.W. Goldman and J.B. Fowlkes, Eds., Advanced Medical Publishing, Madison, WI, 349-358

[19] BS EN 16016-1:2011 Non destructive testing - Radiation method - Computed tomography Part 2: Principles, equipment and samples, British Standard

[20] Christoph, R., Neumann, H.J., 2011, X-ray Tomography in Industrial Metrology – Werth Messtechnik ISBN: 9783862360093

[21] BS EN 16016-1:2011 Non destructive testing - Radiation method – Computed tomography Part 1: Terminology, Britisch Standard

[22] Geochemical Instrumentation and Analysis, http://serc.carleton.edu/research_education/geochemsheets/techniques/CT.html, as it is on October 2011

[23] Carmignato, S., Dreossi, D., Mancini, L., Marinello, F., Tromba, G., Savio, E., 2009 Testing of X-ray Microtomography Systems Using a Traceable Geometrical Standard. Measurement Science and Technology 20:084021

[24] Reisinger, S., KasperL, S., Franz, M., Hiller, J., Schmid, U., 2011, Simulation-Based Planning of Optimal Conditions for industrial computed tomography, DIR International Conference, Berlin

[25] Weckenmann, A., Krämer, P., 2009, Application of computed tomography in manufacturing metrology. Technisches Messen, Oldenbourg. Volume: 76, Pages: 340 – 346

[26] Feldkamp, L.A., Davis, L.C., Kress, J.W., 1984, Practical cone-beam algorithm, J. Opt. Soc. AM. A 1, 612-619

[27] International Vocabulary of Metrology – Basic and General Concepts and Associated Terms VIM, 3rd edition, JCGM 200:2008

[28] Weckenmann, A., Krämer P., Hoffmann, J., 2007, "Manufacturing Metrology – State of the Art and Prospects", 9th International Symposium on Measurement and Quality Control (ISMQC), pp. 1-8, Chennai

[29] Voltan, A., 2010, Metrological performance verification of optical Coordinate Measuring Systems, Phd Thesis, University of Padova

[30] Bosch, J.A., 1995, "Coordinate measuring machines and systems", Marcel Dekker, New York, USA

[31] Schwenke, H., Neuschaefer-Rube, U., Pfeifer, T., Kunzmann, H., 2002, Optical methods for dimensional metrology in production engineering CIRP Ann. 51 685–99

[32] Weckenmann A, Krämer P, 2009, Assessment of measurement uncertainty caused in the preparation of measurements using computed tomography. CD-ROM, Proc. IMEKO XIX World Congress, 1888–1892. ISBN 978-963-88410-0-1

[33] Christoph, R., Neumann, H.J., 2004, Multisensor coordinate metrology" Verlag moderneindustrie, Munich, Germany

[34] Miguel, P. A. C., King, T. G., 1995, Co-ordinate measuring machines—concept, classification and comparison of performance tests Int. J. Qual. Reliab. Manage. 12 48–63

[35] Brunke, O., Santillan, J., Suppes, A., 2010, Precise 3D dimensional metrology using high-resolution x-ray computed tomography *Proc. SPIE* 7804 78040O

[36] Andreu, V., Georgi, B., Lettenbauer, H., Yagüe, J.A., 2009, Analysis of the error sources of a Computer Tomography Machine. Proc. Lamdamap conference 462-471

[37] Neuschaefer-Rube, U., Bartscher, M., Neukamm, M., Härtig, F., 2009, Dimensional Measurements with Micro-CT(Test Procedures and Application). Oral Presentation at "Microparts Interest Group Workshop" NPL Teddington

[38] Carmignato, S., Pierobon, A., 2011, Preliminary Results of the 'CT Audit' Project: First International Intercomparison of Computed Tomography Systems for Dimensional Metrology. DIR Berlin

[39] Carmignato, S., 2007, Traceability of dimensional measurements in computed tomography, Proc. 8th A.I.Te.M. Conf., Montecatini, Italy, ISBN/ISSN: 88-7957-264-4

[40] Lettenbauer, H., Imkamp, D., 2005, Einsatz der 3D-computertomographie in der dimensionelle messtechnik, VDI Berichte 1914, pp.201-208

[41] Telasi, S., 2007, Measure completely and accurately – x-ray computed tomography integrated with a multisensor CMM, Metromeet Int. Conf., Bilbao

[42] Wenig, P., Kasperl, S., 2006, Examination of the Measurement Uncertainty on Dimensional Measurements by X-ray Computed Tomography. ECNDT

[43] Bartscher, M., Neukamm, M., Koch, M., Kniel, K., Härtig, F., Neuschaefer-Rube, U., 2010, Dimensional control of technical components with computed tomography. CIMi2010, Porto – Portugal

[44] ISO/TS 15530-3, 2004, Geometrical Product Specifications (GPS) – CMMs: Technique for determining the uncertainty of measurement – Part 3: Use of calibrated workpieces or standards, ISO Geneve 2004

[45] I.H. Lira, W. Wöger: Evaluation of the uncertainty associated with a measurement result not corrected for systematic effects, Meas. Sci. Technol., vol. 9, 1998, pp. 1010-1011

[46] Bartscher, M., Ehrig, K., Staude, A., Goebbels, J., Neuschaefer-Rube, U., Application of an Industrial CT reference Standard for Cast Freeform Shaped Workpieces, 2011, DIR Berlin

[47] Kasperl, S., Hiller, J., Krumm, M., 2008, "Computed Tomography Metrology in Industrial Research & Development", International Symposium on NDT in Aerospace, Fürth, Germany

[48] ASTM International, http://www.astm.org/index.shtml as it is on 6th December 2011

[49] E 1570-00: Standard Practice for Computed Tomographic (CT) Examination. West Conshohocken, PA: ASTM International (2000).

[50] E 1672 -01: Standard Guide for Computed Tomography (CT) System Selection. West Conshohocken, PA: ASTM International (2001).

[51] E 1695 -01: Standard Test Method for Measurement of Computed Tomography (CT) System Performance. West Conshohocken, PA: ASTM International (2001).

[52] E 1935-03: Standard Test Method for Calibrating and Measuring CT Density. West Conshohocken, PA: ASTM International (2003).

[53] British Standards Institution, http://www.bsigroup.com/, as it is on 6th December 2011.

[54] BS EN 16016-3:2011 Non destructive testing - Radiation method - Computed tomography Part 3: Operation and interpretation, British Standard

[55] BS EN 16016-4:2011 Non destructive testing - Radiation method - Computed tomography Part 4: Qualification, Britisch Standard

[56] VDI, http://www.vdi.eu/index.php?id=2675, as it is on December 7th 2011

[57] ISO 10360-2:2009, Geometrical product specifications (GPS) - Acceptance and reverification tests for coordinate measuring machines (CMM) - Part 2: CMMs used for measuring linear dimensions. ISO, Geneva, 2009

[58] ISO/DIS 10360-8 (2011-06-16), Geometrical product specifications (GPS) - Acceptance and reverification tests for coordinate measuring machines (CMM) - Part 8: CMMs with optical distance sensors. ISO, Geneva, 2011

[59] ISO, http://www.iso.org/iso/home.html, as it is on December 7th 2011

[60] VDI/VDE 2617 Blatt 13, (2011-12): Accuracy of coordinate measuring machines - Characteristics and their testing - Guideline for the application of DIN EN ISO 10360 for coordinate measuring machines with CT-sensors - VDI/VDE 2630 Blatt 1.3: Computed tomography in dimensional measurement. VDI, Duesseldorf, 2011.

[61] ISO/WD 10360-11 (2011-07-27), Geometrical product specifications (GPS) - Acceptance and reverification tests for coordinate measuring machines (CMM) - Part 11: Computed tomography. ISO, Geneva, 2011.

[62] Trapet Precision Engineering, http://www.trapet.de, as it is on 12th December

[63] Lettenbauer, H., Weiss, D., Georg, B., 2009, Verification of the Accuracy of Computed Tomography, Quality Digest Magazine

[64] Weckenmann, A., Krämer, P., 2009, Assessment of measurement uncertainty caused in the preparation of measurements using computed tomography, XIX IMEKO Worl Congress, Lisbon

[65] Bartscher, M., Neuschaefer-Rube, U., Wäldele, F., 2004, Computed Tomography - A Highly potential Tool for Industrial Quality Control and Production near Measurements, VDI BERICHTE

[66] Schulze, M., Neugebauer, M., Meess, R., Brzoska, J., Jung, A., Staude, A., Ehrig, K., 2010, Der Einfluss unterschiedlicher Materialzusammensetzung auf das dimensionelle Messen von Mikroobjekten mittels Mikro-Computertomographie, DGZfP 2010

[67] Hilpert, U., Bartscher, M., Neugebauer, M., Goebbels, J., Weidemann, G., Bellon, C., 2007, Simulation-aided computed tomography (CT) for dimensional measurements, DIR 2007 France

[68] Cantatore, A., Andreasen, J. L., Carmignato, S., Muller, P., De Chiffre, L., 2011, Verification of a CT scanner using a miniature step gauge, In: Proceedings of the 11th euspen International Conference, Como

[69] Nardelli, V., Arenhart, F., Donatelli, G., Porath, M., 2011, Using calibrated parts and integral surface analysis to investigate dimensional CT measurements, DIR Berlin

[70] Kiekens, K., Tan, Y., Kruth, JP., Voet, A., Dewulf, W., Parameter Dependent Thresholding for Dimensional x-ray Computed Tomography, 2011, DIR Berlin

[71] S. Favretto, 2008, "Applications of X-ray computed microtomography to material science: devices and perspectives", PhD. Thesis, Supervised by Prof. E. Lucchini, Università degli studi di Trieste e Dr L. Mancini, Sincrotrone Trieste S.C.p.A.

[72] Patent August 12th 2009 "Carmignato S., Pierobon A., Marinello F., Savio E.,"Metodo di controllo e taratura per sistemi di tomografia computerizzata",PD2009A000242.

[73] Carmignato, S., Pierobon, A., Marinello, F., Savio, E., 2010, Olympic Gauge: A New Reference Standard for Testing X-ray Microtomography Systems, In: Proceedings of Euspen. Delft, 31/05- 04/06 2010, vol. 1, p. 217-220, ISBN: 978-0-9553082-8-4

[74] ISO/IEC 17043:2010, Conformity assessment – General requirements for proficiency testing. ISO, Geneva, 2010.

[75] H. Schwenke, W. Knapp, H. Haitjema, A. Weckenmann, R. Schmitt, F. Delbressine (2008)"Geometric error measurement and compensation of machines – An Update". *Annals of the CIRP* 57 (2008) 660-675

[76] Physikalisch-Technische Bundesanstalt -Coordinate Measuring Machines Section- (2002) "VCMM User Manual"

[77] ISO 4287:1997 Geometrical Products Specifications (GPS) - Surfaces texture: Profile method – Terms, definitions and surface texture parameters, ISO Geneve, 1997

[78] Carmignato, S., Pierobon, A., Savio, S., July 2011, First Draft of the report of Interlaboratory Comparison of Computed Tomography Systems for Dimensional Metrology, Laboratory of Industrial and Geometrical Metrology, University of Padova

[79] Jacobs, P., Bernard, D., 2011, Towards a Society for Tomography, DIR Berlin

[80] CT Audit web site, www.gest.unipd.it/ct-audit, as it is on 26th October 2011

[81] ISO 13528:2005, Statistical methods for use in proficiency testing by interlaboratory comparison, ISO, Geneve 2005

[82] Neuschaefer-Rube U., Neugebauer M., Ehrig W., Bartscher M., Hilpert U., (2008) Tactile and optical microsensors: Test procedures and standards. Measurement Science and Technology, vol. 19, 084010.

[83] Hecht, E., 2002, Optics 4th Edition, Addison Wesley, ISBN 0-321-18878-0

[84] ISO 15708-2:2002, Non-destructive testing - Radiation methods - Computed tomography - Part 2: Examination practices, ISO Geneve 2002

[85] Carmignato, S., 2005, Traceability of coordinate measurements on complex surfaces, PhD Thesis, University of Padova

[86] Philips CT Clinical Science, 2007, Considerations in cardiac CT: understanding temporal resolution and rotation speed for improved cardiac imaging, Philips CT White Paper

[87] SkyScan web site, http://www.skyscan.be/products/1172.htm, as it is on 14th October 2010